



TAMPEREEN TEKNILLINEN YLIOPISTO
TAMPERE UNIVERSITY OF TECHNOLOGY

LEO-VILLE MIETTINEN

**THE ROTATIONAL STIFFNESS AND WATERTIGHTNESS OF RD
PILE WALLS IN THE BEDROCK AND PILE INTERFACE**

Master of Science Thesis

Examiner: Professor Tim Lämsivaara
Examiner and topic approved in the
Faculty of Business and Built Envi-
ronment on 8st November 2013

ABSTRACT

TAMPERE UNIVERSITY OF TECHNOLOGY

Department of Civil Engineering

MIETTINEN, LEO-VILLE: The rotational stiffness and watertightness of RD pile walls in the bedrock and pile interface

Master of Science Thesis, 104 pages, 84 appendixes

March 2014

Major: Structural Design

Examiner: Professor Tim Lämsivaara

Key words: pile, wall, drilling, stiffness, watertightness, steel, concrete, rock

There is a need to increase knowledge about support of the base of the wall when piles are drilled into bedrock. Due to the drilling and installation method, there is a small gap between the piles and the bedrock. This gap is generally filled with drill cuttings or soil. The gap can also be grouted with an RM/RF interlock, another injection channel or from inside the pile.

The objective of this study is to determine the rotational stiffness of the base of the pile wall both theoretically and in practice at a test site. The second objective is to determine the effect of grouting on the watertightness of the bedrock drilling hole. The material in the gap must be established when the gap is not grouted to have data for watertightness and rotational stiffness calculations. In this study, different grouting methods are tested to determine optimal grouting practices. The study creates data to develop the RD pile wall design and installation manual and make it more specific. The manual will help designers choose optimal pile size, guide in calculations of stresses on the wall and anchors by taking into account the rigidity of the lower end of the wall and give guidance for estimating the watertightness of the wall.

To verify watertightness, single piles were tested, with two pieces of pile with different grouting methods. The water pressure on each pile was increased in a step-by-step fashion. Between each step, tap was shut down and pressure kept in place. Both water consumption and the drop in pressure were documented. To calibrate leakage and pressure loss, the same test was executed for bedrock hole and also for the plain hose and other equipment. The water leakage across the gap was calculated. The test was performed after all soil was excavated above the bedrock to prevent soil from affecting the watertightness measurements.

Samples of grout, bedrock, and drill cuttings were collected to determine their material properties. To determine rotational stiffness, a horizontal load test was implemented on single piles excavated up to the bedrock. The other way rotational stiffness was verified was through FEM calculations. The calculations and site tests shed light on when the joint has to assumed to be nominally pinned and when rigid or semi-rigid in the structural calculations of an RD pile wall. The calculations also showed the dependency on bedrock drilling depth and rigidity.

Main conclusion concerning rigidity was that piles with grouted gaps were quite rigid. The other result was that both stiffly grouted connections and also less stiff clay in the gap connection did reduce displacement of the wall and therefore smaller pile sizes may be used or rock anchor quantity or size may be reduced. Dense drill cuttings improved watertightness significantly. Where there were not dense drill cuttings in the gap, water consumption was roughly 50 times greater than when dense drill cuttings were present. According to the measurements, piles with grouting had slightly better watertightness than piles that had dense drill cuttings in the gap. Both material types did not fail at a pressure of 10 bar.

TIIVISTELMÄ

TAMPEREEN TEKNILLINEN YLIOPISTO

Rakennustekniikan koulutusohjelma

MIETTINEN, LEO-VILLE: RD-paaluseinän kiertojäykkyys ja vesitiiveys paalun ja kallion rajapinnassa

Diplomityö, 104 sivua, 84 liitesivua

Maaliskuu 2014

Pääaine: Rakennesuunnittelu

Tarkastaja: professori Tim Länsivaara

Avainsanat: Paalu, seinä, poraaminen, jäykkyys vesitiiveys, teräs, betoni, kallio

Porapaalujen tukeutuminen kallioon poratessa kaipaa lisätietämystä. Poraamisen menetelmästä johtuen paalujen ja kallion väliin jää pieni rako. Yleensä rako täyttyy porasoijalla tai maa-aineksella. Rako voidaan myös injektoida käyttäen RM/RF lukkoa, erillistä injektointi kanavaa tai injektoida paalun sisältä käsin.

Tässä tutkimuksessa tavoite on määrittää paaluseinän juuren kiertojäykkyys sekä teoreettisesti tarkastellen että käytännössä koetyömaalla. Toinen tavoite on määrittää porareian injektoinnin vaikutus seinän vesitiiveyteen. Porareian raon materiaali injektointomissa seinissä täytyy määrittää, että saadaan tarvittavaa tietoa vesitiiveyden ja kiertojäykkyyden laskentaan. Työssä testataan erilaisia injektointimenetelmiä jotta löydetään optimaalisin injektointi käytäntö. Tutkimus luo yksityiskohtaisempaa tietoa RD porapaalu seinän suunnittelu ja asennus ohjeeseen. Ohje auttaa suunnittelijaa valitsemaan optimaalisen paalukoon, ohjeistaa miten seinän alapään vaikutus otetaan huomioon seinän ja ankkureiden mitoituksessa ja ohjeistaa seinän vedentiiveyden arvioinnissa.

Veden tiiveyden määrittämiseksi kaksi jokaista eritavoin injektoitua paalua testattiin. Paalut testattiin portaittain kasvavalla vedenpaineella. Portaiden välissä veden tulo katkaistiin ja paine jätettiin paaluun. Vesimenekki ja painehäviö mitattiin paaluista. Todellisen vesimenekin ja painehäviön arvioimiseksi mitattiin kallio reikä ja pelkän letkujen, mittareiden ja liitosten vastaavat arvot. Hävikkien perusteella saadaan kallioraon kautta kulkeutuvan vesimenekin määrä. Testi suoritettiin kallion päällä olevien maiden kaivuun jälkeen, jotta maaperä ei vaikuttaisi vesitiiviysmittauksiin.

Injektoinnin, kallion ja porasoijan näytteiden avulla tutkittiin materiaali ominaisuuksia. Kiertojäykkyyden määrittämiseksi vaakavoima kuormituskoe tehtiin yksittäisille kallioon poratuille paaluille. Maat poistettiin ennen koetta. Kiertojäykkyys määritettiin toisaalta FEM-laskennan avulla. Testit ja laskelmat antoivat tietoa liitoksen määrittämiseen milloin liitos määritetään jäykäksi niveleksi tai osittain jäykäksi RD paalu seinän rakenteellisessa mitoituksessa. Laskelmat esittävät myös kallioporaus syvyyden vaikutuksen kiertojäykkyyteen.

Tärkein päätelmä jäykkyydestä oli että injektoitu rako kallioreiässä teki paaluista melko jäykkiä. Toinen tulos oli, että sekä jäykkä injektoitu liitos että vähemmän jäykkä savea raossa liitos vähensivät siirtymää seinässä ja siten mahdollisesti pienempää paalukokoa voidaan käyttää tai kallioankkureiden määrää tai kokoa voi vähentää. Tiivis porasoija paransi vesitiiveyttä merkittävästi. Tapauksessa jossa kallioreian raossa ei ollut tiivis porasoija, vesimenekki oli noin 50-kertaa suurempi kuin tiiviin porasoijan tapaus. Injektoidut paalut olivat mittausten mukaan hieman vesitiiviimpiä kuin tiiviin porasoijan tapaukset. Kumpikaan materiaalityyppi ei rikkoutunut edes testatussa 10 baarin paineessa.

PREFACE

This Master's thesis was funded by and written for Ruukki. The examiner of the thesis was Tim Länsivaara, professor of civil engineering at the Tampere University of Technology. I would like to thank Veli-Matti Uotinen, Vesa Järvinen, Hannu Jokiniemi and Hannu Vesamäki at Ruukki for their tips and for supervising this thesis. Thank you for the interesting topic with both theoretical and practical aspects in infrastructure construction. Thanks also goes to Ossi Hakanen, CEO of Suomen Teräspaalaus Oy, and the other personnel of Suomen Teräspaalaus Oy for building the test site needed in this thesis.

I would also like to thank Jukka Rantala for tips and assistance with Ansys modeling. Jukka calculated the rotational stiffness needed to make the table and charts discussed in paragraph 4.1.2. My gratitude goes to all the staff of the Tampere University of Technology who participated in loading or material tests. Thanks to all who introduced construction sites using RD piles walls and shared your practical experiences. I would also like to thank my girlfriend Hannele and my family for their support.

Helsinki 7 March 2014

Leo-Ville Miettinen

TABLE OF CONTENTS

List of symbols and abbreviations.....	vi
1 Introduction to RD pile walls.....	1
1.1 Basics	1
1.2 Supports of RD pile walls	4
1.3 RD pile wall supports in rock	6
1.3.1 Grouting drilling holes.....	7
2 Theory	9
2.1 Rigid, semi-rigid and nominally pinned joints.....	9
2.2 Effects of joint type on RD pile wall structure	11
2.3 Watertightness.....	12
2.3.1 Solution for watertight retaining walls	14
3 Field survey: RD pile wall and rock interface	16
3.1 Preparation	16
3.2 Testing arrangement.....	22
3.2.1 Watertightness	22
3.2.2 Drill cuttings, grouting and bedrock samples	27
3.2.3 Horizontal load test for single piles	43
3.3 Other remarkable findings from the Masku test site.....	51
3.4 Experience from other ongoing RD pile wall sites	57
4 Rotational stiffness of RD pile walls using the results of the field survey	61
4.1 Rock-pile rigidity calculation, Ansys FEM.....	61
4.1.1 Rotational stiffness analysis in Ansys to be used in RD pile wall dimensioning examples in GeoCalc.....	68
4.1.2 Drilling depth in relation to rotational stiffness.....	72
4.2 RD pile wall calculations using different joint types.....	81
5 proposed decision.....	87
5.1 Supporting pile wall into the rock.....	88
5.2 Pile and bedrock interface grouting	88
5.3 Limitations of this study	89
5.4 Suggestions for further research.....	91
References	93

LIST OF SYMBOLS AND ABBREVIATIONS

grout	“A setting material, usually cement and water, containing sometimes additives or a limited amount of fine aggregates, which transfers load from the bearing element or the micro-pile shaft to the ground and/or contributes to corrosion protection” (EN14199)
drilling fluid/mud	“Water or a suspension of bentonite, polymers or clay, in water with or without cement and other additions, for stabilization of borehole walls and for flushing” (EN14199)
drill cuttings	Small pieces of rock that break away due to the action of the bit teeth [37]
multi-stage grouting	"High pressure grouting through a tube-à-manchettes, special valves or post-grouting tubes after the grout previously placed in the borehole has set" (EN14199)
filling	“Grouting under no applied fluid pressure other than the height of grout fluid. Sometimes referred to as gravity grouting or as tremie grouting” (EN14199)
nominally pinned joint	“A nominally pinned joint should be capable of transmitting the internal forces, without developing significant moments which might adversely affect the members or the structure as a whole.” (EN 1993-1-8)
rigid joints	“Joints classified as rigid may be assumed to have sufficient rotational stiffness to justify analysis based on full continuity.” (EN 1993-1-8)
semi-rigid joint	“A joint which does not meet the criteria for a rigid joint or a nominally pinned joint should be classified as a semi-rigid joint. NOTE: Semi-rigid joints provide a predictable degree of interaction between members, based on the design moment-rotation characteristics of the joints. Semi-rigid joints should be capable of transmitting the internal forces and moments.” (EN 1993-1-8)
gap	In this thesis, the theoretical gap between the RD pile and the bedrock
$f_{ck,cube}$	Characteristic compressive cube strength of concrete at 28 days
K_a	Coefficient for horizontal active earth pressure [3]
K_p	Coefficient for horizontal passive earth pressure [3]
M	Tangent modulus [29]
m	Modulus number (Vianova Systems Finland Oy 2010, Novapoint GeoCalc, Supported Excavation Theory)
σ'	Effective vertical stress [29]

σ_a	Reference pressure =100kPa [29]
σ_0	Initial stress level
β	Stress exponent
S_j	“The rotational stiffness of a joint” (EN 1993-1-8)
$S_{j,ini}$	“The slope of the elastic range of the design moment-rotation characteristic” (EN 1993-1-8)
$S_{j,ini}$	“The initial rotational stiffness of a joint” (EN 1993-1-8)
$M_{j,Rd}$	“Design moment resistance of a joint” (EN 1993-1-8)
$M_{j,Ed}$	Bending moment applied to a joint (EN 1993-1-8)
φ_{Ed}	Corresponding rotation between connected members [11]
RD® pile	Ruukki’s special piles installed by drilling in difficult ground and environmental conditions. The piles may be drilled through all natural soil layers all the way into the bedrock.
RD® pile wall	Based on Ruukki’s RD piles (RD170–RD1200) and installed by drilling, RD pile walls are suitable for retaining wall structures in difficult ground conditions.
overburden drilling casing system in overburden drilling	Drilling into the soil [34] Overburden drilling with casing-like steel pipe or pile [34]
under-reaming system	Drilling system where the drilling bit can withdraw from the casing after drilling. There can be movable part like wings, or the drilling bit can be eccentric, which allows removal of the bit from the casing. [35]
concentric drilling system	System with a ring bit and a pilot bit [34, 35]

1 INTRODUCTION TO RD PILE WALLS

1.1 Basics

Ruukki's RD pile walls are composed of RD piles and interlocking sections. Interlocks are welded onto the piles in the workshop. There are two different interlocks available: RM/RF and E21 (shown in figure 1.1). The most recent RM/RM interlock includes a hole for grouting. Using the injection channel, the gap between the pile and the bedrock can be grouted to improve the watertightness and rotational stiffness of the wall. The drilling hole must be oversized because of the interlocks. When using the most recent RM/RF interlock, the required oversize of the drilling is less than for RD pile walls with E21 interlocks as one can see in table 1.1. The RM/RF interlock type is more recommendable due to the smaller oversize of the drilling hole and the injection channel included. E21 interlocks can be provided as well if the customer prefers E21.



Figure 1.1: Two different Ruukki interlocks: RM/RF interlock (left) and E21 interlock (right) [1].

Pile	Pile diameter [mm]	Interlock type	
		Ruukki RM/RF	Ruukki E21
		Ring diameter [mm]	Ring diameter [mm]
RD170	168,3	222	-
RD220	219,1	273	-
RD270	273,0	327	-
RD320	323,9	378	-
RD400	406,4	460	500
RD500	508,0	562	602
RD600	610,0	664	704
RD700	711,0	765	-
RD800	813,0	867	-
RD900	914,0	968	-
RD1000	1016,0	1070	-
RD1200	1220,0	1274	-

Table 1.1: Pile diameters and drilling bit diameter when using RM/RF and E21 interlocks.

RD pile walls can be drilled using different drilling systems. At present, there are two main systems in use. One is the concentric ring bit system, which has a pilot bit that drills the area inside the pile and a ring bit that makes the drilling hole wide enough for piles and interlocks. The pilot can be extracted and reused, but the ring bit remains underground. The ring bit can be welded onto the casing shoe. The ring bit set, including a ring bit and a casing shoe, can be factory-assembled to be an integrated part of the casing. The ring bit can also come as a separate part, which is then attached to the pilot bit before drilling. The separate ring bit, or “solitary ring bit,” is shown in figure 1.2 [34].

Only ring bits integrated into the pile provide horizontal support, as they are connected to the pile and there is no gap between the bedrock and the ring bit. In theory, some bending moment support is also provided to the toe of the pile due to friction between the integrated ring bit and the bedrock.

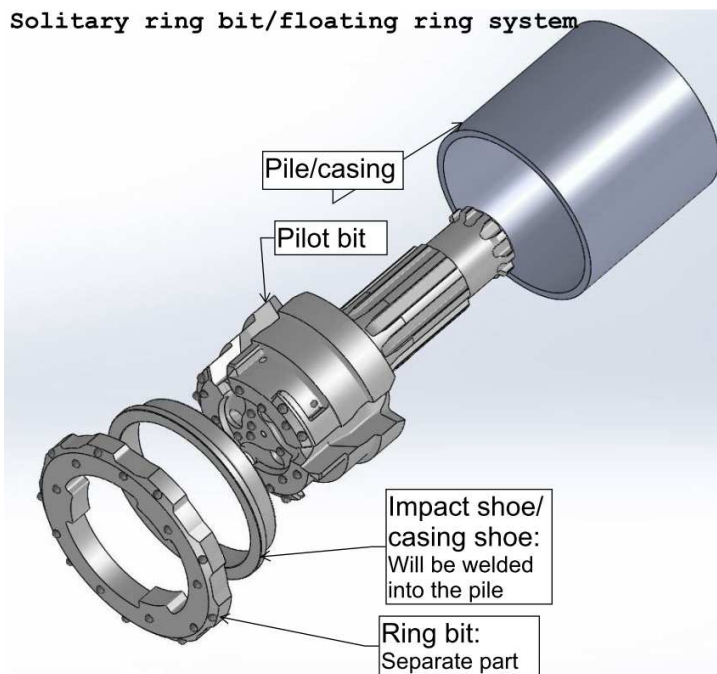


Figure 1.2: Solitary ring system, manufacturer Robit

The other drilling system that is frequently used is called the under-reaming drilling system. In that system, the pilot bit contains movable parts. When the pilot is plugged through the pile, the wings like those in figure 1.3 remain closed. When drilling begins, the wings open and are able to drill a hole large enough for the pile and interlocks. When the pile is at the target level, the wings can then be closed by rotating the bit in the reverse direction. The pilot can be withdrawn from the pile and be reused. There are also eccentric pilot bits with no movable parts [35]. Extractable under-reaming pilot bits do not provide horizontal or bending moment support to the pile toe. Vertical support is obviously provided by all drilling systems. Horizontal support comes from grouting the bedrock drilling hole or from spreading drill cuttings or soil into the drilling hole gap.

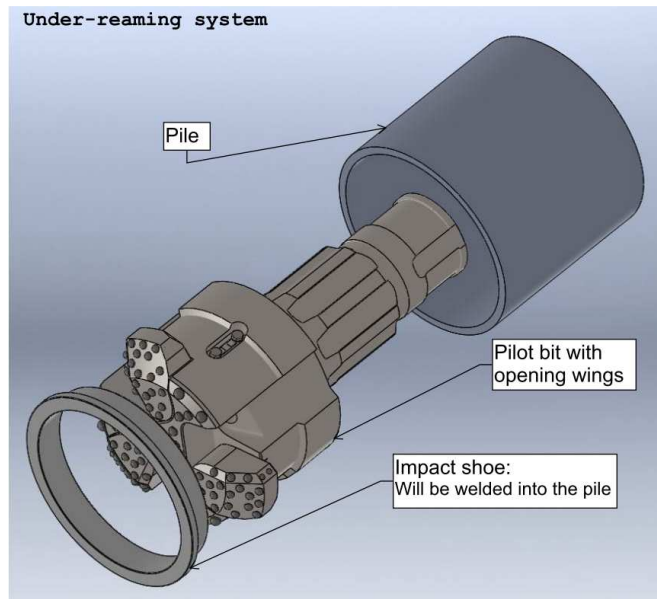


Figure 1.3: Under-reaming drilling system, manufacturer Robit

Ruukki has many pile dimensions and wall thickness and steel grade options to select the optimum pile for a specific construction project [1]. Pile dimensions from RD170 (168.3 mm) to RD1200 (1220.0 mm) can be used. The RD pile wall bending stiffness and capacity can therefore be very high. High bending stiffness and wall capacity may reduce the need for rock anchorage or other support systems.

As can be seen in figure 1.4, there is a theoretical gap between the ground and the pile wall as well as between the bedrock and the pile wall. The gap in the drilling hole is filled with drill cuttings or soil above the bedrock that has fallen down into the gap. The gap can also be grouted by injection section to improve watertightness and rotational stiffness. In this thesis, the need for and effects of grouting will be analyzed in more detail.

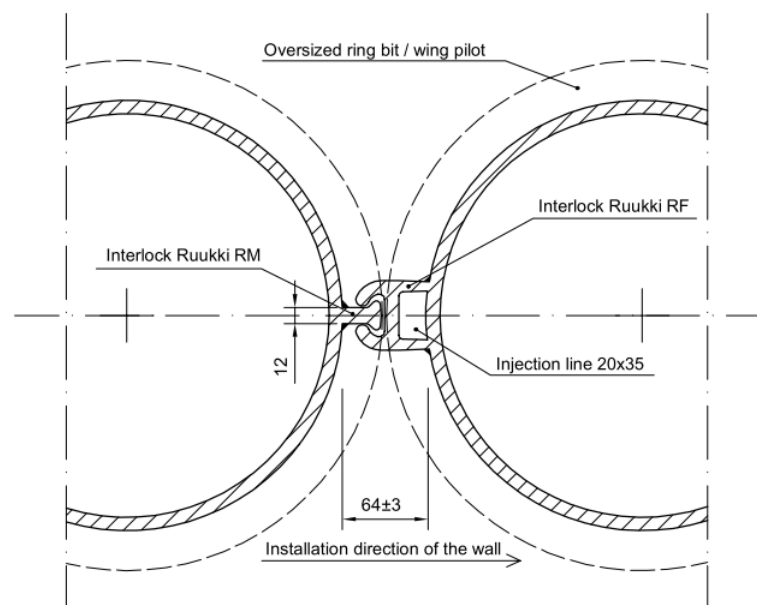


Figure 1.4: Cross-section of an RD pile wall with RM/RF interlocks [Ruukki 2013]

1.2 Supports of RD pile walls

RD pile walls can be supported using rock or ground anchors. Figure 1.5 shows a one-level anchor support used in Western metro line project in Finland. More support levels can be used depending on the depth of excavation. For example, in Kalasatama Centre project, one to three support levels were used. [2]



Figure 1.5: Western metro line project, retaining wall for entrance to new metro station. RD pile wall supported by one anchor level [2]

RD pile walls can be supported inside the excavation like a sheet pile wall. An RD pile wall in Trondheim supported from the inside is shown in figure 1.6. In the figure, the wall is supported inside the excavation at four levels with beams attached to the wall to spread the load from the compression members. Compression members are supported with another RD pile wall in the opposite direction. In that case, an additional support structure was built. One weak point when it comes to using supporting frames is that the structures require space inside the excavation and may restrict movement at the construction site. The purpose of the support structures is to take horizontal loads and thus decrease both wall displacement and stress on the wall.



Figure 1.6: RD610*10 RD pile wall supported from the inside. Picture was taken by Ruukki at a road tunnel construction site on the E6 in Trondheim, Norway on October 25, 2011.

One good application that uses the high load capacity of the pile wall is the use of an RD pile wall as a bearing basement wall as seen in figure 1.7. When the RD pile wall is part of the building, the wall can be supported at the basement and intermediate floor level. In this case, the RD pile wall is used as permanent structure. As built structures, the floors provide permanent support. Additional temporary supporting structures may still need to be used.

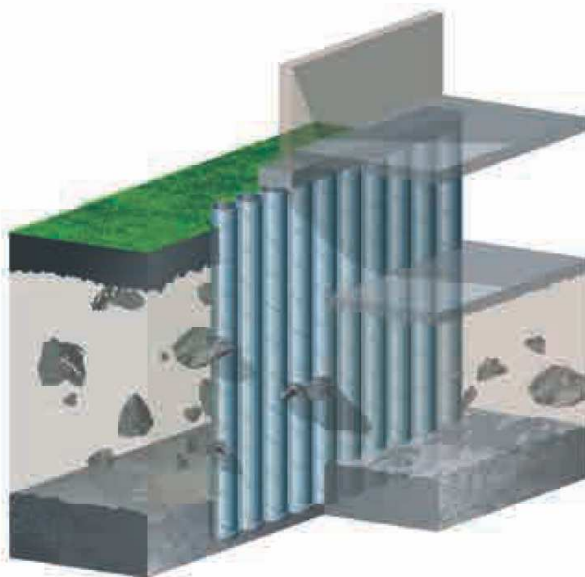


Figure 1.7: Building with a basement with an RD pile wall as a bearing basement wall [1]

1.3 RD pile wall supports in rock

When the passive ground pressure of the soil is not enough to support the wall, the base of the retaining walls must be supported horizontally [5]. The same options used to support sheet pile walls can also be used to support RD pile walls. A rock dowel as shown in figure 1.8 can be drilled into the bedrock to withstand horizontal loads. In the case of RD pile walls, rock dowels can be installed inside the piles. Similar to rock dowels, piles of lesser diameter drilled deeper than wall can be used to withstand horizontal loads.

Another option to ensure the horizontal capacity of the wall toe is to build the toe beam seen in figure 1.8. Toe beams are usually made from reinforced concrete [5]. The beam is bolted onto the bedrock using toe bolts. Another use of toe beams is to improve watertightness at the bottom of the pile wall. Using toe beams is the main method for sealing the toe of sheet pile walls.

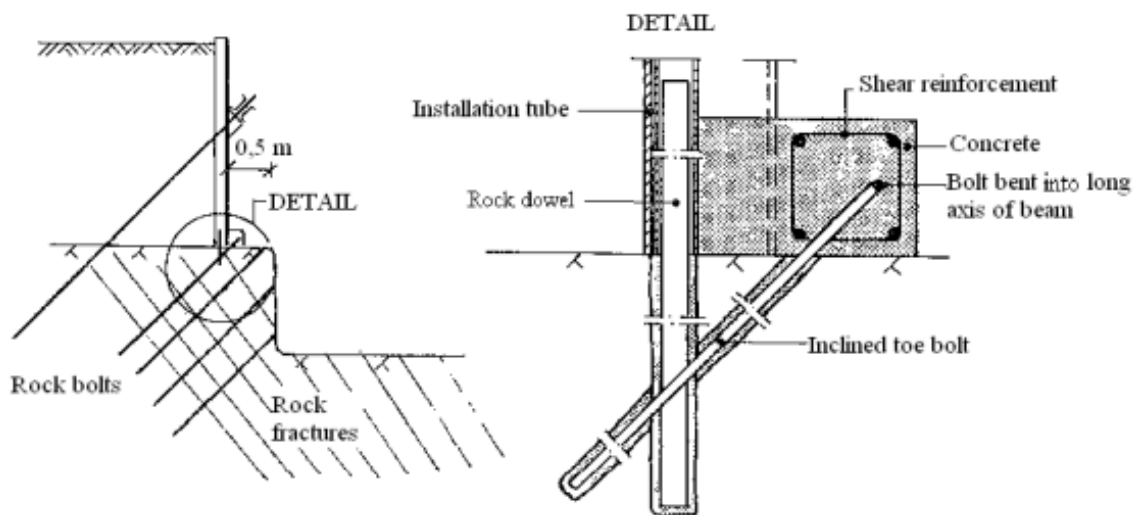


Figure 1.8: Detail of rock dowels, inclined toe bolt and toe beam [Niamh Collins 2011, Originally: Suomen Rakennusinsinöörien Liitto. 1989, Rakennuskaivanto-ohje RIL 181-1989]

For RD pile walls, there is an additional option to ensure horizontal support of the pile wall. Support is generated when the pile wall is drilled deep enough into the bedrock. An example of a pile wall drilled into the bedrock is shown in figure 1.9. Drilling the pile wall into the bedrock also provides rotational stiffness at the toe of the RD pile wall. When piles are drilled into the bedrock, watertightness also is improved. Both watertightness and rotational stiffness can be improved when the pile toe is grouted. Pile walls drilled into bedrock will be discussed in more detail later in this thesis.

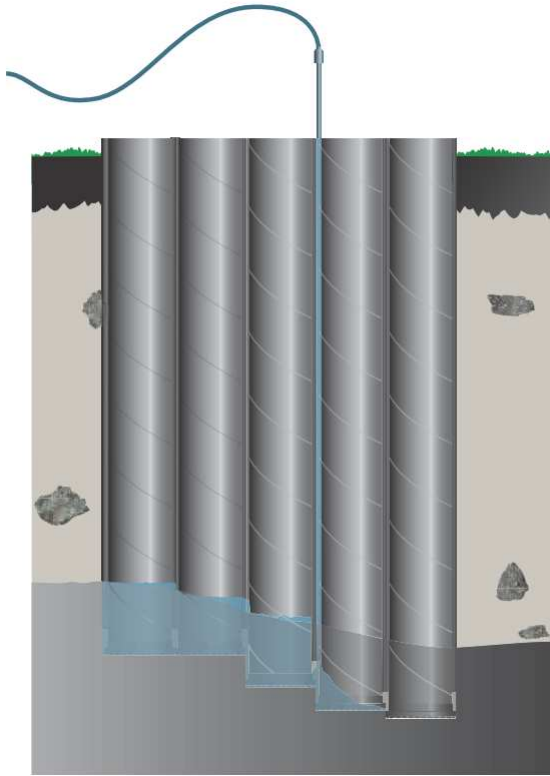


Figure 1.9: RD pile wall drilled into the bedrock. In the figure, the toe is grouted through the RF interlock. [1]

1.3.1 Grouting drilling holes

In many cases of oversized holes in the bedrock as seen in figure 1.4, grouting is a reasonable way to improve the watertightness of the pile wall. Another benefit of grouting the bedrock drilling hole is that the grouting material further stiffens the toe of the RD pile wall. Grouting makes rotational stiffness and watertightness more predictable.

In RD pile walls, the grouting is usually done through the RF injection line shown in figure 1.4 and figure 1.9 when using the latest RM/RF interlocks. This method is similar to the “single-step grouting through a load-bearing element” mentioned in EN 14199 and shown in figure 1.10 c). As in figure 1.10 d), the RF injection line can be perforated if the grouting needs to be spread more widely than the drilling hole bottom. Experience at the test site has shown that drilling holes in RF injection channels are not needed when grouting only bedrock. The test site will be discussed further in chapter 3. If soil stabilization or tightening is required, holes in the injection line can be useful. When using holes in the injection channel, it is important to keep in mind that that grouting tends to erupt where the drag is the lowest, and as such, the bedrock drilling hole will not be grouted as reliably as it would be without holes. Additional injection channels, steel pipe, etc. can be added if both the bedrock drilling hole and the soil behind the RD pile wall need to be grouted or if there is a need to improve grout spreading. Additional

injection lines can be added in the flank of piles ending at the bottom level or any level in pile wall. This principle is shown in figure 1.10.f).

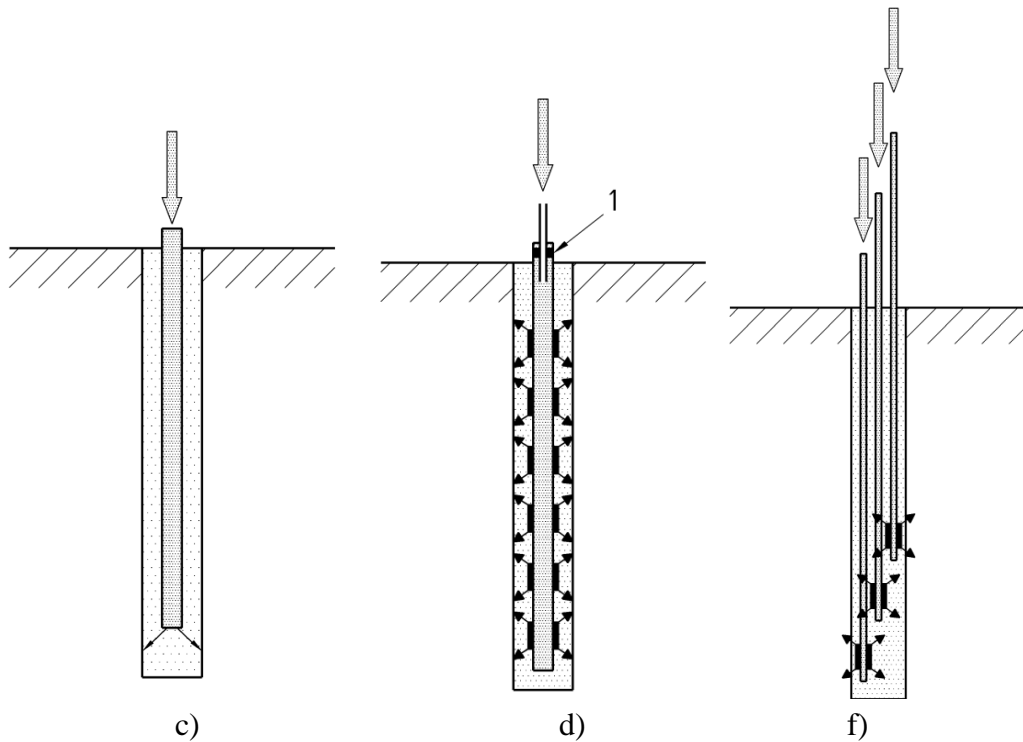


Figure 1.10 c): Single-step grouting through a load-bearing element, d) Single-step grouting through a tube-à-manchettes, f) Single-step grouting through several post-grouting tubes [EN-14199]

EN 14199 establishes the principles for drilling hole testing and pre-grouting. In a soil conditions where the bedrock is weathered or strongly fissured, testing and pre-grouting may be necessary for boreholes in bedrock. Pre-grouting the drilling hole can reduce uncontrolled loss of grout and ensure successful grouting. Water leakage can be measured to determine if pre-grouting is needed. If water leakage is no greater than 5 l/min in a 10-minute test at 0.1 MPa pressure, pre-grouting is not typically required. Cement-based grouting material is used in pre-grouting. Using sand/cement grout when the rock is partially filled or has open fissures can reduce grout consumption. More specific instructions can be found in EN14199. [EN 14199]

The instructions for pre-grouting can be applied with RD pile walls. When the rock is badly weathered, curtain grouting in the bedrock may be a good idea. Curtain grouting may spread into the gap between the pile and the bedrock and the block injection lines. In that case, grouting via injection line may not successfully grout the bedrock. The rotational stiffness and watertightness will be determined from the properties of the pre-grouting material. In many cases, the pre-grouting is done using higher water-to-cement ratio, meaning the material will not be as tight and strong.

2 THEORY

The Finnish Porapaalutusohje 2001 currently specifies that pile walls should be drilled into the bedrock to a depth of at least three times the pile diameter, albeit to a minimum of 0.5 m and a maximum of 1.5 m. Further, the end of the pile must be more than 3 m lower than the excavation level or designed blast-breaking level. Limits are placed on single piles that have sufficient bearing capacity at the point of pile, and sliding is prevented. In very demanding cases, the horizontal capacity of the drilled pile should be calculated using numerical calculation methods verified by measurements or loading tests in similar conditions. [6]

Moreover, the guidelines in the most recent excavation guide in Finland, “1-263-kaivanto-ohje-lausuntoversio-10.6” (currently circulating in a version dated 31 October 2013), indicate that pile walls should be drilled 0.5 m to 1.5 m into the bedrock to ensure reliable horizontal loads at the toe of pile wall. [4]

According to RIL 254-2011 Paalutusohje 2011, piles drilled and grouted in the bedrock can be regarded as rigid joints. [10] This definition is nevertheless a generalization and cannot be taken literally without limitations. RIL 254 discusses horizontally loaded piles only when the piles are supported by ground. In the case of RD pile walls, drilled rock shaft can only be supported horizontally, and the rate of rotational stiffness must therefore be estimated with greater precision.

Eurocode standards EN 1536, EN 1538 EN 12063 EN 14199, EN 1997 and EN 1993-5 do not specify the drilling depth for drilled piles or drilled pile walls. According to EN 1536, designers should specify minimum drilling depths for piles that penetrate the bedrock. When there is steep bedrock, piles should be excavated deeper or toe dowels should be used [EN 1536]. EN 14199 specifies that the drilling depth should be included in the project specifications.

2.1 Rigid, semi-rigid and nominally pinned joints

Joints in steel structures are discussed in EN 1993-1-8. There, joints are classified as rigid joints, semi-rigid joints and nominally pinned joints depending on strength or stiffness [11]. Figure 2.1 shows the classification of joints by rotational stiffness. When the rotational stiffness is in zone 1, the joint can be regarded as continuous in the model. In the model, the bending moment will all be transferred by the joint. In zone 3, the joint is classified as nominally pinned and will not transfer any bending moment in the model.

Joint classification for boundaries other than column base is shown in figure 3.1. The rotational stiffness requirement for rigid joints depends on whether the bracing system

reduces the horizontal displacement by at least 80%. In RD pile walls, horizontal supports such as rock anchors can be considered a bracing system. The higher the RD pile wall, the more likely anchors will reduce the horizontal displacement by more than 80%.

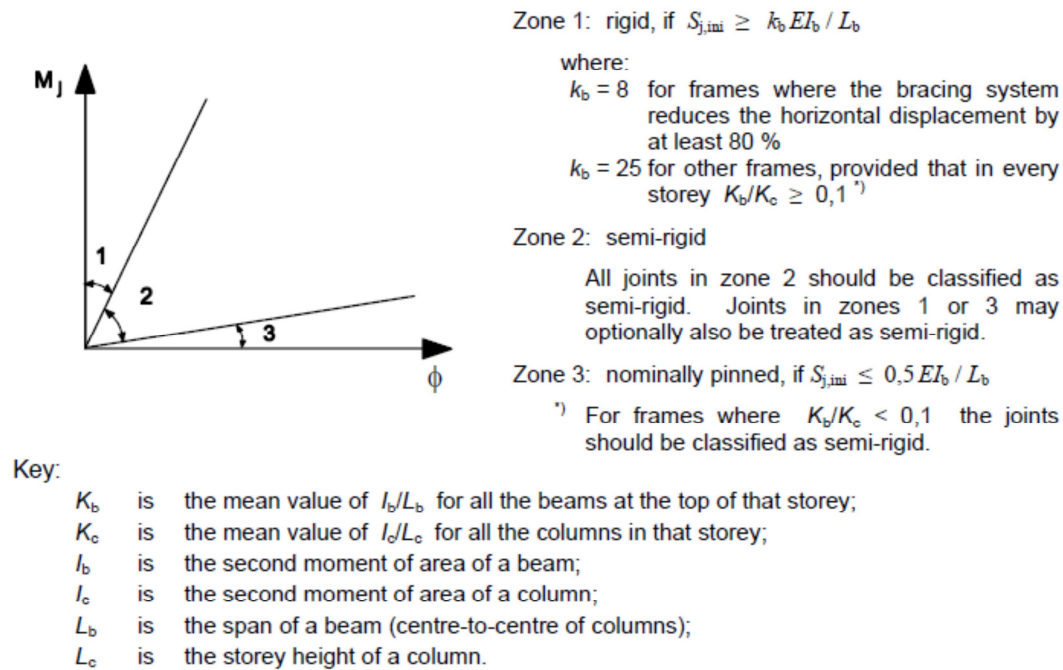


Figure 2.1: Classification of joints by stiffness [11]

When using the moment-rotation characteristic of a joint, linearized approximations can be used as long as the curve lies wholly below the design moment-rotation characteristic [EN 1993-1-8, 2005, paragraph 5.1.1]. In this thesis, linearized approximations were used for the calculations. In this thesis, S_j represents rotational stiffness instead of $S_{j,ini}$ which cannot be defined reliably (see section 4.1). S_j and $S_{j,ini}$ are shown in figure 2.2.

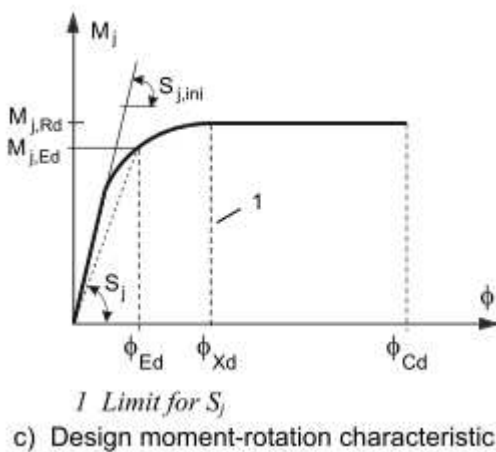


Figure 2.2: Design moment-rotation characteristic for a joint, EN 1993-1-8

According to EN 1993-1-8, all tested joints can be classified as full-strength joints, because in all tested piles, $M_{j,Rd}$ is greater than $M_{c,pt,Rd}$. The EN 1993-1-8 definition of full-strength joints is shown in figure 2.3. The piles were drilled relatively deeply, with the ratio of drilling depth to pile diameter at 4.6 or the ration of drilling depth to drilling hole diameter at 3.7.

5.2.3.3 Full-strength joints

- (1) The design resistance of a full strength joint should be not less than that of the connected members.
- (2) A joint may be classified as full-strength if it meets the criteria given in Figure 5.5.

a) Top of column



$M_{j,Rd}$

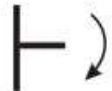
Either

$$M_{j,Rd} \geq M_{b,pt,Rd}$$

or

$$M_{j,Rd} \geq M_{c,pt,Rd}$$

b) Within column height



$M_{j,Rd}$

Either

$$M_{j,Rd} \geq M_{b,pt,Rd}$$

or

$$M_{j,Rd} \geq 2 M_{c,pt,Rd}$$

Key:

$M_{b,pt,Rd}$ is the design plastic moment resistance of a beam;

$M_{c,pt,Rd}$ is the design plastic moment resistance of a column.

Figure 5.5: Full-strength joints

Figure 2.3: EN 1993-1-8: Full-strength joints [11]

2.2 Effects of joint type on RD pile wall structure

The RD pile wall examples in this thesis were designed according to Eurocode standards. In Eurocode, steel structures are designed according to EN 1993-1-1 etc. EN 1997-1 is the standard for geotechnical design. There are three design approaches in EN 1997-1. Approach 2 was used for this thesis. This approach includes two design methods. Partial factors can be applied to actions (DA2) or to the effects of actions (DA2*) [26]. DA2* was used for the calculations in thesis, because GeoCalc uses displacement in its calculations. DA2 adds safety factors into the material values and loads, which would cause the program to incorrectly calculate the displacement. The supporting forces also turn out incorrect when the displacement is not correct. In DA2*, safety is added at the end of the calculations when verifying the conditions of the ultimate limit state. [25, 26]

In nominally pinned joints, there is no support moment at the bottom of the pile wall. Thus, the maximum bending moment is somewhere between the bottom and the top of the pile wall. In that case, dimensioning the wall is a simple task.

Another extreme case is when the joint is rigid. In this case, the support moment may sometimes be larger and be the most determinant point in the wall. The advantage of rigid joint is that the bending moment in the span decreases significantly. The other advantage is that there is a remarkable decrease in wall displacement [31].

Semi-rigid joints fall somewhere between nominally pinned and rigid joints. Semi-rigid joints decrease moment and displacement in the wall. At the same time, they also increase the support moment.

In Finland, Dimension Approach 2 is used when calculating supporting walls [26]. Other countries' national annexes are available, for example, at:

<http://eurocodes.fi/Muiden%20maiden%20kansalliset%20liitteet/Contentsmuidenmaidenliitteet.htm>

When dimensioning RD pile walls according to Eurocode 1997 Design Approach 2, there are two things to verify: limit state of rupture and excessive deformation [3, paragraph 2.4.7.3.4.3].

In cases where deformation is the main determinant, rigid joints are best if they do not increase the support moment too much. There is not one optimum joint type that is suitable in every case. There are calculation examples that clarify the optimal usage of joints later on in this thesis.

2.3 Watertightness

There are no set watertightness requirements for rock construction in Finland. The individual designer and Finnish building authorities decide the permissible water leakage limits in units like $l/(\text{min} \cdot 100 \text{ m})$ or $(\text{number of leaks})/\text{m}^2$ for each individual project [27]. Studies suggest that a “watertightness class” should be developed, but as of July 2013, there was no such class [27]. For example, “*Länsisatama Jätkäsaari maanalaiset tilat*” project in Helsinki, Finland, the rock facades grouting was required and the rooms below ground level required to be under-drained, gunite-lined and (water) tightened [12].

When watertightness is required, geometric tolerances may be stricter than in SFS-EN 1536 2011, paragraph 8.2 [32]. In SFS EN 1536, there are no specific watertightness requirements other than that watertightness should be defined in the execution specification. EN 14199 does not specify exact watertightness values. Neither EN 1993 4-1 nor EN 1993-4-2 contain watertightness requirements.

In terms of watertightness, RD pile walls fall somewhere between steel tanks (EN 1993-4-2) because of the piles, concrete structures (EN 1992-3) because of the grouting and solid rock (EN 1997). The only watertightness classification found was the tightness class for concrete structures (see Table 2.1). RD pile walls will generally have a tightness class of 1, because their function is to keep water and soil out of the excavation while still permitting a limited amount of leakage. In cases where lowering the groundwater level is not allowed, the tightness class could be 2 or 3.

Table 2.1: Classification of tightness (EN 1992-3, Table 7.105)

Tightness Class	Requirements for leakage
0	Some degree of leakage acceptable, or leakage of liquids irrelevant.
1	Leakage to be limited to a small amount. Some surface staining or damp patches acceptable.
2	Leakage to be minimal. Appearance not to be impaired by staining.
3	No leakage permitted

EN 1992-3 contains requirements for different tightness classes. In concrete, water-tightness is based on calculations and limiting crack width. EN 1992-3 also contains joint specifications, but there are no exact requirements concerning water leakage levels. The crack width control in the standard cannot be directly extrapolated to the bedrock drilling holes of RD pile walls, as part of the wall is subject to compression stress and part of the wall is subject to tensile stress. For example, at the bedrock level ground side, the grout material is subject to tensile stress, and thus there are probably cracks at the interface of the steel pile wall and the grouted material. At the same time, the ground side deeper in the drilling hole or at the top of rock level on the excavation side, the grout material is subject to compression stress, and there are likely no cracks.

The D'Arcy coefficient of permeability can be calculated from a water consumption test at the test site. The equation for calculating the D'Arcy coefficient of permeability is shown below as equation 2.1. In RD pile walls, the simplest way to calculate water leakage is to calculate water consumption using the D'Arcy coefficient of permeability formula. If the other variables are known, the volume of water (Q) can be determined using the formula. Then, water leakages in specific RD pile wall projects can be estimated using the coefficient of permeability defined from the leakage data and geometrical information at the test site. Grouted gap material values can be regarded as similar to concrete, taking into consideration the water-to-cement ratio, which plays the most significant role in the water permeability of concrete. The rise of water permeability when the proportion of water is increased is shown in figure 2.4. Figure 2.4 does not include units or magnitude. The source document [33] contains a similar graph in which the water permeability at a water-to-cement ratio of 0.55:1 is approximately $2 \text{ cm/sec} \cdot 10^{-10}$ equal to $20 \text{ m/sec} \cdot 10^{-12}$. In figure 2.4, the equivalent water permeability is approximately $15 \text{ m/sec} \cdot 10^{-12}$.

$$k = \frac{Q * L}{t * A * h}$$

k = D'Arcy coefficient of permeability $\left(\frac{m}{s}\right)$

Q = Volume of water in m^3

L = Length of the test sample in meters (to the nearest 0.001 m)

t = Elapsed time in seconds

h = Applied pressure head in meters of water

A = Area of the test sample in m^2

Equation 2.1: The D'Arcy coefficient of permeability equation [13]

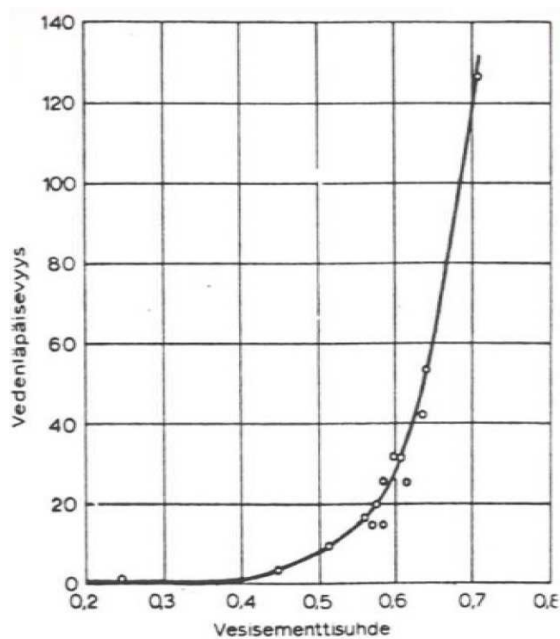


Figure 2.4: Water-to-cement ratio. The vertical axis shows the water permeability (in $m/sec * 10^{-12}$), and the horizontal axis is the water-to-cement ratio. Source: Iso-Mustajärvi, P, 2008, RTEK-3140 Betonitekniikka course material, Tampere University of Technology. Figure originally from A.M.Neville, *Properties of concrete*, fourth edition, 1996

2.3.1 Solution for watertight retaining walls

EN 12060 contains very general specifications for sealing retaining walls. For example, if there is clay between the bedrock and the retaining wall, the interval must be sealed according to the design requirements. In projects with strict watertightness requirements, the watertightness of the interlocks should be tested if there is no practical experience in building watertight walls. [14]

The toes of retaining walls are not automatically watertight [4]. Water tends to flow below the retaining wall if the wall is not embedded down to the bedrock [4]. In such cases, the interface between the bedrock and the retaining wall must be sealed, because the bedrock is not flat, and steel sheet is only partially in contact with the bedrock [4]. The sealing can usually be done after excavation [4]. Sealing done after excavation

should begin by welding steel plates onto the retaining wall and filling any remaining holes, for instance, with polyurethane [4]. Any minor leakages that remain can be sealed with the toe beam [4]. An under-drainage system is required to successfully build the toe beam casting [4]. After the concrete hardens, the under drainage system should be grouted shut [4]. Jet grouting the soil above the bedrock until it overlaps at least one meter of wall is another potential technique for sealing the toe of a retaining wall [4]. Jet grouting is done from the ground level before excavation [4]. The bedrock must also be grouted if the rock is fractured [4]. The leakage can be limited sufficiently if the wall is embedded deep enough into the impermeable soil layer.

With RD pile walls, drilling the pile wall into the bedrock and grouting the drilling hole in the bedrock is a widely used technique for sealing RD pile wall toe. The theoretical gap due to oversized drilling bit is filled with drill cuttings or soil. Filling the gap with soil, however, is unreliable, and it is hard to predict leakage levels. In the test site results, there is one outcome in specific soil conditions. The water penetration test results are shown in appendix 1, and the water penetration calculations can be found in appendix 12.

In the Western metro line Koivusaari station project in Finland, RD pile wall interlocks were sealed using a bitumen-based sealant [15]. The interface between the bedrock and the pile wall was sealed by extending the pile at least 0.5 meters into the bedrock and grouting the drilling hole into the rock. Steel pipes were welded to every other WOM-WOF (figure 2.5) interlocks as depicted in figure 2.6. The grouting was done through steel pipes [15]. Developed later, the RM/RF interlock, which includes an injection channel, has replaced the WOM-WOF interlock. The RM/RF interlock is shown in figure 1.1.



Figure 2.5: Discarded WOM-WOF interlock [15]



Figure 2.6: Grouting pipe welded next to the WOM-WOF interlock [15]

3 FIELD SURVEY: RD PILE WALL AND ROCK INTERFACE

There are two main objectives in this field survey. The first objective is to investigate the watertightness of the RD pile wall. The second is to study the rotational stiffness of the RD pile wall. In order to research the watertightness and rotational stiffness, the material in the bedrock drilling hole must be studied as well. The sealing of the interlocks was not included in the tests, because the sealing of interlocks is more guided and easier to test. The test site can be seen in figure 3.8.

3.1 Preparation

Field investigations were conducted before deciding on the test site. Figure 3.1 shows percussion drilling to determine the depth of the bedrock at the test site. The results of percussion drilling are given in appendix 16. Tests were conducted at maximum 5-meter intervals. RIL 263-2013 generally recommends 10-meter intervals and 5-meter intervals when the bedrock is very irregular [4]. The groundwater level was measured using a standpipe.



Figure 3.1: Percussion drilling at the test site in Masku, Finland

The RD pile wall was built from eight piles. Two ungrouted piles were tested. The second grouting type was piles with normal RF interlock grouting. The third type was grouted piles with shorter RF interlocks that ended above the rock level. Short interlocks had drilled holes on one side of the RF interlock at 1-meter intervals, one pile with 10 mm holes and another with 16mm holes. A fourth type was grouted via interlocks with the attached specially designed injection ring made from a 20x40x3 steel section and welded next to the RF interlock as seen in figure 3.2. To allow the grout to move into injection ring, the section had to make a larger hole toward the RF interlock. The upper surface of the steel section was drilled with 10 mm holes. The purpose of the injection ring was to spread the grouting more perfectly in the bedrock drilling hole.



Figure 3.2: Grouting piece

In terms of single piles, there were five types of piles. The RF interlock injection channel in the single piles was substituted with a 20x40x3 steel profile called an injection channel in this thesis. The first type was a pile with only an injection channel. The second featured an injection channel and an attached injection ring. The third type was a pile with internal grouting. The fourth and fifth pile types were not grouted. Internally grouted piles and piles with no grout had no injection channel. Instead types 3 and 4 had RM (male) interlocks in 3 directions at the length of bedrock drilling to ensure that the piles remained in the drilling hole when drilling and when measuring water leakage. Piles with three one-meter interlocks are shown in figure 3.3.



Figure 3.3: *Piles with three one-meter welded male interlocks (RM)*

The piles in the horizontal load test were supposed to be similar to the piles with injection channels. Because of changes in the test plans after the piles had already been manufactured, the excess male interlocks had to be removed. The interlocks were removed using an angle grinder and a gas cutting machine. The piles could not be damaged on account of the load testing; a minor part of interlock, up to approximately 6 to 7 mm, was therefore left in place. This can be seen in figure 3.4. That extra bit of steel had no effect in the pile testing, as the bending stiffness of the pile did not increase significantly. Also, 7 mm is rather small compared to the width of the gap (27 mm in theory) in the bedrock drilling hole and the displacement in the bedrock during the load test. In other words, the remaining interlock pieces had no contact with the bedrock.



Figure 3.4: *Interlocks removed from single 220/10 piles used in the horizontal load test*

As shown in figure 3.5, the RD pile wall was drilled through the various layers of soil into the bedrock. Both the solitary ring system and the under-reaming drilling system, manufactured by Robit, were used in the test site. The single 220/10 piles were all

drilled using the solitary ring system. In the RD pile wall, both systems were used. The drilling of each pile was documented. Drilling depth progress was documented in terms of time. Comments concerning flushing, such as when drill cuttings started to flow from the inside of the pile, were documented. The drilled material, including the bedrock level, was observed from the drill cuttings and the propagation speed.



Figure 3.5: Test site in Masku, Finland. Piles drilled through soil into the bedrock

The grouting work was also documented. This included the water-to-cement ratio of the various mixing batches, the grouting pressures, grout consumption and comments for each pile in the terms of time. Grout consumption was measured according to the level of grout in the grouting device. The level of grout was then converted to liters. The grout container and mixer device is shown in figure 3.6. A centimeter-to-liter conversion table is given in appendix 15. The grouting was made from water and cement CEM II/A-LL 42.5 R; its compression strength ranged from 42.5 to 62.5 MPa after 28 days in 40mm x40mm x160 mm prism test specimens [16,17]. A water-to-cement ratio of 0.55:1 was used in the test. This ratio is the maximum allowed for grouting according to EN 14199. Lower water-to-concrete ratios tend to be too thick for grouting. The thick grout mixtures tended to cause blockages in the injection adaptor seen in figure 3.7 and the injection line. Other causes of blocks when grouting may have been the high temperature (+25 °C) and fast reactive cement used. There were not blocking issues when grouting from inside the pile using the manchette shown in figure 3.12. The internal grouting was done at the bottom of the pile while the pile was full of water. The grout was poured to the bottom of the pile via long hose. Then the manchette closed the top of

pile. The grout was intended to go only into the gap between the pile and the bedrock. The piles were filled with water because of the water penetration test, and piles for the horizontal load test were not allowed to be full of grout. In some piles, after grouting at rather high pressure (approximately 5-10 bar), the grout probably went partially back into the pile when the pressure went down in the pile. That was the main reason why the internally grouted piles were not as well grouted as those done by RF or RF and injection ring. To get realistic results in the water penetration test, hardened grout had to be drilled away in some of the piles.



Figure 3.6: Grout container and mixer device. The upper container had a mixer. The grout was poured into the lower container where it was pressurized into a hose



Figure 3.7: The left side shows the grouting adapter used to channel the grout from the hose to the RF injection channel. The right side shows the grout's tendency to block the injection adapter and injection channel. The injection adapter channel was made from a metal block drilled with three smaller holes, which caused also blockages during grouting.

The soil in the test site was mostly backfilled soil. The excavation and drilled piles are shown in figure 3.8. The upper layer of soil was approximately one meter of coarse gravel backfill. The second layer was a mixture of boulder, mold, organic matter and clay. At different places above the bedrock, there was sand, gravel or clay. The bedrock was mainly undamaged solid rock and was 3.3 to 4.4 meters below ground level [appendix 16]. There were two types of bedrock at the test site. One was gray-colored rock and another was a reddish rock. There was no big difference in strength between the two bedrock types. Figure 3.5 shows the drilling of the RD pile wall.



Figure 3.8: Test site in Masku, Finland. Piles drilled through soil into the bedrock. The piles were grouted and excavated to the bedrock.

Test site construction and in-situ measurements took approximately three weeks. The schedule followed is given in table 3.1. After the test site was measured, material tests were carried out. Testing of the soil, grouting material and rock were done at the Tampere University of Technology. The horizontal load test was organized and executed by Tampere University of Technology as well.

Table 3.1: *Timetable of RD pile wall test site and measurements***Timetable of RD pile test site and measurements**

	From	To
Drilling of piles	23 Jul 2013	25 Jul 2013
Grouting	26 Jul 2013	29 Jul 2013
Excavation	30 Jul 2013	31 Jul 2013
Rock samples	2 Aug 2013	5 Aug 2013
Concrete samples	26 Jul 2013	5 Aug 2013
Water penetration test	5 Aug 2013	8 Aug 2013
Horizontal load test	9 Aug 2013	9 Aug 2013
Concrete and rock material test	9 Sept 2013	9 Sept 2013
Soil material test	7 Oct 2013	20 Dec 2013

3.2 Testing arrangement**3.2.1 Watertightness**

The focus was on the watertightness of the interface between the rock and the pile wall. Water leaks at the bottom of the pile wall are much harder to observe visually than leaks from the interlocks. That is why Ruukki wanted more careful research on this topic.

An in-situ water penetration test was chosen. The test is performed from inside of the pile to the ground, not from one side of the wall to the other. The reason for making the test simpler was that there were four different scenarios to measure. If a test of the entire wall were chosen, four different walls of considerable length would need to be built. This would obviously entail considerable expense with limited return on that investment. By testing single piles, it was possible to compare the watertightness of piles without grouting, piles with grouting using interlocks, piles with grouting using interlocks and an injection ring and piles grouted from inside the pile. The water penetration of the rock was also tested to determine the proportion of water penetration from pile to rock. Hose leakage was also tested. This allowed for calculating of the water consumption from the pile to the gap between the pile and the rock. The results for the single piles were different from the results for the wall. Single piles can leak in a 360-degree radius, and the distance that water has to travel is approximately half of what it would be in the case of a wall, where water has to penetrate from side to another. The area and the length of water path can be calculated to determine the quantity of the leakage. The single pile case does not take into account the path of water through the interlock.

The water penetration tests were carried out after excavation to ensure more realistic results. The drag of water in the soil did not affect into water consumption in the test. In the test, five pressure steps were used. First, piles were pressurized into a constant water pressure of 0.035 MPa, and leakages were measured over a five-minute period. Then the hose was closed and pressure held constant. Next, the drop in pressure over five minute was measured at 0 minutes, 1 minute, 3 minutes and 5 minutes. The hose was then pres-

surized again, this time to 0.175 MPa, and the leakages were measured. Then hose was closed again, and the drop in pressure was measured at 0 minutes, 1 minute, 3 minutes and 5 minutes. The same procedure was repeated at 0.7 MPa 0.35 MPa and 0.525 MPa. There were two piles of each type except for the bedrock hole test and the hose test, where there was only one test. The instruments used in water penetration test are shown in figures 3.9 to 3.13.



Figure 3.9: Pressure instrument, scale 1 bar = 0.1 MPa, accuracy approximately 0.25 bar = 0.025 MPa.



Figure 3.10: Water consumption instrument, scale 0.1 liter, accuracy approximately 0.025 liter



Figure 3.11: Gas-powered, pressure-controlled water pump



Figure 3.12: Hydraulic-powered manchette used in water penetration test and internal grouting of the piles



Figure 3.13: Mechanically powered manchette for measuring the watertightness of the bedrock hole

3.2.1.1 Results

In the test, leakages through the hose were the major source of uncertainty. The other uncertainty was the limited number of tests. The leakage through the hose was much higher than leakage through the gap in a case of grouted gap. Some grouted gap tests showed that the hose did let less through than the grouted gap, which cannot be the real situation. It is not possible to draw any conclusions about the differences between the various grouting methods except that the grouting from inside the pile was not executed perfectly due to the grouting method used, as mentioned in paragraph 3.1. Another source of uncertainty was that the water pumping system and the instrument were not accurate enough in pressures lower than 0.5 bar = 0.05MPa. As a result, filling the hose at 0.35 bar was difficult and inaccurate. In other words, the starting point of the leakage was not accurate. It was not possible to fill the hose at 0 MPa, because the accuracy of the visual pressure instrument is approximately 0.25 MPa. Also, the grout flowed into the drilling of some ungrouted piles. Water consumption may therefore be underestimated at some point.

The best comparable results were for total water leakage from pressure steps 2 to 5. For those, the inaccuracy of the instruments and in filling the hose did not affect the results. Because of the uncertainty caused by leakage and the difference in the structures, test results should be examined critically. For grouted piles in particular, the average watertightness was very close to zero and below bedrock leakage. Instead, it was observed that the leakage was much greater in gaps filled with soil or drill cuttings than in the grouted bedrock drilling hole. Appendix 1 includes a table with the exact numbers.

In appendix 12, the water penetration is calculated using different material permeability values. It can be found that the water penetration of the drill cuttings measured in ungrouted piles was comparable to that of dense sand. Dense sand yielded the same 3.3 liter water consumption as the drill cuttings tested on the site, when permeability of the sand was $3 \cdot 10^{-6}$ m/s. The permeability of sand can range from $1 \cdot 10^{-2}$ m/s to $1 \cdot 10^{-6}$ m/s [19]. Using the received value for drill cuttings, the leakage calculation showed that for a RD pile wall 220/10 under 5 m of water pressure, piles drilled 0.5 m into the bedrock would exhibit a leakage of 2.0 liters/m/hour. The assumption was that drill cuttings or soil would become as dense as in the test. By comparison, the leakage of the grouted gap assumed to be as permeable as concrete would be $1.0 \cdot 10^{-6}$ liter/m/hour, which is almost zero. When compared to the calculate leakage of 0.08 liters/m/hour through an interlock, drillings cuttings will leak 25 times more than interlocks. On the other hand, leakage through grouted gaps is insignificant compared to leakage through interlocks.

Leakage through the grout may be slightly higher if the grouting is cracked or loose from the pile wall due to a high level of stress. It may be reasonable to use a shorter water path length in calculations when the grout is exposed to high stress. On the other hand, in cases where the piles are concreted from inside, the water path is much longer below the pile than assumed in the calculation. The water has to penetrate through concrete. When the drilling hole is not grouted and the piles are concreted, a major portion of the water leakages will go through the “hole” below the interlock. Interlocks are usually around 100 mm shorter than the piles at each end of the pile. In such cases, the leakage is much smaller than calculated. Overall, when the grout is continuous and mostly free of cracks, the wall seems to be very watertight. In projects where there is strict water-tightness requirement, grouting the gap or toe beam is a good option.

For comparison, the water leakage from interlocks in the same structure would be 0.1 L/(m*hour) as per appendix 12. Here, the calculation was done as in annex E of SFS EN 12063. The calculations there are for sheet pile interlocks, but they can obviously be applied to RD pile wall interlocks. RD pile wall interlocks are at least as watertight as sheet pile interlocks due to less damage in the interlocks on account of a more gentle installation method. In EN 12063, the discharge equation for one interlock was deduced into the form in equation 3.1 [14]. The total discharge can be calculated from equation 3.2.

$$Q_1 = \rho * H(0.5 * h)$$

ρ = the inverse joint resistance in meters per second (m/s) [14]

H and h are shown in figure 3.14.

Equation 3.1: Discharge of one interlock

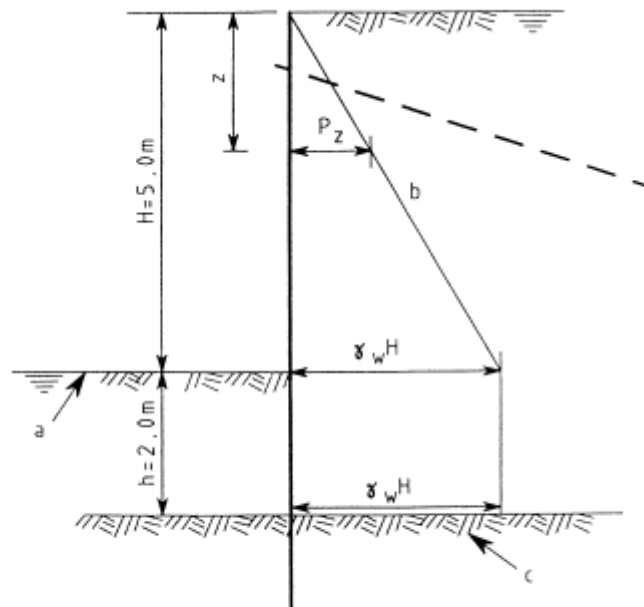
$$Q = nQ_1 = \frac{L}{b} Q_1$$

n = "the total number of interlocks in the sheet pile wall for the excavation" [14]

L = "the length of the perimeter of the excavation in meter " [14]

b = "system width of the sheetpiles in meter." [14]

Equation 3.2: Total discharge into the excavation [14]



Legend

a excavation level b resulting water pressure c impermeable layer

Figure 3.14: Example of an excavation in which the water level has been lowered about 5 m [14]

3.2.2 Drill cuttings, grouting and bedrock samples

Different test samples were collected at the Masku test site. Samples of drill cuttings, hardened grout, material mixtures from grouted drilling holes and bedrock were taken.

Figure 3.15 shows grouted drilling hole samples collected by diamond drilling. The site was excavated until the bedrock and piles were cut shorter to access with the drill. Pure grout samples were made from a plugged piece of rubber hose. Grout made for grouting the piles was filled into the piece of hose. Adiabatic curing was neglected for some of the samples, and the samples did not even remain solid when removing the

hose around the grout sample. The samples with decent adiabatic curing were solid and about as strong as the drilled grout samples. For the adiabatic curing, the samples were placed in the shade, and both ends of the hose were closed.



Figure 3.15: Grouting samples were collected from the drilling hole next to pile using a diamond drill. Masku test site

The bedrock samples were drilled next to the RD pile wall as shown in figure 3.16. The rock samples represented rock conditions after pile wall had been drilled. The samples were also drilled right next to the pile wall to allow for visual examination and for collection of break-off pieces of the grout from deeper in the drilling hole. After the samples were drilled out of the bedrock, smaller rock samples were made at the laboratory. The technique for doing so is shown in figure 3.16.



Figure 3.16: *Bedrock sample drilled next to the RD pile wall at the Masku test site. Figures show the process of drilling for bedrock sample. Both stages were drilled with a diamond drill.*

It was possible to collect soil samples and samples of drill cuttings, hardened drill cuttings and some grouting without drilling. Figure 3.17 shows the samples taken from the Masku test site with the exception of the rock samples. Obviously, the soil and non-hardened drill cutting samples were disturbed in the sampling process by taking them out their natural place and form.



Figure 3.17: Masku test site grouting, drill cuttings and soil samples going to Tampere university of Technology laboratory

Cylindrical test samples were made in length-to-diameter ratio of 1. Hardened drill cutting and hardened soil samples were cubes. The hardened drill cutting samples included cement. The soil samples potentially included cement. As such, all specimens are equal to EN 1992-2 $f_{ck,cube}$ values (SFS EN 12504-1). The rock values are characteristic mean values. The drilling soil sample was treated as concrete, because it is more like concrete than solid rock. The $f_{ck,cube}:f_{ck}$ ratio is approximately 1.25:1 based on the calculated average from SFS EN 1992-1 in table 3.1. The bedrock samples and some of the grout test samples were approximately cylindrical with a diameter of 52 mm and a height of 52 mm. These cylindrical samples are shown in figures 3.19, 3.21, 3.22 and 3.23. The d52*h52 grout samples were collected from inside the grouted pile, which was grouted from inside the pile. Smaller grout samples collected from the bedrock drilling hole could be only up to 27 mm, so d25*h25 cylinders were chosen. Drill cutting samples were taken after the horizontal load test, some after the piles were removed from drilling holes and another by hammering the piece of material while piles were in drilling hole. The pieces of drill cuttings were made into cubes as large as possible. Cubes were approximately 10 mm to 19 mm on each side. The test specimen dimensions are shown in appendix 17. There were difficulties making the smaller samples (cubes and cylinders) exactly symmetrical. The asymmetry of the samples probably made them easier to break due to stress on the specimen that was not even at every point of the sample, meaning samples may reach the breaking point on one side while the other side is not fully stressed. It was possible to break the samples a little too early in the test, and the ultimate strength was lower than the actual strength.

The samples were tested at the structural laboratory of the Tampere University of Technology. The tests were executed using a powered control system. The hydraulic testing machines used for the testing are shown in figures 3.19 and 3.20. Force and displacement were measured at 0.5-second intervals.



Figure 3.18: *Specimens of grout and hardened drill cuttings with cement ready for the compression test*

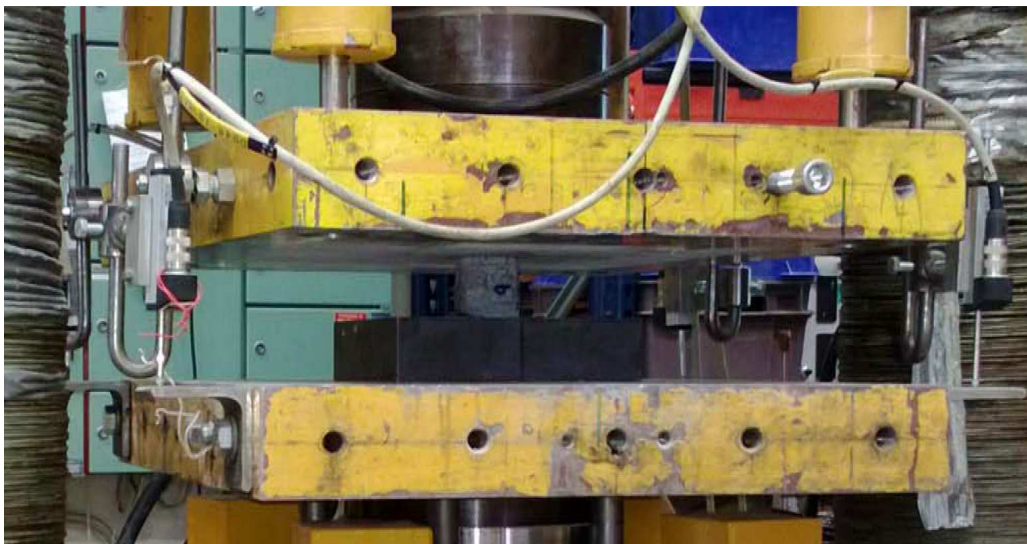


Figure 3.19: *The hydraulic testing machine used to test larger samples ($d=h=52$ mm)*



Figure 3.20: *Servo-controlled hydraulic actuator used to test smaller samples. In the picture, the hydraulic testing machine is inclined quite noticeably, because the specimen was not a perfectly symmetrical cylinder.*



Figure 3.21: *Grout samples after the compression test*



Figure 3.22: *Bedrock samples after the compression test. The sample fractured only on half before the hydraulic testing machine was stopped. The force dropped dramatically after the fracture.*



Figure 3.23: *Bedrock samples after a sudden brittle failure in the compression test*

The elastic modulus of the rock samples was determined from the compression test results using the load range starting from the first measured load point up to 33% of the ultimate load. In some cases, the first measured point was more than 5% of the ultimate force. Ranges of 2% to 33% are used in the EN 14580 standard to determine elastic modulus. The lower range was chosen to be higher than 0%, because the samples were

not perfectly smooth. It took some force before the whole area of the sample was fully stressed. This inaccuracy is emphasized, because in the tests, only one load step was used instead of the three load steps mentioned in EN 14580. Near failure load the elastic modulus was not constant. By defining the elastic modulus of the grout material and the hardened soil, the same stress range was used as when testing the rock samples.

3.2.2.1 Results

The elastic modulus of the rock was near the values found in the literature, but the ultimate strength was much lower than the literature values (see table 3.2). The lower ultimate strength can be explained by fragmentation of the rock when the piles were drilled.

Table 3.2: *Ultimate compression strength (Puristuslujuus) and elastic modulus (Kimmokerroin) values for different rock types (Kivilajit). Cited 14 Nov 2013. Available at: https://noppa.aalto.fi/noppa/kurssi/rak-50.2122/luennot/Rak-50_2122_luentoaineisto_3.pdf*

Kivilaji	Puristuslujuus	Kimmomoduli
	MN/m ²	MN/m ²
Graniitti	200...350	70 000
Gneissi	140...300	60 000
Kiilleliuska	130...210	110 000
Kvartsiitti	200...300	80 000
Leptiitti	270...420	70 000
Amfiboliitti	180...420	110 000
Kalkkikivi	60...150	50 000
Pegmatiitti	160...310	60 000
Rapakivi	120...180	60 000
Pegmatiitti	260...350	100 000

The elastic modulus was calculated at the range of 2% to 33% from the ultimate strength if the test result was constant. Otherwise, it was calculated at the stress level of 50% from the ultimate strength. The area selected was where the elastic modulus was at its maximum value. The maximum value is more representational than the 2% to 33% area in many cases, because test specimens were not perfectly flat. In the 2% 33% area, the elastic modulus values were significantly lower than the maximum E values in some cases. The maximum elastic modulus value in this test is nevertheless lower than the real value, because in the case of concrete, the elastic modulus of rock and soil tends to decrease as stress increases. The maximum values were determined using figures to find the approximate maximum value area and selecting a wide enough range within that area. Therefore, the E values are not exact maximum values. Selecting the exact maximum elastic modulus values at the exact measurement point was not appropriate, because the E value was much higher at that exact point than the overall “trend.” This inaccuracy was probably caused by the test instruments.

“Clay (concrete)” material test samples were collected from the sides of piles that were grouted from inside the piles. The material was surprisingly solid even it did rise from the gap in the horizontal load test. The material seen in figure 3.24 was clay, which may include a little cement even though the sample taken from the gap was pure clay [appendix 20]. Partly grouted material or at least slightly harder material seemed to be about 0.5 m, and the remaining 0.5 m was pure clay. In the material test, the sample probably went hard when the sample had time to harden and the water content decreased. According to the Ansys FEM calculation, the displacement was equal to the displacement measured at the test site when the material elastic modulus value in the gap had an elastic modulus 1000 times lower than the weakest “clay (+concrete?)” value shown in table 3.3. The elastic modulus value used in Ansys model was approximately 10 MPa, which is equivalent to that of to dry crust clay [18].

Table 3.3: Conclusions of material test on 9 September 2013 (in MPa)

Material test										
			fck,cube	fck,cube	fck,cube	fck	fctm	E_mean	E	E
Material		samples	Average	Max	Min	Average	Average	Average	Max	Min
Concrete		7	33.5	38.9	25.3	26.8	2.7	24306	35450	10550
clay(+concrete?)		3	14.1	22.5	6.2	11.2	1.5	21067	26900	10150
cuttings or clay+grout		4	23.6	36.2	15.5	18.9	2.1	22040	33245	12365
cuttings or sand+grout		4	30.7	45.7	19.0	24.5	2.5	23600	36750	10350
cuttings or clay+grout*		2	35.1	36.6	33.5	28.1	2.8	37800	55300	20300
			\bar{R}	R	R					
Rock 1		5	60.0	80.0	48.8	-	-	93334	150370	44320
Rock 3		5	67.7	100.2	29.2	-	-	115592	186800	45710
Rock 5		5	46.6	71.8	22.6	-	-	49840	89520	21550
Average			58.1					86255		
* grouting was flowed from the different pile										
			fck,cube		fck	fctm				E
			Min		Min	Min				Min
weakest clay(+concrete?) sample					6.2	5.0	0.9	-	-	10150



Figure 3.24: Horizontal load test. Grouted pile where gap was filled with clay. The material may have small amounts of cement mixed in, even though sample taken from the gap did not contain cement.

The elastic modulus of the rock was usually constant; however, in chart 3.1 the elastic modulus was constant from 0 kN to around 25 kN as well as from 25 kN to around 175 kN. In chart 3.2, the modulus is constant except at the low-force level where the roughness of the sample has an impact.

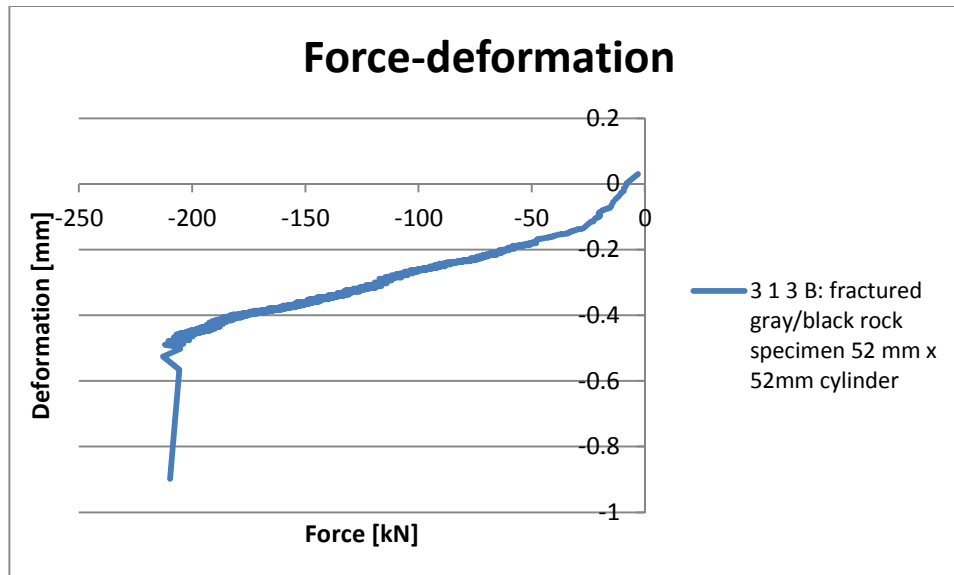


Chart 3.1: Rock testing. The elastic modulus was partially constant.

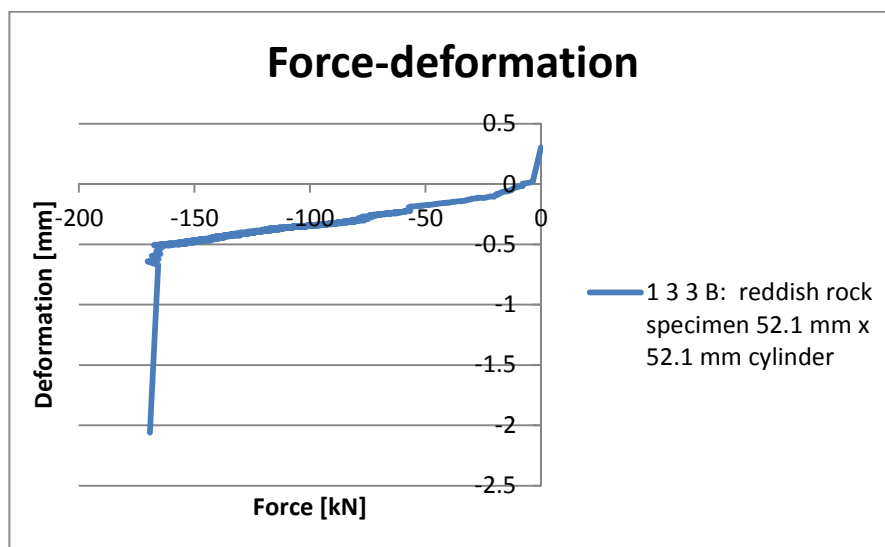


Chart 3.2: Rock testing. The elastic modulus was constant except very at low force.

The soil samples shown in figures 3.25 to 3.27 were analyzed at the Earth and Foundation Structures laboratory; the laboratory report can be found in appendix 20. Sample 1 was taken next to the ungrouted pile and drilled using the solitary ring system. Above the gap, the soil was clay. Samples 2 and 3 were collected next to pile drilled with an under-reaming drilling bit. The soil above samples 2 and 3 was sand/moraine. The grain-size distributions of the samples are quite similar to gravel with fine soil. Accord-

ing to the Nuutti Vuorimies project manager in TTY, the weight of tested soil samples in appendix 20 were too small in all samples but sample 1. The grain size analysis is therefore inaccurate for the other samples. The minimum weight for samples of a maximum grain size of 32 mm is about 10 kg and for grain size 4mm about 0.2 kg [appendix 23]. In sample 3, the rock size is slightly bigger, and there is little fine soil, likely because that pile was flushed for an additional half hour. The other side of pile with extra flushing was empty. This is not typical when drilling RD pilot walls. Such extra flushing may occur if the pilot gets stuck in the pile and extra flushing is used to try to free it.



Figure 3.25: Soil samples 1-3. The samples were taken in the gap of the 440/12.5 pile wall next to the ungrouted piles.

Charts 3.3 and 3.4 and the soil samples in figures 3.25 and 3.26 reveal the difference in the drill cuttings between the drilling systems used at the test site. It appeared that the largest rock pieces (10-25 mm) tended to remain in the gap and that the smaller rocks flew away from inside the pile. The finest mass both flew away and also filled the rest of the gap. The gap appeared to be filled with drilled rock pieces that were almost the same size as the extra size of the pilot. The rest of the volume of the gap was filled with fine soil or drill cuttings. There was no evident difference between the under-reaming drilling bit and the solitary ring system except that the under-reaming drilling bit yielded slightly larger rock pieces than the solitary ring bit. This can be explained by the bigger openings in the pilot system (see figures 3.28 and 3.29). In the solitary drilling system, the ring bit has only little openings in the outer face of the ring bit. The wing pilot in contrast has larger holes from the bottom to the gap when wings are opened. In wing pilot system, the rocks can theoretically be as large as the gap.



Figure 3.26: Soil samples 9-10 were collected at the top of ground level after each pile had drilled into the bedrock. The drill cutting samples flew out of the pile while drilling the bedrock.



Figure 3.27: Sample 10. These sample rocks seem to be split out of bedrock on account of their very sharp edges. The samples were taken in the gap of the 440/12.5 pile wall next to the ungrouted piles.



Figure 3.28: Robit solitary ring bit attached to a pile. 440/12.5 pile RD pile wall at the Masku test site



Figure 3.29: The under-reaming drilling bit manufactured by Robit. At the left, the wings are closed, and at the right, the wings are partly open.

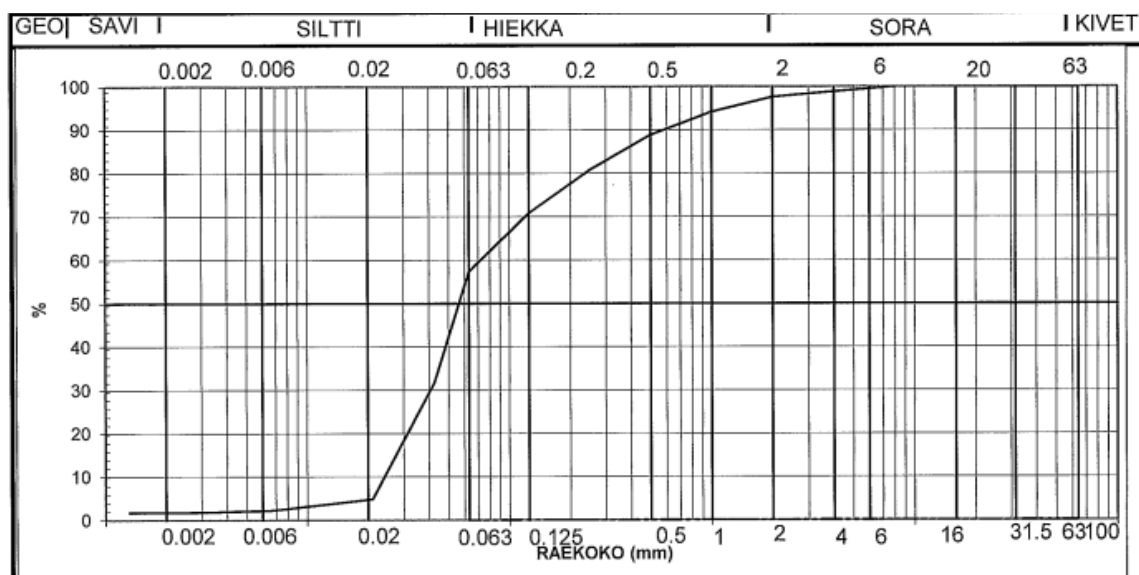


Chart 3.3: Granulation of soil sample 1. Sampled next to the pile drilled with the ring bit

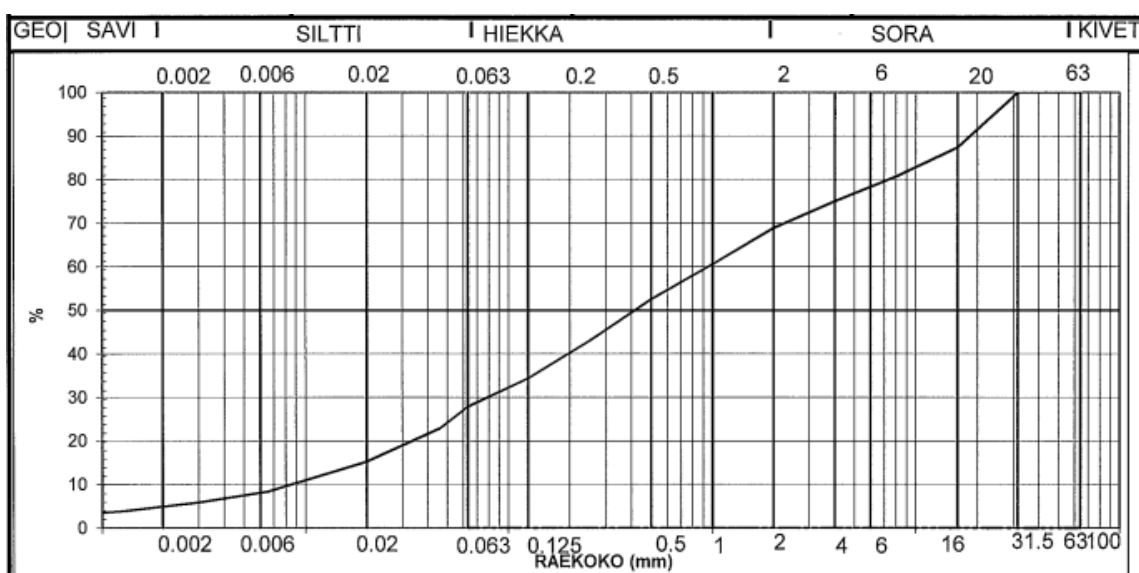


Chart 3.4: Granulation of soil sample 2. Sampled next to the pile drilled with the under-reaming drilling bit

Table 3.4: “Basic soils are soils with uniform grading (i.e., they consist of particles of only one size range) as specified in Table 1 8” (SFS-EN ISO 14688-1)

Table 1 — Particle size fractions

Soil fractions	Sub-fractions	Symbols	Particle sizes mm
Very coarse soil	Large boulder	LBo	> 630
	Boulder	Bo	> 200 to 630
	Cobble	Co	> 63 to 200
Coarse soil	Gravel	Gr	> 2,0 to 63
	Coarse gravel	CGr	> 20 to 63
	Medium gravel	MGr	> 6,3 to 20
	Fine gravel	FGr	> 2,0 to 6,3
	Sand	Sa	> 0,063 to 2,0
	Coarse sand	CSa	> 0,63 to 2,0
	Medium sand	MSa	> 0,2 to 0,63
	Fine sand	FSa	> 0,063 to 0,2
Fine soil	Silt	Si	> 0,002 to 0,063
	Coarse silt	CSi	> 0,02 to 0,063
	Medium silt	MSi	> 0,006 3 to 0,02
	Fine silt	FSi	> 0,002 to 0,006 3
	Clay	Cl	≤ 0,002

Equation 3.3 is used to calculate sand and gravel water permeability values. This equation was used even though sample 1 is defined as having silt as a principal fraction according to EN 14688 (see table 3.4). Sample 2 can be defined as medium sand. Appendix 12 shows the calculated water permeability of samples. As one can see, the water permeability of sample 2 ($3.5 \cdot 10^{-6}$ m/s) is very close to the tight packed drill cuttings tested in the water penetration test. Sample 1 is much more permeable at $2.7 \cdot 10^{-5}$. It must be stressed that the water permeability values are very rough estimates. The drill cuttings/clay materials, in contrast, were much more watertight (see table 3.5) than the estimates for samples 1 and 2. The drill cutting/ clay sample had no rocks and was in tight packed form, which explains the huge difference to other samples. Also, at least some of the drill cutting samples included cement. The drill cuttings/clay sample indicates the watertightness of the bedrock drilling hole to be nearly as watertight as a grouted drilling hole. The variation in the watertightness is hugely dependent on the material in the gap. Loose soil allows considerable water to pass. Grouted drilling holes lead to very tight rock-pile wall contacts.

$$k = C \left[\frac{100 * d_{10} * n}{1 - n} \right]^2$$

Equation 3.3: *C is the Hazen constant (1/(m*s)), which has an average value of 2. d10 is the grain size at which there is 10% of the whole material smaller. Finally, n is porosity. [19]*

Table 3.5: Water permeability of the drill cutting/clay sample 23 from the pile grouted internally with no success (see section 3.1). The water permeability was calculated with the coefficient of consolidation defined in the Casagrande method after an odometer test. The left column shows the effective normal stress of the sample [kPa]. The right column shows the water permeability [m/s]. [Appendices 20 and 22]

Vedenläpäisevyyskerroin	
Casagrande	
porras	k, m/s
100	2,1E-09
200	5,8E-10
400	2,4E-10
800	1,5E-10
1600	6,7E-11

When considering the rotational stiffness aspect of sample 1, for example, the desired material value is the tangent modulus seen in equation 3.4. The tangent modulus is non-linear modulus value for soil. In the FEM calculation used in this thesis, the soil was determined to be a concrete with non-linear elastic modulus values equal to the tangent modulus values calculated from equation 3.4. From appendix 20, the graininess of sample 1 can be seen in chart 3.3. and angle of internal friction of 38° was defined. The sample best corresponds to a medium dense moraine when comparing to “sillan geotekniset suunnitteluperusteet” appendix 4 table 2 soil material values [28]. The values $m=800$ and $\beta=0.5$ were selected. The tangent modulus and compression strain values were calculated in table 3.6 for the FEM calculations. Equation 3.5 was used to calculate the compression strain value.

$$M = m * \sigma_a * \left(\frac{\sigma}{\sigma_a}\right)^{1-\beta}$$

Equation 3.4: Equation for tangent modulus [28]

$$\varepsilon = \int_{\sigma_0}^{\sigma} \frac{d\sigma}{M} = \frac{1}{m * \beta} * \left[\left(\frac{\sigma}{\sigma_a}\right)^\beta - \left(\frac{\sigma_0}{\sigma_a}\right)^\beta \right], \text{ in which } \beta \neq 0$$

Equation 3.5: Equation for soil compressive strain. [28]

Table 3.6: Tangent modulus and compression strain values for soil sample 1 taken from the drilling hole of the RD 400/12.5 pile drilled by the ring bit system. Measurements were taken up to 1600 kPa, and the remainder was estimated [appendix 20].

Sample 1 Tangent modulus values

σ' [kPa]	β	m	σ_a [kPa]	M [MPa]	σ_0 [kPa]	ϵ
1	0.5	800	100	8.0	0	0.0003
10	0.5	800	100	25.3	0	0.0008
100	0.5	800	100	80.0	0	0.0025
500	0.5	800	100	178.9	0	0.0056
1000	0.5	800	100	253.0	0	0.0079
5000	0.5	800	100	565.7	0	0.0177
10000	0.5	800	100	800.0	0	0.0250
30000	0.5	800	100	1385.6	0	0.0433
100000	0.5	800	100	2529.8	0	0.0791
200000	0.5	800	100	3577.7	0	0.1118

3.2.3 Horizontal load test for single piles

Tests were done on site to improve the reliability of the theoretical rotational stiffness calculation. Single 220/10 piles of approximately two meters in length were horizontally loaded, and the displacement and strain were measured at a few levels along the pile.

In order to prepare piles for the horizontal test, a thick steel plate was welded to the top of the piles to prevent deformation at the loading point of the pile and therefore improved the accuracy of the measured displacement. Also, the spacing piece in contact with pile was the same shape as the surface of the pile to even out the force on the pile. A drawbar 25 mm in diameter was drilled through the pile tested to generate force on the pile. The drawbar was bolted onto the RD pile wall which was made from much strong 440/12.5 piles. A hydraulic jack was attached behind the spacing piece to exert force on the drawbar. Next to the jack, there was an instrument to measure the exact force on the drawbar. The last part was the base plate and bolt. The test equipment are shown in figure 3.30.



Figure 3.30: *Horizontal load test. UngROUTED pile tested at the moment*

To measure the exact displacement of the pile, a separate supporting wall frame was built behind the pile tested. The displacement instruments were attached the frame, so that the force of the tested pile could not affect the results measured. The displacement of the piles was measured at three levels: at the force level of the pile, at the middle of the pile and near bedrock level. To be on the safe side, four strain sensors were glued onto the pile to determine the stress on the pile during the test. Strain sensors were attached at two levels: near rock level and halfway up on both the compression and tension side of the pile. The strain and displacement instruments are shown in figure 3.31.



Figure 3.31: *The displacement instruments were installed near the bedrock level on the glued blade to keep the sensor from slipping along the surface of the pile. Below the displacement instrument is a strain sensor glued to the tension side of the pile.*

To prevent different piles from behaving differently in the load test, the piles with a grouting channel were set 90 degrees from the direction of the load. Grouting profile at the neutral axis of the pile has only a small impact on the bending stiffness of the pile in comparison to a profile added at the compression or tension side of the pile. Also, a profile 90 degrees from the load direction will not have contact to bedrock before the pile itself. In theory piles with a grouting channel had some additional rotational stiffness in measured piles compared to the piles with no channel, because the piles with a grouting profile were able to spread the stress wider into the grout or drill cuttings than piles with no grouting channel. On the other hand, real RD pile walls have interlocks on both sides of the pile, meaning that the rotational stiffness will be even higher than in the test case.

3.2.3.1 Results

In the field survey, the displacement was measured at three levels. The first level was a little higher than the bedrock level. The second sensor was located approximately one meter from the bedrock, and the third was at almost the same level as the horizontal load. The displacement at the exact height of the load was calculated when there was a difference in height. The method of least squares was used to calculate the shape of the pile. The deflection curve should be $y = a \cdot x^2 + b \cdot x$. The $a \cdot x^2$ comes from the deflection of the pile. As one can see from figure 3.32, the deflection is dependent on the moment and shank of the force at the base of the cantilever. When the moment is the same, the

deflection is function of X to the power of 2. On the other hand, when calculating an example where the deflection is calculated at the end of the cantilever and at the mid-way point ($x=L/2$), the deflection is $FL^3/(3EI)$ at the end and $FL^3/(12*EI)$ at the midway point. In other words, the difference is four times larger at the end of the cantilever. Assuming that deflection at the end of cantilever is 1, the deflection at the half must be $(L/2)^2 = 1/4$.

Attempts were made to add constant c to the equation, but the formula did not fit any case other than that of the pile with very loose material in the gap. At the point where $x=0$ (bedrock level), the formula gave negative y values, which is not the case. At the bedrock level, the pile seemed to deflect more than be displaced into the grouting material. From figure 3.33, it is evident that there was approximately a 2 mm gap between the grouting material and the steel pile at the bedrock level. The displacement measurements indicate that the displacement was even lower (1.6 mm) 17 centimeters above the bedrock level. The method of least squares indicates that the displacement at the bedrock level is very close to 0 mm, meaning that the entire “gap” was due to deflection of the pile. After releasing the horizontal load, the gap disappeared almost completely.

The gap of test pile 22 was filled mainly with clay. There may also have been partly grouted clay as the internal grouting of the pile was unsuccessful. In this case, the formula $y=a*x^2+b*x+c$ worked best, because the pile exhibited approximately 15 mm displacement at the bedrock level. Appendix 9 shows the estimated deflection of the pile, and chart 3.6 shows the force-displacement correlation in pile 22 during the load test. The force was relieved, because the jack displacement had a limited functional range. The drawbar had to be tightened and the jack released at some point.

Taulukko 1 Ulokkeen ja kaksitukisen palkin eräiden kuormitustapausten kimmoviivoja.

$$\langle x-a \rangle^n = (x-a)^n, \text{ jos } x-a \geq 0, \text{ mutta } \langle x-a \rangle^n = 0, \text{ jos } x-a < 0$$

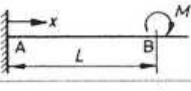
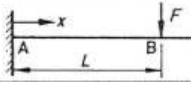
1		$v = \frac{M}{2EI} [x^2 - \langle x-L \rangle^2]$	$v_B = \frac{ML^2}{2EI} \quad v'_B = \frac{ML}{EI}$
2		$v = \frac{F}{6EI} [3Lx^2 - x^3 + \langle x-L \rangle^3]$	$v_B = \frac{FL^3}{3EI} \quad v'_B = \frac{FL^2}{2EI}$

Figure 3.32: [Outinen.H, Salmi.T, 2004 Lujuusopin perusteet]



Figure 3.33: Grouted pile (number 20) at the maximum horizontal load. The horizontal displacement and deformation of the pile at the bedrock level was approximately 2 mm on the tensile stress side of the pile.

Chart 3.5 reveals the difference between the pile deformation and additional displacement from the rotational angle caused by bedrock-pile joint stiffness. The difference in the case of the grouted pile in chart 3.5 was much smaller than in the pile with clay in the drilling hole in chart 3.6. As one can see, there is no clear elastic slope, and it is thus not possible to determine $S_{j,ini}$. In addition, measurements at very low horizontal load were not accurate. For example, in chart 3.5, the slope $S_{j,ini}$ in the very beginning is considerably lower than S_j . Instead of using $S_{j,ini}$, it is more realistic to use S_j to specify the joint as rigid or nominally pinned. S_j is linearized from a load scope of 0 kN to the maximum elastic load for the pile.

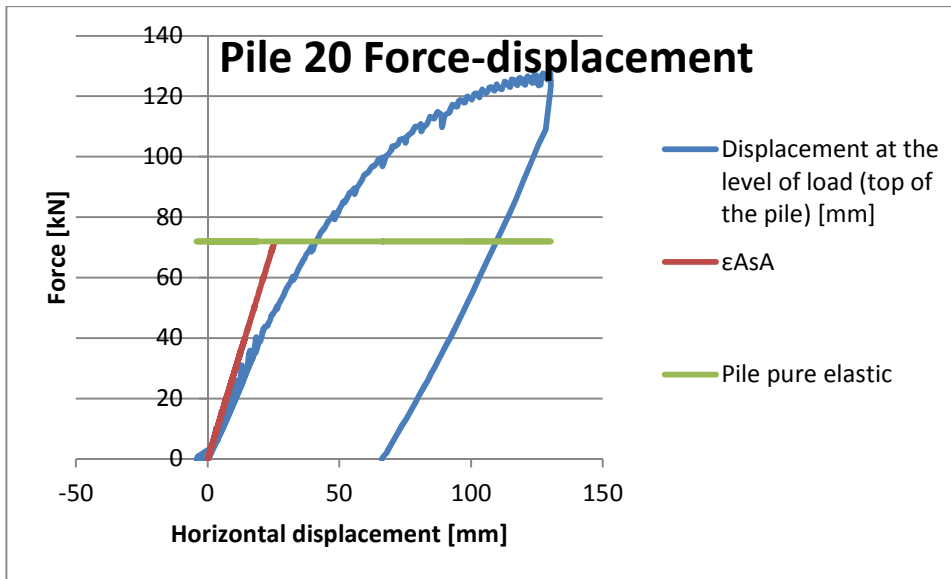


Chart 3.5: Drilled into bedrock, gap grouted. The pile was loaded horizontally until it went into the plastic range.

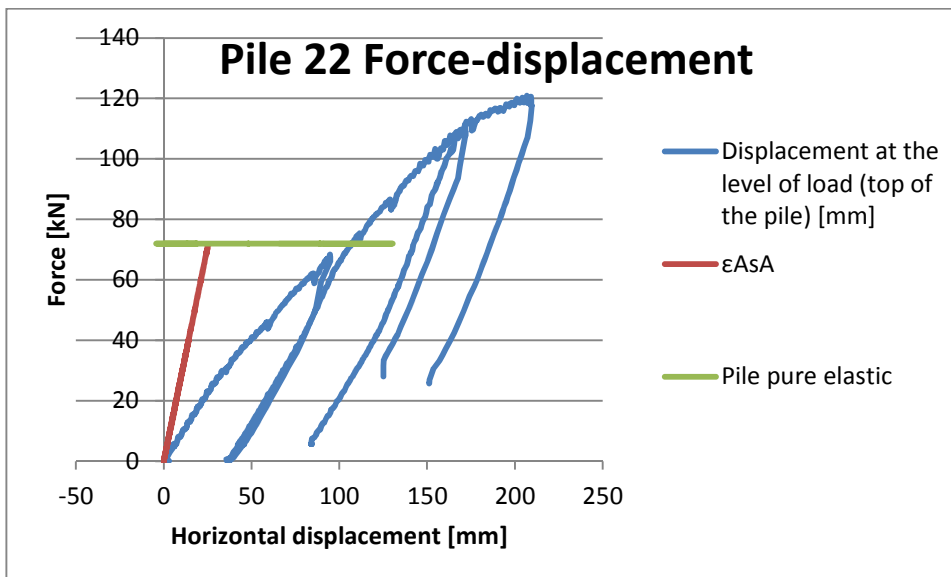


Chart 3.6: Pile drilled into bedrock, gap filled with clay and potentially a small amount of cement. The pile was loaded horizontally until it went into the plastic range.

The displacement at the top of pile is reduced by elastic deflection of the pile. The rest of the displacement is due to the flexibility of the joint. The theoretical joint in the upper level of the bedrock consists of pile deflection in the bedrock pile and the tilt of the pile and horizontal displacement. The horizontal displacement in the drill hole is ignored, because it is relatively small compared to the displacement at the top of pile caused by tilt and deflection.

As one can see from the calculation (appendix 2), the 220/10 piles tested were not categorized as having a rigid joint or nominally pinned joint according to EN 1993 (see

figure 2.1). Therefore, the joints had to be treated as semi-rigid joints. Two out of four piles were included in the calculation as they represented the stiffest and least stiff piles.

In the test site case, grouted pile number 10 was 67.5% out of the rigid joint in cases where bracing is assumed taking over 80% of horizontal displacement and 21.6% in cases where bracing took less than 80%. On the other hand, the joint is was 1085.3% stiffer than a nominally pinned joint. When the gap was basically filled with clay, the joint was almost nominally pinned joint. It was only 1.82 times stiffer than the limit for a nominally pinned joint.

It should be noted that pile length affects EN 1993 rigidity classifications as seen in figure 2.1. In other words, if grouted pile number 10 were about five times longer, the requirement for a rigid joint would be met. That means the load (result of soil pressure) would be at a level of approximately 10 meters, and the RD pile wall would be 30 meters high. In that case, the joint would also be more rigid, because the shearing force would be much smaller with the same bending moment. The stress at the top of the bedrock and the gap would decrease in that case.

Chart 3.7 shows the dependency of rotational stiffness on load level according to the results of the site test. The stiffness rises at first, perhaps because the gap between the pile and the bedrock may not be 100% full of grout and the grout itself have air/water pores inside due to the relatively high water-to-cement ratio (0.55:1). At some point, the stiffness decreases as the load increases. The decreasing stiffness may be explained by tendency of the elastic modulus of concrete and grout to decrease as the stress level rise. The overall linearized approximation of the rotational stiffness is a rather good approximation for grouted piles.

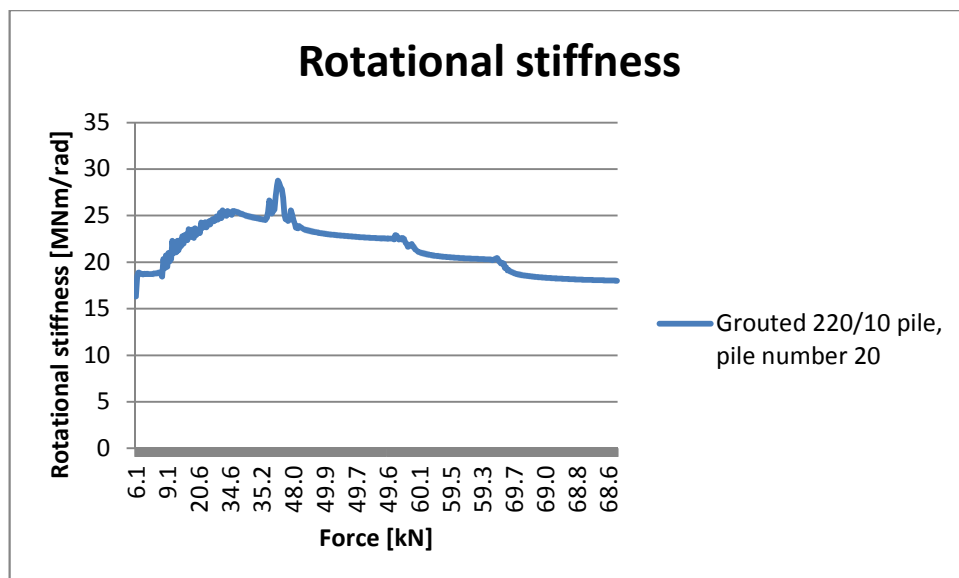


Chart 3.7: Pile drilled into bedrock, gap grouted. The pile was loaded horizontally until it went into the plastic range. The chart shows the rotational stiffness calculated from the load test data..

The behavior of the pile with clay in the gap (see chart 3.8) was very similar to the grouted pile in chart 3.7, except that the grouted pile was much stiffer. Also, the joint of the pile with no grouting exhibited plastic deformation in pile's elastic load range. The reason that the rotational stiffness starts at zero in chart 3.9 and slowly increases over the second loading of the pile with clay in the gap is that clay was moved out of gap as in figure 3.24.

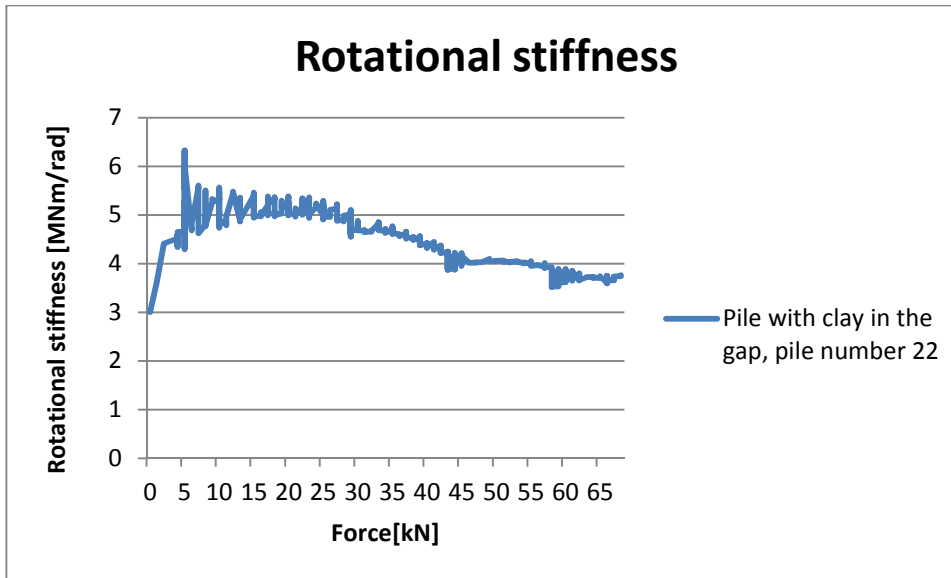


Chart 3.8: Rotational stiffness of the pile with clay in the drilling hole gap. The chart shows the rotational stiffness calculated from the load test data.

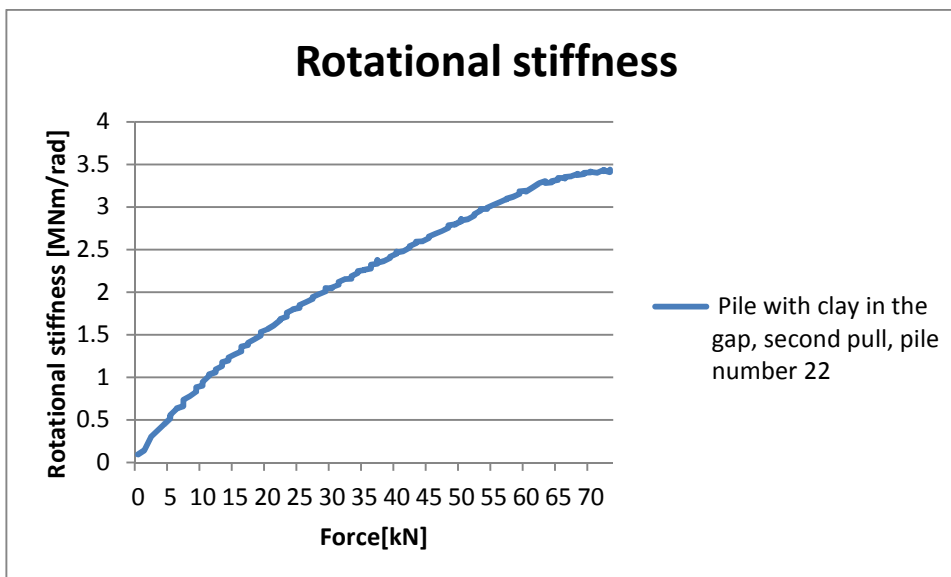


Chart 3.9: Rotational stiffness of the pile with clay in the drilling hole gap. Second loading of the pile after the first load was released due to the limited functional range of the jack. The chart shows the rotational stiffness calculated from the load test data.

The grouted pile exhibited more elastic behavior (see chart 3.10). The pile only exhibited some plastic deformation at a load of 89.7 kN, when the elastic limit of the pile was 73.1. Some of the deformation was due to plastic deflection of the pile.

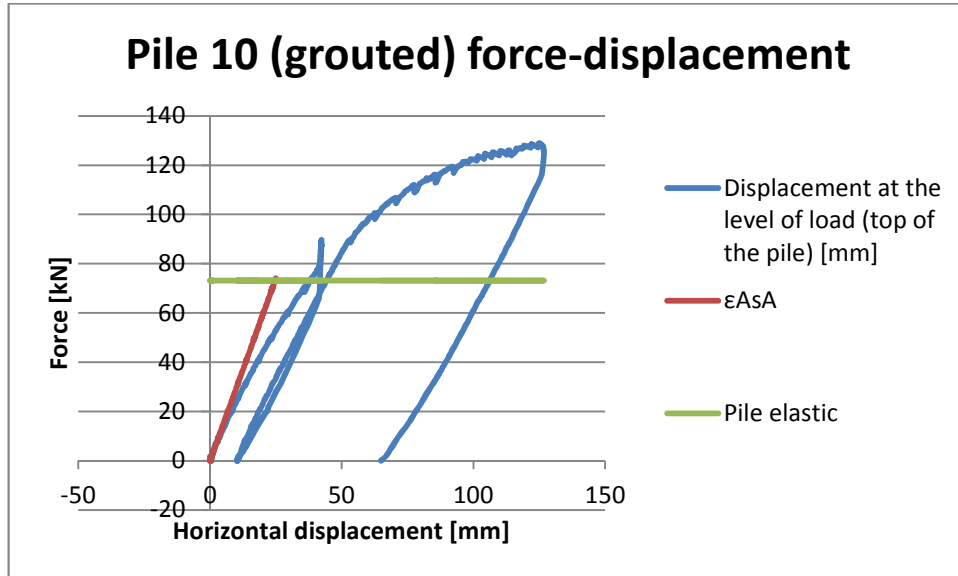


Chart 3.10: Pile drilled into bedrock, gap grouted. The pile was loaded horizontally until it went into the plastic range. The discontinuity in the displacement around 40 mm was due to the fact that the measuring device was not able to move like pile at that point.

3.3 Other remarkable findings from the Masku test site

A water-to-cement ratio of 0.55:1 was mostly used for grouting at the test site. Thicker mixtures tended to cause blockages in the hose, grouting adapter and RF injection channel. When lower amounts of water are used, plasticizing ingredients should be included. Unnecessary restrictions in the system, e.g., in the hoses, the injection adapter, etc., should be avoided to prevent blockages. For example, the injection adapter channel should be smooth unlike the one used at the test site (see figure 3.7).

The grouting mass will not flow through the injection channel if the channel is filled with soil or other materials. The upper end of injection channel should be closed to prevent material from dropping from the upper side when piles next to the injection are drilled. If the grouting mass does not flow through the injection channel, the channel should be cleared. The most effective way to clear the channel is to insert a thin pipe into the bottom of the channel and inject pressurized water or air into the channel. Pressurized air, for instance, can be used to check whether the channel is blocked. If grout hardens in the injection channel, it will be virtually impossible to use later on.

The background of an RD pile wall can be grouted by making from 10 mm to 16 mm holes in the side of the RF interlock at, for instance, 500 mm intervals and blocking the holes with plastic plugs to keep soil from pouring into the channel. If plastic plugs are not used, the channel should be cleared before grouting. When using background grouting, extra injection channels should be used to ensure injection into the bedrock drilling

holes if the drilling holes require grouting. The background grouting will probably spread primarily into the area where the oversized drilling bit loosened the soil as seen in figure 3.34. Background grouting supposed to make a “concrete” wall behind the RD pile wall with thickness equal to the excess drilling. At the test site, some parts of the wall background were grouted.

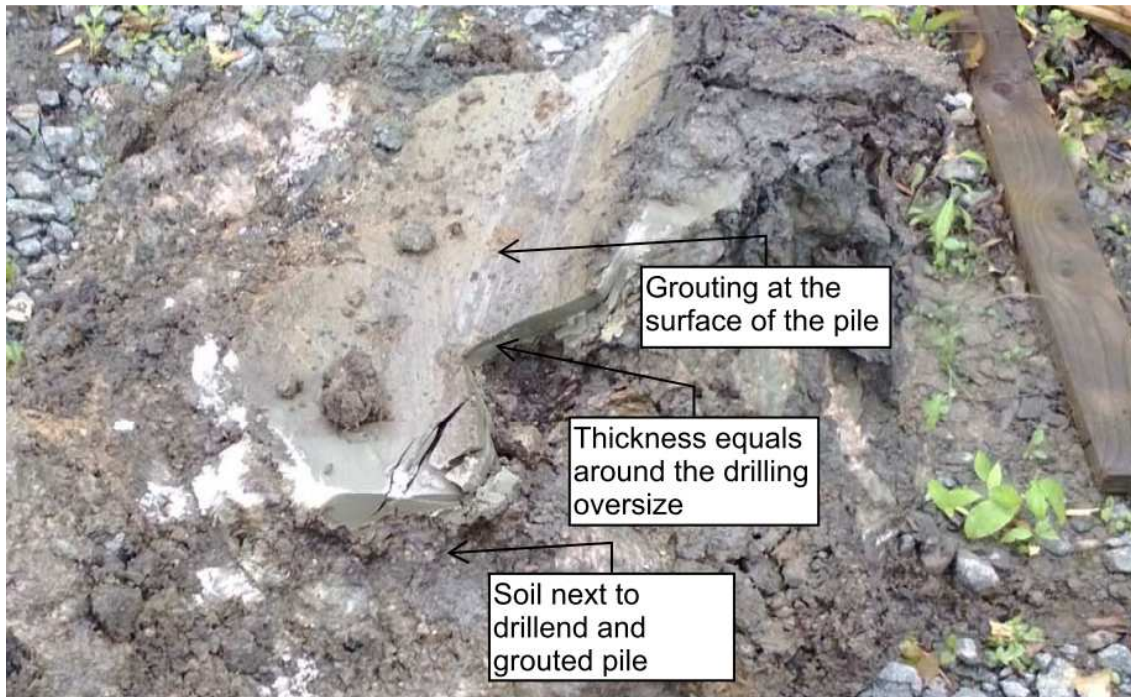


Figure 3.34: Soil pieces collected next to the pile with background grouting. The grouting was spread mostly into the excess drill space next to pile. This picture was taken at the Masku test site.

When designing RD pile walls, attention should be paid into interlock lengths. If the RF interlock is too long and ends at too low a level, the RF interlock may stop the previous pile’s ring bit. This occurs when a pile is drilled deeper than the previous pile. The contractor should pay attention when the bedrock proves deeper than in the ground survey and cut the RF interlock shorter if necessary.

If the top of a male interlock fills with soil or rock, it should be cleared to avoid additional friction in the interlocks. In some cases, high friction may damage the interlocks. Using interlock sealant will keep soil from finding its way between the interlocks as easily. Sealant mass may function as a lubricant and decrease friction even more.

The volume of grouting material used should be two to three times more than theoretical mass needed. Grouting material tends to spread first along the path with the least amount of drag. Using more than the theoretical volume of grout mass will make it more likely that the grout will flow into the wanted target after any unnecessary places or paths are filled.

At the test site, grouting pressures were generally 2 to 8 bar. The maximum pressure indicated by the equipment at the test site was 18 to 19 bar. When using RF rings, the

resistance of the grout increased and the pressure rose. Table 3.7 shows that internal grouting tended to require slightly higher pressure to penetrate the soil in the drilling hole than grouting via an RF interlock. When grouting from inside the pile, the grout first had to penetrate the area below the pile into the gap. It was also observed that after the grout reached the drilling hole gap, the pressure tended to drop. The reason may be that the pile had to ascend a little for the grout to spread. When pile moved, the grout had a free path to flow. It would be necessary to observe if the pile ascends during grouting when pile is internally grouted. If pile ascends, it should be driven to ensure that pile is at the bottom of the drilling hole. Driving the pile is necessary, especially when pile will be vertically loaded.

Table 3.7: Grouting pressures needed at the test site

Pressure need to penetrate the grout into the drilling hole gap

Pile	Type	Pressure when grout started to flow[Bar]	Pressure when stop grouting[Bar]	Comment
1	-			
2	-			
3	Injection ring	18	18	Grout did not flow
4	Injection ring	5	15	Blocked before designed volume
5	Holed RF	8	8	
6	Holed RF	4	2	
7	RF	2	6	
8	-	-	-	
9	RF	2	8	
10	Injection ring	0	18	Injection adapter tend to block
11	-			
12	-			
13	Injection ring	-	-	Grout did not flow
14	Injection ring	5	5	
15	-			
16	-			
17	-			
18	-			
19	RF	5	6	
20	RF	2	7	
21	Internal grouting	10	1	Mass flow without resistance when quit grouting
22	Internal grouting	2	5	
23	Internal grouting	5	4	Max pressure was 7 bar

maximum pressure of equipment used in test was 19bar

AVERAGE		
Injection ring	5	10
Holed RF	6	5
RF	2.75	6.75
Internal grouting	5.67	3.33

One finding was that drilling tends to stabilize, and drill cuttings only began to flush out of the inside of the pile after 1 to 1.5 meters. For further site investigation, 2 meters of soil over the bedrock should be reasonable in soil conditions similar to those at the

Masku RD pile test site. The test site had 3 to 4 meters of soil over the bedrock. Less soil to drill reduces the excavation required. Also, shorter piles can be used, and there are fewer challenges associated with unwatering the excavation.

The best grouting method according to the results from the test site was grouting via RF interlocks. In theory, the injection ring is even better due to wide spreading at the base of the toe of the injection channel. At the test site, the injection ring method proved to be less reliable due to the tendency of blockages to form in the channel. Considering the reliability, cost and rather small advantage given by the injection ring, it is not worth using without additional product developments. Other good grouting methods seemed to be grouting through the pile. When grouting from inside the piles, the grout begins spreading at the pile toe level and may therefore spread better than in RF grouting. On the other hand, after forcing grout into the gap at rather high pressure, the grout may flow back into the pile once the path for the grout is created if there is no counter pressure in the pile. To prevent soil from flowing into the drill cuttings and replacing the grout, extra volume of grout should be used. If the pile is concreted and the drilling hole is grouted at the same time with a high-slump mixture at additional pressure, there is automatically counter pressure in the pile. Inside grouting can be used, for example, in cases where grouting through an RF interlock fails for some reason. That section of the RD pile wall can be grouted through the pile.

The gaps in the test site RD pile wall were tightly packed with moraine/drill cuttings alongside the piles that were not grouted. The grout spread in a 25 to 45-degree angle up from the injection channel when there was tightly packed soil/drill cuttings in the gaps. The spreading of the grout is shown in figure 3.36. The tightly packed soil in and above the drilling hole is shown in figure 3.35. Such tightly packed frictional soil made it more difficult for the grout to spread all over the gap without an injection ring. The test site results reveal that grout replaced the cohesion soil in the gap of single pile quite perfectly, as evident in figure 3.37. Somehow one of the piles with an injection ring showed worse grouting results. Figure 3.38 shows how only about 50% of the drilling hole was filled with grout. That said, the deepest 50 cm out of total 100 cm drilled was hard material, probably grouting. The grouting may have been more successful if more than the theoretical grout volume were used. Figure 3.39 shows cement material in the pile that was not grouted. The nearest grouted pile was about 1.5 meters away. Above the bedrock, no cement path was found. The cement probably flowed through a suitable crack in the bedrock. Watertightness may be insufficient in RD pile walls with a non-continuous grouted gap caused by tightly packed soil in the gap. This may occur when the diameter of the pile is larger than the pile drilled into the bedrock. In such cases, it is likely that the grout will spread more widely at the bedrock level when there is no more than tightly packed soil. When the grout spreads at the bedrock level, it may improve watertightness compared to non-continuous grouting. It was observed from the bedrock level in the gap in the bedrock hole that the grout tended to break when drilling samples

or removing the wall. For the calculations in this thesis, it was assumed that the entire drilling hole was filled with drill cuttings, soil or grouting mass.



Figure 3.35: Tightly packed moraine in and above the drilling hole. Some grouting material may be mixed into the moraine. This photo was taken at the Masku test site.



Figure 3.36: Grout spread in a 25 to 45 degree angle from the toe of the RF interlock's injection channel. The RF interlock ended 100 mm above the toe of the pile. The pile diameter was 508 mm, and the pile was drilled 500 mm into bedrock. The soil that the grout had to replace was tightly packed moraine in the gap. The bedrock, the drilling hole and the RD pile wall were washed using a pressurized washer. Any moraine with only a little grout was probably washed away, and only solid grout material remained. This photo was taken at the Masku test site.



Figure 3.37: Pile grouted through the injection channel. The grout perfectly replaced the clay/drill cuttings in the gap.



Figure 3.38: Pile grouted through the injection channel and an injection ring. The grout replaced the clay/drill cuttings in the gap only on one side. There was harder material for 50 cm out of a total of 100 cm drilled. Harder material was noticed using a metal pipe. The first 50 cm consisted of soft clay and suddenly the pipe stopped.



Figure 3.39: The pile had grouting around the pile even though pile was not grouted. A piece of the material was tested at the Tampere University of Technology laboratory.

3.4 Experience from other ongoing RD pile wall sites

For the Urheilupuisto metro station in the Länismetro project, there were extra tight requirements regarding watertightness. Next to the construction site, there was a ground-supported building. The soil at the site was basically thick organic clay, and the groundwater level was near ground level. Lowering groundwater level was thus not acceptable. (Collins, N 2011)

The main structure for ensuring watertightness was a sheet pile wall. Where the excavation was deep, an RD pile wall was used for extra security. The RD pile wall was drilled in front of the sheet pile wall. The RD piles were RD 600/10 piles, and the interlocks were E21W/E21N interlocks with a drilling diameter 96 mm wider than pile itself. The interlock type is shown in figure 3.40. The gap was not grouted. Instead, the piles were filled with high-slump mix concrete, K40, S5, max 16 mm aggregate, self-compacting concrete (interview memo). The strength of K40 concrete is between C30/37 and C35/45 Eurocode EN 1992. WOM-WOF interlocks were also used in another section of the pile wall.

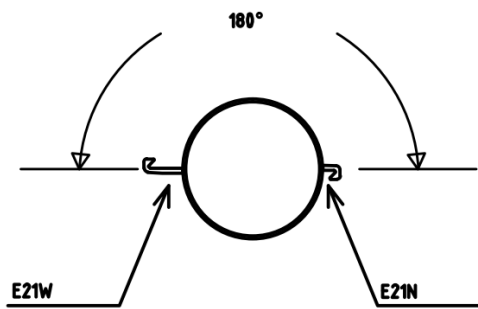


Figure 3.40: The interlock type used in the RD pile wall in the Länsimetro Urheilupuisto project. Picture: Ruukki

According to construction manager Erkki Virtanen of Peab Infra Oy, there were no leaks between the RD pile wall and the bedrock [Appendix 22: interview memo]. As of 16 June 2013, not all of the RD piles were excavated all the way from the ground level to the bedrock. The deepest RD piles excavated down to bedrock had about 9 meters of water pressure in the gap between the bedrock and the pile wall. Some of gaps had been filled with material similar to solid concrete up to the top of the bedrock level. Solid material was not breakable with a sharp metal stick (figure 3.41). Appendix 18 gives the actual drilling depth and bedrock level of piles P126 and P273. Solid material was found in the gap of concreted pile (P126) a height of 6.4 meters drilled 1 meter into the bedrock. So, in that case, the concrete climbed 1 meter from bottom of the pile to the top of the bedrock as a result of approximately 150 kPa in pressure ($24 \text{ kPa/m} \times 6.4 \text{ m}$). By contrast, pile P273, 7.5 meters high and drilled 1.5 meters into the bedrock, had no solid concrete-like material at the top of the bedrock. Instead of solid material, the gap was filled with drill cuttings or glacial till from the soil near the top of the bedrock level.



Figure 3.41: *Solid material in the gap of pile P126, Länsimetro, Urheilupuisto*

In the Länsimetro Koivusaari metro station, the RD pile wall bedrock drilling hole was grouted successfully as shown in figure 3.42. In Koivusaari, the rock drilling hole was grouted using 20 mm pipes located on the ground side of the wall. About 50% of the pipes could not be opened with pressurized air. The bedrock was also curtain grouted before grouting the drilling hole. Curtain grouting tends to rise into the drilling hole, which explains both the high number of blocked injection channels and the success of the grouting. There were no leakages from the drilling hole [Appendix 22: interview memo].



Figure 3.42: Grouted drilling hole in the bedrock. Picture: Länsimetro Koivusaari metro station, taken after excavation by Westerlund, Antti 13 August 2013

4 ROTATIONAL STIFFNESS OF RD PILE WALLS USING THE RESULTS OF THE FIELD SURVEY

4.1 Rock-pile rigidness calculation, Ansys FEM

The FEM model was created with ANSYS R14.5. In the model, the bedrock was modeled as hard concrete with only little tension capacity. The gap material was modeled as concrete when the gap was grouted and as a concrete with only little tension capacity when drill cuttings or soil were used. The pile was structural steel with values set equal to S440J2H material values. In the model, concrete was modeled with isotropic plastic hardening [7]. The hardening of the concrete and bedrock materials was set very close to zero. When the material reaches the yield stress, the stress no longer increases. The very soft clay material in the drilling hole had to be modeled as non-breakable concrete material with the hardening set close to zero. In the site test, the displacement of the pile was so large that the material compressed from 27 mm to 13 mm. This made the theoretical compression strain approximately 50%, which is huge. In reality, clay material extruded out of the drilling hole on the compression side of the pile. That kind of behavior cannot be modeled; however, as the remaining material still supports the pile, material had to be modeled as non-breakable. The steel was modeled with kinetic hardening [9]. The difference between kinetic and isotropic hardening is shown in chart 4.1. Bedrock on the x, y and z axes are supported from each side of the bedrock block.

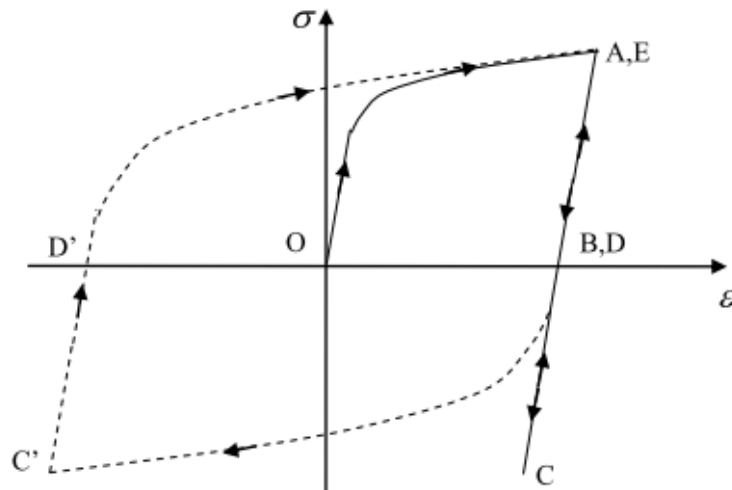


Fig. 2 $\sigma\epsilon$ diagram of uniaxial cyclic test.

— Isotropic hardening
 ---- Kinematic hardening

Chart 4.1: Cyclic loading [8]

The FEM calculations were made using frictional contact between materials with the frictional coefficient value set to both 0.1 and 0.5. The coefficient of friction for steel on concrete varies in the literature from 0.47 to 0.65 depending on the stress level and whether the material is wet or dry [20,21]. The coefficient of friction for concrete on rock ranges from 0.5 to 0.8 in the literature [22,23,24]. The force was set equal to the maximum elastic horizontal load (see figure 4.1). If the model was not able to resolve, the force was reduced. Characteristic values for the materials and load were used.

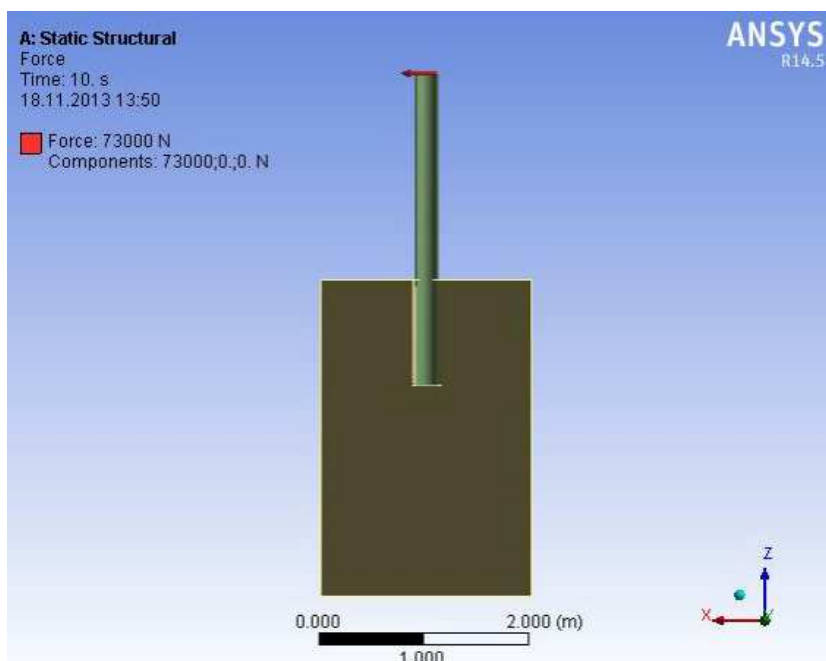


Figure 4.1: FEM model modeling pile rotational stiffness. Pile 10, grouted gap

The element mesh was produced automatically by ANSYS, with the mesh defined as denser on contact faces. The maximum mesh size was set to 50 mm, but the mesh realized was much denser as seen in figure 4.2. The pile mesh, for example, was approximately as thick as the pile, i.e., 10 mm.

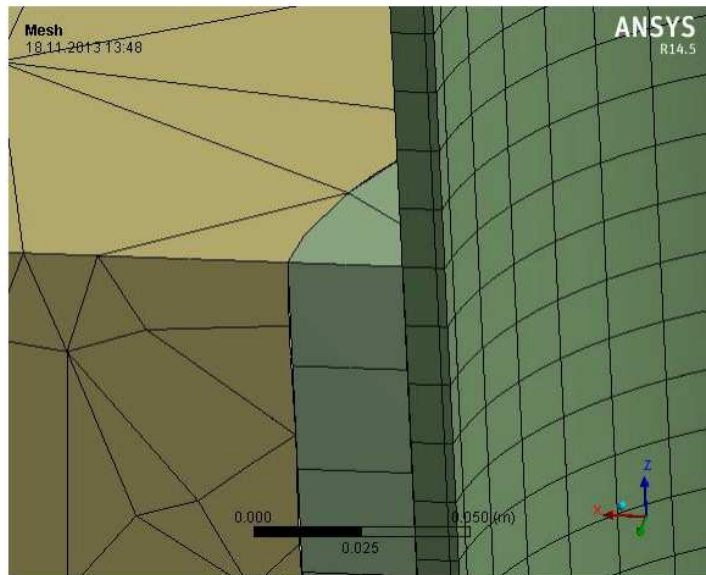


Figure 4.2: FEM model: The mesh was made denser at points of contact between materials. Pile 220/10 test pile number 10, grouted gap

Figure 4.3 shows a horizontal displacement very close to the displacement measured at the test site. Also, the displacement at the bedrock level was very similar.

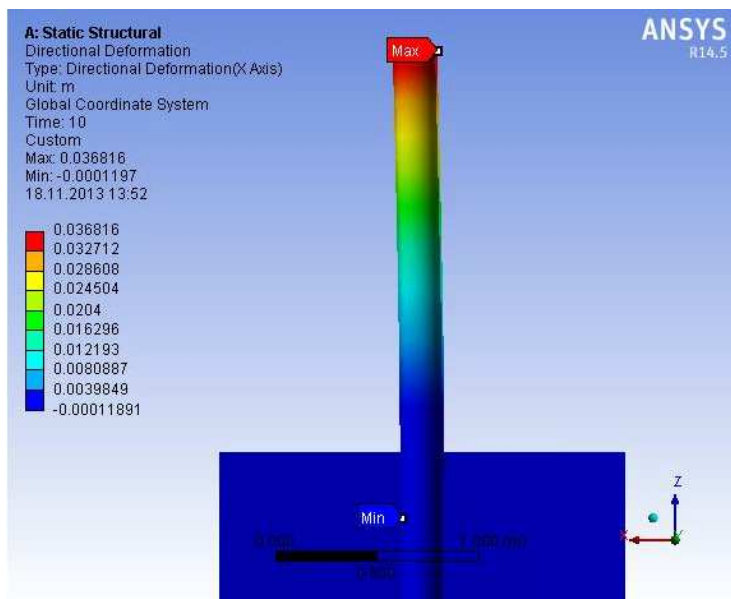


Figure 4.3: FEM model: Horizontal displacement at maximum load. Pile 10, grouted gap

Another model was made modeling the grout, rock and soil as linear materials with no breaking point. The results were inaccurate, even when pile was drilled into the bed-rock about twice its diameter and the gap was grouted. In the grout, there was a maximum tensile stress of 6MPa. The ultimate tensile strength of grout was about 3 MPa. When the piles are drilled less, the inaccuracy becomes even larger. At lower loads, the stress naturally remains lower and the material therefore models in a linear range.

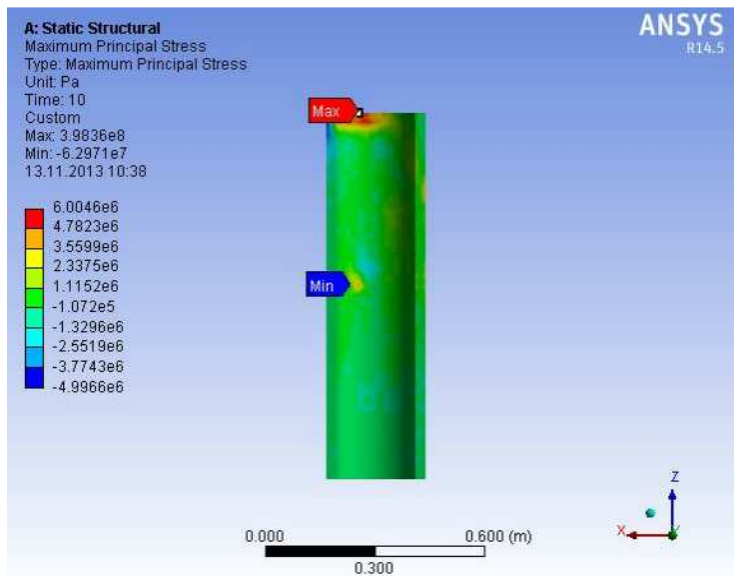


Figure 4.4 FEM model: Tensile stress in grout when material model is linear. Pile 10, grouted gap

The horizontal displacement of the pile at bedrock level was very small when the gap was grouted as seen in figure 4.8 and in the deformation shape in figure 4.5. The deformation shape fit the shape where the horizontal displacement of pile was zero at the bedrock level quite well. Moreover, when fitting the deflection curve, the direction of the displacement at the bedrock level was opposite to that of the load. That cannot be the case. The fitted deflection curve is shown in figure 4.6. The method of least squares was used to fit the curve.

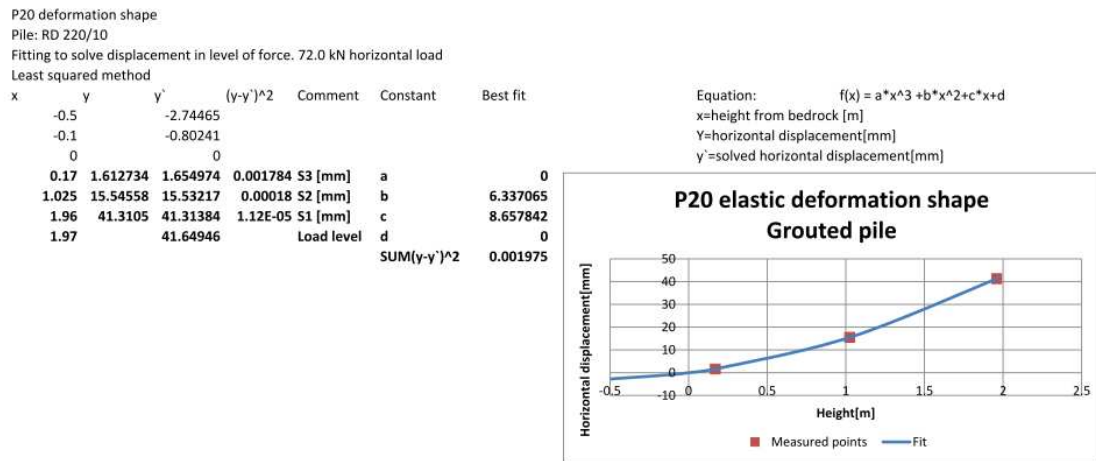


Figure 4.5: Least squared method fitting to horizontally loaded grouted test pile 20. The deflection curve was calculated using three points measured during the Masku horizontal load test. The displacement at the top of the bedrock (constant d) was forced into 0. This figure is also shown in appendix 3.

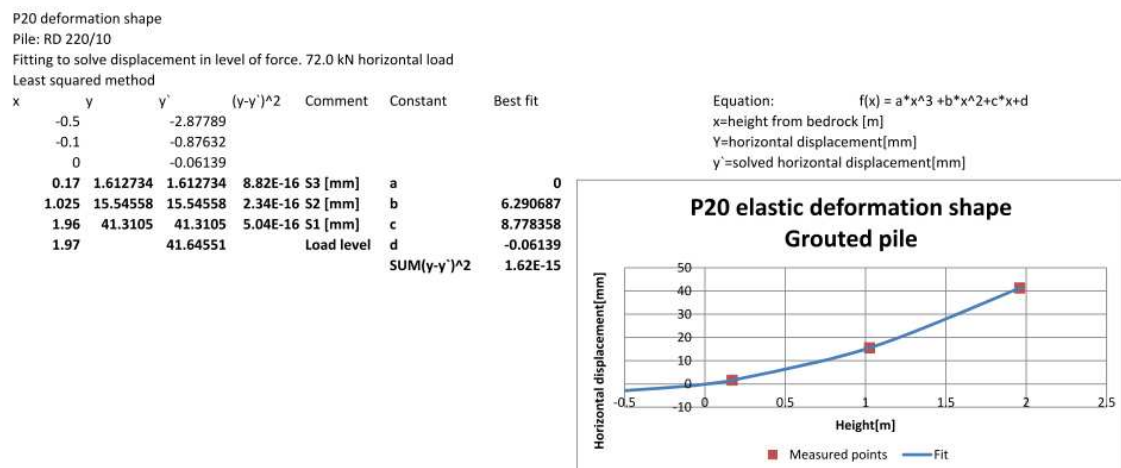


Figure 4.6: Least squared method fitting to horizontally loaded grouted test pile 20. The deflection curve was calculated using three points measured during the Masku horizontal load test. This figure is also shown in appendix 3.

Ansys FEM calculated the rotational stiffness in a very linear fashion. Chart 4.1 shows the graph of calculation where the structure was loaded with many partial loads until reaching the elastic limit. The FEM analysis was more linear than the measured rotational stiffness cited in paragraph 3.2.3.1. That said, the largest variance from the average value was only 0.3%. In calculations, a linearized approximation is much easier to work with. Because of linearity, a partial safety coefficient can be added after the FEM calculations.

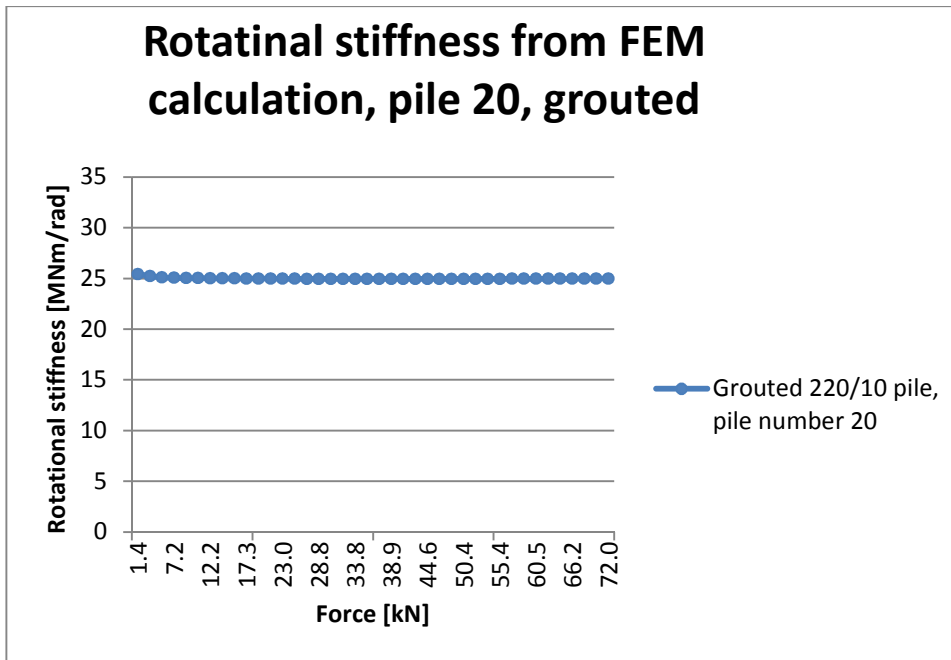


Chart 4.1: RD 220/10 pile drilled 1 meter into bedrock, gap grouted. The pile was loaded horizontally until it went into the plastic range. Linear material model. The chart shows the rotational stiffness according to the FEM analysis.

In the non-linear material model shown in chart 4.2, the rotational stiffness was less linear than in the linear material model. The highest rotational stiffness for the grouted pile in the non-linear model is approximately 30% from elastic load. The additional rotational stiffness at 30% load is 4.2% higher than the rotational stiffness at the load point of yield stress. The model behaved somewhat differently when the pile drilling hole was very poorly grouted and the gap included mainly clay. See section 3.1 for the reason for the grouting failure. Chart 4.3 shows that rotational stiffness increases as the bending moment in the joint increases. This was also the case in the linear model. The model therefore calculated the rotational stiffness too low at the low stress level in the case of clay in the bedrock. The rotational stiffness value at the elastic limit is about 25% too high as seen in appendix 21, and the rotational stiffness should therefore be divided by 1.25 when used in RD pile wall dimensioning. The reason why the rotational stiffness tended to rise in that specific model was not clarified.

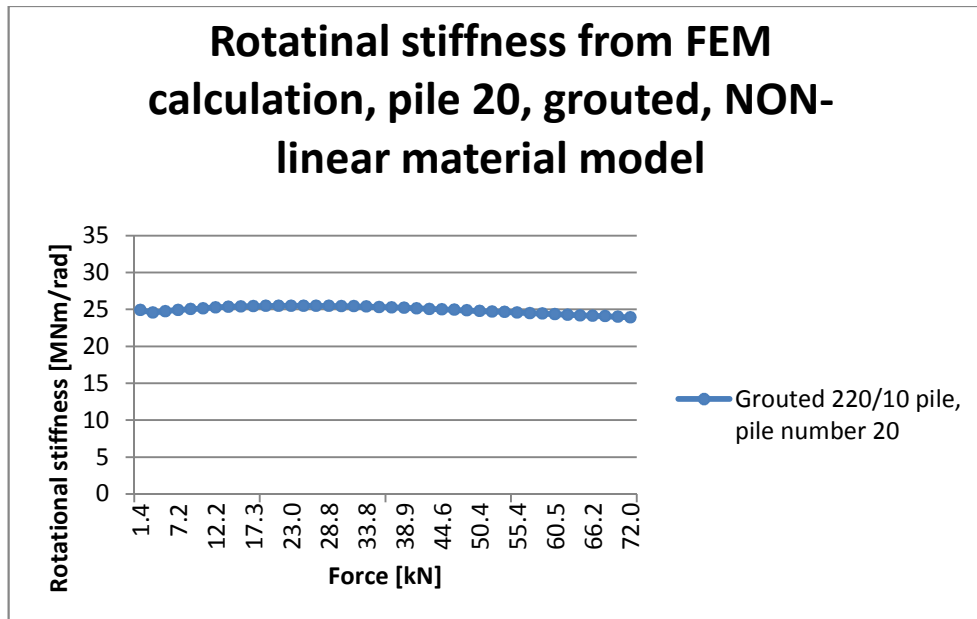


Chart 4.2: RD 220/10 pile drilled 1 meter into bedrock, gap grouted. The pile was loaded horizontally until it went into the plastic range. Non-linear material model. The chart shows the rotational stiffness according to the FEM analysis.

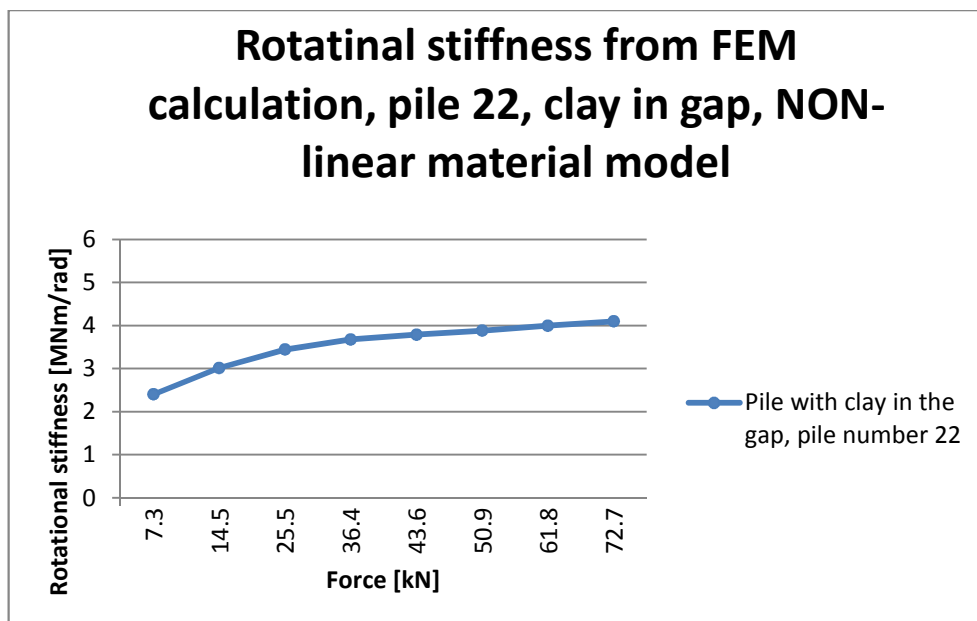


Chart 4.3: RD 220/10 pile drilled 1 meter into bedrock, gap filled with very poorly grouted clay. The pile was loaded horizontally until it went into the plastic range. Non-linear material model. The chart shows the rotational stiffness according to the FEM analysis.

As one can see from table 4.1, the FEM analysis estimates the horizontal displacement due to pure joint (deducting the displacement of the pile itself) to be approximately 20% lower than the actual horizontal displacement in the site load test. By way of comparison, table 4.1 also shows a calculation where friction is set to 0.1 (and the mate-

rial model is linear). A friction value of 0.1 very closely approximates the clay case. Still, there was much more variation between the different piles calculated.

Table 4.1: FEM model displacement compared to the piles tested at the site. A clearer version is included in appendix 21.

Appendix 21: rotational stiffness of test piles versus FEM calculation

Pile	Pile length [m]	Material in the gap of the drilling hole in bed rock	Max elastic force [kN]	Measured displacement when max elastic force [mm]	Displacement due to FEM without extra springs and large deflection allowed, friction 0.5	FEM displacement compared to tested	Displacement from joint, measured	Comment	Non-linear 0.5friction vs. reality TOTAL	Non-linear 0.5friction vs. reality JOINT	Displacement due to FEM without extra springs and large deflection allowed, linear model friction 0.1	Linear 0.1friction vs. reality TOTAL	Linear 0.1friction vs. reality JOINT
10	1.97	Grouted	73.1	38	35.9	-5.5 %	13.3	sand above rock level	-5.5 %	-15.8 %	37.3	-1.8 %	-5.3 %
11	1.99	Drilling mud	72.4	38.9	36.2	-6.9 %	14.2	sand above rock level	-6.9 %	-19.0 %	37.2	-4.4 %	-12.0 %
20	2	Grouted	72	41.3	37.5	-9.2 %	16.6	clay above rock level	-9.2 %	-22.9 %	37.9	-8.2 %	-20.5 %
22**	1.98	Grout/clay	72.7	108.1	39.4	-63.6 %	83.4	clay above rock level	-63.6 %	-82.4 %	38.3	-64.6 %	-83.7 %
22***	1.98	Grout/clay	72.7	108.1	95.7	-11.5 %	83.4	clay above rock level	-11.5 %	-14.9 %	108.5	0.4 %	0.5 %

*Non-grouted tight, drilling mud

**weakest clay-concrete sample values

***weakest clay-concrete sample values/1000

4.1.1 Rotational stiffness analysis in Ansys to be used in RD pile wall dimensioning examples in GeoCalc

The bedrock stress level in the linear material model is shown in figure 4.7 and is very high. The maximum compression is approximately 200 MPa. Many bedrock materials are at their breaking point at such high stress levels. This thesis does not discuss the details of bedrock design resistance. In the FEM calculations, the bedrock was assumed to be unfragmented and have same strength as the bedrock tested in site test. The stress in the bedrock is higher when pile is drilled to only a short depth. Deeper drilling reduces stress on the bedrock. Many times, the bedrock is fragmented at the top, and drilling may damage the bedrock even more. Short drilling depths should thus be avoided if there are no structures providing horizontal support. Horizontal support can be provided using rock dowels or toe beams as discussed in section 1. When the excavation level is below the toe of the RD pile wall near wall as seen in figure 1.8, extra horizontal support should be used. Another option is to drill pile wall below the excavation level next to wall.

If grouted 500/12.5 piles were drilled just 254 mm into the bedrock, the grout would obviously fail before the bedrock would. The stress on grout is greater than the stress on rock. The grout compression stress in figure 4.7 is about 240 MPa. For comparison, appendix 19 includes a hand calculation in which pile is assumed to be solid and that maximum compression is 156 MPa. This hand calculation yields relatively less stress the deeper the drilling.

The Ansys FEM calculations for GeoCalc were made using the linear model and a friction coefficient of 0.1. In that model, the differences between the FEM model and reality were rather small as seen in appendix 21. Pure rotational stiffness values were

used without an extra coefficient. The linear model could be used in this case, because drilling depth was set as much as 3.94 times diameter.

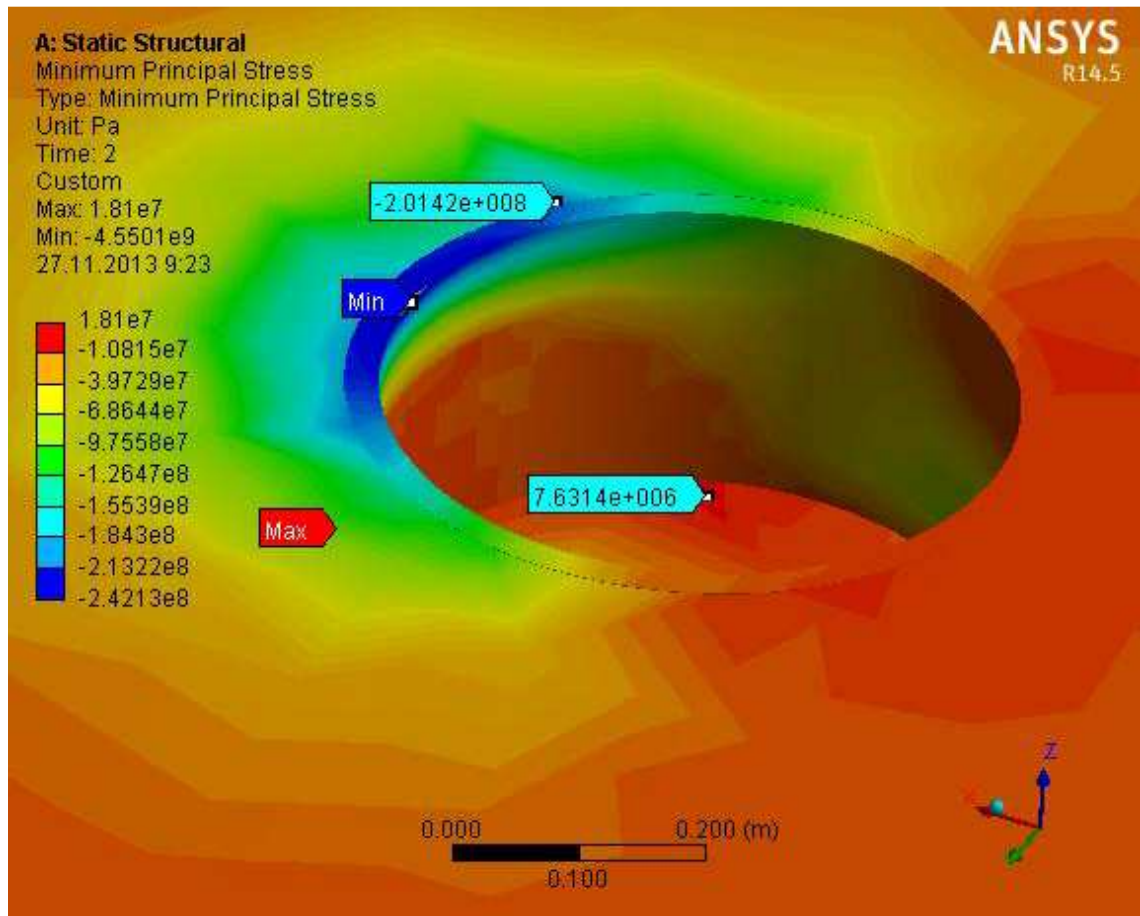


Figure 4.7: Stress in bedrock. 500/12.5 pile maximum elastic horizontal load, drilled 254mm into bedrock

In the Ansys FEM calculations, the pile length above the bedrock level was one third of the height in the GeoCalc model. The horizontal load was located at the top of the cut piles. The horizontal load was chosen to be equal to the maximum elastic load. In this case, the deflection in the bedrock and the gap will not increase more than the elastic load. The bending moment in upper level of the bedrock was 1035 kNm when the horizontal load was equal to elastic load, or 444 kN. This is calculated in appendix 2. The load was located one-third of the way from the bedrock, because the load from soil and groundwater is basically triangular, increasing linearly starting from zero at the surface level and reaching a maximum value at the deepest level. The pile length above the bedrock level was $7 \text{ m}/3 = 2.333 \text{ m}$. The horizontal load was located at the top of the pile.

Figures 4.8 to 4.10 show the horizontal displacement of the model with the same geometry and loading with different material in drilling hole gap. Figures 4.10 and 4.11 both have soil sample 1 in the drilling hole. Figure 4.11 is loaded with only one-tenth of the load in figure 4.10. The partial load was calculated due the non-linearity of soil sample 1, demonstrated by the fact that the bedrock level displacement in figure 4.11 is

not 10 times less than in figure 4.10. The displacement at the top of the bedrock and the toe of the pile were used in the GeoCalc model to imitate similar rotational stiffness. This method of generating bending stiffness is not as accurate method as a torsional spring would be. For example, the horizontal displacement is different at the different points on pile cross-section due to deflection of the pile, as seen in figure 4.10. Because displacement is dependent on load, the load level was taken into account the calculation in appendix 2. In linear cases, the displacement at specific load levels can be derived from the displacement at the elastic load without significant inaccuracy. For soil sample 1, the calculation in the FEM analysis also had to be done at the load level, derived from bending moment level applied in the GeoCalc calculations. Calculation process is an iterative process, because fixing the bedrock support conditions in GeoCalc, discussed in section 4.2, also changes the bending moment in the pile at the top of the bedrock level. Changing bending moment obviously changes the displacement in the drilling hole as well. In linear material or piecewise linear material, such as grout at low stress levels, the desired displacement is easy to calculate. In non-linear material models, such as the one in figure 4.11, the displacement can only be calculated by FEM. The GeoCalc calculations are given in section 4.2.

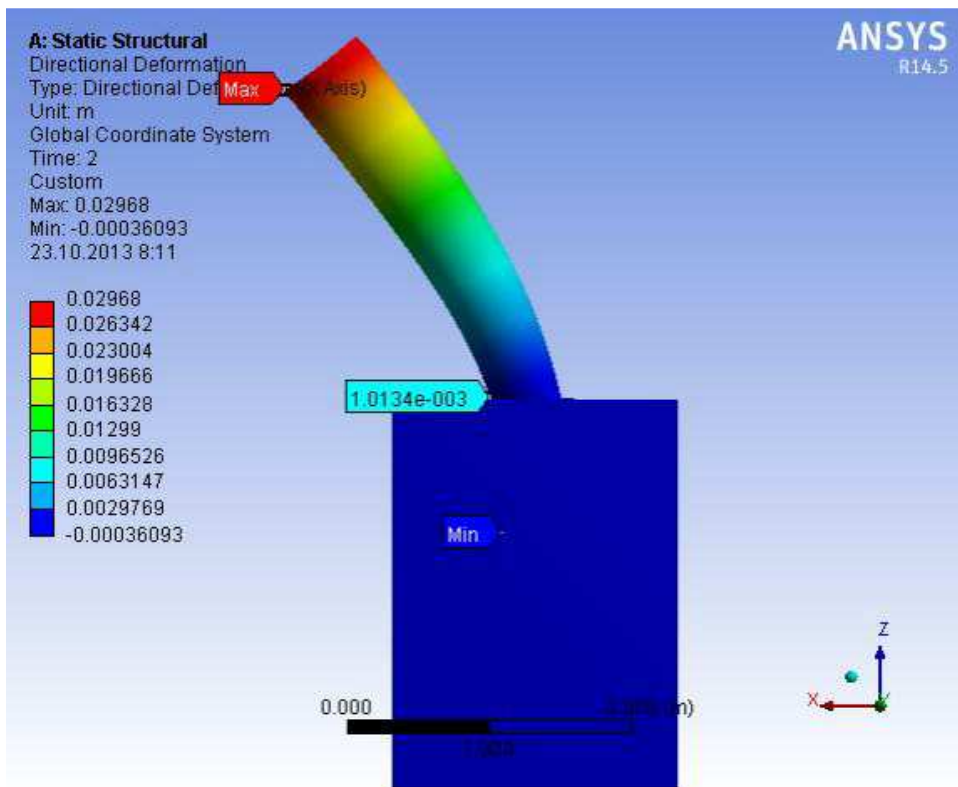


Figure 4.8: Deformation of the RD500/12.5 pile grouted in the bedrock. The pile was loaded with the maximum horizontal elastic load.

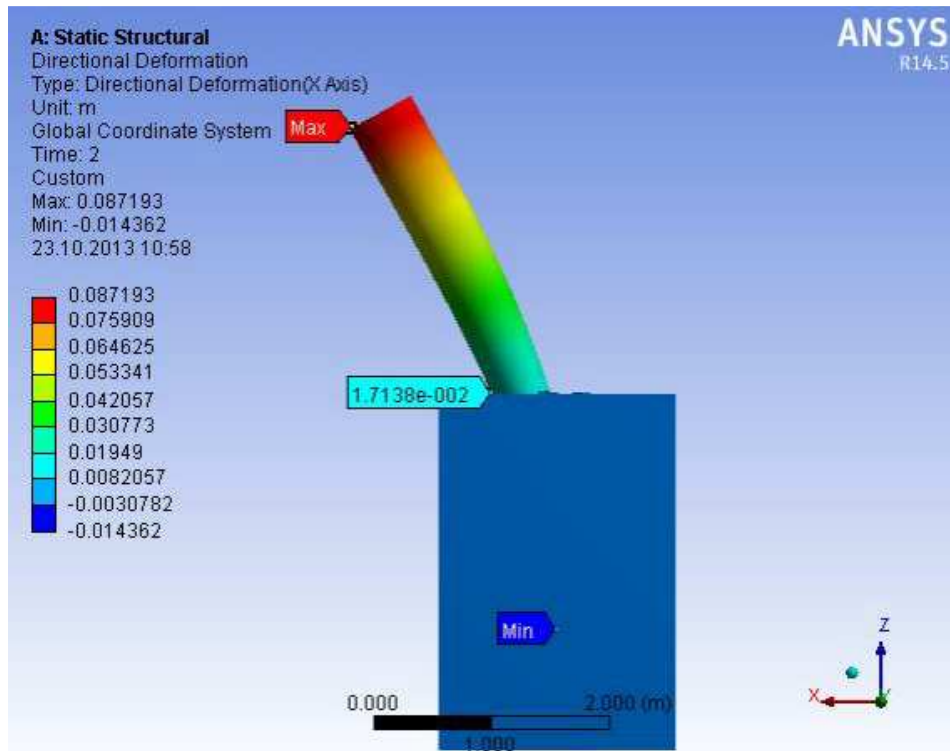


Figure 4.9: Deformation of the RD500/12.5 pile with clay in the gap. The pile was loaded with the maximum horizontal elastic load.

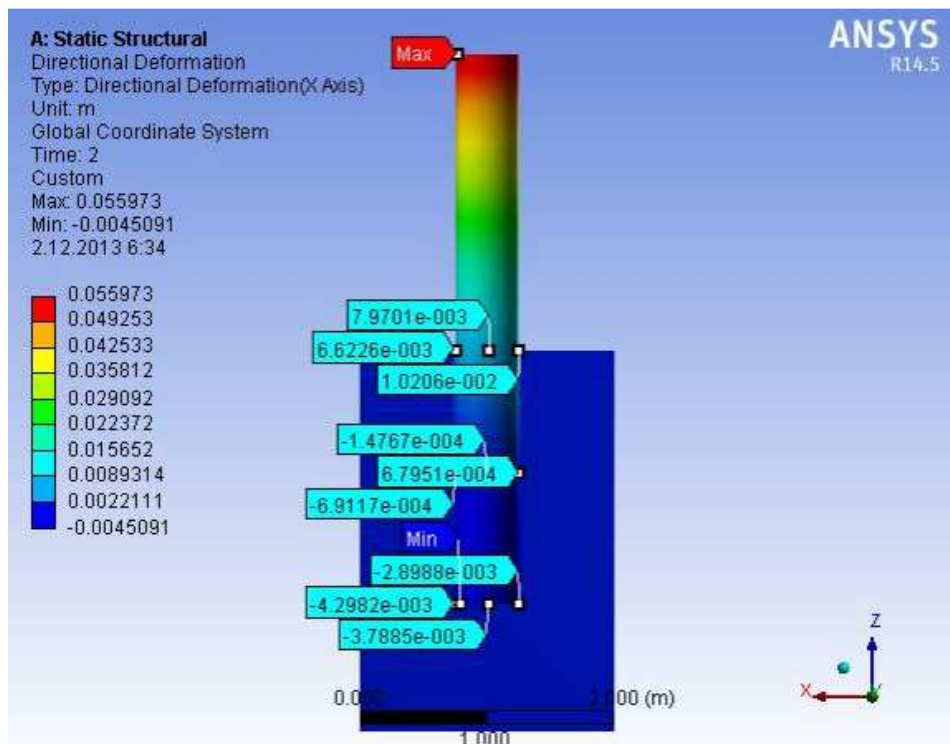


Figure 4.10: Deformation of the RD500/12.5 pile with soil sample 1 in the gap. The pile was loaded with the maximum horizontal elastic load.

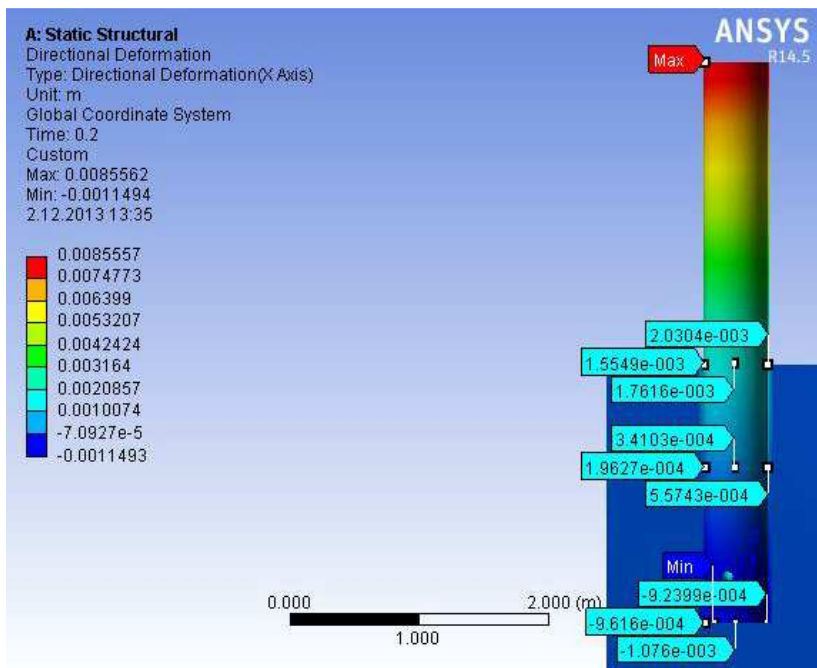


Figure 4.11: Deformation of the RD500/12.5 pile with soil sample 1 in the gap. The pile was loaded with 0.1 times the maximum horizontal elastic load.

4.1.2 Drilling depth in relation to rotational stiffness

The Ansys model was loaded in many load steps to identify rotational stiffness at each step. The average values from material laboratory test were used in the FEM analysis (see table 3.3). The values represent characteristic values. The load height, bedrock material, pile material and dimensions remained same. The rotational stiffness was calculated for a few different drilling depths in cases where there was grout material and weak clay-like material in the bedrock drilling hole gap. The pile length above the bedrock was same used in the calculations in section 4.1.1. 1220/12.5 piles were calculated using a pile length of 3 meters, because the displacement gave erroneous results when pile length to pile diameter below 2. A friction coefficient of 0.5 was used in the FEM calculations. A non-linear material model was used. After the FEM calculations, an extra coefficient of 0.8 for rotational stiffness was used to compensate for the 20% smaller displacement in the FEM calculations versus the load test results. In non-linear material model with a friction coefficient of 0.5, the rotational stiffness value had to be multiplied by 0.8 to obtain more realistic value. A comparison of the FEM calculation and load test results was presented in section 4.1.

The FEM analysis shows that when RD piles are drilled only a short length into the bedrock, rotational stiffness decreases as bending moment in the joint increases. Chart 4.4 shows the results of the FEM analysis. In the site test, 220/10 piles were drilled one meter (4.6 times diameter) into the bedrock. In both the site test (see chart 3.7) and the FEM analysis as seen in chart 4.2, the drop at the elastic load level was much smaller due to of deeper drilling. Also, the FEM analysis in chart 4.5 shows a much smaller

drop in rotational stiffness at the high load level when the piles are drilled at least twice their diameter into the bedrock. Chart 4.6 shows the rotational stiffness of the grouted RD1200/12.5 pile at the load level at different drilling depths.

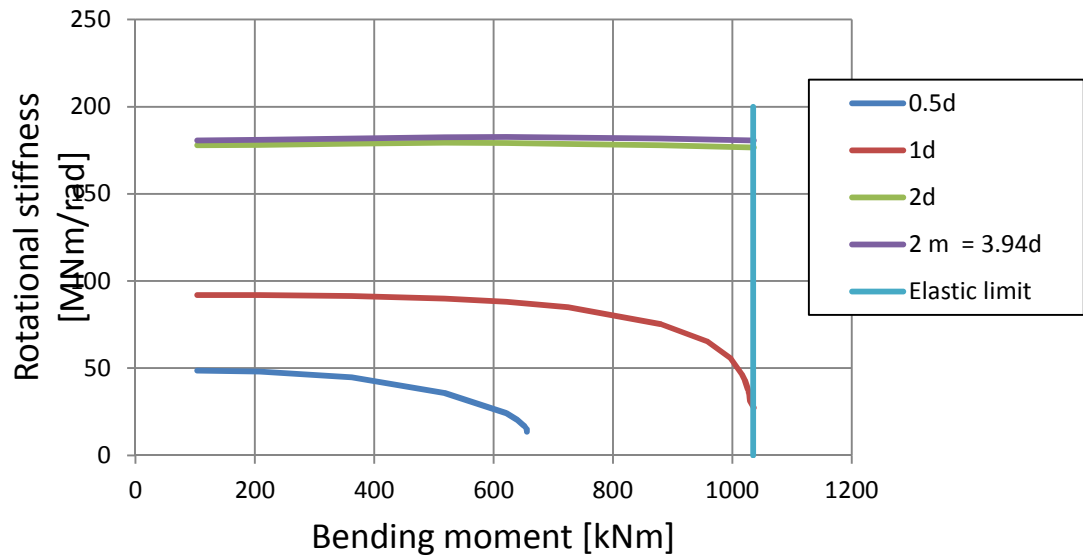


Chart 4.4: Rotational stiffness of a single 500/12.5 RD pile drilled 254mm = 0.5*diameter to 2000mm = 3.94*diameter into the bedrock. The piles are grouted.

There is a drilling depth for maximum joint rotational stiffness after which deeper drilling does not significantly increase rotational stiffness. The reasonable drilling depth mostly depends on the material in the gap. The pile size also affects the maximum reasonable drilling depth. Table 4.2 reveals that a pile drilled 1.016 m = 2*diameter results in nearly maximum rotational stiffness. Drilling two meters into the bedrock will not greatly increase the rotational stiffness. In theory, when considering rotational stiffness, drilling into unfragmented rock should be to a depth of not more than twice diameter.

The rotational stiffness at the elastic limit alone is not a good indicator, because in FEM calculations, the stiffness will drop significantly when approaching the elastic limit load. The rotational stiffness should be selected at the point in which the structure will be loaded. Because the bending moment depends on the rotational stiffness at the toe of RD pile wall and the rotational stiffness depends on the bending moment level, calculations must be iterative to be more accurate. First, the rotational stiffness should be selected, for instance, at the level of elastic limit. Then, the RD pile wall bending moment should be calculated and checked to see whether the bending moment is near to the assumed value. If not, a new rotational stiffness should be selected.

Table 4.2: 500/12.5 $f_y=440\text{MPa}$ pile rotational stiffness in relation to drilling depth. The stiffness values are calculated at the failure load. The bedrock drilling holes are grouted.

Material in the drilling hole**	Drilling depth (m)	Horizontal displacements at load level			Stiffness (MNm/rad)	Failure bending moment (kN*m)	Comment
		Total (mm)	Pile deflection, calculated in appendix 2 (mm)	Joint (Total-pile) (mm)			
Grout	0.254	120.5	9.5	112.2	13.6	655.7	
Grout	0.508	101.3	15.0	88.2	27.4	1035.9	*
Grout	1.016	28.7	15.0	15.6	154.9	1035.9	*
Grout	2	28.4	15.0	15.3	158.0	1035.9	*
Clay	0.508				1.0	163.3	
Clay	0.762				2.7	244.9	
Clay	1.016				5.4	419.3	
Clay	1.524				13.1	762.0	
Clay	2.032				21.1	919.2	
Clay	2.54				27.4	919.2	

*Elastic bending moment, calculation ended

** Material value from material test.

Pile length 2.333m

From chart 4.5, one can see that in this thesis, the rotational stiffness of the toe of the RD pile wall is determined at the pile's elastic range stress level. After the pile reaches the plastic range, its deformation rapidly increases displacement at the top of the pile wall. The calculations taking into account the deflection of the piles assume that the displacement from pile deformation at the top of the pile is linear. That assumption is not valid after the elastic limit stress level.

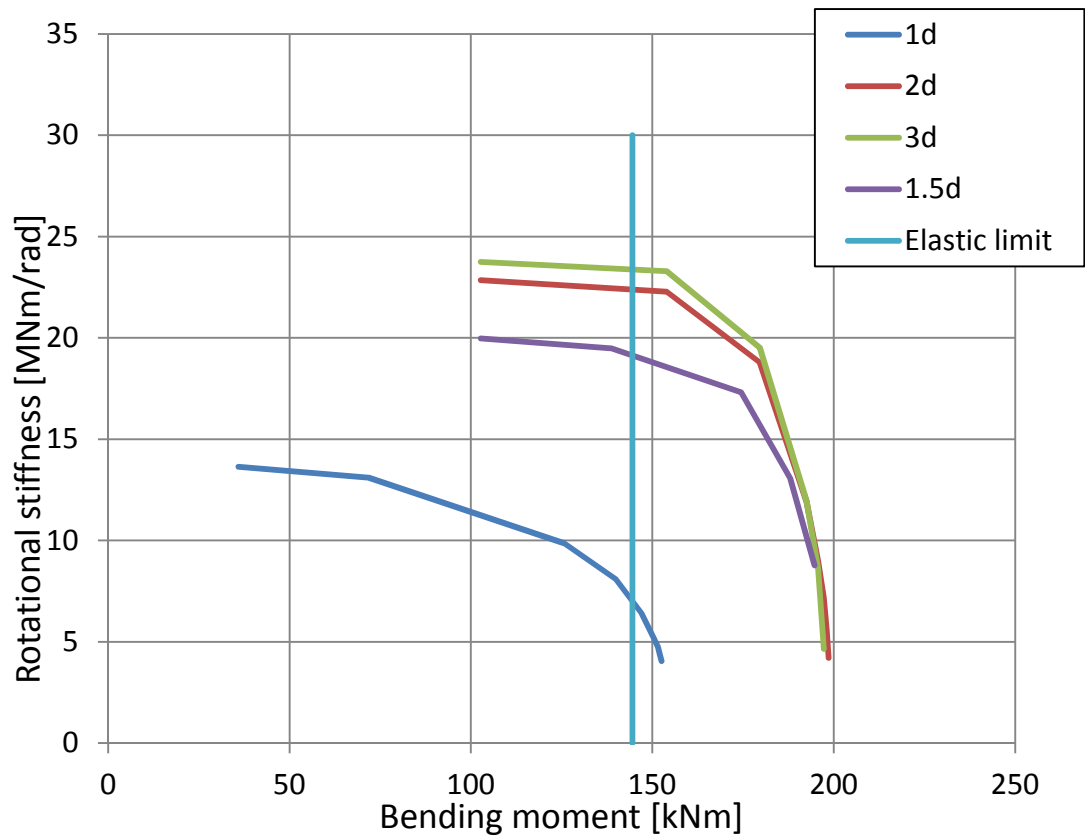


Chart 4.5: Rotational stiffness of a single 220/10 RD pile drilled 220 mm = 1*diameter to 660 mm = 3*diameter into the bedrock. The piles are grouted.

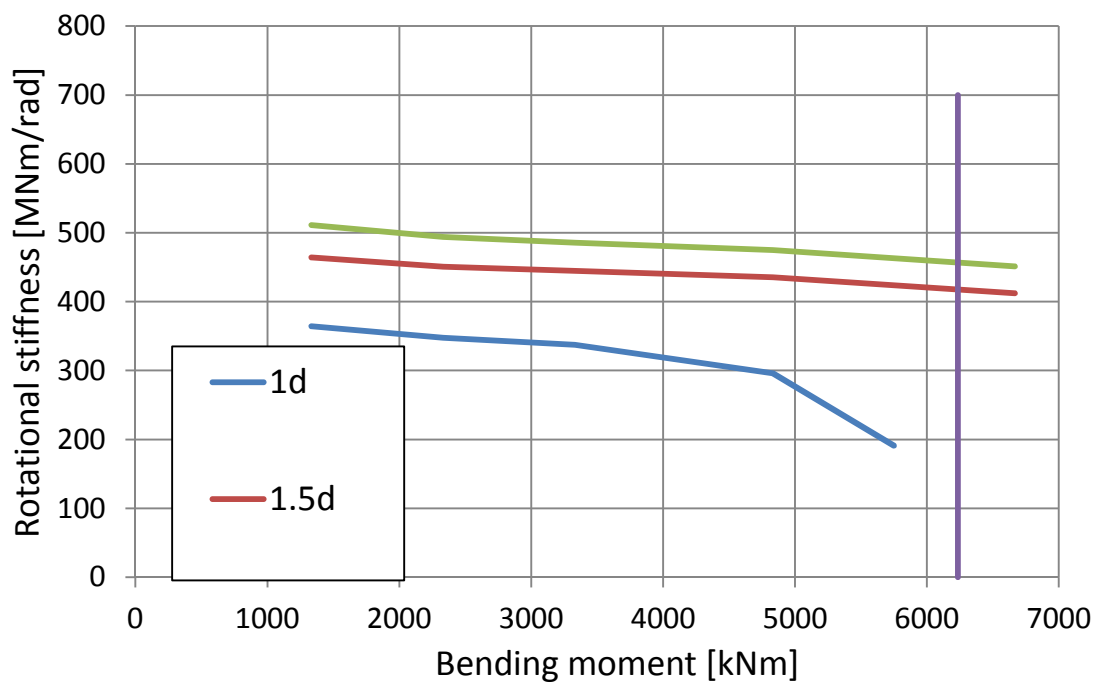


Chart 4.6: Rotational stiffness of a single 1220/12.5 RD pile drilled 1*diameter to 2*diameter into the bedrock. The piles are grouted. The load height is 3 m above bed-rock.

The FEM calculations in the case of clay in the drilling hole were not converged after the pile had moved and deflected in the drilling hole enough to reach the bedrock. Therefore, the calculations indicate only the first part of the pile's rotational stiffness. The calculated rotational stiffness values dependent on the bending moment level and drilling depth are shown in charts 4.7 to 4.9. The second part of the rotational stiffness would increase significantly due to bedrock supporting stress; however, the displacement of the wall at this point is so much that it would probably not be accepted. For example, if a pile were drilled with a 27 mm oversize one meter into bedrock, the displacement at the top of RD pile wall would about 270 mm for a 10 meters height wall if the wall were cantilever. In that case, the wall would probably be supported by a toe beam, significantly limiting the displacement. The typical calculated displacements at the bedrock level are much smaller than those seen in appendix 10, in which the displacement is approximately 2 mm.

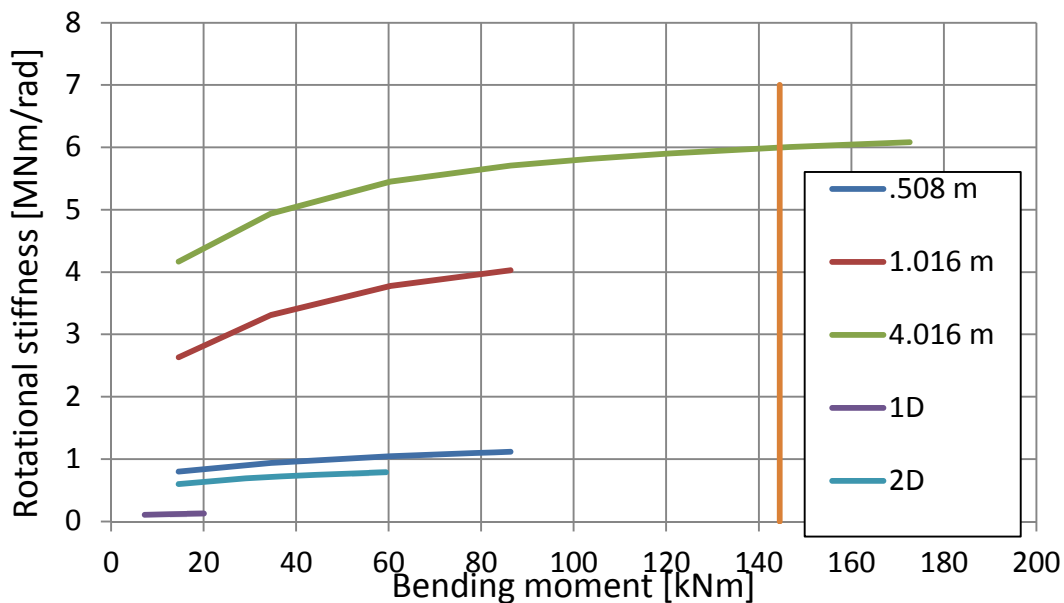


Chart 4.7: Rotational stiffness of a single RD 220/10 pile drilled $2.3 \times \text{diameter}$ to $18.3 \times \text{diameter}$ into the bedrock. The drilling holes of the piles are filled with clay.

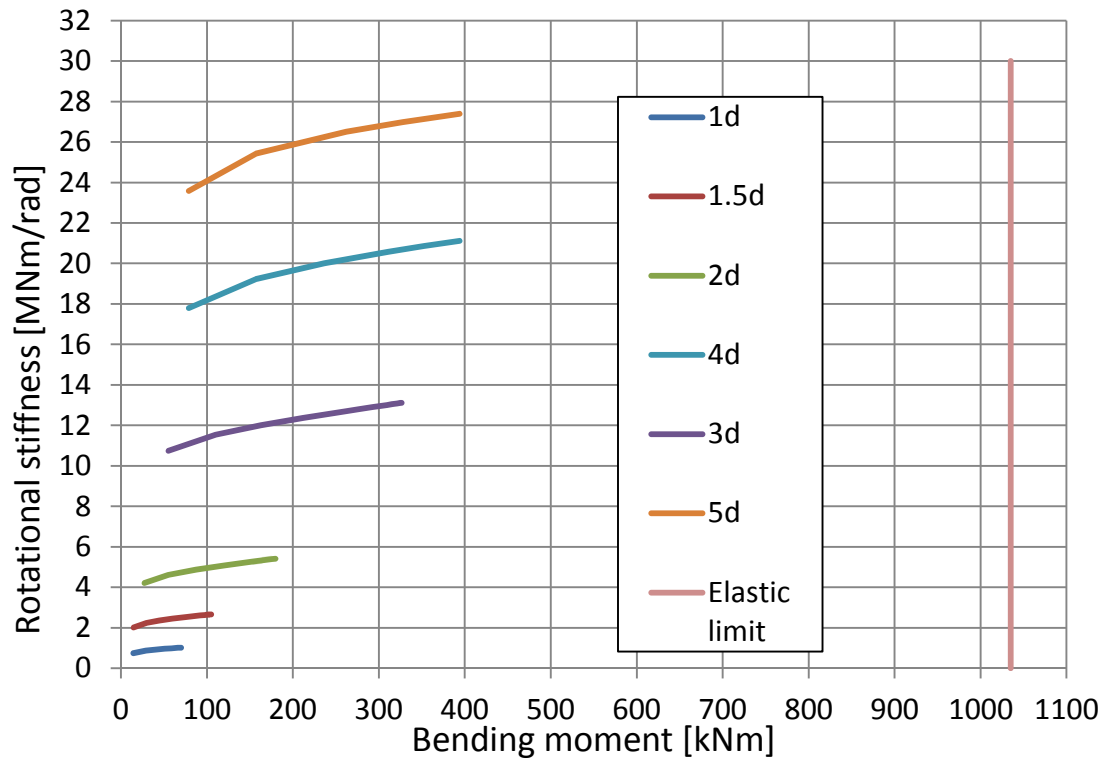


Chart 4.8 Rotational stiffness of a single RD500/12.5 pile drilled 1*diameter to 5*diameter into the bedrock. The drilling holes of the piles are filled with clay.

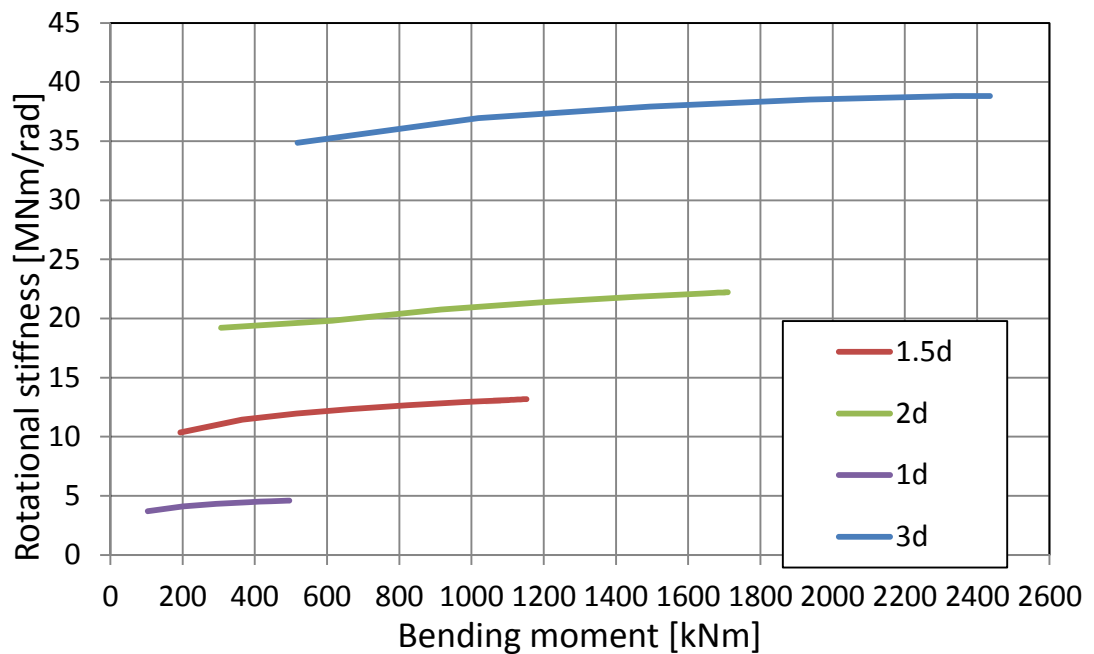


Chart 4.9: Rotational stiffness of a single RD1200/12.5 pile drilled 1*diameter to 3*diameter into the bedrock. The drilling holes of the piles are filled with clay.

Drilling depths of one and two times the pile's diameter (1d and 2d) were picked to estimate other pile sizes than the calculated RD220/10, RD500/12.5 and RD1200/12.5 piles. These piles are supposed to be drilled into the bedrock to a depth of at least three

times the pile's diameter. The reason for picking those drilling depths was that when the piles are grouted, the rotational stiffness does not increase much after a $2d$ drilling depth. When dimensioning a pile wall, a shorter drilling depth than the designer's specified drilling depth should be used for several reasons. When determining drilling depth, the sloping and roughness of the bedrock should be taken into account. When the designer uses a specific rotational stiffness value derived from the drilling depth in dimensioning the RD pile wall, a longer drilling depth may need to be used in the construction plan depending on the specific ground survey. Many times, the driller detects the bedrock level right away when one side of the pile reaches the bedrock. If drilling depth is measured from the first contact with the bedrock, the other side of the pile may not even reach the bedrock. In such a case, the rotational stiffness of the pile wall naturally will not fulfill the theoretical rotational stiffness. One diameter ($1d$) should be added to the calculated drilling depth on account of the bedrock sloping and another $1d$ in case the bottom of the drilling hole is filled with clay and grout will spread 1:2. Grout is then spread fully in the drilling hole. So, in a case where $3d$ is assumed for drilling the RD pile wall into the bedrock, $1d$ is justified for use in dimensioning the wall, anchors, etc. For ungrouted pile walls, $1d$ should be reduced in the structural calculations. On the other hand, a stiffer connection may be worse when considering the ultimate strength of the wall. That is why the real drilling depth should be calculated as well.

The results of table 4.3 can only be used directly for the piles mentioned in the table. Because the RD220/10 and RD 500/12.5 piles analyzed had different wall thicknesses, RD220/10 had to be replaced with an RD220/12.5 pile. In the rotational stiffness fitting, RD220/10 was replaced by RD220/12.5; the rotational stiffness estimate was calculated using the ratio of stiffness of pile RD220/10 and RD/12.5. The EI ratio of a 12.5 mm wall to a 10 mm wall is 1.207. When using thicker or thinner walls, the values should be adjusted proportionally by the EI ratio of pile in table versus the pile intended for use. The rotational stiffness will not decrease as rapidly, because the rotational stiffness of the connection will be affected by both the bending stiffness of the pile (EI) and the stiffness of the drilling hole surface (grout and bedrock). Table 4.5 calculates the same case with RD500/12.5, RD500/10 and RD500/8 piles. As shown, the rotational stiffness decreases slightly less than the EI of the pile. Inversely, when increasing the thickness of a pile wall, the rotational stiffness increases slightly less than the bending stiffness of the pile. When increasing rotational stiffness values for thicker piles, rotational stiffness values ends up being slightly overestimated, though it is very close, the inaccuracy being less than 2% in a one specific case shown in table 4.5.

Table 4.3 shows the difference between linear fitting and a better non-linear cubic function, which better fits the piles calculated. Appendix 8 shows least squared method fitting for other piles at different drilling depths and different load levels and with different materials in the drilling hole. At some point, the cubic fitting will overestimate the stiffness. At those points, a linear fitting is used. Appendix 8 contains more rotational stiffness estimation tables for all pile sizes. In the table, a correlation factor of $1/1.25 = 0.8$ is included; there is more on the correlation factor in section 4.1. Tables 4.4 and

4.3 reveal the major difference between grouted and ungrouted piles. The stiffness of piles with soft material in the drilling hole is typically 1-5% of that of a grouted pile when piles drilled one to two times diameter in to the bedrock. The difference decreases when drilling deeper. Chart 4.10 shows the rotational stiffness of grouted piles of different diameters. Chart 4.11 illustrates the cubic fit of piles not analyzed in the FEM analysis using least squares method. More specific calculations are given in appendix 8. Three piles and zero position values for rotational stiffness were known.

Table 4.3: Rotational stiffness of the grouted piles drilled 1d into the bedrock at 0.5*elastic bending moment level. This table can be used only at bending moment levels ranging from 0 to 0.5*elastic bending moment. S_i [MNm/rad] is the rotational stiffness of the pile's connection to the bedrock.

Appendix 8 Drilling depth and pile size relation to rotational stiffness

correlation factor $1/1.25 = 0.8$ is included, more of correlation factor in paragraph 4.1

Rotational stiffness of other pile sizes are fitted, drilling hole grouted

1d drilling depth, 0.5x elastic load

Pile	Diameter [mm]	Analysed according to FEM analysis	Cubic fit	Linear fit	Difference	Single piles: fitted S_i [MNm/rad]	Wall (RM-RF): fitted S_i [MNm/rad*m]
RD170/12.5	168.3		6.9	9.7	2.8	6.90	29.68
RD220/12.5	219.1	12.6	12.8	12.6	-0.2	12.62	44.58
RD270/12.5	273		20.8	23.7	2.9	20.78	61.68
RD320/12.5	323.9		29.8	34.1	4.4	29.76	76.71
RD400/12.5	406.4		46.9	51.0	4.1	46.93	99.76
RD500/12.5	508	71.9	71.8	71.9	0.1	71.79	125.51
RD550/12.5	559		85.5	86.2	0.7	85.50	137.24
RD600/12.5	610		99.9	100.5	0.7	99.85	148.15
RD700/12.5	711		129.6	128.9	-0.8	128.86	166.27
RD750/12.5	762		145.1	143.2	-1.9	143.18	173.34
RD800/12.5	813		160.6	157.5	-3.1	157.49	179.58
RD900/12.5	914		191.1	185.8	-5.3	185.84	190.02
RD1000/12.5	1016		220.7	214.5	-6.3	214.48	198.59
RD1200/12.5	1220	271.7	271.7	271.7	0.0	271.74	211.64

Table 4.4: Rotational stiffness of the piles with clay in the drilling hole, piles drilled 1d into the bedrock at 0.5*elastic bending moment level. This table can be used only at bending moment levels ranging from 0 to 0.5*elastic bending moment. S_i [MNm/rad] is the rotational stiffness of the pile's connection to the bedrock.

Rotational stiffness of other pile sizes are fitted, clay in the drilling hole
Least squared method

1d drilling depth, 0.05x elastic load

Pile	Diameter [mm]	Analysed according to FEM analysis	Cubic fit	Linear fit	Difference	Single piles: fitted S_j [MNm/rad]	Wall (RM-RF): fitted S_j [MNm/rad*m]
RD170/12.5	168.3		0.12	0.08	-0.05	0.077	0.33
RD220/12.5	219.1	0.10	0.18	0.10	-0.08	0.100	0.35
RD270/12.5	273		0.26	0.23	-0.03	0.226	0.67
RD320/12.5	323.9		0.34	0.34	0.00	0.340	0.88
RD400/12.5	406.4		0.49	0.54	0.04	0.495	1.05
RD500/12.5	508	0.77	0.72	0.77	0.05	0.722	1.26
RD550/12.5	559		0.85	0.97	0.11	0.852	1.37
RD600/12.5	610		0.99	1.16	0.17	0.993	1.47
RD700/12.5	711		1.30	1.54	0.24	1.302	1.68
RD750/12.5	762		1.47	1.74	0.26	1.474	1.78
RD800/12.5	813		1.66	1.93	0.28	1.656	1.89
RD900/12.5	914		2.05	2.32	0.27	2.048	2.09
RD1000/12.5	1016		2.49	2.70	0.22	2.485	2.30
RD1200/12.5	1220	3.48	3.49	3.48	-0.01	3.480	2.71

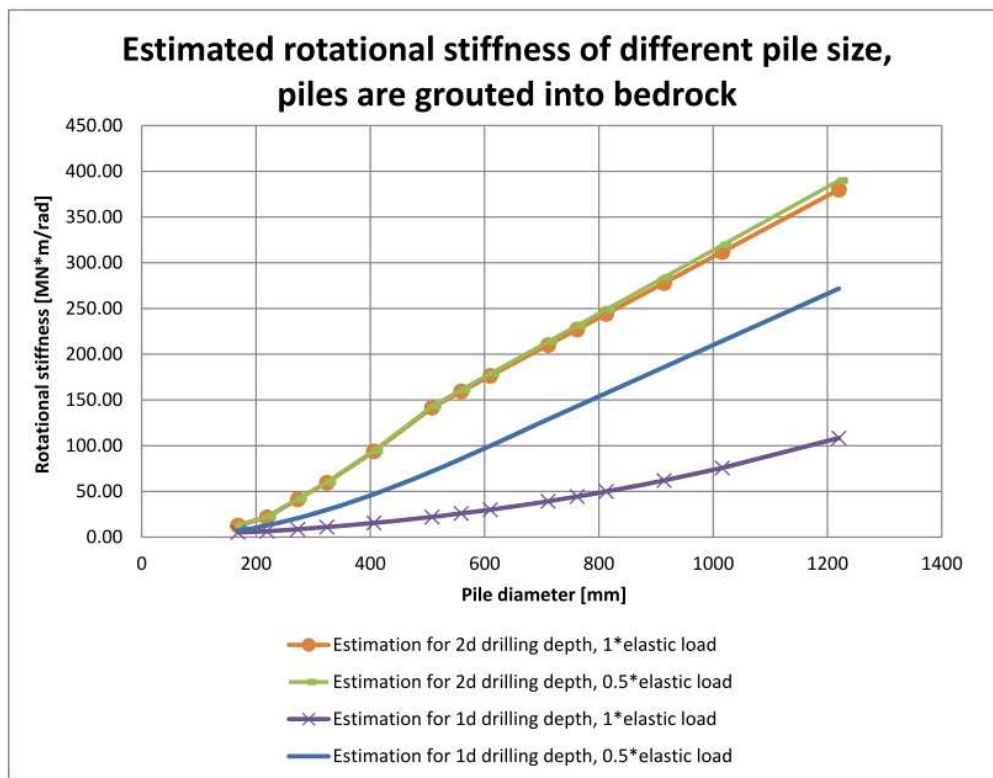


Chart 4.10: Rotational stiffness estimates for different pile sizes when the piles are drilled 1d or 2d into the bedrock and grouted. The rotational stiffness is shown at the maximum elastic bending moment and half moment.

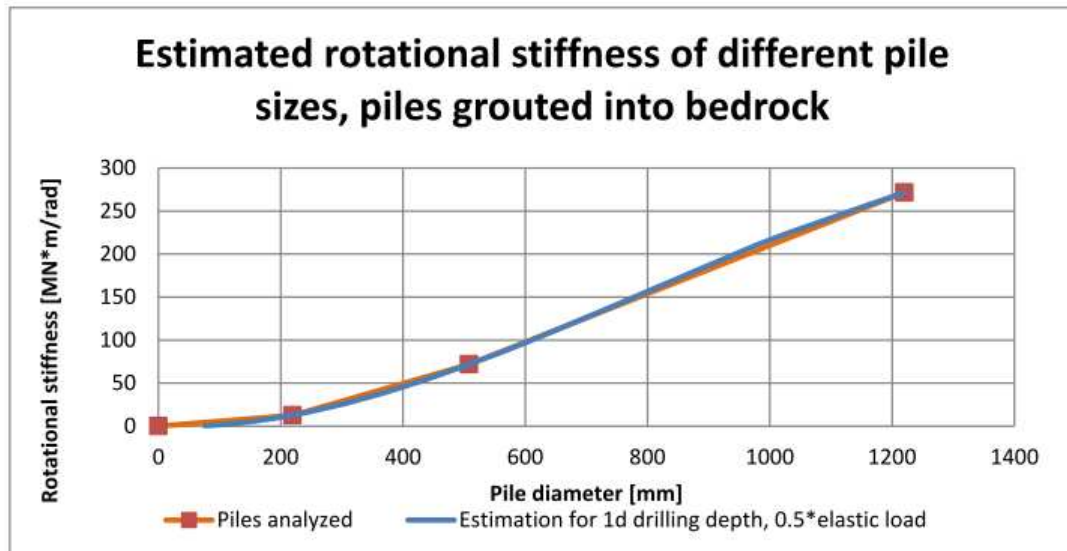


Chart 4.11: Rotational stiffness of the grouted piles drilled 1d into the bedrock at 0.5*elastic bending moment level. The rotational stiffness for the remaining piles was estimated by cubic fit.

Table 4.5: Wall thickness in relation to rotational stiffness of the pile's connection to the bedrock. The table features calculations for same case as in section 4.1.1 with 500/12.5, 500/10 and 500/8 piles.

0.5* elastic load			Pile lenght		2.333 m					
Pile	Elastic load [kN]	Elastic bending moment[kN*m]	f _{total}	f _{pile}	S (0.5*F)	W _{el} [cm ³]	EI [kN*m ²]	EI vs. 500/12.5	S(0.5*F) vs. 500/12.5	relational increase of S
500/8	292	681	19.91	6.42	117.7395	1546.5	82488	0.66	0.66	0.52 %
500/10	361	841	19.96	6.42	144.9311	1910.2	101893	0.81	0.81	0.18 %
500/12.5	444	1036	19.98	6.42	178.1846	2352.6	125486	1.00	1.00	0.00 %

0.85* elastic load			Pile lenght		2.333 m					
Pile	Elastic load [kN]	Elastic bending moment[kN*m]	f _{total}	f _{pile}	S (0.5*F)	W _{el} [cm ³]	EI [kN*m ²]	EI vs. 500/12.5	S(1*F) vs. 500/12.5	relational increase of S
500/8	292	681	38.42	6.42	49.65	1546.5	82488	0.657	0.669	1.72 %
500/10	361	841	38.66	6.42	60.87	1910.2	101893	0.812	0.820	0.96 %
500/12.5	444	1036	38.97	6.42	74.25	2352.6	125486	1.000	1.000	0.00 %

1* elastic load *			Pile lenght		2.333 m					
Pile	Elastic load [kN]	Elastic bending moment[kN*m]	f _{total}	f _{pile}	S (0.5*F)	W _{el} [cm ³]	EI [kN*m ²]	EI vs. 500/12.5	S(1*F) vs. 500/12.5	relational increase of S
500/8 *	292	681	101.38	6.42	16.73	1546.5	82488	0.657	0.419	-36.19 %
500/10 *	361	841	88.99	6.42	23.76	1910.2	101893	0.812	0.596	-26.62 %
500/12.5 *	444	1036	67.01	6.42	39.88	2352.6	125486	1.000	1.000	0.00 %

* unkonverged solution in FEM analysis

4.2 RD pile wall calculations using different joint types

All geotechnical calculations were done using Novapoint GeoCalc 2.4. The model was based on the example model by Vianova Systems Finland Oy shown in the document

“Tukiseinä: Vianova Systems Finland Oy: Versio 2.3:27.01.2012.” Figure 4.12 shows GeoCalc model, in which the RD pile wall connection to the bedrock is modeled as a hinge. For the GeoCalc calculations, typical RD pile wall conditions were chosen. Above the bedrock, there is one meter of moraine. Above the moraine is a layer of clay, and at the ground surface is a layer of rock waste. Rock waste layers are typically hard to penetrate with sheet piles, so an RD pile wall may be the only option. The GeoCalc calculation procedure is introduced in reference 36. Calculation examples can be found in reference 31.

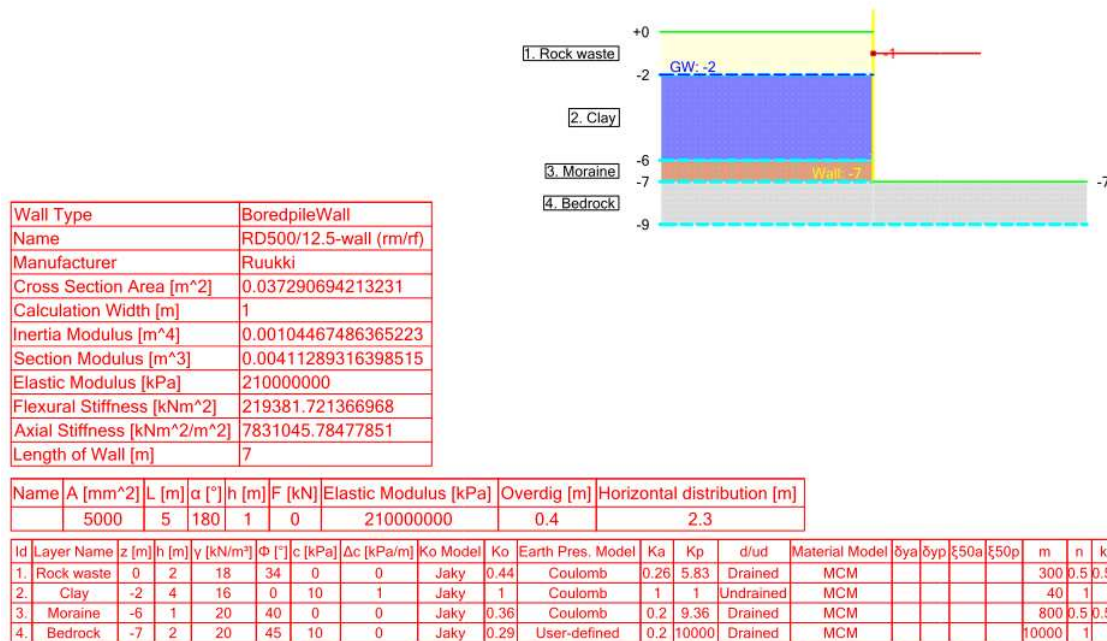


Figure 4.12: RD pile wall GeoCalc calculation example. This figure is also in appendix 6.

It was not simple to estimate rotational stiffness into the GeoCalc geotechnical model. In GeoCalc, it is not possible to create rotational support from a spring. The rotational stiffness values S_j were calculated in appendix 2 according to SFS EN 1993-1-8 in appendix 2. There are two options for adjusting the rotational stiffness in GeoCalc. The bedrock has to be made of soil, and the pile must be drilled into that soil. One option is to give the bedrock very high m and K_p values. The other option is to add a horizontal anchor at the bedrock level. There is limitation concerning anchors in GeoCalc. Anchors at the bedrock level cannot be activated before upper anchors are activated. As a result, piles in the bedrock will deflect more than in real life before the upper anchor levels will be activated. Bigger deflection at the beginning of excavation is compensated by using stiffer bedrock values and anchors at the level of the bedrock. The stiffness parameters of bedrock and extra anchor were set that the total deflection was equivalent to the deflection in the Ansys FEM model. Horizontal support can be added at the bottom level of the pile using a rock bolt. A bending-moment-free RD pile wall can be made by end-

ing the pile wall at the bedrock level and adding a rock bolt at the bottom level of the pile.

Table 4.6 compares different example models. A 500/12.5 pile wall was calculated using different bedrock supports. Bending moments, forces and displacements at the top of bedrock were compared. Hinge connections used in comparison had vertical and horizontal support created by a very stiff anchor and no bending moment support. In the “rock” option, the pile extended into the rock. The rock was modeled as soil with very high m and K_p values. In the “anchor+rock” model, the pile was extended into the rock as in the “rock” model, but an extra anchor was also added at the bedrock level. The Ansys model most accurately represents the behavior of the bedrock connection. The Ansys model displacement is 84 times smaller than the “anchor+rock” connection. The “anchor+rock” example greatly underestimates the effect of the bedrock when the drilling hole of the pile wall is grouted.

Table 4.6: Bending moments and displacements compared by type of joint at the toe of pile wall and with or without a rock anchor. The RD500/12.5 pile is grouted into the bedrock. Hinge, “anchor+rock” and “rock” are example calculations included in Novapoint GeoCalc 2.4 and are also discussed in Vianova Systems Finland Oy 2012 [31].

Geocalc calculations

Pile

500/12.5

Comparing bending moment and displacement of Novapoint Geocalc 2.4. example models

	Hinge	Anchor+rock	Rock	Ansys
M_support [kNm]	0	158	120	1810
M_wall [kNm]	217	135	175	
F_anchor [kNm]	225	160	190	
F_anchor in rock [kNm]	-	230	-	
Rock bolt [kNm]	150	50	86	
Displacement_upper level of rock [mm]	0.15	1.17	2.38	0.16

Models without rock bolts were tested in this thesis, and the models did not work at all. Horizontal displacement went in the opposite direction as loading, which cannot be the case. The GeoCalc models were calculated with a rock bolt. Because rock bolts bring horizontal displacement to approximately zero at the toe of the pile, the displacement at the upper level of the bedrock in the GeoCalc models is set to be the displacement difference between the upper level of the bedrock and the toe of the pile. The different treatment of displacement in the bedrock drilling hole in Ansys and GeoCalc models is illustrated in figure 4.13. For example, displacements calculated in Ansys are given in figure 4.8.

Pile's displacement in bedrock Pile's deflection is ignored

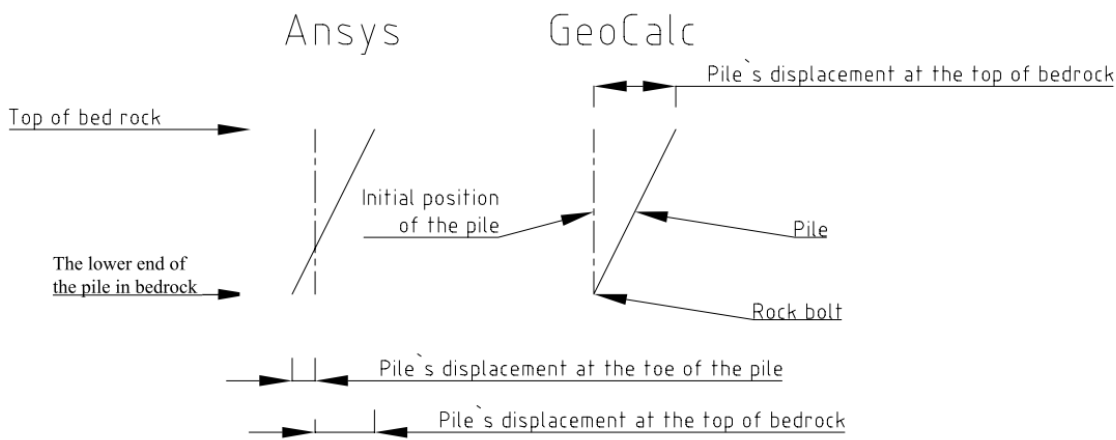


Figure 4.13: Comparison of pile displacement in the Ansys and GeoCalc models

The required displacement for the GeoCalc model at a specific bending moment level is calculated in appendix 2. For example, the displacement of 500/12.5 piles grouted into the bedrock at the top of the bedrock level is 1.01 mm and at the toe of pile is -0.37 mm at the elastic load (see figure 4.8). From the difference in the pile's displacement at the top of the bedrock and at the toe of pile and considering the bending moment level, the target displacement in the GeoCalc calculation will be 0.16 mm at a bending moment level of 250 kNm/m. A displacement of 0.16 mm can only be satisfied by using both high m ($=10000$) and K_p ($=10000$) values and an additional horizontal anchor at the bedrock level. The effect of added bending moment stiffness in the joint increased the maximum moment from 220 to 250 kNm (see figures 4.14 and 4.15). The maximum bending moment moved from the span to the support. On the other hand, the maximum displacement of the RD pile wall decreased significantly from 10 mm to 4.75 mm. In that case, the structural dimensioning was not restrictive. According to the calculation in appendix 2, the utilization rate of the RD pile wall structural capacity was only 18.6%. If there were a building with a pile foundation, the maximum horizontal displacement allowed would be 10 mm [31]. According to the calculation in appendix 2, the pile size can be downsized to 320/10 if the bottom of the pile wall is grouted. In that case, the horizontal displacement is still a greater determinant than the structural strength of the pile.

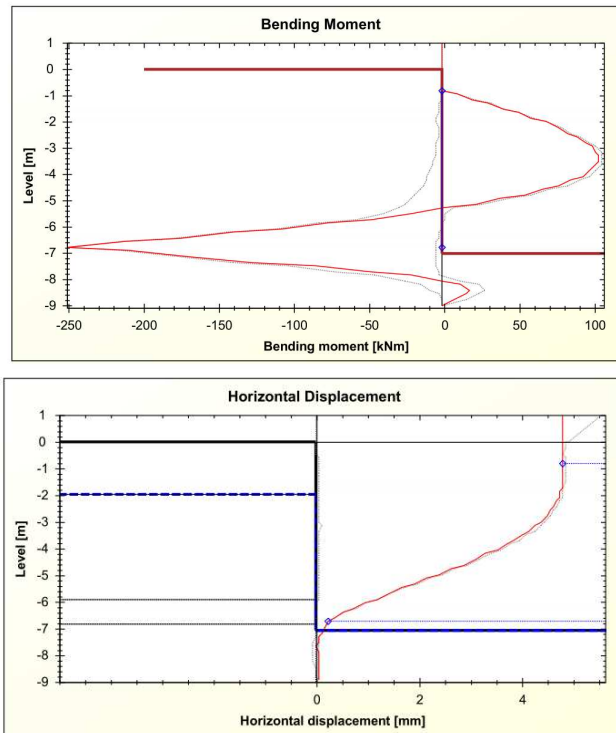


Figure 4.14: 500/12.5 RD pile wall with connection reflecting the rotational stiffness of a pile wall grouted into the bedrock. Better figures are included in appendix 5.

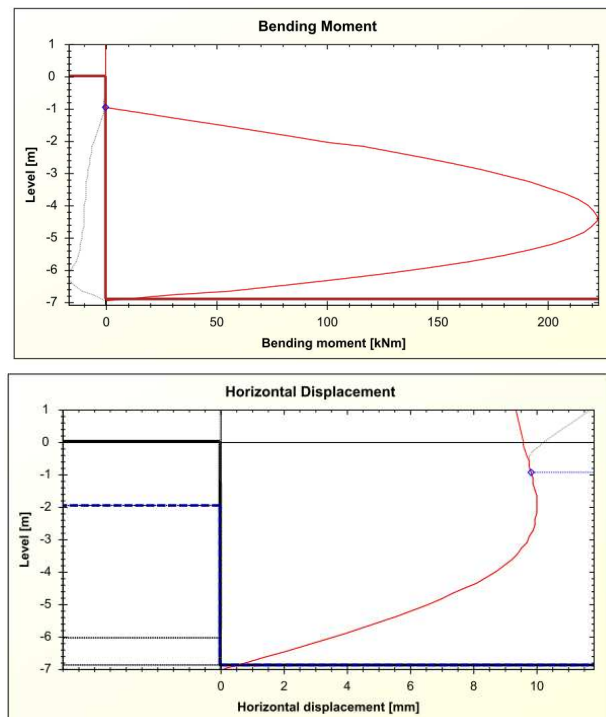


Figure 4.15: 500/12.5 RD pile wall with a bending-moment-free connection. The model was calculated using the example model by Vianova Systems Finland Oy. Better figures are included in appendix 5.

When testing the GeoCalc model by modifying the drilling depth of the cantilever RD pile wall, the calculations evidenced the weakness of the model. When decreasing or increasing the drilling depth, the horizontal displacement rises. The reason is that with a smaller drilling depth, the stiffness of the anchor at the bedrock level should be reduced to fit the Ansys displacement. When increasing the drilling depth, the distance between the additional anchor and the rock bolt increases and pile will deflect more while the bedrock modeled as soil is not stiff enough. A better model in GeoCalc could be to model with no bedrock and with additional anchors frequently added through the bedrock.

Another material that may appear in the gap is clay. In the horizontal load test, there was one pile tested that had clay and very little or no cement in the gap. As seen in figure 4.9, the displacement rises dramatically. Second weakest material tested was soil sample 1. The rotational stiffness of clay, the weakest material, and soil sample 1 were calculated in appendix 2. The calculations show that very different materials dry crust clay and soil sample behave same way at low stress level. Clay had as a linear material elastic modulus and sample 1 had non-linear elastic modulus. Even though the soil sample has a much higher elastic modulus at high stress levels, the rotational stiffness is very similar from 0*elastic load to 0.1*elastic load. At the full elastic load, the rotational stiffness of medium dense moraine (soil sample 1) in the gap is almost twice as large as with dry crust clay in the gap (58870 kNm/rad vs.33440 kNm/rad). These values are included in appendix 2. Although piles with a much softer material in the drilling hole and thus lower rotational stiffness than grouted piles, the mobilized support bending moment is still remarkable as seen in appendix 10. The GeoCalc calculation in appendix 10 represents both clay and the soil sample 1. Table 4.7 shows the effect of joint rotational stiffness on horizontal displacement. Even without grouting, the joint of a pile wall in the bedrock will decrease displacement by 25% in that specific case compared to nominally pinned joint.

Table 4.7: Horizontal displacement of the wall with different fixing to the bedrock. The rotational stiffness is shown at a specific bending moment level.

RD 500/12.5 Geocalc example joint comparison

Jointype	Rotational stiffness according to Ansys calculation	Bending moment of the join in Geocalc	Displacement difference toe- top of bed rock	Maximum displacement of the wall	displacement decrease vs nominally pinned
	[MN*m/rad]	[kN*m/m]	[mm]	[mm]	[%]
Grout	164	250	0.191	4.9	51 %
soi sample1	33.4	150	2.6	7.5	25 %
clay sample	34.2	150	2.3	7.5	25 %
nominally pinned	0	0	-	10	-

5 PROPOSED DECISION

This thesis' objective of specifying the rotational stiffness of the pile wall was reached partly. The site tests and FEM calculations yielded accurate rotational stiffness values for RD220/10, RD500/12.5 and 1200/12.5 at different drilling depths and for the different material values investigated in this thesis. The horizontal load test was conducted for clay, grout and tightly packed drill cuttings with cement present in the drilling hole. Frictional soil or pure drill cuttings were not load-tested. For other pile sizes, the non-linear fitting was done using the investigated pile sizes.

Simple RD pile wall dimensioning examples were made to illustrate the effect of rotational stiffness. Displacement of the wall and stress on the wall were made using GeoCalc. Calculations showed that grouting the bedrock drilling hole significantly decreases displacement and that drill cuttings as well as very soft materials like clay also provide rotational support for the wall. Pile size, the number of anchors or anchor size can be reduced with a stiffer connection to the bedrock.

The other objective of investigating the effect of grouting on watertightness was mainly reached. The study showed the method used to calculate water leakage through the drilling hole, and leakage was also compared to leakage via interlocks. The method used to calculate watertightness in this thesis was not very accurate, however. The water permeability of material can vary significantly. The inaccurate water penetration test equipment also limited the conclusions of the tests. The permeability of water was defined for drill cuttings from drilled single piles in water penetration tests. The spreading of grouting from drilling holes of single piles to other holes created additional inaccuracy for tests of the water permeability of drill cuttings. The soil material test in the laboratory provided water permeability values as well. Grout permeability values were investigated in the literature, since the water permeability of concrete is rather small and water penetration test margin of error was too big to conclude water permeability values for grout.

Material investigation of drill cuttings or soil in the drilling hole was performed. Grading analysis was performed on drill cuttings found in the RD pile wall drilling hole at the Masku test site. The strength and elastic properties of hardened grout and bedrock next to the drilled RD pile wall were examined. Also, some hardened drill cuttings with cement samples were solid enough to be tested.

Some useful experiences from site practices was gleaned from the Masku RD pile test site and other RD pile construction sites. Different grouting methods were tested to determine a best practice for grouting RD pile drilling holes in bedrock. The background grouting of the RD pile wall was tested.

5.1 Supporting pile wall into the rock

The wall can be supported by toe bolts when pile wall is not drilled into the bedrock. When using toe bolts, sufficient watertightness must be addressed. This can be done by constructing a toe beam after excavation. In that case, leakages may occur before beam is made.

A more useful way to address both the watertightness and structural stiffness of the pile wall is to drill piles deep enough into the bedrock. When piles are deep enough in the bedrock, toe beams and toe bolts are no longer needed.

A reasonable theoretical drilling depth according to rotational stiffness analysis seems to be around two times the diameter of the pile when the bedrock drilling hole is grouted. The stiffness does not increase much if the piles are drilled deeper. If drilling hole is not grouted and there is a risk that clay-like soft materials will fill the drilling hole gap, the rotational stiffness will increase from a drilling depth of two times diameter to at least 18.3 times diameter for the RD220/10 pile analyzed. The rotational stiffness of the pile with soft material in the drilling hole gap is a fraction of the grouted pile's stiffness at typical drilling depths. According to the material test, medium dense moraine in the drilling hole exhibited behavior similar to dry crust clay in the gap at the stress level in the calculated example.

With regards to the 2d drilling depth, a shorted drilling depth than will actually be executed can be used in pile wall dimensioning due the bedrock sloping and potentially imperfect grouting at the toe of the pile wall. For non-grouted piles, a 1d reduction is sufficient. In fractured bedrock cases, the drilling depth has to be considered on a case-by-case basis. Also, the real drilling depth should be calculated, because it may be the worst case scenario.

When the bedrock drilling hole of an RD pile wall is not grouted, the rotational stiffness of the connection should be assumed to both very stiff like grouted and also nominally pinned or as stiff as clay. RD pile wall should be dimensioned using both cases. According to EN 1993-1-8, both grouted and clay gaps are defined as semi-rigid joints in most cases.

To achieve watertight structures, drilling holes should be grouted. The drilling depth of one time diameter is the absolute minimum to establish continuous grout spreading in drilling hole. Deeper drilling into the bedrock is recommended. When piles are drilled to only 1d in the bedrock, a toe beam or some other form of horizontal support should be executed. When there is not a watertightness requirement and the rotational stiffness of the bedrock connection is not required, the drilling hole does not need to be grouted.

5.2 Pile and bedrock interface grouting

Soil conditions play a major role in grouting. If there is clay above the bedrock, grouting the base of the pile wall is reasonable to achieve a significant improvement in rotational stiffness. Grouting the base will decrease horizontal displacement of the pile wall

and will decrease the bending moment in the middle of the pile wall. Smaller displacement makes it possible to decrease pile size, anchor size or the number of anchors in some cases. Grouting the base of the pile wall may thus save customers money. Grouting the drilling hole also prevents horizontal movement of the wall in the drilling hole. In theory, the whole wall may move in the drilling hole by a length equal to the drilling oversize. This may occur when the hole is empty or contains a very soft material, such as clay.

Another reason to grout the gap is to improve watertightness. The watertightness of an ungrouted gap in the pile wall is more unreliable and will not be as tight as if it were grouted. In some projects, grouting the gap may be only option due to strict watertightness requirements.

It may be better to grout the RD pile wall toe before doing any curtain grouting to avoid grouting channel blockages. If the bedrock is badly fractured, it may be better to do curtain grouting before toe grouting to prevent grout from flowing only into the fractured bedrock. RF interlocks cannot be reused in grouting if the channel is not cleared after grouting. Piles can be concreted before or after toe grouting or at the same time. If grouted first and the grout tends to flow into the pile without designed reinforcement, the grouting should be done after the pile is concreted.

5.3 Limitations of this study

To determine rotational stiffness, the drill cuttings and soil in the gap between the bedrock and the pile wall were calculated as a modified concrete. The ultimate compression, tensile strength and elastic modulus were modified. Treating soil as a concrete may result in some inaccuracy. There was no clear horizontal load test case where the gap was filled with only soil or drilling mud without any cement, and as such, the result is not fully reliable. In a case where there was grouting or tightly packed drill cuttings with cement in the gap, the result of the theoretical FEM calculations and the practical load test results were almost the same.

The Ansys FEM model worked quite well when pile was fully and successfully grouted or when there were tightly packed soil/drill cuttings with cement in the gap. In the case of very loose material in the gap, however, the elastic modulus of the material had to be set very low. The grout material elastic modulus had to be divided by 1000 to equal the deformation in the tested pile. That said, the elastic modulus equals that of dry crust clay. The strength of the material must even then be similar to the strength of grout, and strain is therefore much larger than with concrete material. Elastic modulus assumption conflicts with the measured modulus of the clay sample though in different conditions due to the drying and possible hardening of potential cement. The strain must be that big, because in reality, the pile displacement in the bedrock drilling hole was more than 10 mm in a 27 mm gap. In site test, the clay behaved differently in the gap. Clay tends to rise from the drilling hole. In the FEM model, that kind of behavior is not easy to model.

The GeoCalc calculations and Mathcad calculation linked to GeoCalc were made to be very simple examples. The calculations may not include all the instructions from SFS EN 1997, etc. The purpose of the calculations was to demonstrate the effect of the rotational stiffness at the bottom of the pile on the dimensioning of the pile wall. The rotational stiffness from the horizontal load test and FEM calculations could not be modeled in GeoCalc very accurately, because torsional spring could not be added in GeoCalc. The rotational stiffness was modeled in GeoCalc by setting the pile displacement in the drilling hole to be same as in the Ansys FEM calculations.

The FEM calculations were made using Ruukki RD piles and the recommended oversized drilling for FM/RF interlocks. The sizes were picked from source [1]. The rotational stiffness will not be same if the drilling oversize is different or if the piles have different dimensions.

The GeoCalc calculations may not be accurate. In the model where bedrock is modeled by using both rock as a soil and an additional anchor at the top of the bedrock level, the behavior was different when using different drilling depths. The anchor and bedrock parameters should be selected carefully to obtain a realistic deflection inside the bedrock. Also, an extra additional anchor or even several anchors should be added inside the bedrock to limit pile deflection inside the bedrock. It is worth considering creating a better model. The best and simplest model would be a model with support and the rotational spring at the top level of the bedrock. In GeoCalc, that is not possible at the moment.

The design resistance of bedrock is discussed very briefly in this thesis. This matter should be considered when drilling piles to a short depth or when the rock excavation is next to a RD pile wall.

The calculated water leakages through the bedrock drilling hole were rather excessive. The water permeability values were calculated values from the water penetration test and analyzed from the soil samples. When working on this thesis and other development work in Ruukki for nine months any leakage problems through the drilling hole was not heard. The leakages measured and calculated in thesis may not accurately reflect the real situation because of the huge variation in soil permeability values due to different soils. In the test, the water flowed upwards from the toe. In real RD pile walls, the water flow direction is partly downward, which tends to compact the soil in the drilling hole gap. Another uncertainty is the movement of soil particles into the drilling hole gap and away from the gap, carried by water. In real project monitoring, it may be reasonable to carry on to find out if the calculations are accurate or not. When the RD pile wall piles are concreted, the water path will be more limited, flowing mainly through the area below the interlock.

The rotational stiffness of the toe of the pile wall is determined only until the elastic limit stress level of the piles. After the piles become plastic, the rotational stiffness decreases rapidly as the piles themselves will deform more and more with only a little additional force.

5.4 Suggestions for further research

This study shows that the material in the gap between the piles and the bedrock may vary depending on the drilling conditions, bedrock type and soil on top of the bedrock. Ongoing RD pile wall sites should be study more accurately to take advantage of packed drill cuttings for structural aspects and watertightness. If the appearance of tightly packed drill cuttings in the gap can be assumed reliably, there may be no need to grout the gap in some cases.

More research should be done to understand the grouting of bedrock drilling holes. From the research at the test site, some information was found. Most focus should be paid to preventing the interlock injection channel from blocking at the toe of the channel. The top of channel can easily be closed when drilling the next piles. Another remarkable thing would be to test the effect of different water-to-cement ratios on grout spreading. The use of water-reducing agents may also be tested. At the Masku test site, a 0.55:1 water-to-cement ratio was used without any additives. More water makes the grout weak, and less water would make the grout mass too thick to grout. In upcoming RD pile test sites, the optimal thickness of the soil above the bedrock should be approximately two meters when using 220 to 500 piles.

In this thesis, the rotational stiffness of the RD pile wall was determined using specific pile sizes, gap materials and bedrock values. This thesis gives information how to determine rotational stiffness using FEM calculations but does not give simple equations for rough estimates of rotational stiffness. With the simple calculation equations in this thesis, where pile is assumed to be solid, the rotational stiffness of the drilling hole will predicted with greater inaccuracy the more drilling depth increases. Pile deflection must be taken into account in a hand calculation. It would be useful if there were an equation to calculate the required drilling depth to fulfill the rotational stiffness required or an equation to predict the rotational stiffness in each case. It may be calculated from the deflection curve using the geometrical values of the hole and pile, the drilling depth and the material values of the gap and bedrock; however, the additional value of a hand calculation may be restricted, because the rotational stiffness of any pile can be approximated from piles already investigated. The rotational stiffness tables in appendix 8 would be slightly more accurate, if the RD220/10 pile would be replaced by the RD220/12.5 pile after analyzing it. After that, the remaining pile sizes could be calculated more accurately. The rotational stiffness tables for ungrouted piles with a deeper drilling depth can be calculated, because the rotational stiffness increases even after a drilling depth of twice the pile diameter.

At the moment, it is not possible in GeoCalc to add torsion spring at the bottom of RD pile wall to add rotational stiffness. One of the easiest ways to create rotational stiffness is by using torsion springs. The value of the spring could be taken from this thesis for different pile sizes, drilling depths, etc.

The evaluation of frictional soil or drill cuttings in the drilling gap was not as reliable as clay or drill cuttings with cement or grout due to lack of a load test. Horizontal load

tests for different soil materials could be considered. That said, the extreme cases of clay as the least stiff material and grout as most stiff material were investigated, and the different soil materials in between those materials will not produce much benefits.

REFERENCES

- [1] Retaining wall solution for all conditions: Ruukki RD pile wall. [WWW]. [2013]. Available at:
<http://www.ruukki.com/~media/Files/Infrastructure-solutions/Retaining%20walls%20brochures%20and%20data%20sheets/Ruukki-RD-pilewall%20EN.pdf>

- [2] Uotinen, V-M Jokiniemi, H: 2012: RD PILE WALL – A NEW WAY TO BUILD MICROPILE RETAINING WALL STRUCTURES

- [3] SFS-EN 1997-1, 2005, Eurocode 7: Geotechnical design. Part 1: General rules

- [4] RIL 263-2013 Kaivanto-ohje LUONNOS 3.6.2013

- [5] Collins N 2011 Master's thesis: Support and sealing at the toe of a retaining wall extending to bedrock: theory and practice

- [6] Tiehallinto (Juha Heinonen,. Sami Eronen,. Jouko Lehtonen etc., 2001, Porapaalutusohje: Suunnittelu- ja toteuttamisvaiheen ohjaus.

- [7] Raveendra Babu R. 1 , Gurmail S. Benipal 2, and Arbind K. Singh 3, Plasticity-based constitutive model for concrete in stress space 2006

- [8] PLASTICITY. Flow rule for kinematic hardening. Cited on 05 November 2013. Available at:
http://www.solid.iei.liu.se/Education/TMHL55/TMHL55_lp1_2010/lecture_notes/plasticity_flow_rule_kinematic_hardening.pdf

- [9] Čanađija, M. & Brnić, J, A MIXED ISOTROPIC - KINEMATIC HARDENING MODEL FOR THERMOPLASTICITY 2008

- [10] Riihimäki T etc., RIL 254-2011 paalutusohje, 2011

- [11] European Standard EN 1993-1-8:2005, Eurocode 3: Design of steel structures. Part 1-8: Design of joints, 2005

- [12] "HKR (Helsingin kaupungin rakennusvirasto) -Rakennuttaja", 2011 JÄTKÄSÄÄREN MAANALAISET TILAT LUOLAN UUDISRAKENNUS HANKESUUNNITELMA 2011, HELSINGIN KAUPUNKI, TASKE, KSV, STARA

- [13] MAIN ROADS Western Australia, 1998 WATER PERMEABILITY OF HARD-ENED CONCRETE. Available at:
https://www.mainroads.wa.gov.au/Documents/wa625_2.pdf
- [14] European Standard EN 12063:1999 Execution of special geotechnical work. Sheet-pile walls
- [15] Peisa, A: Lemminkäinen infra Oy, 2012. RD-paaluseinä osana Länsimetron Rakentamista, presented in “Teräspaalu päivä 26.1.2012 Messukeskus, Helsinki”. Available at:
<http://www.ruukki.fi/~media/Finland/Files/Infra/Seminaarimateriaalit/Teraspaalupaiva%202012/RDpaalusein%20osana%20Lnsimetron%20rakentamista%20Annina%20Peisa%20Lemminkinen.ashx>
- [16]] European Standard EN 197-1:2012. Cement. Part 1: Composition, specifications and conformity criteria for common cements
- [17] European Standard EN 196-1:2005. Methods of testing cement. Part 1: Determination of strength
- [18] Aalto University. Course Rak 50.2122, Geotekniikan perusteet, Osa A-johdatus ja painuma. Cited on 22 October 2013. Available at:
https://www.google.com/url?sa=t&rct=j&q=&esrc=s&frm=1&source=web&cd=2&cad=rja&ved=0CCsQFjAB&url=https%3A%2F%2Fnoppa.aalto.fi%2Fnoppa%2Fkurssi%2Frak-50.2122%2Fluennot%2FRak-50_2122_luento1b.pdf&ei=3FZmUpf3Ks2y7Ab614DAAg&usg=AFQjCNF5Wp-3bhuya-9YSDqc4qgrNWetMw&bvm=bv.55123115,d.ZGU
- [19] Leivo, V, Rantala, J, 2000, maanvaraisten alapohjarakenteiden kosteuskäyttötymien. Available at:
http://dspace.cc.tut.fi/dpub/bitstream/handle/123456789/20771/leivo_%20rantala_maanvaraisten_alapohjarakenteiden.pdf?sequence=3
- [20] Rabbat, B. and Russell, H. (1985). ”Friction Coefficient of Steel on Concrete or Grout.” *J. Struct. Eng.*, 111(3), 505–515.
- TECHNICAL PAPERS
- [21] Baltay, P. and Gjelsvik, A. (1990). ”Coefficient of Friction for Steel on Concrete at High Normal Stress.” *J. Mater. Civ. Eng.*, 2(1), 46–49.
- TECHNICAL NOTES
- [22] Dvorak, J and Novak, L. 1994 Soil conservation and silviculture

- [23] Eran Cenciper, robot and machines design. 2012. Cited on 27 November 2013. Available at:
<http://www.robot-and-machines-design.com/en/Tables-Lists/549-Static-and-Dynamic-Friction-Coefficient-Table.html>
- [24] Stanford University. Cited 27 November 2013. Available at:
<http://www.stanford.edu/~tyzhu/Documents/Some%20Useful%20Numbers.pdf>
- [25] Eurokoodin soveltamisohje: Geotekninen suunnittelu – NCCI 7 (10.6.2011)
- [26] NATIONAL ANNEX FI TO SFS-EN 1997-1 EUROCODE 7: GEOTECHNICAL DESIGN
- [27] Ritola, J and Vuopio, J 2002, VTT: Research notes 2147 Kalliotilojen vesitiiveyden hallinta
- [28] Tolla. P, Manelius. M and Immonen J., Tiehallinto, 2007, Sillan geotekniset Suunnitteluperusteet. Cited on 1 December 2013. Available at:
http://alk.tiehallinto.fi/sillat/julkaisut/sillan_geosuunn.pdf
- [29] Tadesse. S, 2003.COMPUTATION OF SOIL COMPRESSIBILITY USING TANGENT MODULUS APPROACH. Cited on 1 December 2013. Available at:
<http://etd.aau.edu.et/dspace/bitstream/123456789/1190/1/Desalegne.pdf>
- [30] Länsivaara.T, Painumalaskentamenetelmien käyttökelpoisuuden arviointi JAN-BUN TANGENTTIMODUULIMENETELMÄ. Cited on 1 December 2013. Available at: <http://alk.tiehallinto.fi/thohje/pdf/3200630-03i.pdf>
- [31] Vianova Systems Finland Oy. 2012, versio 2.3 Novapoint GeoCalc: Tukiseinä Available at: http://docs.vianova.fi/GeoCalc/2.3/NPGeoCalc_Tukiseina.pdf in Finnish
- [32] SFS-EN 1536, 2011: EXECUTION OF SPECIAL GEOTECHNICAL WORK. BORED PILES
- [33] The Aberdeen Group 1989, Permeability of Concrete: Low water-cement ratio and 7-day moist-cure make concrete more impermeable.
- [34] Atlas Copco, Ground Engineering ProductsProduct catalogue. Cited on 12 December 2013. Available at:
http://www.atlascopco.us/Images/6991%201570%2001a_Symmetrix%20catalogue_english_lowres_tcm795-1777630.pdf

[35] Mitsubishi Materials, Casing advance system in overburden drilling. Cited on 12 December 2013. Available at: <http://mrt.mitsubishicarbide.com/en/product/gk18b.pdf>

[36] Vianova Systems Finland Oy, 2011, Supported Excavation Theory Versio 2.2
Available at:
http://docs.vianova.fi/GeoCalc/2.3/NPGeoCalc_Supported_Excavation_Theory.pdf

[37] Schlumberger. Cited 21 December 2013. Available at:
<http://www.glossary.oilfield.slb.com/en/Terms.aspx?LookIn=term%20name&filter=cuttings>

APPENDIX 1: Water penetration test

Measurer: Leo-Ville Miettinen, Ruukki

Start Date 6 Jul 2013 Time 9:00

End Date 8 Aug 2013 Time 16:00

water consumption									
Number	Pile	Grouting method	Drilling depth	L/5min	L/5min	L/5min	L/5min	L/5min	0.35bar-7bar
Hose	-	-	-	0.7	1.3	1.4	0.5	0.8	4
9	220/10	RF grouting	1000mm	5	0	2	0	1	3
12	220/10	None: Bedrock hole	2000mm	0.8	0.9	0.9	0.5	2.1	4.4
13	220/10	Injection ring	1000mm	1	0.8	1	1.7	2.2	5.7
14	220/10	Injection ring	1000mm	0.8	0.4	1.1	0.7	0.6	2.8
15.1	220/10	-	1000mm	5	3	1	2	1	7 *)
15.2	220/10	-	1000mm	1.3	2.5	2.3	1.7	1.9	8.4 *)
16	220/10	-	1000mm	3	2.3	1.7	1	1.4	6.4
18	220/10	-	2000mm	83.5	87.9	-	-	-	342.8
19	220/10	RF grouting	1000mm	0.3	1.1	1.4	1.4	1.1	5
21	220/10	Internal grouting	1000mm	2	1	2	1	1	5
23	220/10	Internal grouting	1000mm	17.8	3.5	1.7	1.2	1	7.4

*) Pile was not grouted but at least some grout had flowed into the drilling hole.

Average 0.35bar-7bar

	[L]	-hose
Hose	4	0
Bedrock	4.4	0.4
RF grouting	4	0
Injection ring	4.25	0.25
Internal grouting	6.2	2.2
Dense soil/drilling mud	7.3	3.3
Loose soil	342.8	338.8

Appendix 2

Site investigation calculations of rotational stiffness of RD piles
220/10 piles drilled 1 meter into bedrock, 2-meter cantilever

Subscripts named based on
pile numbers. P10, P11, P20,
P22 -> 10, 11, 20, 22

$$f_y := 440 \text{ MPa}$$

$$\gamma_{M0} := 1$$

Pile site investigation geometry (measured on the compression side of the piles
when the rock was not planar)

Pile 10

$$L_{1.10} := 1.97 \text{ m} \quad \text{Pile 10 height of horizontal load from bedrock}$$

$$L_{d1.10} := 1.96 \text{ m} \quad \text{Height of displacement sensor 1}$$

$$L_{d2.10} := 1.025 \text{ m} \quad \text{Height of displacement sensor 2}$$

$$L_{d3.10} := 0.17 \text{ m} \quad \text{Height of displacement sensor 3}$$

$$L_{s1.10} := 0.12 \text{ m} \quad \text{Height of strain sensor 1}$$

$$L_{s2.10} := 0.082 \text{ m} \quad \text{Height of strain sensor 2}$$

$$L_{s3.10} := 0.95 \text{ m} \quad \text{Height of strain sensor 3}$$

$$L_{s4.10} := 0.995 \text{ m} \quad \text{Height of strain sensor 4}$$

Pile 11

$$L_{1.11} := 1.99 \text{ m} \quad \text{Height of horizontal load from bedrock}$$

$$L_{d1.11} := 2.00 \text{ m} \quad \text{Height of displacement sensor 1}$$

$$L_{d2.11} := 1.03 \text{ m} \quad \text{Height of displacement sensor 2}$$

$$L_{d3.11} := 0.14 \text{ m} \quad \text{Height of displacement sensor 3}$$

$$L_{s1.11} := 0.12 \text{ m} \quad \text{Height of strain sensor 1}$$

$L_{s2.11} := 0.10 \text{ m}$ Height of strain sensor 2

$L_{s3.11} := 1.10 \text{ m}$ Height of strain sensor 3

$L_{s4.11} := 1.08 \text{ m}$ Height of strain sensor 4

Pile 20

$L_{1.20} := 2.00 \text{ m}$ Height of horizontal load from bedrock

$L_{d1.20} := 2.00 \text{ m}$ Height of displacement sensor1

$L_{d2.20} := 1.00 \text{ m}$ Height of displacement sensor2

$L_{d3.20} := 0.12 \text{ m}$ Height of displacement sensor3

$L_{s1.20} := 0.06 \text{ m}$ Height of strain sensor1

$L_{s2.20} := 0.06 \text{ m}$ Height of strain sensor2

$L_{s3.20} := 1.06 \text{ m}$ Height of strain sensor3

$L_{s4.20} := 1.08 \text{ m}$ Height of strain sensor4

Pile 22

$L_{1.22} := 1.98 \text{ m}$ Height of horizontal load from bedrock

$L_{d1.22} := 1.97 \text{ m}$ Height of displacement sensor1

$L_{d2.22} := 1.05 \text{ m}$ Height of displacement sensor2

$L_{d3.22} := 0.09 \text{ m}$ Height of displacement sensor3

$L_{s1.22} := 0.16 \text{ m}$ Height of strain sensor1

$L_{s2.22} := 0.06 \text{ m}$ Height of strain sensor2

$L_{s3.22} := 1.00 \text{ m}$ Height of strain sensor3

$L_{s4.22} := 1.01 \text{ m}$ Height of strain sensor4

Horizontal load test 9.8.2013

D1= Height of the displacement instrument number one from bed rock

D2= Height of the displacement instrument number two from bed rock

Et cetera

S1= Height of the strain gauge number one from bed rock

S1= Height of the strain gauge number two from bed rock

Et cetera

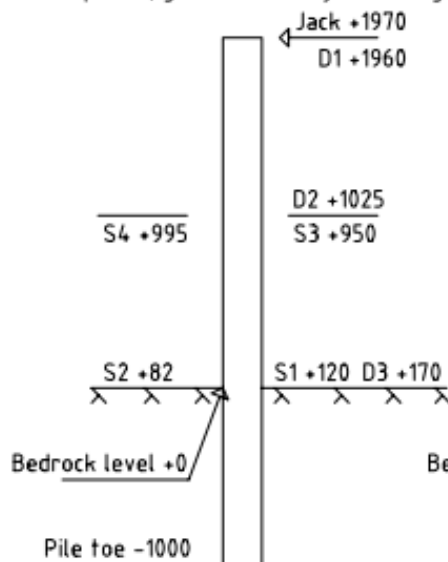
Jack= Height of the load from bed rock

The level of bedrock is selected the level of bed rock at the compression side of the pile

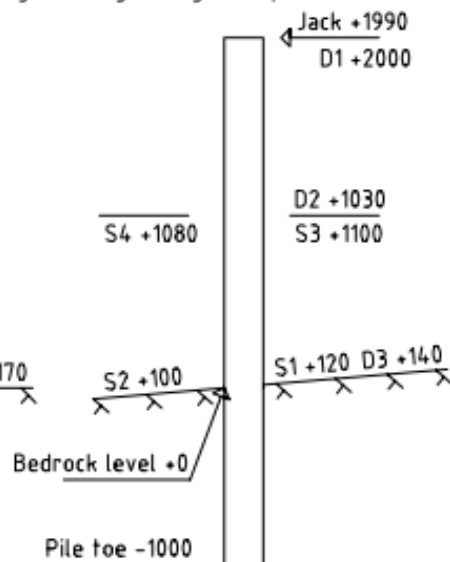
Units: (mm)

Piles: RD220/10, S440J2H

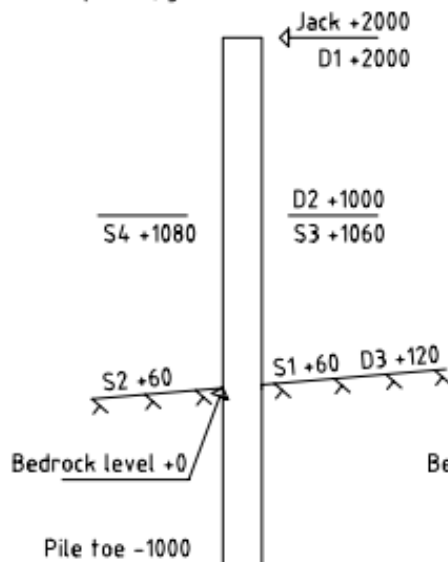
Test pile 10, grouted with injection ring



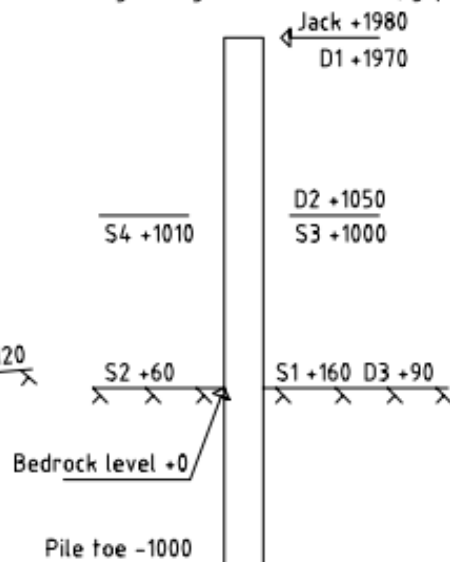
Test pile 11, non-grouted, grouting was spread from elsewhere



Test pile 20, grouted with RF channel



Test pile 22, internal grouting, grouting was unsuccessful, gap mainly clay



Pile dimensions, real values not theretical values

$$d_{220_10} := 219.5 \text{ mm} \quad \text{Outer diameter}$$

$$t_{220_10} := 9.92 \text{ mm} \quad \text{Thickness of pile}$$

$$d_{inner_220_10} := d_{220_10} - 2 \cdot t_{220_10} = 199.66 \text{ mm} \quad \text{Inner diameter}$$

$$A_{220_10} := \pi \cdot \frac{(d_{220_10}^2 - d_{inner_220_10}^2)}{4} = (6.531 \cdot 10^3) \text{ mm}^2$$

$$E_s := 210 \cdot \text{GPa}$$

$$EI_{220_10} := \frac{\pi}{64} \cdot (d_{220_10}^4 - d_{inner_220_10}^4) \cdot E_s = (7.548 \cdot 10^3) \text{ kN} \cdot \text{m}^2$$

$$W_{220_10} := \frac{\pi}{4} \cdot \frac{\left(\left(\frac{d_{220_10}}{2} \right)^4 - \left(\frac{d_{inner_220_10}}{2} \right)^4 \right)}{\frac{d_{220_10}}{2}} = 327.483 \text{ cm}^3$$

Theoretical displacement at the level of horizontal force at the elastic deformation level

$$M_{el} := \frac{W_{220_10} \cdot f_y}{\gamma_{M0}} = 144.092 \text{ kN} \cdot \text{m}$$

$$F_{elastic_10} := \frac{M_{el}}{L_{1,10}} = 73.143 \text{ kN}$$

$$F_{elastic_11} := \frac{M_{el}}{L_{1,11}} = 72.408 \text{ kN}$$

$$F_{elastic_20} := \frac{M_{el}}{L_{1,20}} = 72.046 \text{ kN}$$

$$F_{elastic_22} := \frac{M_{el}}{L_{1,22}} = 72.774 \text{ kN}$$

Check if the shear force is restricting moment capacity (EN 1993-1-1).

$$A_v := \frac{2 \cdot A_{220_10}}{\pi} = 0.004 \text{ m}^2 \quad \text{When round profile (EN 1993-1-1)}$$

$$V_{Ed} := F_{elastic_10} = (7.314 \cdot 10^4) \text{ N} \quad \text{Elastic load}$$

$$V_{pl.Rd} := \frac{A_v \frac{f_y}{\sqrt{3}}}{\gamma_{M0}} = (1.056 \cdot 10^6) \text{ N}$$

Plastic shear capacity

$$V_{c.Rd} := V_{pl.Rd}$$

$$V_{pl.Rd} := \left(\frac{V_{Ed}}{V_{c.Rd}} \right) = 0.069 \quad \square < \square \quad 0.5$$

— $\square > \square$ Shear load does not affect bending moment capacity

Checking elastic shear force vs. shear capacity

$$I := \frac{EI_{220_10}}{E_s} = (3.594 \cdot 10^7) \text{ mm}^4$$

$$S_{220_10} := A_{220_10} \cdot \frac{d_{220_10}}{2} = (7.168 \cdot 10^5) \text{ mm}^3$$

S = the first moment of area about the centroidal axis of that portion of the cross-section between the point at which the shear is required and the boundary of the cross-section (EN 1993-1-8)

$$\tau_{Ed} := \frac{V_{Ed} \cdot S_{220_10}}{I \cdot t_{220_10}} = 147.057 \text{ MPa}$$

$$\frac{\tau_{Ed}}{\frac{f_y}{\sqrt{3} \cdot \gamma_{M0}}} = 0.579 \quad \square < 1$$

Pile 10 rotational stiffness

$$f_{pile_10} := F_{elastic_10} \cdot \frac{L_{1.10}^3}{3 \cdot EI_{220_10}} = 24.697 \text{ mm}$$

$$f_{real_10} := 38.42 \text{ mm}$$

$$L_{1.10rock} := L_{1.10} + 0.3 \text{ m} = 2.27 \text{ m}$$

$$f_{pile_10rock} := F_{elastic_10} \cdot L_{1.10} \cdot \frac{L_{1.10rock}^2}{3 \cdot EI_{220_10}} = 32.791 \text{ mm}$$

This is too little. We cannot assume that there is support at the bedrock level.

$$\theta_{74kN_10} := \frac{f_{real_10} - f_{pile_10}}{L_{1.10}} = 0.00697$$

$$S_{j_10} := \frac{M_{el}}{\theta_{74kN_10}} = (2.068 \cdot 10^4) \frac{kN \cdot m}{rad}$$

$$S_{j_ini_10} := 25 \cdot \frac{EI_{220_10}}{L_{1.10}} = (9.578 \cdot 10^4) \frac{kN \cdot m}{rad}$$

$$L_{rigid_10} := \frac{S_{j_ini_10}}{S_{j_10}} \cdot L_{1.10} = 9.122 \text{ m}$$

$$\frac{S_{j_10}}{S_{j_ini_10}} = 21.6\%$$

In structures where bracing system reduces horizontal displacement by at least 80%

$$S_{j_ini_10_braced} := 8 \cdot \frac{EI_{220_10}}{L_{1.10}} = (3.065 \cdot 10^4) \frac{kN \cdot m}{rad}$$

$$\frac{S_{j_10}}{S_{j_ini_10_braced}} = 67.5\%$$

$$S_{j_ini_10_pinned} := 0.5 \cdot \frac{EI_{220_10}}{L_{1.22}} = (1.906 \cdot 10^3) \frac{kN \cdot m}{rad}$$

Displacement from FEM model was 26.8mm. Difference is due to shear deformation (approx. 10% difference).

F=73.4 kN, calculated f value from displacement data using y(x)=ax^2+b*x function in Excel 2st order polynomy because

What if the the pile starts to bend from point x=0.3

Angle of rotation

Linear rotational stiffness of joint P10 from F=0 to Fmax(elastic)

the initial rotational stiffness of a joint: EN 1993-1-8

Pile 10 length when bedrock joint is rigid

"rigidness rate"

the initial rotational stiffness of a joint

"rigidness rate"

the initial rotational stiffness of a joint: Nominally pinned

$$\frac{S_{j_{10}}}{S_{j_{ini_{10_pinned}}}} = 1085.3\%$$

"nominally pinned rate"

Joint is considered semi-rigid

Pile 22 rotational stiffness

$$f_{pile_{22}} := F_{elastic_{20}} \cdot \frac{L_{1.22}^3}{3 \cdot EI_{220_{10}}} = 24.699 \text{ mm}$$

$$f_{real_{22}} := 106.9 \text{ mm}$$

displacement from FEM model was 26.8mm. Difference is due to shear deformation (approx. 10% difference).

F=72.8 kN, calculated f value from displacement data by using $y(x)=ax^2+b*x$ function in excel
2st order polynomy because

$$\theta_{74kN_{22}} := \frac{f_{real_{22}} - f_{pile_{22}}}{L_{1.22}} = 0.04152$$

Angle of rotation

$$S_{j_{22}} := \frac{M_{el}}{\theta_{74kN_{22}}} = (3.471 \cdot 10^3) \frac{kN \cdot m}{rad}$$

Linear rotational stiffness of joint P22 from F=0 to Fmax(elastic)

$$S_{j_{ini_{22}}} := 25 \cdot \frac{EI_{220_{10}}}{L_{1.22}} = (9.53 \cdot 10^4) \frac{kN \cdot m}{rad}$$

the initial rotational stiffness of a joint: Rigid

$$\frac{S_{j_{22}}}{S_{j_{ini_{22}}}} = 3.6\%$$

"rigidness rate"

In structures where bracing system reduces horizontal displacement by at least 80%

$$S_{j_{ini_{22_braced}}} := 8 \cdot \frac{EI_{220_{10}}}{L_{1.22}} = (3.05 \cdot 10^4) \frac{kN \cdot m}{rad}$$

the initial rotational stiffness of a joint

$$\frac{S_{j_{22}}}{S_{j_{ini_{22_braced}}}} = 11.4\%$$

"rigidness rate"

$$S_{j_{ini_{22_pinned}}} := 0.5 \cdot \frac{EI_{220_{10}}}{L_{1.22}} = (1.906 \cdot 10^3) \frac{kN \cdot m}{rad}$$

the initial rotational stiffness of a joint: Nominally pinned

$$\frac{S_{j_22}}{S_{j_ini_22_pinned}} = 182.1\%$$

"nominally pinned rate"

Joint is considered semi-rigid

Calculation to help create charts in Excel and other extras

$$M_{elasti_10} := F_{elastic_10} \cdot L_{1.10} = 144.092 \text{ kN} \cdot \text{m}$$

$$\frac{L_{1.10}^3}{3 \cdot EI_{220_10}} = 0.337648762 \frac{\text{mm}}{\text{kN}}$$

$$\frac{L_{1.11}^3}{3 \cdot EI_{220_10}} = 0.348037238 \frac{\text{mm}}{\text{kN}}$$

$$\frac{L_{1.20}^3}{3 \cdot EI_{220_10}} = 0.35331044 \frac{\text{mm}}{\text{kN}}$$

$$\frac{L_{1.22}^3}{3 \cdot EI_{220_10}} = 0.342816767 \frac{\text{mm}}{\text{kN}}$$

$$W_{1220_12_5} := 14169.3 \cdot \text{cm}^3$$

$$M_{el1220_12_5} := \frac{W_{1220_12_5} \cdot f_y}{\gamma_{M0}} = (6.234 \cdot 10^3) \text{ kN} \cdot \text{m}$$

$$W_{220_10} := 328.5 \cdot \text{cm}^3$$

$$M_{el220_10} := \frac{W_{220_10} \cdot f_y}{\gamma_{M0}} = 144.54 \text{ kN} \cdot \text{m}$$

GeoCalc 500/12.5 pile RD pile wall example

$$L_{500_12.5} := \frac{7}{3} \text{ m} = 2.333 \text{ m}$$

Height of the load. 1/3*
height from bedrock to
upper face of soil

$$f_y := 440 \text{ MPa}$$

$$\gamma_{M0} := 1$$

Theoretical pile dimension values

$$d_{500_{12.5}} := 508.0 \text{ } mm \quad \text{Outer diameter}$$

$$t_{500_{12.5}} := 12.5 \text{ } mm \quad \text{Thickness of pile}$$

$$d_{inner_{500_{12.5}}} := d_{500_{12.5}} - 2 \cdot t_{500_{12.5}} = 483 \text{ } mm \quad \text{Inner diameter}$$

$$d_{500run} := d_{500_{12.5}} + 64 \text{ } mm = 0.572 \text{ } m \quad \text{Run of the pile in wall}$$

$$A_{500_{12.5}} := \pi \cdot \frac{(d_{500_{12.5}}^2 - d_{inner_{500_{12.5}}}^2)}{4} = (1.946 \cdot 10^4) \text{ } mm^2$$

$$E_s := 210 \cdot GPa$$

$$EI_{500_{12.5}} := \frac{\pi}{64} \cdot (d_{500_{12.5}}^4 - d_{inner_{500_{12.5}}}^4) \cdot E_s = (1.255 \cdot 10^5) \text{ } kN \cdot m^2$$

$$EI_{500_{12.5}wall} := \frac{EI_{500_{12.5}}}{d_{500run}} = (2.194 \cdot 10^5) \text{ } kN \cdot m$$

$$W_{500_{12.5}} := \frac{\pi}{4} \cdot \frac{\left(\left(\frac{d_{500_{12.5}}}{2} \right)^4 - \left(\frac{d_{inner_{500_{12.5}}}}{2} \right)^4 \right)}{\frac{d_{500_{12.5}}}{2}} = (2.353 \cdot 10^3) \text{ } cm^3$$

$$W_{500_{12.5}wall} := \frac{W_{500_{12.5}}}{d_{500run}} = (4.113 \cdot 10^3) \frac{1}{m} \cdot cm^3$$

Theoretical displacement at the level of horizontal force at the elastic deformation level

$$M_{el_{wall}} := \frac{W_{500_{12.5}wall} \cdot f_y}{\gamma_{M0}} = (1.81 \cdot 10^3) \frac{1}{m} \cdot kN \cdot m$$

$$M_{el} := \frac{W_{500_{12.5}} \cdot f_y}{\gamma_{M0}} = (1.035 \cdot 10^3) \text{ } kN \cdot m$$

$$F_{elastic_500_12.5} := \frac{M_{el}}{L_{500_12.5}} = 443.628 \text{ kN}$$

Pile 500/12.5 rotational stiffness

$$f_{pile_500_12.5} := F_{elastic_500_12.5} \cdot \frac{L_{500_12.5}^3}{3 \cdot EI_{500_12.5}} = 14.97 \text{ mm}$$

$$f_{real_500_12.5} := 29.7 \text{ mm}$$

$$\theta_{500_12.5} := \frac{f_{real_500_12.5} - f_{pile_500_12.5}}{L_{500_12.5}} = 0.00631 \text{ Angle of rotation}$$

$$S_{j_500_12.5} := \frac{M_{el}}{\theta_{500_12.5}} = (1.64 \cdot 10^5) \frac{\text{kN} \cdot \text{m}}{\text{rad}} \quad \text{Linear rotational stiffness of joint from F=0 to Fmax(elastic)}$$

$$S_{j_ini_500_12.5} := 8 \cdot \frac{EI_{500_12.5}}{L_{500_12.5}} = (4.302 \cdot 10^5) \frac{\text{kN} \cdot \text{m}}{\text{rad}} \quad \text{the initial rotational stiffness of a joint: EN 1993-1-8}$$

$$S_{j_500_12.5} \ll S_{j_ini_500_12.5} \quad \text{Is not considered a rigid joint}$$

$$L_{rigid_500_12.5} := \frac{3 \cdot S_{j_ini_500_12.5}}{S_{j_500_12.5}} \cdot L_{500_12.5} = 18.4 \text{ m} \quad \text{Pile length when bedrock joint is rigid, 3x load level}$$

$$\frac{S_{j_500_12.5}}{S_{j_ini_500_12.5}} = 38.1\% \quad \text{500/12.5 "rigidness rate"}$$

$$S_{j_ini_500_12.5_pinned} := 0.5 \cdot \frac{EI_{500_12.5}}{L_{500_12.5}} = (2.689 \cdot 10^4) \frac{\text{kN} \cdot \text{m}}{\text{rad}} \quad \text{the initial rotational stiffness of a joint: Nominally pinned}$$

$$\frac{S_{j_500_12.5}}{S_{j_ini_500_12.5_pinned}} = 609.8\% \quad \text{500/12.5 "nominally pinned rate"}$$

GeoCalc calculation, grouted joint: stiffness of the joint is assumed to be constant (F/f is linear)

$$M_{Geocalc} := 250 \text{ kN} \cdot \frac{\text{m}}{\text{m}}$$

$$M_{Ansys} := M_{el_wall} = (1.81 \cdot 10^3) \frac{1}{\text{m}} \cdot \text{kN} \cdot \text{m}$$

$$f_{rock_ansys} := 1.01 \text{ mm} - (-0.37 \text{ mm}) = 1.38 \text{ mm}$$

$$f_{rock_geocalc} := \frac{M_{Geocalc}}{M_{Ansys}} \cdot f_{rock_ansys} = 0.191 \text{ mm}$$

In GeoCalc, f must be the difference in displacement at the upper level of the bedrock and the bottom of the pile.

320/10 pile displacement check

$$M_{Geocalc} := 205 \text{ kN} \cdot \frac{\text{m}}{\text{m}}$$

$$W_{320_10wall} := 1935 \cdot \frac{\text{cm}^3}{\text{m}}$$

$$M_{el_wall_300_10} := \frac{W_{320_10wall} \cdot f_y}{\gamma_{M0}} = 851.4 \frac{1}{\text{m}} \cdot \text{kN} \cdot \text{m}$$

$$L_{320_10} := L_{500_12.5} = 2.333 \text{ m}$$

$$d_{320run} := 323.9 \text{ mm} + 64 \text{ mm} = 387.9 \text{ mm}$$

$$F_{el320_10} := \frac{M_{el_wall_300_10} \cdot d_{320run}}{L_{320_10}} = 141.539 \text{ kN}$$

$$M_{Ansys} := M_{el_wall_300_10} = 851.4 \frac{1}{\text{m}} \cdot \text{kN} \cdot \text{m}$$

$$f_{rock_ansys} := 0.49 \text{ mm} - (-0.67 \text{ mm}) = 1.16 \text{ mm}$$

$$f_{rock_geocalc} := \frac{M_{Geocalc}}{M_{Ansys}} \cdot f_{rock_ansys} = 0.279 \text{ mm}$$

GeoCalc calculation, clay joint: stiffness of the joint is assumed a constant (F/f is linear)

$$f_{real_500_12.5} := 87.2 \text{ mm}$$

$$\theta_{500_12.5} := \frac{f_{real_500_12.5} - f_{pile_500_12.5}}{L_{500_12.5}} = 0.03096 \text{ Angle of rotation}$$

$$S_{j_500_12.5} := \frac{M_{el}}{\theta_{500_12.5}} = (3.344 \cdot 10^4) \frac{\text{kN} \cdot \text{m}}{\text{rad}} \text{ Linear rotational stiffness of joint from F=0 to Fmax(elastic)}$$

$$M_{Geocalc} := 150 \text{ kN} \cdot \frac{\text{m}}{\text{m}}$$

$$M_{Ansys} := M_{el_wall} = (1.81 \cdot 10^3) \frac{1}{\text{m}} \cdot \text{kN} \cdot \text{m}$$

$$f_{rock_ansys} := 17.14 \text{ mm} - (-14.36 \text{ mm}) = 31.5 \text{ mm}$$

$$f_{rock_geocalc} := \frac{M_{Geocalc}}{M_{Ansys}} \cdot f_{rock_ansys} = 2.611 \text{ mm}$$

Geocalc calculation, Soilsample is in joint:

$$M_{Geocalc} := 150 \text{ kN} \cdot \frac{\text{m}}{\text{m}}$$

Bending moment and rotational stiffness were iterated due to non-linear stiffness.

$$M_{Ansys} := M_{el_wall} = (1.81 \cdot 10^3) \frac{1}{m} \cdot kN \cdot m$$

$$f_{rock_ansys} := 8.0 \text{ mm} - (-3.8 \text{ mm}) = 11.8 \text{ mm} \quad \text{From figure 4.1.1.5}$$

$$f_{rock_geocalc} := \frac{M_{Geocalc}}{M_{Ansys}} \cdot f_{rock_ansys} = 0.978 \text{ mm} \quad \text{Linear assumption}$$

$$M_{Ansys} := M_{el_wall} \cdot \frac{1}{10} = 180.967 \frac{1}{m} \cdot kN \cdot m$$

$$f_{real_500_12.5} := 56.0 \text{ mm}$$

$$\theta_{500_12.5} := \frac{f_{real_500_12.5} - f_{pile_500_12.5}}{L_{500_12.5}} = 0.01758 \quad \text{Angle of rotation}$$

$$S_{j_500_12.5} := \frac{M_{el}}{\theta_{500_12.5}} = (5.887 \cdot 10^4) \frac{kN \cdot m}{rad} \quad \text{Rotational stiffness of joint when pile is at full elastic bending moment}$$

$$f_{rock_ansys} := 1.8 \text{ mm} - (-1.0 \text{ mm}) = 2.8 \text{ mm}$$

$$f_{rock_geocalc} := \frac{M_{Geocalc}}{M_{Ansys}} \cdot f_{rock_ansys} = 2.321 \text{ mm} \quad \text{Non-linear assumption from figure 4.1.1.6}$$

Soil sample rotational stiffness from 0 kN*m to 1810 kN*m (scaled to wall case) in joint:

$$\theta_{500_12.5} := \frac{f_{real_500_12.5} - f_{pile_500_12.5} \cdot \frac{1}{10}}{L_{500_12.5}} = 0.00303 \quad \text{Angle of rotation}$$

$$S_{j_500_12.5} := \frac{M_{el} \cdot \frac{1}{10}}{\theta_{500_12.5}} = (3.42 \cdot 10^4) \frac{kN \cdot m}{rad} \quad \text{Linear rotational stiffness of joint from F=0 to Fmax(elastic)}$$

Theoretical displacement at the level of horizontal force at the plastic deformation level.

$$W_{500_12.5PL} := 3070 \cdot 10^3 \cdot mm^3 = (3.07 \cdot 10^6) mm^3$$

$$M_{PL} := \frac{W_{500_12.5PL} \cdot f_y}{\gamma_{M0}} = (1.351 \cdot 10^3) kN \cdot m \quad \text{Plastic moment capacity}$$

$$M_{PLwall} := \frac{M_{PL}}{d_{500run}} = (2.362 \cdot 10^3) \frac{1}{m} \cdot kN \cdot m \quad \text{Plastic moment capacity of wall}$$

Structural dimensioning of Appendix 5 RD pile wall

Bending moment stress in wall

$$M_k := 250 \text{ kN} \cdot \frac{\text{m}}{\text{m}}$$

From GeoCalc calculation
appendix 5

$$\gamma_F := 1.35$$

A.3A(FI)

$$E_d := \gamma_F \cdot M_k = 337.5 \frac{1}{\text{m}} \cdot \text{kN} \cdot \text{m}$$

$$R_d := M_{el} = (1.035 \cdot 10^3) \text{ kN} \cdot \text{m}$$

Capacity

$$E_d \leq R_d \quad \text{OK!}$$

$$\frac{E_d}{R_d} = 32.6\% \frac{1}{\text{m}}$$

Utilization rate

Downsizing the RD pile wall

Theoretical pile dimension values

$$d_{320_10} := 320.0 \text{ mm}$$

Outer diameter

$$t_{320_10} := 10 \text{ mm}$$

Thickness of pile

$$f_y := 440 \text{ MPa}$$

Steel grade

$$d_{inner_320_10} := d_{320_10} - 2 \cdot t_{320_10} = 300 \text{ mm}$$

Inner diameter

$$d_{320run} := d_{320_10} + 64 \text{ mm} = 0.384 \text{ m}$$

Run of the pile in wall

$$A_{320_10} := \pi \cdot \frac{(d_{320_10}^2 - d_{inner_320_10}^2)}{4} = (9.739 \cdot 10^3) \text{ mm}^2$$

$$E_s := 210 \cdot \text{GPa}$$

$$EI_{320_10} := \frac{\pi}{64} \cdot (d_{320_10}^4 - d_{inner_320_10}^4) \cdot E_s = (2.459 \cdot 10^4) \text{ kN} \cdot \text{m}^2$$

$$W_{320_10} := \frac{\pi}{4} \cdot \frac{\left(\left(\frac{d_{320_10}}{2} \right)^4 - \left(\frac{d_{inner_320_10}}{2} \right)^4 \right)}{\frac{d_{320_10}}{2}} = 731.942 \text{ cm}^3$$

$$W_{320-10wall} := \frac{W_{320_10}}{d_{320run}} = (1.906 \cdot 10^3) \frac{1}{\text{m}} \cdot \text{cm}^3$$

Theoretical displacement at the level of horizontal force at the elastic deformation level.

$$M_{el} := \frac{W_{320-10wall} \cdot f_y}{\gamma_{M0}} = 838.684 \frac{1}{\text{m}} \cdot \text{kN} \cdot \text{m}$$

Structural dimensioning of Appendix 7 RD pile wall

Bending moment stress in wall

$$M_k := 210 \text{ kN} \cdot \frac{\text{m}}{\text{m}}$$

From GeoCalc calculation
appendix 5

$$\gamma_F := 1.35$$

A.3A(FI)

$$E_d := \gamma_F \cdot M_k = 283.5 \frac{1}{\text{m}} \cdot \text{kN} \cdot \text{m}$$

$$R_d := M_{el} = 838.684 \frac{1}{\text{m}} \cdot \text{kN} \cdot \text{m}$$

Capacity

$$E_d \leq R_d \quad \text{OK!}$$

$$\frac{E_d}{R_d} = 33.8\%$$

Utilization rate

Check if the shear force is restricting moment capacity (EN 1993-1-1).

$$A_v := \frac{2 \cdot A_{320_10}}{\pi} = 0.006 \text{ m}^2 \quad \text{When round profile (EN 1993-1-1)}$$

$$V_k := 210 \frac{\text{kN}}{\text{m}}$$

Shear force in the wall. From GeoCalc calculation appendix 7

$$\gamma_F := 1.35 \quad \text{A.3A(FI)}$$

$$V_{Ed} := \gamma_F \cdot V_k = 283.5 \frac{1}{\text{m}} \cdot \text{kN}$$

$$V_{pl.Rd} := \frac{A_v \frac{f_y}{\sqrt{3}}}{\gamma_{M0}} = (1.575 \cdot 10^6) \text{ N}$$

Plastic shear capacity

$$V_{c.Rd} := \frac{V_{pl.Rd}}{d_{320run}} = (4.102 \cdot 10^3) \frac{\text{kN}}{\text{m}}$$

$$V_{pl.Rd} := \left(\frac{V_{Ed}}{V_{c.Rd}} \right) = 0.069 \quad \square < \square \quad 0.5$$

— $\square > \square$ Shear load does not affect bending moment capacity

Checking elastic shear force vs. shear capacity

$$I := \frac{EI_{320_10}}{E_s} = (1.171 \cdot 10^8) \text{ mm}^4$$

$$S_{320_10} := A_{320_10} \cdot \frac{d_{320_10}}{2} = (1.558 \cdot 10^6) \text{ mm}^3$$

S= the first moment of area about the centroidal axis of that portion of the cross-section between the point at which the shear is required and the boundary of the cross-section (EN 1993-1-8)

$$\tau_{Ed} := \frac{V_{Ed} \cdot S_{320_10}}{I \cdot t_{320_10}} \cdot d_{320run} = 144.85 \text{ MPa}$$

$$\frac{\tau_{Ed}}{\frac{f_y}{\sqrt[2]{3} \cdot \gamma_{M0}}} = 0.57 \quad \blacksquare < 1$$

Material properties used in FEM analysis,
Steel

$$f_y := 440 \text{ MPa}$$

$$f_u := 615 \text{ MPa}$$

$$E_s := 200 \text{ GPa}$$

$$e_1 := \frac{f_y}{E_s} = 0.002$$

Elongation at yield stress

$$e_2 := \frac{f_u - f_y}{0.17 - e_1} = (1.043 \cdot 10^3) \text{ MPa}$$

Strain at failure for steel: 17%

APPENDIX 3

P20 deformation shape

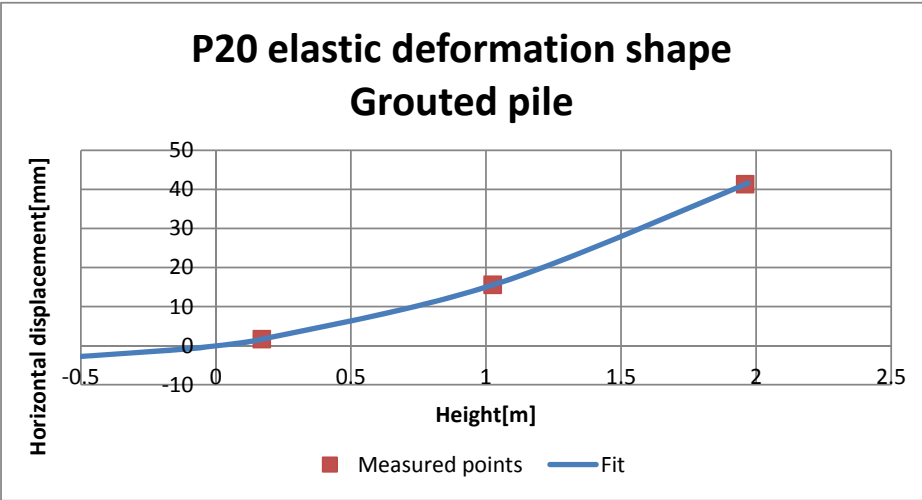
Pile: RD 220/10

Fitting to solve displacement in level of force. 72.0 kN horizontal load

Least squares method

x	y	y`	(y-y`)^2	Comment	Constant	Best fit
	-0.5	-2.74465				
	-0.1	-0.80241				
	0	0				
0.17	1.612734	1.654974	0.001784	S3 [mm]	a	0
1.025	15.54558	15.53217	0.00018	S2 [mm]	b	6.337065
1.96	41.3105	41.31384	1.12E-05	S1 [mm]	c	8.657842
1.97		41.64946		Load level	d	0
SUM(y-y`)^2						0.001975

Equation: $f(x) = a \cdot x^3 + b \cdot x^2 + c \cdot x + d$
x=height from bedrock [m]
Y=horizontal displacement [mm]
y`=solved horizontal displacement [mm]



APPENDIX 4

P20 deformation shape

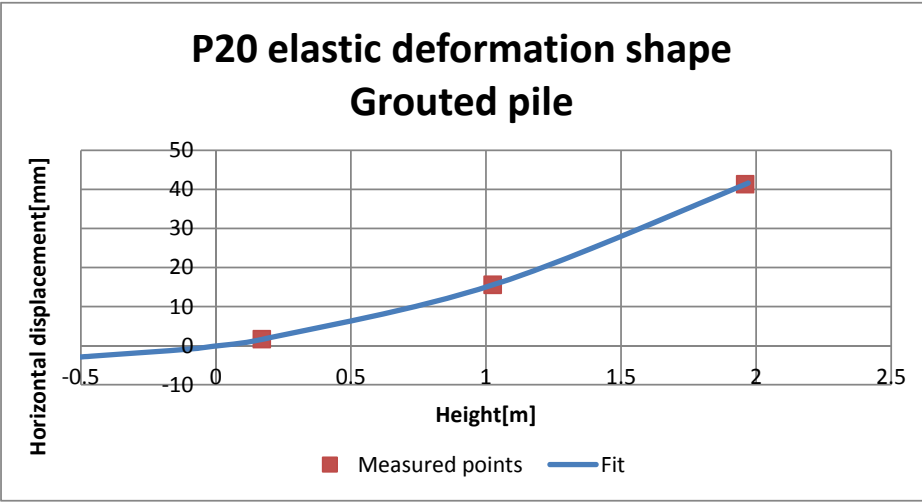
Pile: RD 220/10

Fitting to solve displacement in level of force. 72.0 kN horizontal load

Least squares method

x	y	y`	(y-y`)^2	Comment	Constant	Best fit
	-0.5	-2.8779				
	-0.1	-0.87632				
	0	-0.06139				
0.17	1.612734	1.612732	6.96E-12	S3 [mm]	a	0
1.025	15.54558	15.54558	8.38E-12	S2 [mm]	b	6.290687
1.96	41.3105	41.31049	1.15E-11	S1 [mm]	c	8.778358
1.97		41.6455		Load level	d	-0.06139
			SUM(y-y`)^2			2.69E-11

Equation: $f(x) = a \cdot x^3 + b \cdot x^2 + c \cdot x + d$
x=height from bedrock [m]
Y=horizontal displacement [mm]
y`=solved horizontal displacement [mm]



Appendix 5

Wall Type	BoredpileWall
Name	RD500/12.5-wall (rm/rf)
Manufacturer	Ruukki
Cross Section Area [m^2]	0.037290694213231
Calculation Width [m]	1
Inertia Modulus [m^4]	0.00104467486365223
Section Modulus [m^3]	0.00411289316398515
Elastic Modulus [kPa]	210000000
Flexural Stiffness [kNm^2]	219381.721366968
Axial Stiffness [kNm^2/m^2]	7831045.78477851
Length of Wall [m]	9

Name	A [mm^2]	L [m]	α [°]	h [m]	F [kN]	Elastic Modulus [kPa]	Overdig [m]	Horizontal distribution [m]
	5000	5	180	1	0	210000000	0.4	2.3
	20000	1	180	7	0	210000000	-5.55	1

Id	Layer Name	z [m]	h [m]	γ [kN/m³]	Φ [°]	c [kPa]	Δc [kPa/m]	Ko Model	Ko	Earth Pres. Model	Ka	Kp	d/ud	Material Model	δya	δyp	ξ50a	ξ50p	m	n	k
1.	Täyttö	0	2	18	34	0	0	Jaky	0.44	Coulomb	0.26	5.83	Drained	MCM					300	0.5	0.5
2.	Savi	-2	4	16	0	10	1	Jaky	1	Coulomb	1	1	Undrained	MCM					40	1	1
3.	Moreeni	-6	1	20	40	0	0	Jaky	0.36	Coulomb	0.2	9.36	Drained	MCM					800	0.5	0.5
4.	Kallio	-7	2	20	45	10	0	Jaky	0.29	User-defined	0.2	10000	Drained	MCM					10000	1	1

1. Rock waste

1. Täyttö

2. Clay

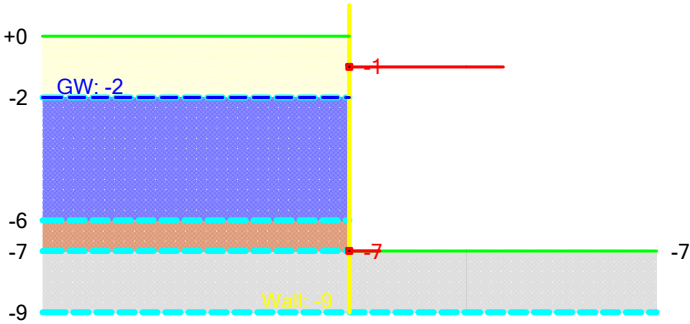
2. Savi

3. Moraine

3. Moreeni

4. Bedrock

4. Kallio



/RD pile wall 500/12.5

Pile drilled into bedrock. Bedrock as a soil and reinforced with anchor at the upper level of bedrock

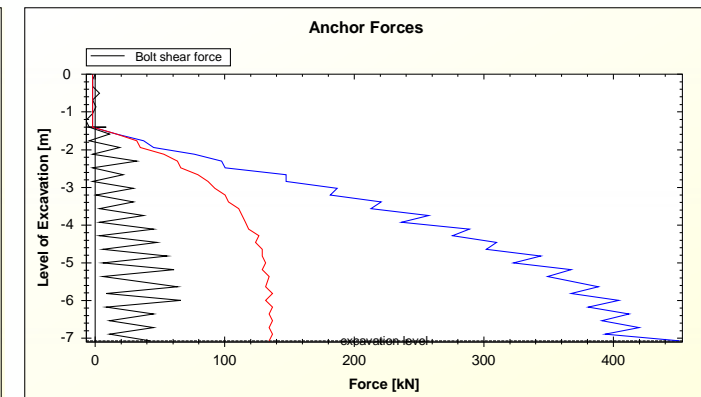
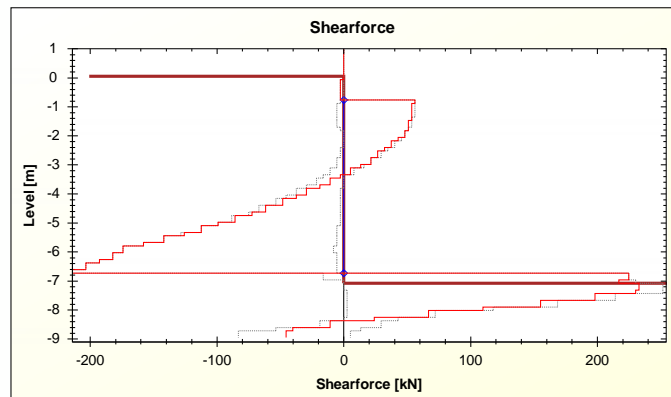
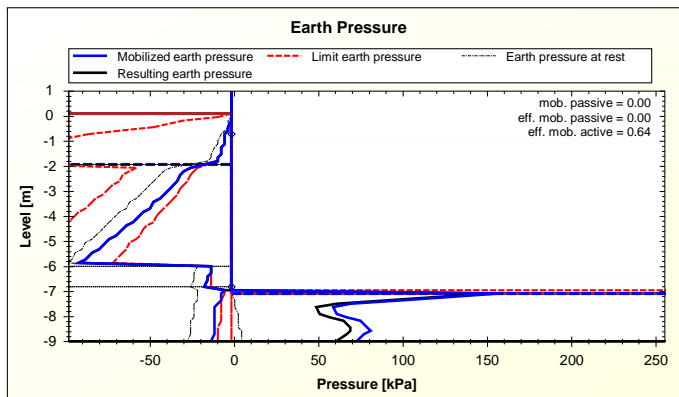
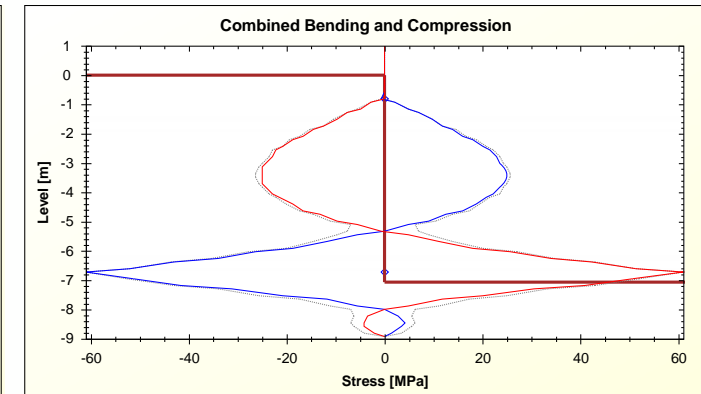
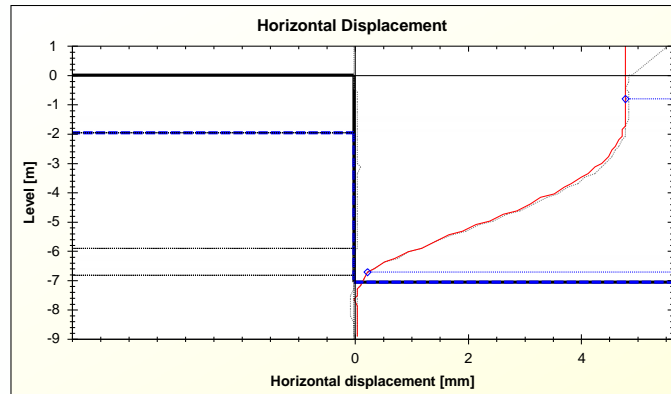
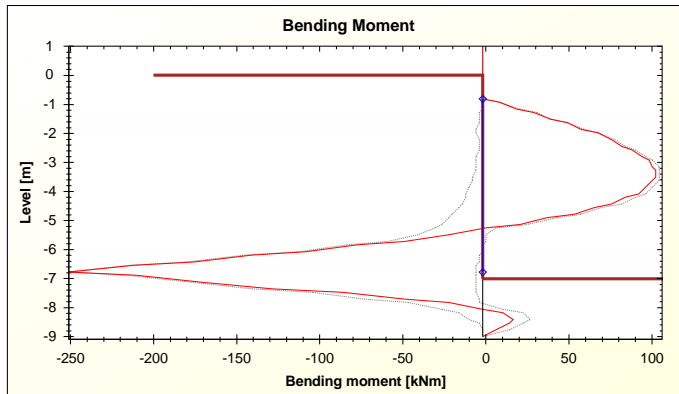
Leo-Ville Miettinen/

Novapoint GeoCalc 2.4 (19.10.2013 14:42)

Appendix 5

Calculation Graphs Excavation Level -7.09 m

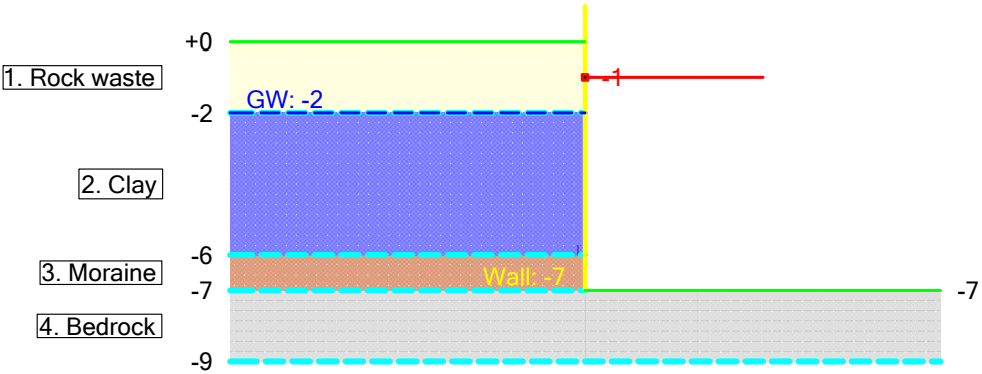
Tukiseinä luku 9/Porapaaluesimerkki
ViaNova
Porapaalu, tuki kallion pinnassa
Novapoint GeoCalc 2.4 (18.10.2013 10:34)



Wall Type	BoredpileWall
Name	RD500/12.5-wall (rm/rf)
Manufacturer	Ruukki
Cross Section Area [m^2]	0.037290694213231
Calculation Width [m]	1
Inertia Modulus [m^4]	0.00104467486365223
Section Modulus [m^3]	0.00411289316398515
Elastic Modulus [kPa]	210000000
Flexural Stiffness [kNm^2]	219381.721366968
Axial Stiffness [kNm^2/m^2]	7831045.78477851
Length of Wall [m]	7

Name	A [mm^2]	L [m]	α [°]	h [m]	F [kN]	Elastic Modulus [kPa]	Overdig [m]	Horizontal distribution [m]
	5000	5	180	1	0	210000000	0.4	2.3

Id	Layer Name	z [m]	h [m]	γ [kN/m³]	Φ [°]	c [kPa]	Δc [kPa/m]	Ko Model	Ko	Earth Pres. Model	Ka	Kp	d/ud	Material Model	δya	δyp	ξ50a	ξ50p	m	n	k
1.	Rock waste	0	2	18	34	0	0	Jaky	0.44	Coulomb	0.26	5.83	Drained	MCM					300	0.5	0.5
2.	Clay	-2	4	16	0	10	1	Jaky	1	Coulomb	1	1	Undrained	MCM					40	1	1
3.	Moraine	-6	1	20	40	0	0	Jaky	0.36	Coulomb	0.2	9.36	Drained	MCM					800	0.5	0.5
4.	Bedrock	-7	2	20	45	10	0	Jaky	0.29	User-defined	0.2	10000	Drained	MCM					10000	1	1



/RD pile wall 500/12.5

Pile drilled at the level of bedrock. Bending moment free support

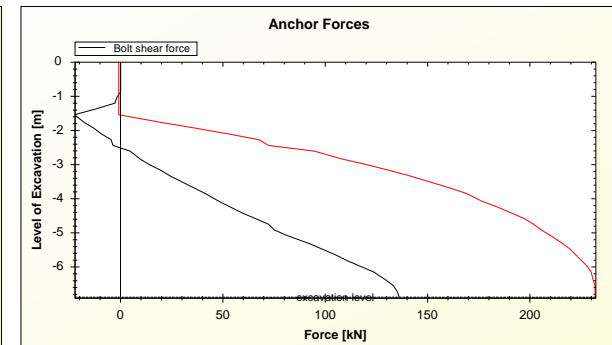
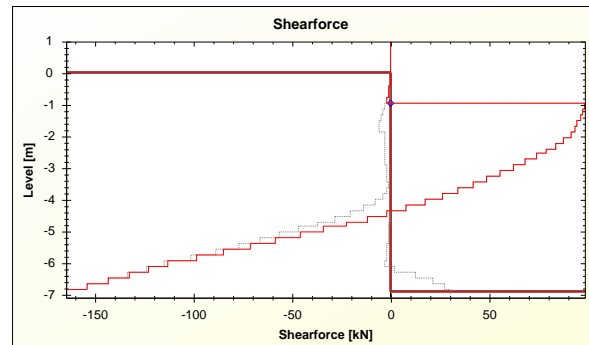
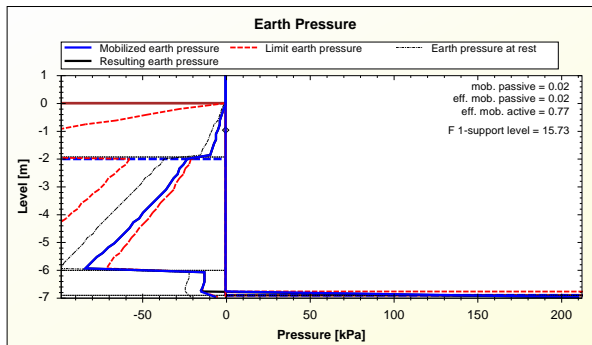
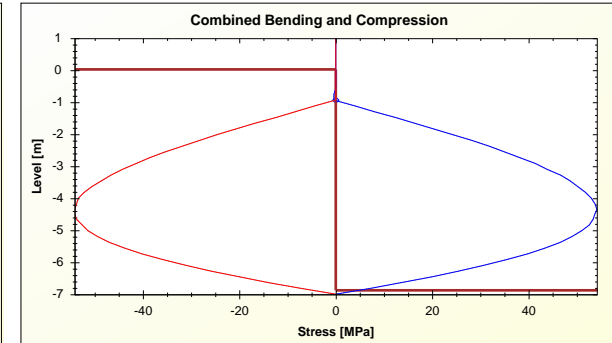
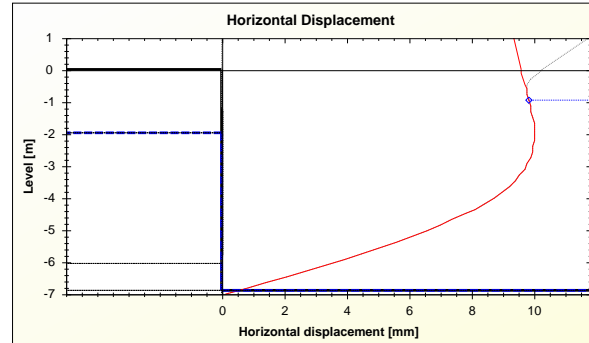
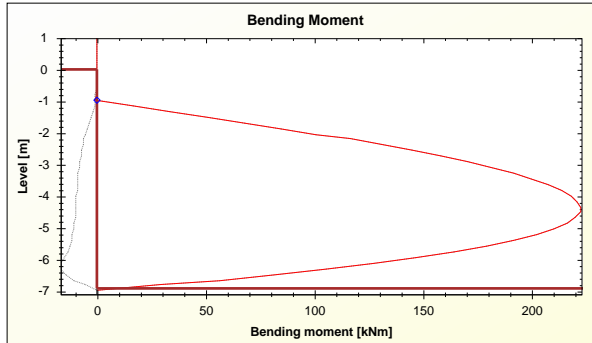
Leo-Ville Miettinen/

Novapoint GeoCalc 2.4 (19.10.2013 14:38)

Appendix 6

Calculation Graphs Excavation Level -6.91 m

RD pile wall 500/12.5
Pile drilled at the level of bedrock. Bending moment free support
Leo-Ville Miettinen/
Novapoint GeoCalc 2.4 (19.10.2013 14:46)



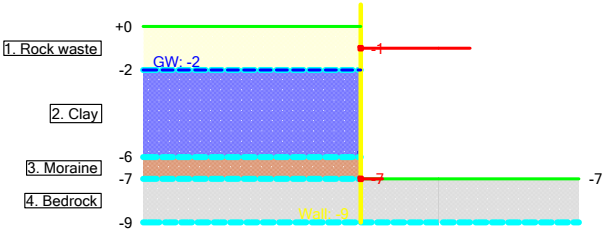
Appendix 7

Wall Type	BoredpileWall
Name	RD320/10-wall (rm/rf)
Manufacturer	Ruukki
Cross Section Area [m^2]	0.0302494972028052
Calculation Width [m]	1
Inertia Modulus [m^4]	0.000313440123082959
Section Modulus [m^3]	0.00193541292425415
Elastic Modulus [kPa]	210000000
Flexural Stiffness [kNm^2]	65822.4258474214
Axial Stiffness [kNm^2/m^2]	6352394.41258909
Length of Wall [m]	9

Name	A [mm^2]	L [m]	α [°]	h [m]	F [kN]	Elastic Modulus [kPa]	Overdig [m]	Horizontal distribution [m]
	5000	5	180	1	0	210000000	0.4	2.3
	20000	1	180	7	0	210000000	-5.55	1

Id	Layer Name	z [m]	h [m]	γ [kN/m³]	Φ [°]	c [kPa]	Δc [kPa/m]	Ko Model	Ko	Earth Pres. Model	Ka	Kp	d/ud	Material Model	δya	δyp	ξ50a	ξ50p	m	n	k
1.	Rock waste	0	2	18	34	0	0	Jaky	0.44	Coulomb	0.26	5.83	Drained	MCM					300	0.5	0.5
2.	Clay	-2	4	16	0	10	1	Jaky	1	Coulomb	1	1	Undrained	MCM					40	1	1
3.	Moraine	-6	1	20	40	0	0	Jaky	0.36	Coulomb	0.2	9.36	Drained	MCM					800	0.5	0.5
4.	Bedrock	-7	2	20	45	10	0	Jaky	0.29	User-defined	0.2	10000	Drained	MCM					10000	1	1

Result	Value
Anchor 1: Max. force [kN]	152.7
Anchor 2: Max. force [kN]	378.6
Max. bending moment [kNm]	-207
Max. horizontal displacement [mm]	9.5



/RD pile wall 320/10

Pile drilled into bedrock. Bedrock as a soil and reinforced with anchor at the upper level of bedrock

Leo-Ville Miettinen/

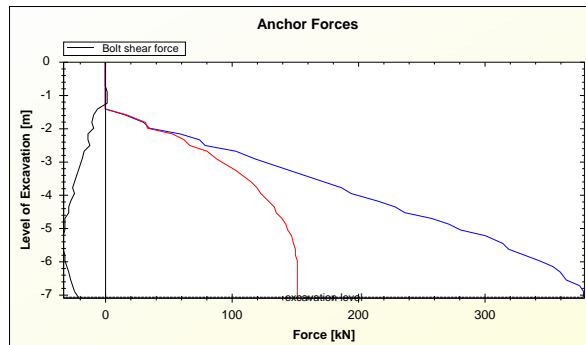
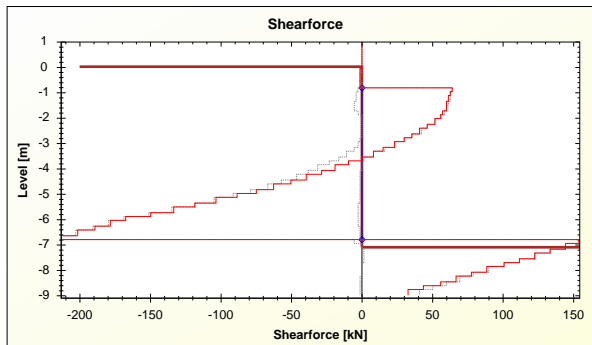
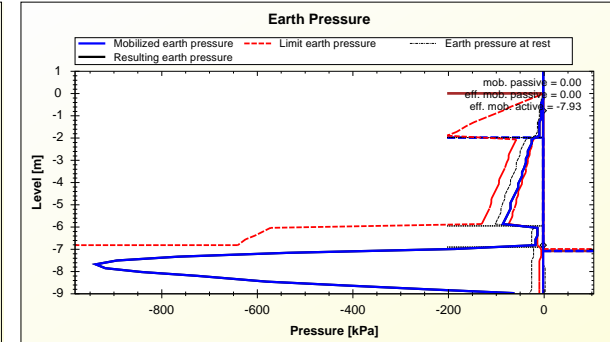
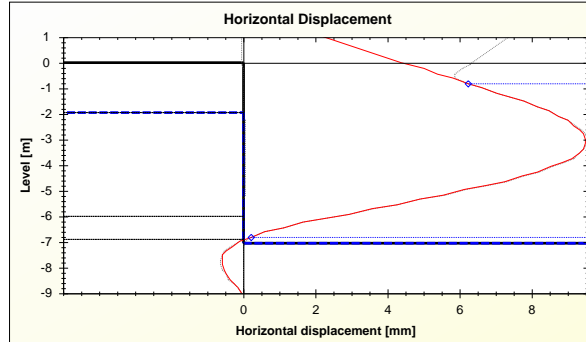
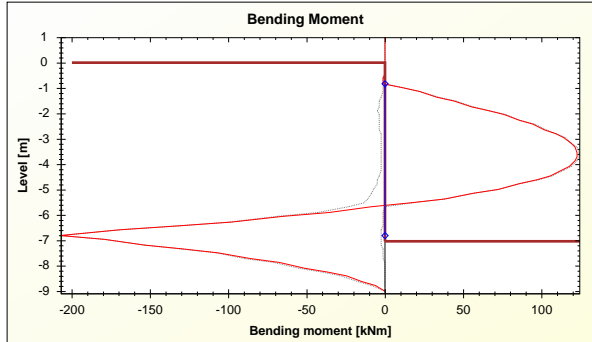
Novapoint GeoCalc 2.4 (21.10.2013 12:56)

Appendix 7

Calculation Graphs Excavation Level -7.09 m

/RD pile wall 320/10

Pile drilled into bedrock. Bedrock as a soil and reinforced with anchor at the upper level of bedrock
Leo-Ville Miettinen/
Novapoint GeoCalc 2.4 (21.10.2013 13:04)



Appendix 8 Drilling depth and pile size in relation to rotational stiffness

Fitting done by using calculated 220/10, 500/12.5 and 1220/12.5 piles
 Rotational stiffness of other pile sizes fitted, drilling hole grouted
 Least squares method

1d drilling depth, 0.5x elastic load

correlation factor $1/1.25 = 0.8$ is included, more on correlation factor in section 4.1

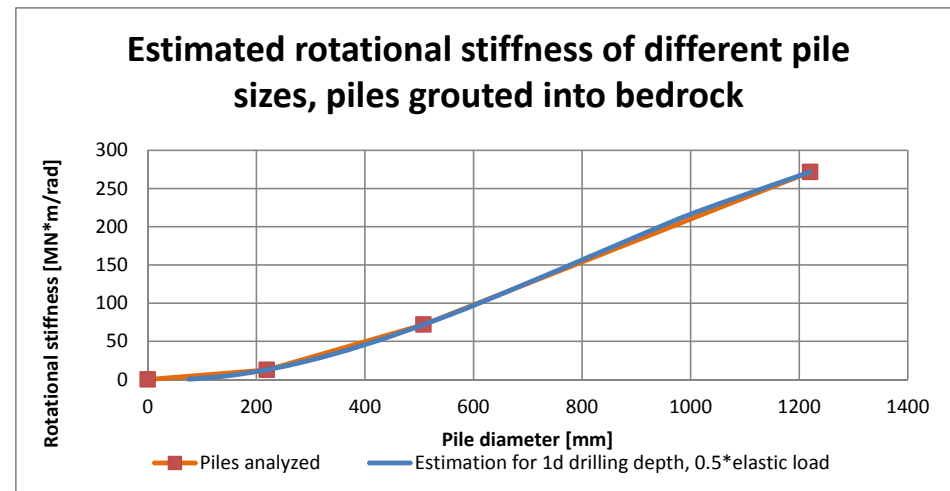
Diameter	Analyzed at	Cubic fit	Linear fit	Difference	Pile
x	y	y'	(y-y')^2	Constant	Best fit
0	0	0	0		
219.1	12.6212	12.81832	0.038854		RD220/10 a
508	71.87738	71.78967	0.007694		RD500/12.5 b
1220	271.7397	271.74104	1.81E-06		RD1220/12.5 c
				d	
				SUM(y-y')^2	0.046549531
76.1		0.52	4.383723	3.86	
88.9		1.05	5.121064	4.07	
114.3		2.44	6.584225	4.14	
139.7		4.29	8.047386	3.76	
168.3		6.90	9.694883	2.80	RD170/12.5
219.1		12.82	12.6212	-0.20	RD220/12.5
273		20.78	23.68	2.89	RD270/12.5
323.9		29.76	34.12	4.36	RD320/12.5
406.4		46.93	51.04	4.11	RD400/12.5
508		71.79	71.88	0.09	RD500/12.5
559		85.50	86.19	0.69	RD550/12.5
610		99.85	100.51	0.66	RD600/12.5
711		129.63	128.86	-0.77	RD700/12.5
762		145.08	143.18	-1.90	RD750/12.5
813		160.62	157.49	-3.13	RD800/12.5
914		191.15	185.84	-5.30	RD900/12.5
1016		220.73	214.48	-6.25	RD1000/12.5
1220		271.74	271.74	0.00	RD1200/12.5

$$\text{Equation: } f(x) = a \cdot x^3 + b \cdot x^2 + c \cdot x + d$$

x=height from bedrock [m]

Y=horizontal displacement [mm]

y'=solved horizontal displacement [mm]



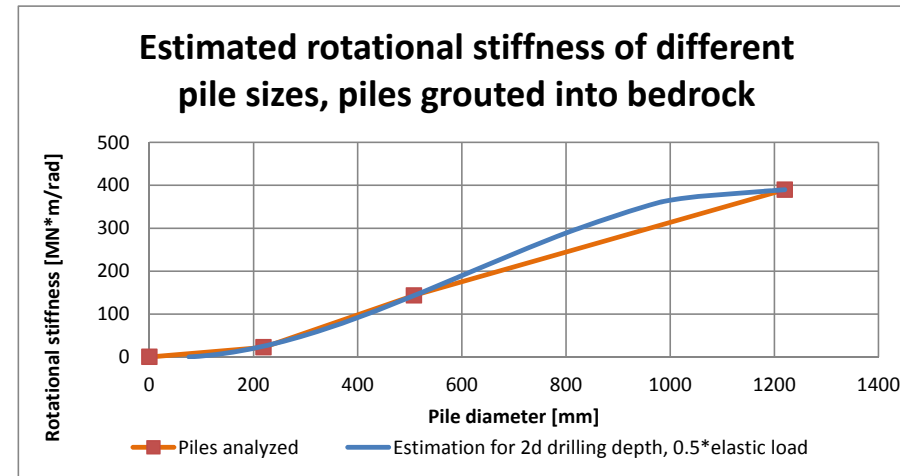
Fitting done by using calculated 220/10, 500/12.5 and 1220/12.5 piles
 Rotational stiffness of other pile sizes fitted, drilling hole grouted
 Least squares method

2d drilling depth, 0.5x elastic load

correlation factor $1/1.25 = 0.8$ is included, more on correlation factor in section 4.1

Diameter	Analyzed at	Cubic fit	Linear fit	Difference	Pile	Constant	Best fit
x	y	y'	(y-y')^2				
0	0	0	0				
219.1	22.40	19.2	7.386964		RD220/10	a	-5.21914E-07
508	143.44	142.83	0.377469		RD500/12.5	b	0.000955817
1220	389.84	389.87	0.000875		RD1220/12.5	c	-0.069715153
		Cubic fit	Linear	Difference		d	0
76.1		0.00	7.78	7.78		SUM(y-y')^2	7.76530699
88.9		0.99	9.09	8.10			
114.3		3.74	11.69	7.95			
139.7		7.49	14.28	6.79			
168.3		12.85	17.21	4.36	RD170/12.5		
219.1		25.12	22.40	-2.72	RD220/12.5		
273		41.58	44.98	3.40	RD270/12.5		
323.9		59.96	66.31	6.35	RD320/12.5		
406.4		94.50	100.87	6.37	RD400/12.5		
508		142.83	143.44	0.61	RD500/12.5		
559		168.54	161.09	-7.45	RD550/12.5		
610		194.67	178.74	-15.93	RD600/12.5		
711		246.03	213.69	-32.34	RD700/12.5		
762		270.95	231.34	-39.60	RD750/12.5		
813		294.63	248.99	-45.64	RD800/12.5		
914		336.26	283.94	-52.31	RD900/12.5		
1016		368.45	319.24	-49.21	RD1000/12.5		
1220		389.87	389.84	-0.03	RD1200/12.5		

Equation: $f(x) = a*x^3 + b*x^2 + c*x + d$
 x=height from bedrock [m]
 Y=horizontal displacement [mm]
 y'=solved horizontal displacement [mm]



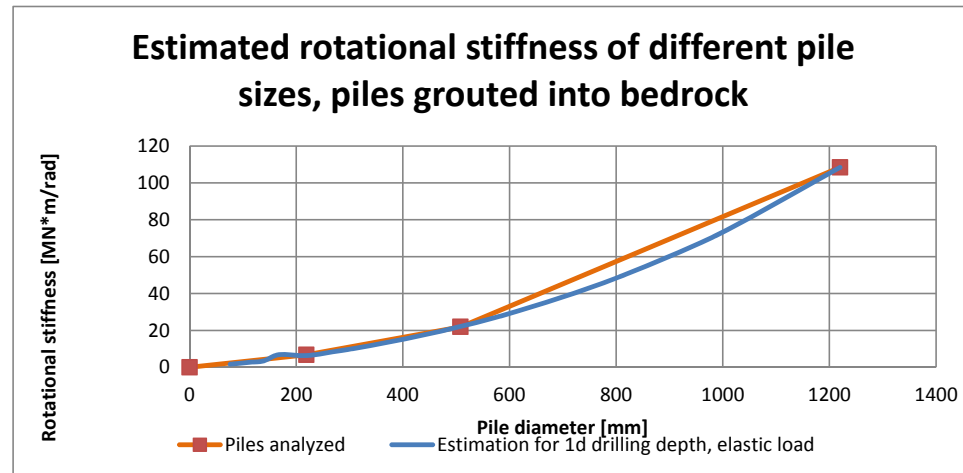
Fitting done by using calculated 220/10, 500/12.5 and 1220/12.5 piles
 Rotational stiffness of other pile sizes fitted, drilling hole grouted
 Least squares method

1d drilling depth, elastic load

correlation factor $1/1.25 = 0.8$ is included, more on correlation factor in section 4.1

Diameter	Analyzed at	Cubic fit	Linear fit	Difference	Pile	Constant	Best fit
x	y	y'	(y-y')^2				
0	0	0	0				
219.1	6.7592	6.36	0.16138		220/10	a	1.33E-08
508	21.92	22.13	0.042286		500/12.5	b	4.07E-05
1220	108.4	108.39	0.000169		1220/12.5	c	0.019468
		Cubic fit	Linear			d	0
76.1		1.72	2.35	0.62		SUM(y-y')^2	0.203835
88.9		2.06	2.74	0.68			
114.3		2.78	3.53	0.75			
139.7		3.55	4.31	0.76			
168.3		6.90	5.19	-1.70	RD170/12.5		
219.1		6.36	6.76	0.40	RD220/12.5		
273		8.62	9.59	0.97	RD270/12.5		
323.9		11.02	12.26	1.24	RD320/12.5		
406.4		15.52	16.59	1.07	RD400/12.5		
508		22.13	21.92	-0.21	RD500/12.5		
559		25.91	28.11	2.20	RD550/12.5		
610		30.02	34.31	4.29	RD600/12.5		
711		39.17	46.58	7.40	RD700/12.5		
762		44.32	52.77	8.45	RD750/12.5		
813		49.84	58.97	9.12	RD800/12.5		
914		61.90	71.23	9.33	RD900/12.5		
1016		75.68	83.62	7.94	RD1000/12.5		
1220		108.39	108.40	0.01	RD1200/12.5		

Equation: $f(x) = a \cdot x^3 + b \cdot x^2 + c \cdot x + d$
 x = height from bedrock [m]
 Y = horizontal displacement [mm]
 y' = solved horizontal displacement [mm]



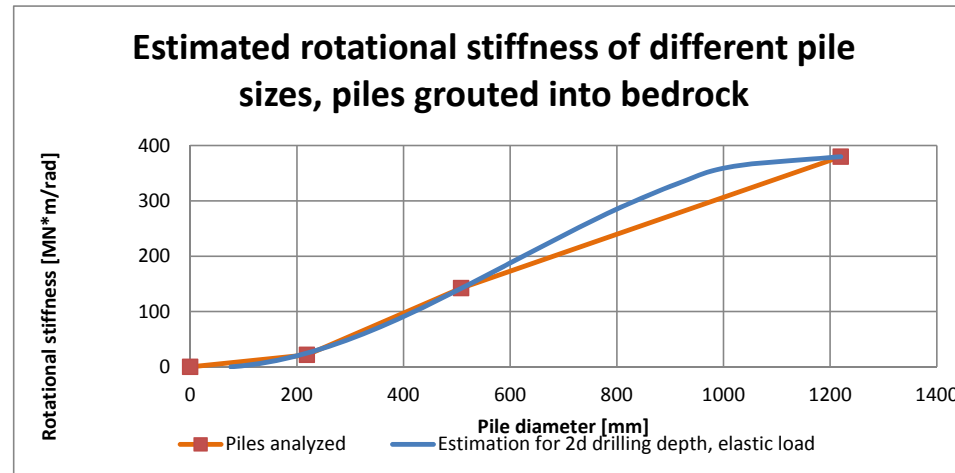
Fitting done by using calculated 220/10, 500/12.5 and 1220/12.5 piles
 Rotational stiffness of other pile sizes fitted, drilling hole grouted
 Least squares method

2d drilling depth, elastic load

correlation factor $1/1.25 = 0.8$ is included, more on correlation factor in section 4.1

Diameter	Analyzed at	Cubic fit	Linear fit	Difference	Pile	Constant	Best fit
x	y	y'	(y-y')^2				
0	0	0	0				
219.1	21.62944	24.96	11.09786		220/10	a	-5.2E-07
508	142.32	141.58	0.542348		500/12.5	b	0.000951
1220	379.92	379.96	0.001318		1220/12.5	c	-0.06936
		Cubic fit	Linear			d	0
76.1		0.00	7.51	7.51		SUM(y-y')^2	11.64153
88.9		0.98	8.78	7.79			
114.3		3.72	11.28	7.57			
139.7		7.45	13.79	6.34			
168.3		12.78	16.61	3.84	RD170/12.5		
219.1		24.96	21.63	-3.33	RD220/12.5		
273		41.31	44.15	2.84	RD270/12.5		
323.9		59.54	65.41	5.87	RD320/12.5		
406.4		93.77	99.88	6.11	RD400/12.5		
508		141.58	142.32	0.74	RD500/12.5		
559		166.98	159.34	-7.64	RD550/12.5		
610		192.76	176.36	-16.40	RD600/12.5		
711		243.29	210.06	-33.23	RD700/12.5		
762		267.72	227.08	-40.64	RD750/12.5		
813		290.87	244.10	-46.76	RD800/12.5		
914		331.29	277.81	-53.49	RD900/12.5		
1016		362.06	311.84	-50.22	RD1000/12.5		
1220		379.96	379.92	-0.04	RD1200/12.5		

Equation: $f(x) = a*x^3 + b*x^2 + c*x + d$
 x =height from bedrock [m]
 Y =horizontal displacement [mm]
 y' =solved horizontal displacement [mm]



Appendix 8 Drilling depth and pile size relation to rotational stiffness

Fitting done by using calculated 220/10, 500/12.5 and 1220/12.5 piles

Rotational stiffness of other pile sizes fitted, drilling hole grouted

Least squares method

1d drilling depth, 0.05x elastic load

correlation factor $1/1.25 = 0.8$ is included, more on correlation factor in section 4.1

Diameter	Analized a	Cubic fit	Linear fit	Difference	Pile	Constant	Best fit
x	y	y'	(y-y')^2				
0	0	0	0				
219.1	0.100422	1.84E-01	0.006960086		RD220/10	a	0.00E+00
508	0.7728	7.22E-01	0.002558827		RD500/12.5	b	2.01651E-06
1220	3.48	3.49E+00	3.69489E-05		RD1220/12.5	c	0.000397294
						d	0
						SUM(y-y')	0.009555862
76.1		0.042	0.034879711	-0.01			
88.9		0.051	0.040746469	-0.01			
114.3		0.072	0.052388317	-0.02			
139.7		0.095	0.064030166	-0.03			
168.3		0.124	0.077138703	-0.05	RD170/12.5		
219.1		0.184	0.1004224	-0.08	RD220/12.5		
273		0.259	0.23	-0.03	RD270/12.5		
323.9		0.340	0.34	0.00	RD320/12.5		
406.4		0.495	0.54	0.04	RD400/12.5		
508		0.722	0.77	0.05	RD500/12.5		
559		0.852	0.97	0.11	RD550/12.5		
610		0.993	1.16	0.17	RD600/12.5		
711		1.302	1.54	0.24	RD700/12.5		
762		1.474	1.74	0.26	RD750/12.5		
813		1.656	1.93	0.28	RD800/12.5		
914		2.048	2.32	0.27	RD900/12.5		
1016		2.485	2.70	0.22	RD1000/12.5		
1220		3.486	3.48	-0.01	RD1200/12.5		

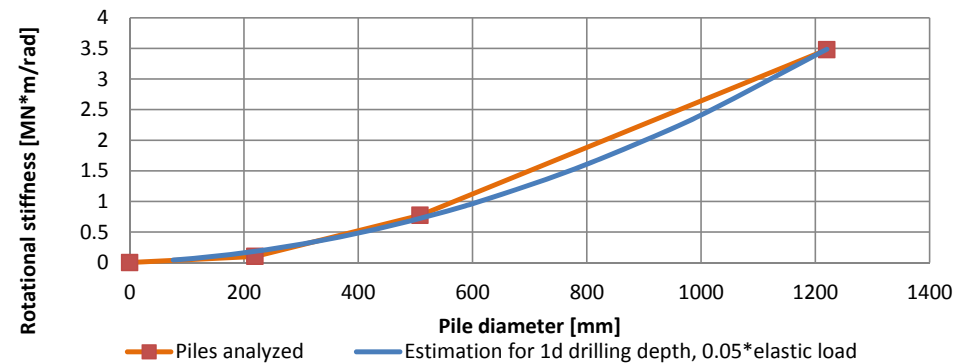
Equation: $f(x) = a \cdot x^3 + b \cdot x^2 + c \cdot x + d$

x=height from bedrock [m]

Y=horizontal displacement [mm]

y'=solved horizontal displacement [mm]

Estimated rotational stiffness of different pile sizes, piles grouted into bedrock



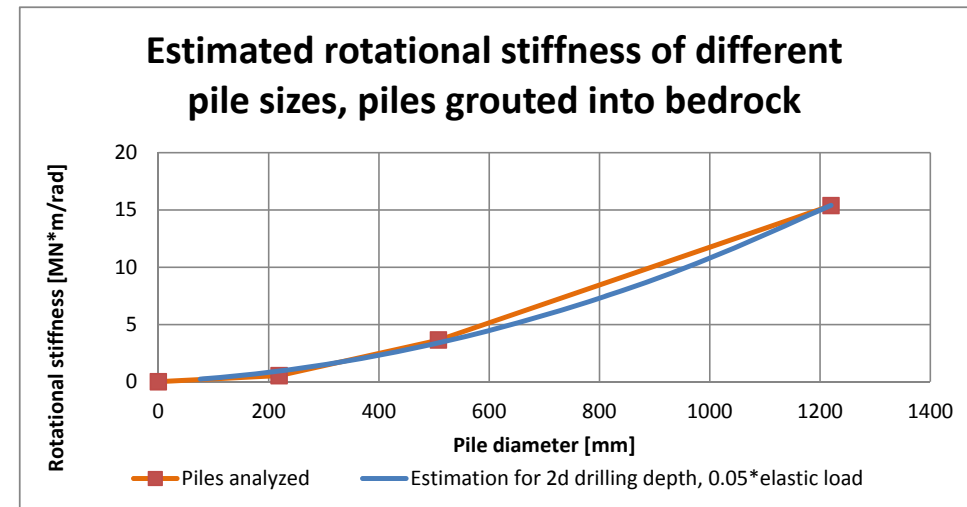
Fitting done by using calculated 220/10, 500/12.5 and 1220/12.5 piles
 Rotational stiffness of other pile sizes fitted, drilling hole grouted
 Least squares method

2d drilling depth, 0.05x elastic load

correlation factor $1/1.25 = 0.8$ is included, more on correlation factor in section 4.1

Diameter	Analyzed a	Cubic fit	Linear fit	Difference	Pile	Constant	Best fit
x	y*	y`	(y-y`)^2				
0	0	0	0				
219.1	0.533977	0.94	0.163061295		RD220/10	a	0
508	3.6432	3.40	0.059941574		RD500/12.5	b	8.34038E-06
1220	15.3768	15.41	0.00086591		RD1220/12.5	c	0.002452793
						d	0
						SUM(y-y`)^2	0.223868778
		Cubic fit	Linear	Difference			
76.1		0.235	0.19	-0.05			
88.9		0.284	0.22	-0.07			
114.3		0.389	0.28	-0.11			
139.7		0.505	0.34	-0.16			
168.3		0.649	0.41	-0.24	RD170/12.5		
219.1		0.938	0.5339768	-0.40	RD220/12.5		
273		1.291	1.11	-0.18	RD270/12.5		
323.9		1.669	1.66	-0.01	RD320/12.5		
406.4		2.374	2.55	0.18	RD400/12.5		
508		3.398	3.64	0.24	RD500/12.5		
559		3.977	4.48	0.51	RD550/12.5		
610		4.600	5.32	0.72	RD600/12.5		
711		5.960	6.99	1.03	RD700/12.5		
762		6.712	7.83	1.12	RD750/12.5		
813		7.507	8.67	1.16	RD800/12.5		
914		9.209	10.33	1.12	RD900/12.5		
1016		11.101	12.01	0.91	RD1000/12.5		
1220		15.406	15.38	-0.03	RD1200/12.5		

Equation: $f(x) = a \cdot x^3 + b \cdot x^2 + c \cdot x + d$
 x=height from bedrock [m]
 Y=horizontal displacement [mm]
 y`=solved horizontal displacement [mm]



Appendix 8 Drilling depth and pile size relation to rotational stiffness

correlation factor $1/1.25 = 0.8$ is included, more of correlation factor in paragraph 4.1

Rotational stiffness of other pile sizes are fitted, drilling hole grouted

1d drilling depth, 0.5x elastic load

Pile	Diameter [mm]	Analysed according to FEM analysis	Cubic fit	Linear fit	Difference	Single piles: fitted S_j [MNm/rad]	Wall (RM-RF): fitted S_j [MNm/rad*m]
RD170/12.5	168.3		6.9	9.7	2.8	6.90	29.68
RD220/12.5	219.1	12.6	12.8	12.6	-0.2	12.62	44.58
RD270/12.5	273		20.8	23.7	2.9	20.78	61.68
RD320/12.5	323.9		29.8	34.1	4.4	29.76	76.71
RD400/12.5	406.4		46.9	51.0	4.1	46.93	99.76
RD500/12.5	508	71.9	71.8	71.9	0.1	71.79	125.51
RD550/12.5	559		85.5	86.2	0.7	85.50	137.24
RD600/12.5	610		99.9	100.5	0.7	99.85	148.15
RD700/12.5	711		129.6	128.9	-0.8	128.86	166.27
RD750/12.5	762		145.1	143.2	-1.9	143.18	173.34
RD800/12.5	813		160.6	157.5	-3.1	157.49	179.58
RD900/12.5	914		191.1	185.8	-5.3	185.84	190.02
RD1000/12.5	1016		220.7	214.5	-6.3	214.48	198.59
RD1200/12.5	1220	271.7	271.7	271.7	0.0	271.74	211.64

Rotational stiffness of other pile sizes are fitted, drilling hole grouted

2d drilling depth, 0.5x elastic load

Pile	Diameter [mm]	Analysed according to FEM analysis	Cubic fit	Linear fit	Difference	Single piles: fitted S_j [MNm/rad]	
RD170/12.5	168.3		12.9	17.2	4.4	12.85	55.33
RD220/12.5	219.1	22.4	25.1	22.4	-2.7	22.40	79.13
RD270/12.5	273		41.6	45.0	3.4	41.58	123.40
RD320/12.5	323.9		60.0	66.3	6.3	59.96	154.58
RD400/12.5	406.4		94.5	100.9	6.4	94.50	200.89
RD500/12.5	508	143.4	142.8	143.4	0.6	142.83	249.70
RD550/12.5	559		168.5	161.1	-7.4	161.09	258.57
RD600/12.5	610		194.7	178.7	-15.9	178.74	265.19
RD700/12.5	711		246.0	213.7	-32.3	213.69	275.73
RD750/12.5	762		270.9	231.3	-39.6	231.34	280.07
RD800/12.5	813		294.6	249.0	-45.6	248.99	283.91
RD900/12.5	914		336.3	283.9	-52.3	283.94	290.33
RD1000/12.5	1016		368.4	319.2	-49.2	319.24	295.59
RD1200/12.5	1220	389.8	389.9	389.8	0.0	389.84	303.61

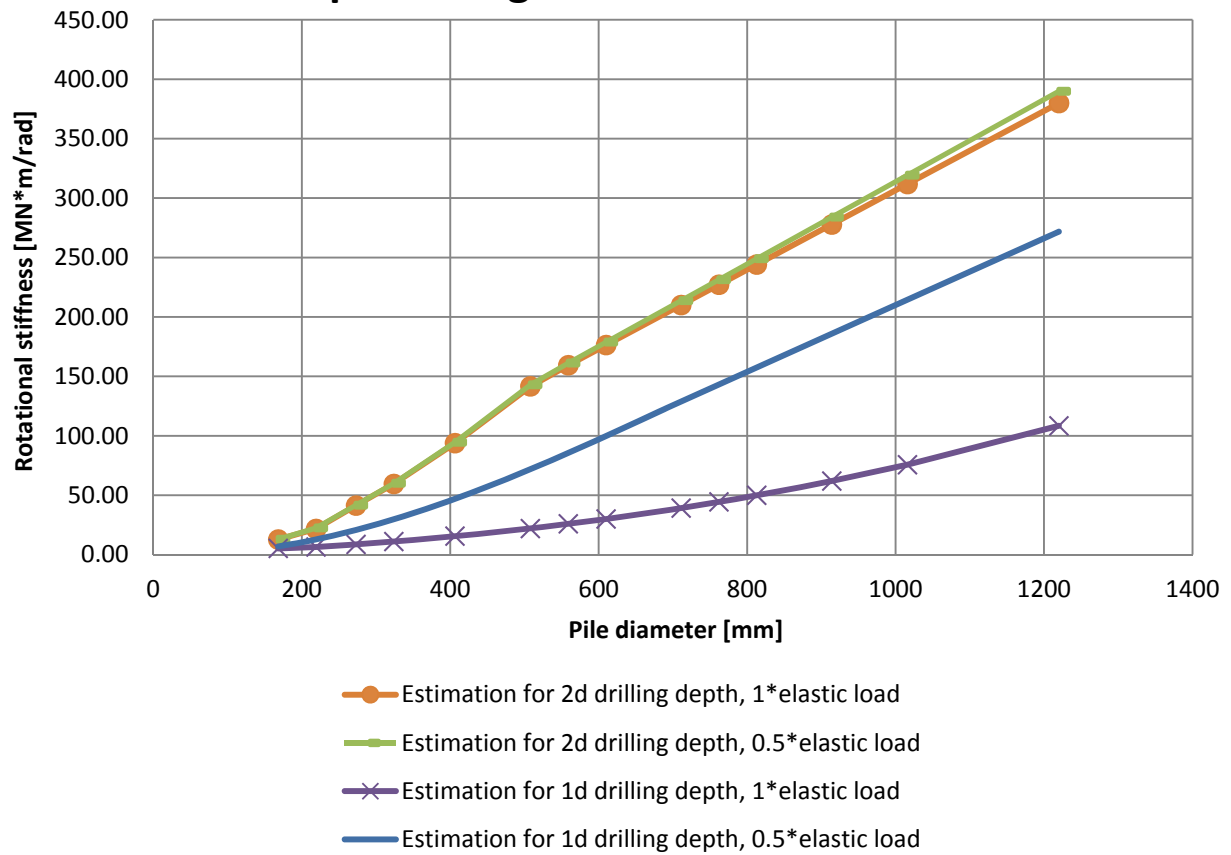
Rotational stiffness of other pile sizes are fitted, drilling hole grouted
1d drilling depth, elastic load

Pile	Diameter [mm]	Analysed according to FEM analysis	Cubic fit	Linear fit	Difference	Single piles: fitted S_j [MNm/rad]	Wall (RM-RF): fitted S_j [MNm/rad*m]
RD170/12.5	168.3		6.9	5.2	-1.7	5.19	22.35
RD220/12.5	219.1	6.8	6.4	6.8	0.4	6.36	22.46
RD270/12.5	273		8.6	9.6	1.0	8.62	25.57
RD320/12.5	323.9		11.0	12.3	1.2	11.02	28.42
RD400/12.5	406.4		15.5	16.6	1.1	15.52	32.99
RD500/12.5	508	21.9	22.1	21.9	-0.2	21.92	38.32
RD550/12.5	559		25.9	28.1	2.2	25.91	41.59
RD600/12.5	610		30.0	34.3	4.3	30.02	44.54
RD700/12.5	711		39.2	46.6	7.4	39.17	50.55
RD750/12.5	762		44.3	52.8	8.4	44.32	53.66
RD800/12.5	813		49.8	59.0	9.1	49.84	56.83
RD900/12.5	914		61.9	71.2	9.3	61.90	63.30
RD1000/12.5	1016		75.7	83.6	7.9	75.68	70.08
RD1200/12.5	1220	108.4	108.4	108.4	0.0	108.39	84.41

Rotational stiffness of other pile sizes are fitted, drilling hole grouted
2d drilling depth, elastic load

Pile	Diameter [mm]	Analysed according to FEM analysis	Cubic fit	Linear fit	Difference	Single piles: fitted S_j [MNm/rad]	Wall (RM-RF): fitted S_j [MNm/rad*m]
RD170/12.5	168.3		12.8	16.6	3.8	12.78	54.99
RD220/12.5	219.1	21.6	25.0	21.6	-3.3	21.63	76.40
RD270/12.5	273		41.3	44.1	2.8	41.31	122.57
RD320/12.5	323.9		59.5	65.4	5.9	59.54	153.48
RD400/12.5	406.4		93.8	99.9	6.1	93.77	199.34
RD500/12.5	508	142.3	141.6	142.3	0.7	141.58	247.52
RD550/12.5	559		167.0	159.3	-7.6	159.34	255.76
RD600/12.5	610		192.8	176.4	-16.4	176.36	261.66
RD700/12.5	711		243.3	210.1	-33.2	210.06	271.05
RD750/12.5	762		267.7	227.1	-40.6	227.08	274.92
RD800/12.5	813		290.9	244.1	-46.8	244.10	278.34
RD900/12.5	914		331.3	277.8	-53.5	277.81	284.05
RD1000/12.5	1016		362.1	311.8	-50.2	311.84	288.74
RD1200/12.5	1220	379.9	380.0	379.9	0.0	379.92	295.89

Estimated rotational stiffness of different pile size, piles are grouted into bedrock



Rotational stiffness of other pile sizes are fitted, clay in the drilling hole
Least squared method

1d drilling depth, 0.05x elastic load

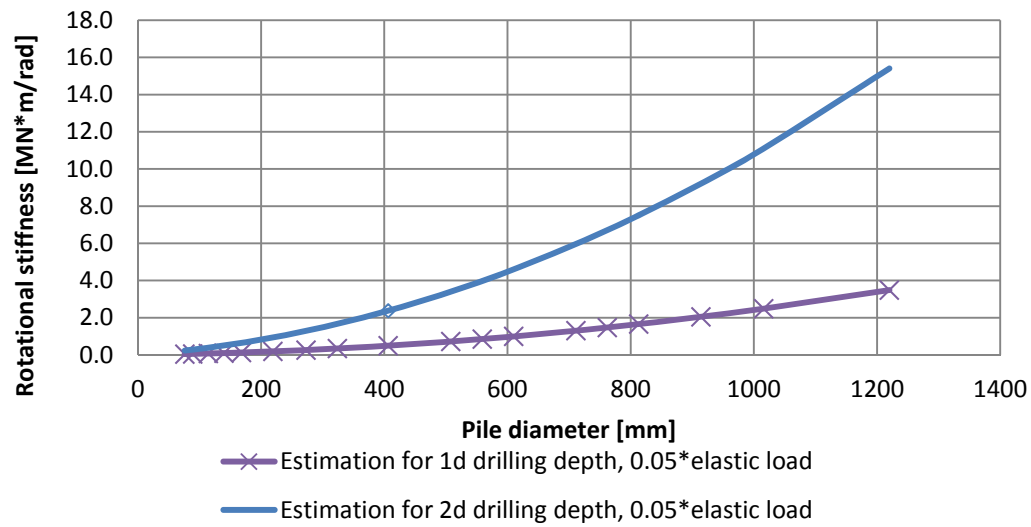
Pile	Diameter [mm]	Analysed according to FEM analysis	Cubic fit	Linear fit	Difference	Single piles: fitted S_j [MNm/rad]	Wall (RM-RF): fitted S_j [MNm/rad*m]
RD170/12.5	168.3		0.12	0.08	-0.05	0.077	0.33
RD220/12.5	219.1	0.10	0.18	0.10	-0.08	0.100	0.35
RD270/12.5	273		0.26	0.23	-0.03	0.226	0.67
RD320/12.5	323.9		0.34	0.34	0.00	0.340	0.88
RD400/12.5	406.4		0.49	0.54	0.04	0.495	1.05
RD500/12.5	508	0.77	0.72	0.77	0.05	0.722	1.26
RD550/12.5	559		0.85	0.97	0.11	0.852	1.37
RD600/12.5	610		0.99	1.16	0.17	0.993	1.47
RD700/12.5	711		1.30	1.54	0.24	1.302	1.68
RD750/12.5	762		1.47	1.74	0.26	1.474	1.78
RD800/12.5	813		1.66	1.93	0.28	1.656	1.89
RD900/12.5	914		2.05	2.32	0.27	2.048	2.09
RD1000/12.5	1016		2.49	2.70	0.22	2.485	2.30
RD1200/12.5	1220	3.48	3.49	3.48	-0.01	3.480	2.71

Rotational stiffness of other pile sizes are fitted, clay in drilling hole
Least squared method

2d drilling depth, 0.05x elastic load

Pile	Diameter [mm]	Analysed according to FEM analysis	Cubic fit	Linear fit	Difference	Single piles: fitted S_j [MNm/rad]	Wall (RM-RF): fitted S_j [MNm/rad*m]
RD170/12.5	168.3		0.65	0.41	-0.24	0.410	1.77
RD220/12.5	219.1	0.53	0.94	0.53	-0.40	0.534	1.89
RD270/12.5	273		1.29	1.11	-0.18	1.114	3.31
RD320/12.5	323.9		1.67	1.66	-0.01	1.662	4.28
RD400/12.5	406.4		2.37	2.55	0.18	2.374	5.05
RD500/12.5	508	3.64	3.40	3.64	0.24	3.398	5.94
RD550/12.5	559		3.98	4.48	0.51	3.977	6.38
RD600/12.5	610		4.60	5.32	0.72	4.600	6.82
RD700/12.5	711		5.96	6.99	1.03	5.960	7.69
RD750/12.5	762		6.71	7.83	1.12	6.712	8.13
RD800/12.5	813		7.51	8.67	1.16	7.507	8.56
RD900/12.5	914		9.21	10.33	1.12	9.209	9.42
RD1000/12.5	1016		11.10	12.01	0.91	11.101	10.28
RD1200/12.5	1220	15.38	15.41	15.38	-0.03	15.377	11.98

Estimated rotational stiffness of different pile size, clay in drilling hole



Appendix 9

P22 deformation shape

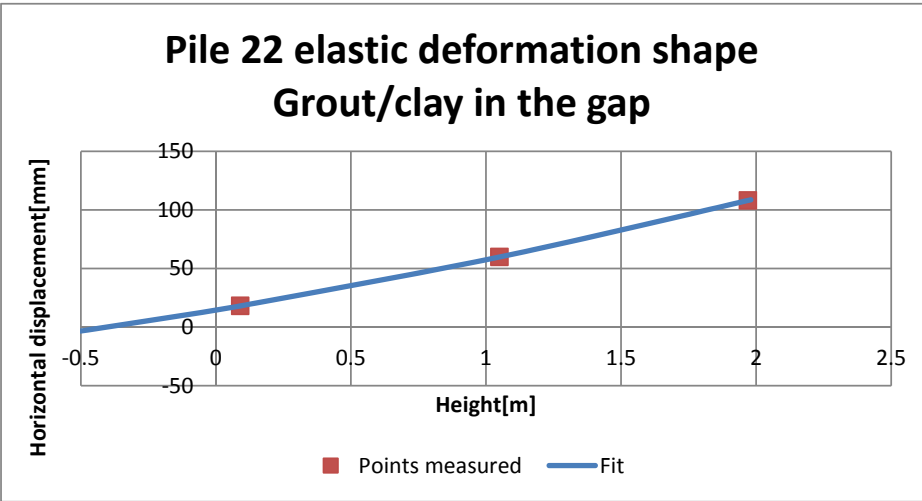
Pile: RD 220/10

Fitting to solve displacement in level of force. 72.7 kN horizontal load

Least squares method

x	y	y`	(y-y`)^2	Comment	Constant	Best fit
	-0.5	-3.28986				
	-0.1	10.859				
	0	14.63127				
0.09	18.10669	18.10669	6.84E-17	S3 [mm]	a	0
1.05	59.91655	59.91655	6.39E-18	S2 [mm]	b	4.701022
1.97	108.1152	108.1152	1.57E-16	S1 [mm]	c	38.19277
1.98		108.6828		Load level	d	14.63127
			SUM(y-y`)^2			2.31E-16

Equation: $f(x) = a \cdot x^3 + b \cdot x^2 + c \cdot x + d$
x=height from bedrock [m]
Y=horizontal displacement [mm]
y`=solved horizontal displacement [mm]



Wall Type	BoredpileWall
Name	RD500/12.5-wall (rm/rf)
Manufacturer	Ruukki
Cross Section Area [m^2]	0.037290694213231
Calculation Width [m]	1
Inertia Modulus [m^4]	0.00104467486365223
Section Modulus [m^3]	0.00411289316398515
Elastic Modulus [kPa]	210000000
Flexural Stiffness [kNm^2]	219381.721366968
Axial Stiffness [kNm^2/m^2]	7831045.78477851
Length of Wall [m]	9

Name	A [mm^2]	L [m]	α [°]	h [m]	F [kN]	Elastic Modulus [kPa]	Overdig [m]	Horizontal distribution [m]
	5000	5	180	1	0	210000000	0.4	2.3

Id	Layer Name	z [m]	h [m]	γ [kN/m³]	Φ [°]	c [kPa]	Δc [kPa/m]	Ko Model	Ko	Earth Pres. Model	Ka	Kp	d/ud	Material Model	δya	δyp	ξ50a	ξ50p	m	n	k
1.	Täyttö	0	2	18	34	0	0	Jaky	0.44	Coulomb	0.26	5.83	Drained	MCM					300	0.5	0.5
2.	Savi	-2	4	16	0	10	1	Jaky	1	Coulomb	1	1	Undrained	MCM					40	1	1
3.	Moreeni	-6	1	20	40	0	0	Jaky	0.36	Coulomb	0.2	9.36	Drained	MCM					800	0.5	0.5
4.	Kallio	-7	2	20	45	10	0	Jaky	0.29	User-defined	0.2	1000	Drained	MCM					1500	1	1

1. Rock waste

1. Täyttö

2.Clay

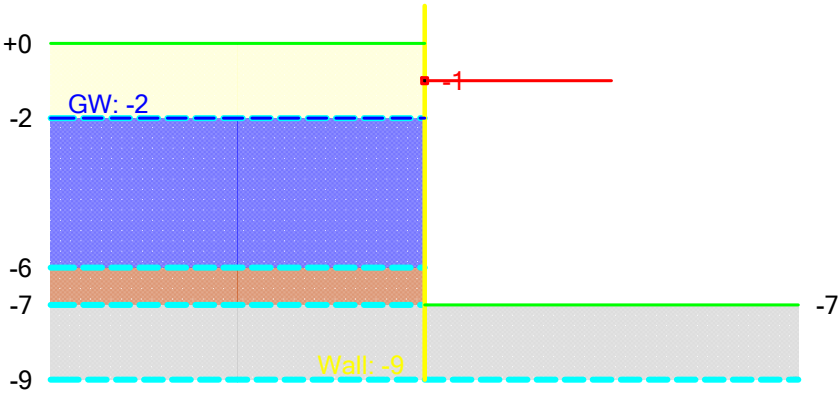
2. Savi

3. Moraine

3. Moreeni

4. Bedrock

4. Kallio



Result	Value
Anchor 1: Max. force [kN]	201.5
Max. bending moment [kNm]	191
Max. horizontal displacement [mm]	7.3

/RD pile wall 500/12.5

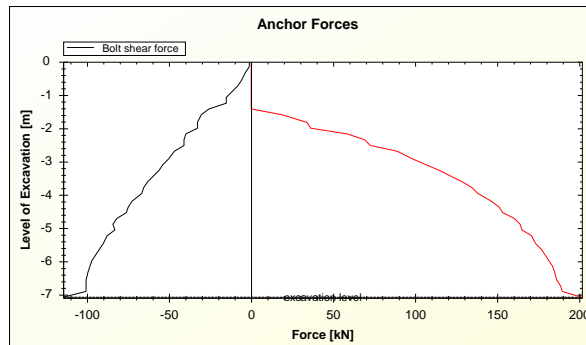
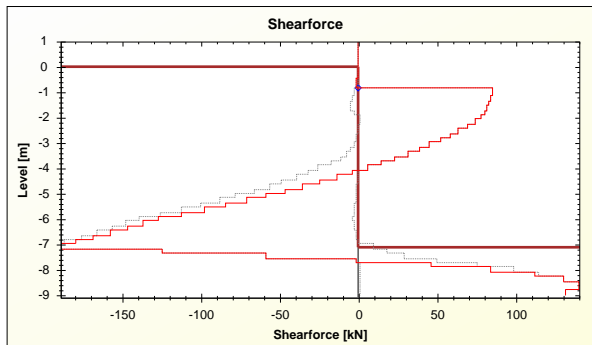
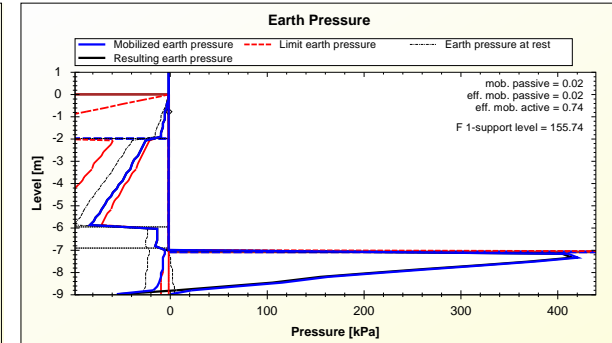
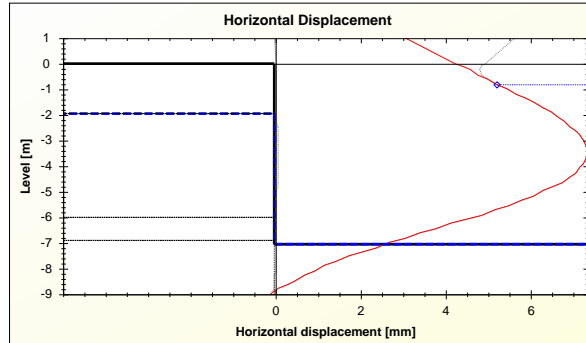
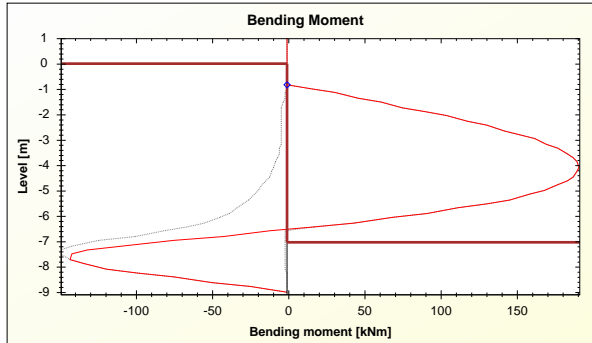
Pile drilled into bedrock. Bedrock as a soil. Clay in gap
Leo-Ville Miettinen/

Appendix 10

Calculation Graphs Excavation Level -7.09 m

/RD pile wall 500/12.5

Pile drilled into bedrock. Bedrock as a soil. Clay in gap
Leo-Ville Mettinen/
Novapoint GeoCalc 2.4 (23.10.2013 14:36)



APPENDIX 11

Directional Deformation

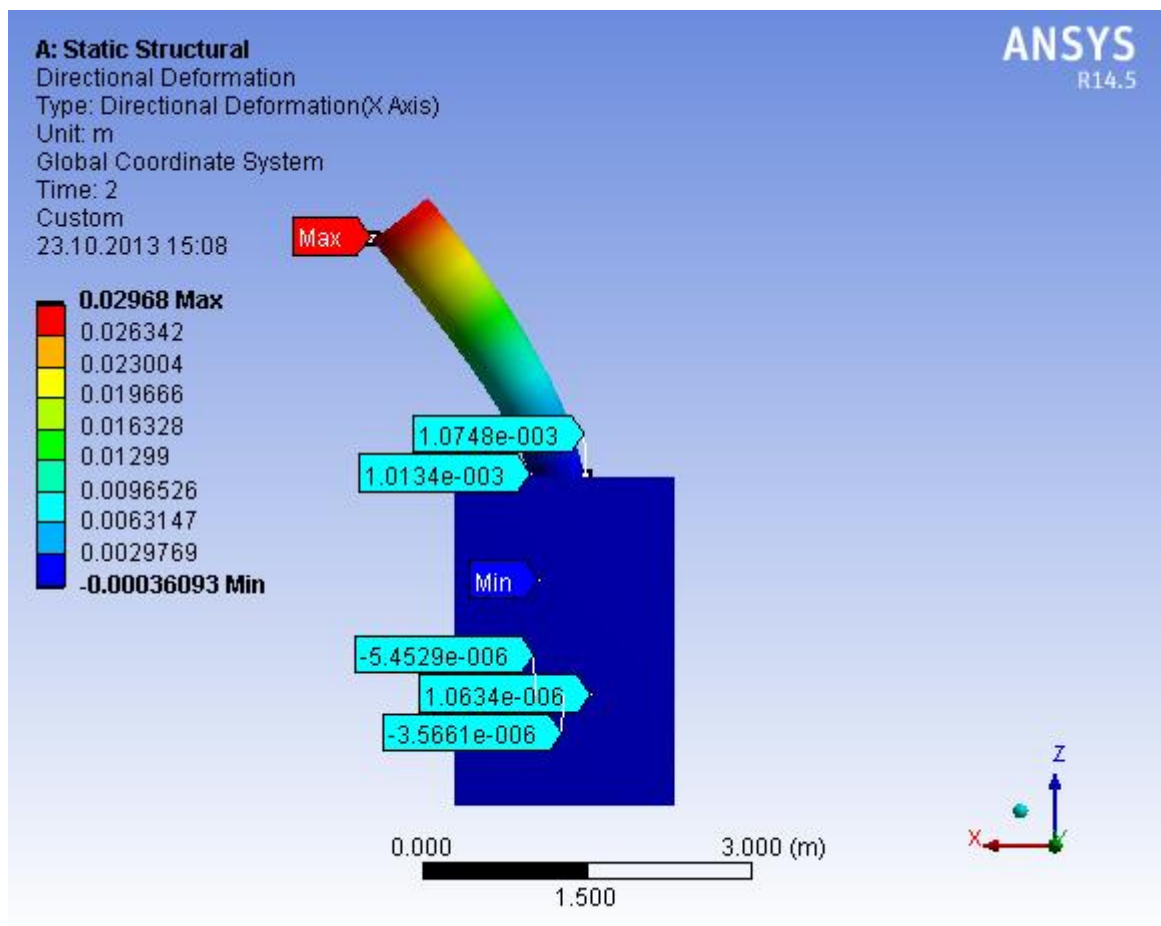
Subject:

Author:

Prepared For:

Date Wednesday, October 23, 2013

Comments:



Appendix 12: Water penetration calculations

Water penetration through drilling hole

$$d_{220_10} := 219.1 \text{ mm}$$

$$d_{220_10drill} := 273 \text{ mm}$$

$$A_{gap} := \left(d_{220_10drill}^2 - d_{220_10}^2 \right) \cdot \frac{\pi}{4} = 0.021 \text{ m}^2$$

Area of the gap

$$L_{220_10drill} := 1 \text{ m}$$

Drilling length of pile 220/10

$$k_{silt} := 10^{-7} \frac{\text{m}}{\text{s}}$$

Permeability of silt

Leino,V, Rantala,J, 2000, maanvaraisten alapohjarakenteisen

kosteuskäyttäytyminen, Available at:

[http://dspace.cc.tut.fi/dpub/bitstream/handle/123456789/20771/leivo_%](http://dspace.cc.tut.fi/dpub/bitstream/handle/123456789/20771/leivo_%20rantala_maanvaraisten_alapohjarakenteiden.pdf?sequence=3)

20rantala_maanvaraisten_alapohjarakenteiden.pdf?sequence=3

$$h := \left(\frac{70 + 52.5 + 35 + 17.5 + 3.5}{5} \right) \cdot \text{m} = 35.7 \text{ m}$$

Water column equal to 0.35-7 bar average (used in site test)

$$L := L_{220_10drill} \cdot 2 = 2 \text{ m}$$

Silt

$$Q := k_{silt} \cdot \frac{h}{L} \cdot A_{gap} = \left(3.719 \cdot 10^{-8} \right) \frac{\text{m}^3}{\text{s}}$$

$$Q := k_{silt} \cdot \frac{h}{L} \cdot A_{gap} = 0.112 \frac{L}{50 \cdot \text{min}}$$

Water leakage through gap in 0.35-7 bar pressure in 50 min

Dense sand

$$k_{sand} := 3.0 \cdot 10^{-6} \frac{\text{m}}{\text{s}}$$

Leino,V, Rantala,J, 2000, page 20

$$Q := k_{sand} \cdot \frac{h}{L} \cdot A_{gap} = 3.347 \frac{L}{50 \cdot \text{min}}$$

Water leakage through gap in 0.35-7bar pressure. About same volume as in test (2.11).

Concrete

$$k_{concrete0.55} := 15 \cdot 10^{-12} \frac{m}{s}$$

Permeability of concrete,
perform as grouting
Figure 2.3.2 [Iso-Mustajärvi,P 2008]

$$Q := k_{concrete0.55} \cdot \frac{h}{L} \cdot A_{gap} = (1.673 \cdot 10^{-5}) \frac{L}{50 \cdot min}$$

Wall made of 220/10 piles

Dense sand

$$h := 5 \text{ m}$$

$$L := 1 \text{ m}$$

Pile drilled 0.5m

$$L_{run220} := 283 \text{ mm}$$

$$A_{gap220wall} := A_{gap} \frac{1 \cdot m}{2 \cdot L_{run220}} \cdot \frac{1}{m} = 0.037 \frac{m^2}{m}$$

$$k_{sand} = (3 \cdot 10^{-6}) \frac{m}{s}$$

$$Q := k_{sand} \cdot \frac{h}{L} \cdot A_{gap220wall} = 1.988 \frac{1}{m} \cdot \frac{L}{60 \text{ min}}$$

Water leakage through gap
in 0.5 bar pressure (5 m
ground water pressure).

Concrete

$$k_{concrete0.55} = (1.5 \cdot 10^{-11}) \frac{m}{s}$$

$$Q := k_{concrete0.55} \cdot \frac{h}{L} \cdot A_{gap220wall} = (9.938 \cdot 10^{-6}) \frac{1}{m} \cdot \frac{L}{60 \text{ min}}$$

Water leakage through gap
in 0.5 bar pressure (5 m
ground water pressure).

$$Q = 0.087 \frac{1}{m} \frac{L}{365 \cdot 24 \cdot 60 \cdot min}$$

Leakage in one year per 1 m wall

Water penetration through interlocks [14]

This calculation imitates the example calculation in SFS-EN 12063,
Appendix E.

$$b := L_{run220} = 0.283 \text{ m}$$

RD 220 pile wall

$$H := h = 5 \text{ m}$$

Height of wall

$$\rho := 5 \cdot 10^{-10} \cdot \frac{\text{m}}{\text{s}}$$

Joint resistance, interlock filled with filler [14]

$$n := \frac{1}{b} = 3.534 \frac{1}{\text{m}}$$

Number of interlocks per meter

$$Q := \rho \cdot H \cdot \frac{H}{2} \cdot n = (2.208 \cdot 10^{-8}) \frac{\text{m}^2}{\text{s}}$$

Discharge per meter of wall

$$Q = 0.08 \frac{1}{\text{m}} \cdot \frac{L}{60 \text{ min}}$$

Water permeability of soil samples

Sample 1

$$k = C \cdot \left[\frac{100 \cdot d_{10} \cdot n}{1 - n} \right]^2 \quad [19]$$

$$C := 2 \cdot \frac{1}{\text{m} \cdot \text{s}}$$

$$d_{10} := 0.025 \text{ mm}$$

(Diagram 3.2.2.1.1)

$$n := 59.5\%$$

Equal to maximum saturated water portion in sample [Appendix 20]

$$k := C \cdot \left(\frac{100 \cdot d_{10} \cdot n}{1 - n} \right)^2 = (2.698 \cdot 10^{-5}) \frac{\text{m}}{\text{s}}$$

Sample 2

$$d_{10} := 0.009 \text{ mm}$$

(Diagram 3.2.2.1.2)

$$n := 59.5\%$$

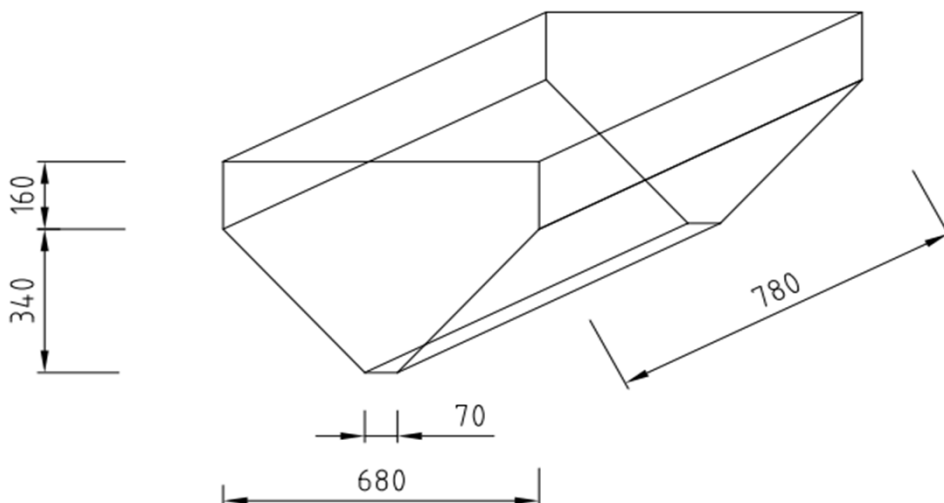
Porosity assumed to be same as sample 1

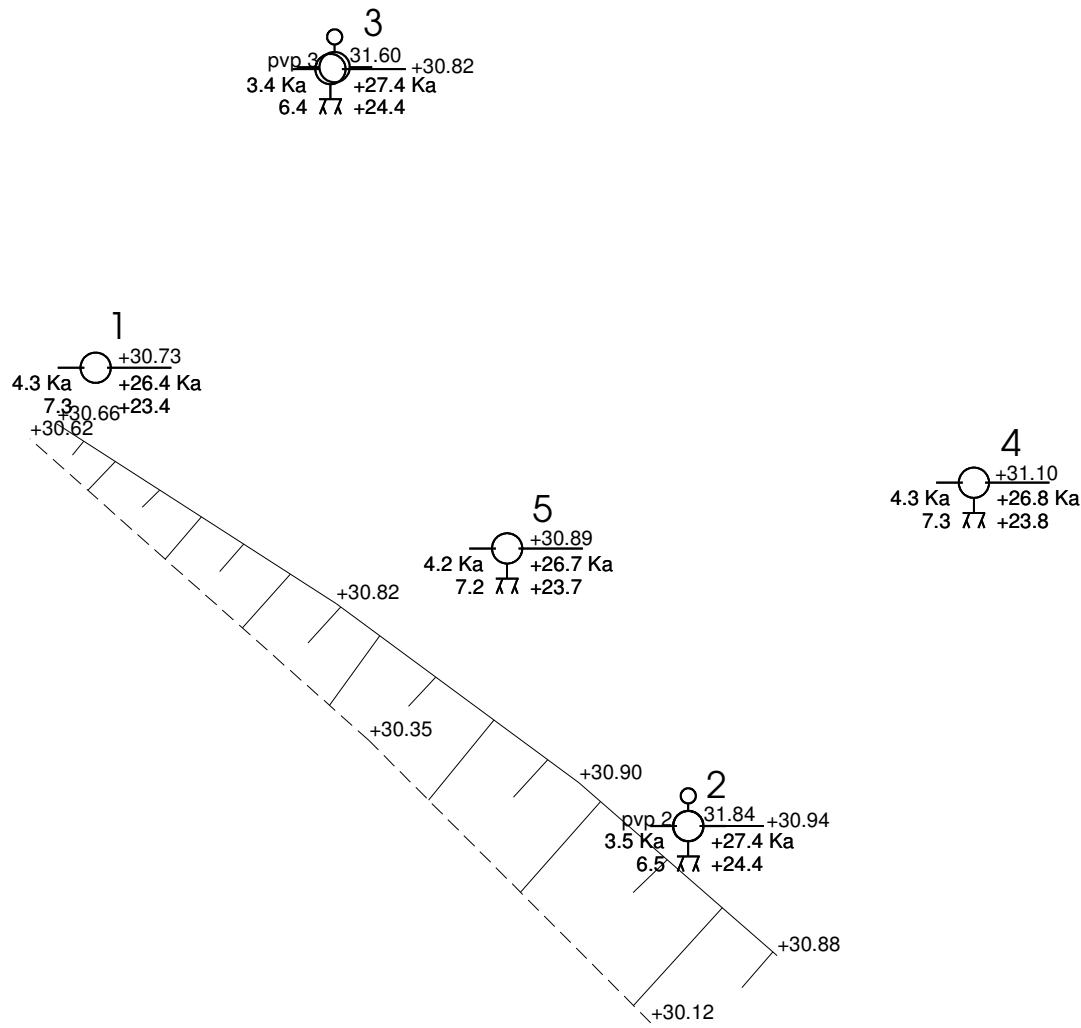
$$k := C \cdot \left(\frac{100 \cdot d_{10} \cdot n}{1 - n} \right)^2 = (3.497 \cdot 10^{-6}) \frac{\text{m}}{\text{s}}$$

Appendix 15 Volume table of grouting container

Distance from the bottom of container [cm]	Volume difference per 1 cm level difference [L]	Volume in containet at specific grout level [L]
1	0.69	0.69
2	0.83	1.51
3	0.97	2.48
4	1.11	3.58
5	1.25	4.83
6	1.39	6.21
7	1.53	7.74
8	1.67	9.41
9	1.81	11.21
10	1.95	13.16
11	2.09	15.24
12	2.23	17.47
13	2.37	19.83
14	2.51	22.34
15	2.65	24.98
16	2.79	27.77
17	2.93	30.69
18	3.06	33.76
19	3.20	36.96
20	3.34	40.31
21	3.48	43.79
22	3.62	47.42
23	3.76	51.18
24	3.90	55.09
25	4.04	59.13
26	4.18	63.32
27	4.32	67.64
28	4.46	72.10
29	4.60	76.71
30	4.74	81.45
31	4.88	86.34
32	5.02	91.36
33	5.16	96.53
34	5.30	101.83

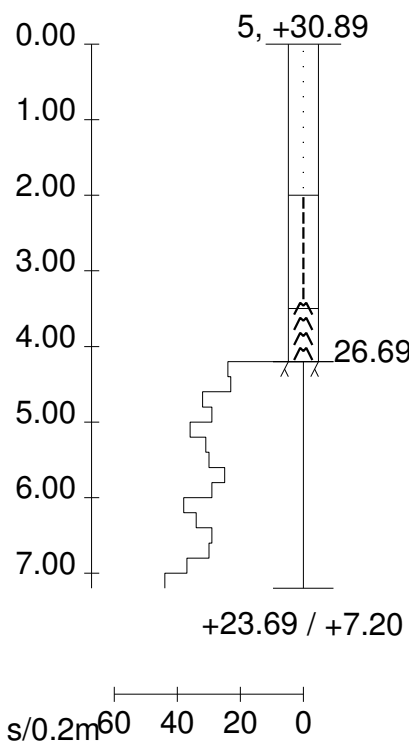
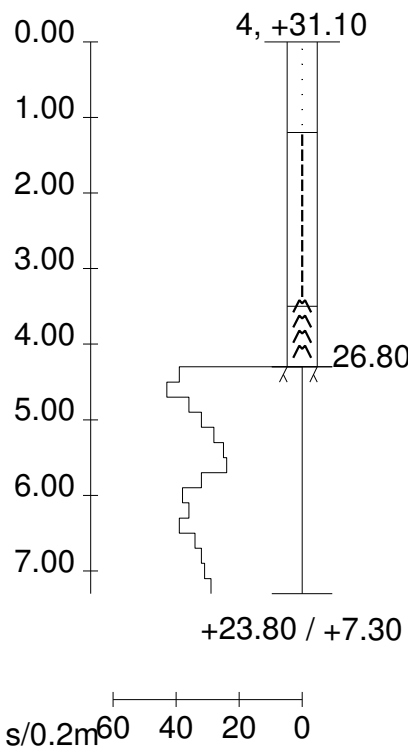
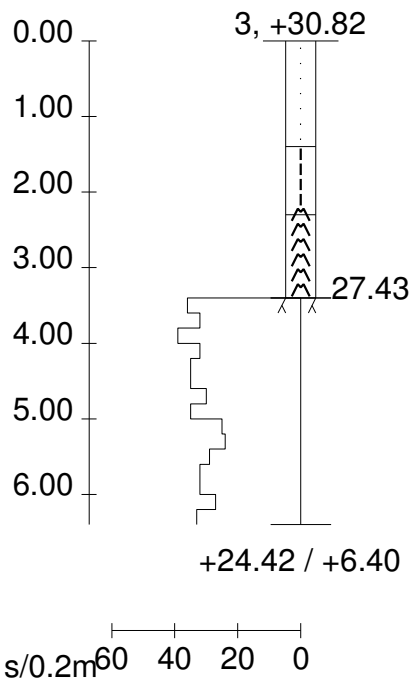
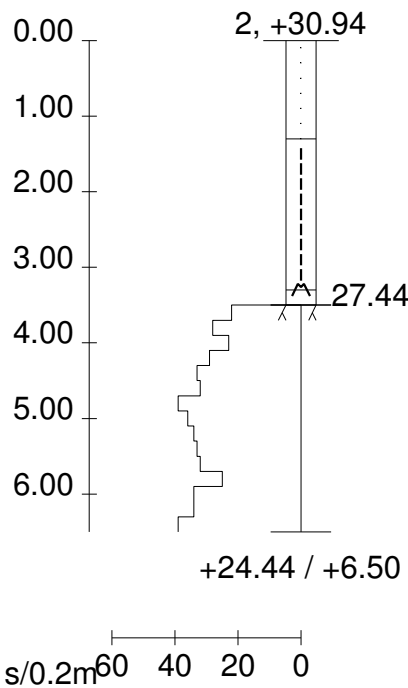
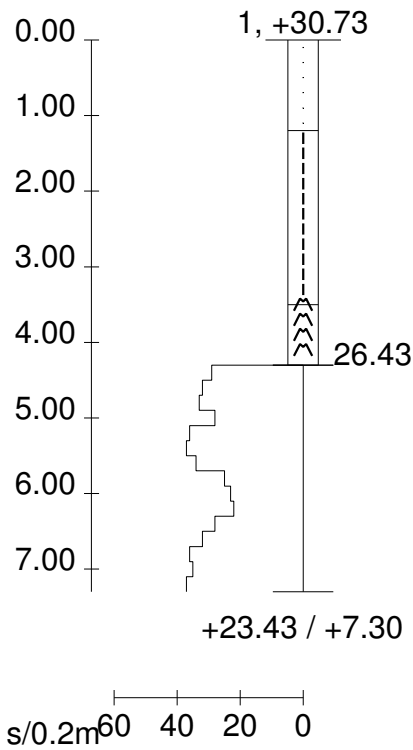
Grouting container





K.osa/Kylä	Kortteili/Tila	Tonitti/Rnro	Viranomaisten arkistomerkitöjä varten	
Rakennustoimenpide			Piirustuslaji	Juoks. nro
Rakennuskohteen nimi ja osoite			Piirustuksen sisältö	Mittakaavat
RD-PAALUSEINÄN TUTKIMUSPORAUS			TUTKIMUSKARTTA	1:100
Piirtänyt	Päiväys	Suunnitteluala, työ- ja piirustusnumero		Muutos
Kalaukset	01.07.2013	GEO		
JPS	Tarkistanut			

KAIRAUSDIAGRAMMIT 1...5

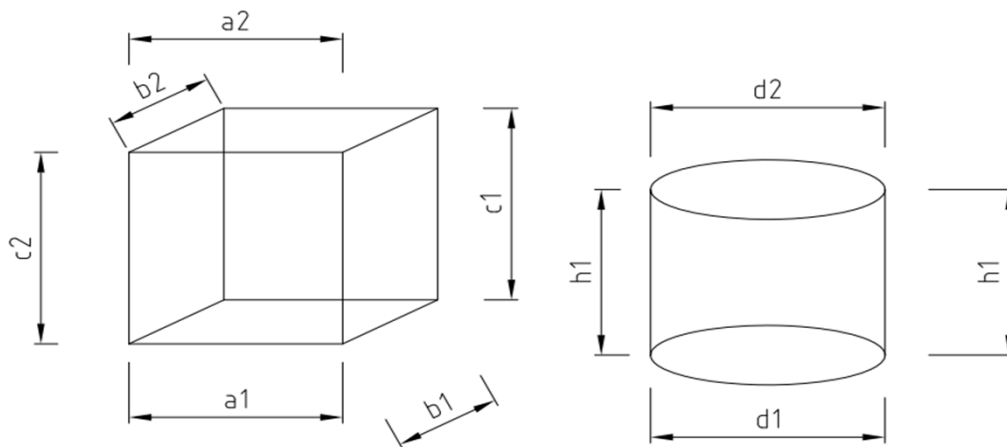


K.osa/Kylä		Kortteli/Tila	Tontti/Rnro	Viranomaisten arkistomerkintöjä varten	
Rakennustoimenpide				Piirustustyyli	Juoks. nro
Rakennuskohteen nimi ja osoite				Piirustuksen sisältö	Mittakaavat
RD-PAALUSEINÄN TUTKIMUSPORAUS				KAIRAUDIAGRAMMIT 1...5	1:100
Piirtänyt		Päiväys		Suunnitteluala, työ- ja piirustusnumero	
Kairaukset		Suunnitellut		Muutos	
JPS		Tarkistanut		GEO	
 Geotiimi Oy				Tammistontie 321, 20900 Turku Puh. (02) 2586 261 Matkapuh. 0400 323 271	

Appendix 17 Grout, rock and drilling cutting samples

				Cube	a1	b1	c1	a2	b2	c2
				Cylinder	d1	d2	h1			h2
Sample	Material	Shape	h/d							
7A	Grout	Cylinder	1		25.3	25.5	22.4			21.5
7B	Grout	Cylinder	1		25	25.8	15.8			16
8A	Grout	Cylinder	1		24.9	25.8	23.6			25.1
8B	Grout	Cylinder	1		24.6	26	14.7			19.6
11_4_1	Grout	Cylinder	1		52.1	52.1	50.9			50.7
11_4_2A	Grout	Cylinder	1		52.1	52.2	49.9			50.4
11_4_2B	Grout	Cylinder	1		52.1	52.2	49.9			50.4
23_1B	Clay(+concrete?)	Cube	1		14.4	15.5	17	14.9	15.3	16.9
24_1A	Cuttings or clay-grout*	Cube	1		11.2	11.2	9.9	11.6	11.2	9.9
24_1B	Cuttings or clay-grout*	Cube	1		10.3	9.3	10.8	10.1	9.6	10.8
26_1A	Clay(+concrete?)	Cube	1		14.1	16.4	17.6	13.8	16.6	17.5
26_1B	Clay(+concrete?)	Cube	1		15.5	17.4	20	15.5	18.1	19.5
30_3A	Cuttings or sand+grout	Cylinder	1		22.1	22.1	20.8			19.9
30_3B	Cuttings or sand+grout	Cylinder	1		22.4	22.1	21.9			21
30_3C	Cuttings or sand+grout	Cylinder	1		22.1	22.1	21.6			21.6
30_3D	Cuttings or sand+grout	Cylinder	1		22.2	22.1	22.4			22
32_1	Cuttings or clay+grout	Cylinder	1		22	21.9	21.1			19.3
32_2A	Cuttings or clay+grout	Cylinder	1		22	22	22.2			21.9
32_2B	Cuttings or clay+grout	Cylinder	1		22	21.8	22			21.7
32_3C	Cuttings or clay+grout	Cylinder	1		22.3	22.2	21.1			20.3
1_3_1	Rock	Cylinder	1		52.1	52.1	52.5			52.5
1_3_2A	Rock	Cylinder	1		52	52	52.3			52.3
1_3_2B	Rock	Cylinder	1		52	52	52.3			52.3
1_3_3A	Rock	Cylinder	1		52.2	52	52			52.5
1_3_3B	Rock	Cylinder	1		52	52.1	51.1			51.5
3_1_1	Rock	Cylinder	1		52	52	51.4			51.1
3_1_2A	Rock	Cylinder	1		52	52	50.9			51.5
3_1_2B	Rock	Cylinder	1		52	52	51.2			51.5
3_1_3A	Rock	Cylinder	1		52	52	52.5			52.4
3_1_3B	Rock	Cylinder	1		52	52	52.3			52.3
5_2_1	Rock	Cylinder	1		52.1	52.1	51.4			52
5_2_2A	Rock	Cylinder	1		52.1	52	51			51.3
5_2_2B	Rock	Cylinder	1		52.1	52.1	51.7			52.2
5_2_3A	Rock	Cylinder	1		52.1	52.1	51.2			51.5
5_2_3B	Rock	Cylinder	1		52.2	52.2	52.5			51.9

* grouting flowed from different pile



APPENDIX 18


**PORAPAALUJEN ASENNUSPÖYTÄKIRJA
PAALUKOHTAISET TIEDOT**
Peab Infra Oy
Paalunumero P126

Urakoitsija TERRAMEK
Työkohte RD600 LU3A MRU
 P-SEINÄ

Paalutyyppi
Porausmenetelmä
Työpiirustus nro
E21
 UPPOPORAUS
 PAALUPORAUSKALLIOSYVYYS
 SUUNNITTELIJAN OHJEIDEN MUKAAN

Poraus

Aloituspvm	14.2.2013	Klo	7.10	Aloitustaso	±	Paalun yläpään taso	±	-1.4
Lopetuspvm		Klo	8.15	Lopetustaso	±	Paalun alapään taso	±	-7.8
Todettu kalliopinnan taso		±	-6,8	Poraussyvyys		6.4	Paalupituus	6.4

PORAUS- SYVYYS (m)	POR. VASTUS (m/h)	POHJAS. Kuvaus	PORAUSHAVAINNOT (pohjavesi, keskeytykset)	PORAUSMENET JA KALUSTO	HUOMAUTUKSET
1			SAVI	H181	TASOSTA -1,4
2			SAVI		1M KALLIOON
3			SAVI		
4			SAVI		5,4 KALLIO ALKAA
5			5,4 KOVA KALLIO		
6			KOVA KALLIO		
7					
8					

Porausvastus (m/h) merkitään vähintään kallioporausken matkalta
Allekirjoitukset: Paalutustyönjohtaja _____
 Valvoja _____

Paalun toteutuneet poikkeamat (sijaintipoikkeamat paalun yläpään katkaisutasossa)

 $\Delta x =$ _____ cm Kaltevuus _____ °
 $\Delta y =$ _____ cm Kaarevuussäde _____ m Tasolla ± _____

Pohjanpuhdistus Pvm _____ Klo _____

Betonointi

 Betonoinnin aloitus Pvm _____ Klo _____
 Betonoinnin lopetus Pvm _____ Klo _____
 Vedenpinnan taso reiässä betonoinnin alkaessa _____ m Yläpään katkaisutason alapuolella

Betonimenekki Teoreettinen: _____ m³ Todellinen: _____ m³

Erityishuomiot betonoinnissa : _____

Huomautukset/havainnot _____

Allekirjoitukset: Paalutustyönjohtaja _____
 Valvoja _____


**PORAPAALUJEN ASENNUSPÖYTÄKIRJA
PAALUKOHTAISET TIEDOT**
Peab Infra Oy
Paalunumero P273
Urakoitsija TERRAMEK
Työkohte RD600 LU3A MRU
M SEINÄ
Paalutyyppi
Porausmenetelmä
Työpiirustus nro
womwof
UPPOPORAUS
PAALUPORAUSKALLIOSYVYYS
SUUNNITTELIJAN OHJEIDEN MUKAAN
Poraus

Aloituspvm	<u>30.1.2013</u>	Klo	<u>11.30</u>	Aloitustaso	±	<u>Paalun yläpään taso</u>	±	<u>-1.4</u>
Lopetuspvm		Klo	<u>14.15</u>	Lopetustaso	±	<u>Paalun alapään taso</u>		<u>-9.1</u>
Todettu kalliopinnan taso		±	<u>-7,6</u>	Poraussyvyys		<u>7.7</u>	<u>Paalupituus</u>	<u>7.7</u>

PORAUS- SYVYYS (m)	POR. VASTUS (m/h)	POHJAS. KUVAUS	PORAUSHAVAINNOT (pohjavesi, keskeytykset)	PORAUSMENET JA KALUSTO	HUOMAUTUKSET
1			SAVI	H181	TASOLTA -1,4
2			SAVI		1,5 KALLIOON
3			SAVI		
4			SAVI		
5			KIVIÄ, RIKKON KALLIO		
6			RIKKON KALLIO 6,2 PUN KALLIO		6,2 KALLIO ALKAA
7			PUN KALLIO		
8			PUN KALLIO		
9					
10					

Porausvastus (m/h) merkitään vähintään kallioporausken matkalta
Allekirjoitukset: Paalutustyönjohtaja _____
Valvoja _____

Paalun toteutuneet poikkeamat (sijaintipoikkeamat paalun yläpään katkaisutasossa)

 $\Delta x =$ _____ cm Kaltevuus _____ °
 $\Delta y =$ _____ cm Kaarevuussäde _____ m Tasolla ± _____

Pohjanpuhdistus Pvm _____ Klo _____

Betonointi

Betonoinnin aloitus Pvm _____ Klo _____
Betonoinnin lopetus Pvm _____ Klo _____
Vedenpinnan taso reiässä betonoinnin alkaessa _____ m Yläpään katkaisutason alapuolella

Betonimenekki Teoreettinen: _____ m³ Todellinen: _____ m³

Erityishuomiot betonoinnissa : _____

Huomautukset/havainnot _____

Allekirjoitukset: Paalutustyönjohtaja _____
Valvoja _____

Appendix 19: Simplified calculation to determine drilling depth of RD pile

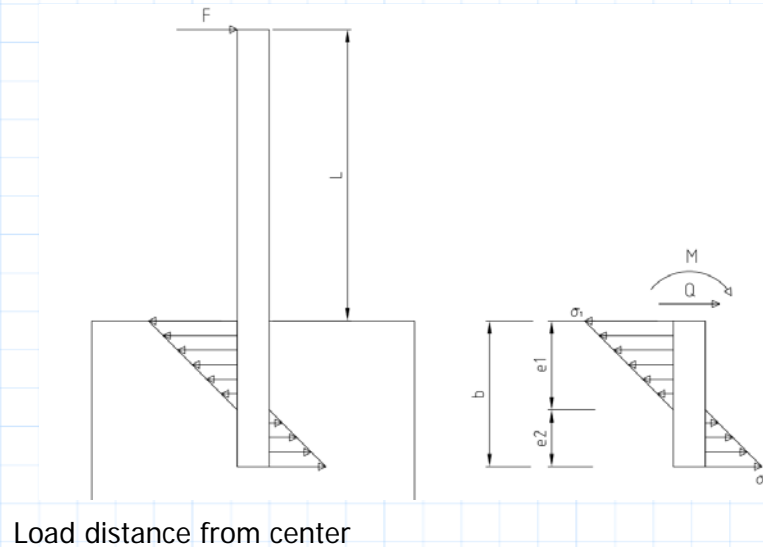
$$F := 444 \text{ kN}$$

$$L := \frac{7 \text{ m}}{3} = 2.333 \text{ m}$$

$$a := 508 \text{ mm}$$

$$b := \frac{508}{2} \text{ mm}$$

$$e := \frac{b}{2} = 127 \text{ mm}$$

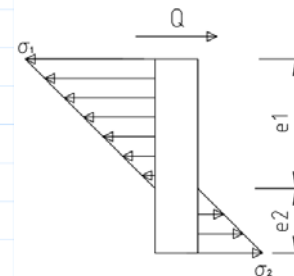


From shear force

$$\sigma_{1Q} := \frac{F}{a \cdot b} \cdot \left(1 + \frac{6 \cdot e}{b}\right) = 13.764 \text{ MPa}$$

[Rakentajain kalenteri 2004]

$$\sigma_{2Q} := -\frac{F}{a \cdot b} \cdot \left(1 - \frac{6 \cdot e}{b}\right) = 6.882 \text{ MPa}$$



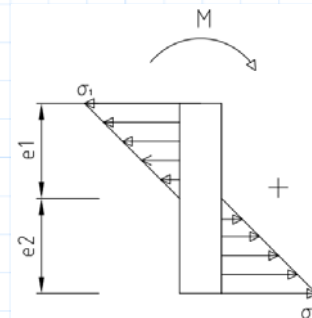
From bending moment

$$M := F \cdot L = (1.036 \cdot 10^3) \text{ m} \cdot \text{kN}$$

$$e_1 := \frac{b}{2} = 0.127 \text{ m}$$

$$e_2 := \frac{b}{2} = 0.127 \text{ m}$$

$$e_{12} := \frac{2}{3} e_1 + \frac{2}{3} e_2 = 0.169 \text{ m}$$



Distance between force resultants

$$M_{support} := M$$

Supporting moment = external moment

$$M_{support} := 2 \cdot \boxed{F_1} \cdot \frac{e_{12}}{2}$$

$$M_{support} := M = (1.036 \cdot 10^3) \text{ kN} \cdot \text{m}$$

In that case $F_1 = F_2$ and $e_1 = e_2$

otherwise $M = \frac{2}{3} \cdot F_1 \cdot e_1 + \frac{2}{3} \cdot F_2 \cdot e_2$

$$F_1 := \frac{\boxed{\sigma_{1M}}}{2} \cdot e_1 \cdot a$$

$$\sigma_{1M} := 2 \cdot \frac{\boxed{F_1}}{e_1 \cdot a}$$

$$\sigma_{1M} := 2 \cdot \frac{M_{support}}{e_{12} \cdot e_{12} \cdot a} = 142.246 \text{ MPa}$$

$$\sigma_{2M} := \sigma_{1M} = 142.246 \text{ MPa}$$

From shear force and moment

$$\sigma_1 := \sigma_{1Q} + \sigma_{1M} = 156.01 \text{ MPa}$$

approximately 240 in FEM calculation

$$\sigma_2 := \sigma_{2Q} + \sigma_{2M} = 149.128 \text{ MPa}$$

Horizontal displacement due from joint. Pile assumed to be extremely stiff

$$d_{oversize} := 27 \text{ mm}$$

Oversize of the drilling on one side of the pile

$$E_{grout} := 24.3 \text{ GPa}$$

$$\varepsilon_1 := \frac{\sigma_1}{E_{grout}} = 0.0064$$

$$\varepsilon_2 := \frac{\sigma_2}{E_{grout}} = 0.0061$$

$$\Delta x_1 := \varepsilon_1 \cdot d_{oversize} = 0.173 \text{ mm}$$

Displacement at rock level

$$\Delta x_2 := \varepsilon_2 \cdot d_{oversize} = 0.166 \text{ mm}$$

Displacement at toe of pile

$$\Delta x := (\Delta x_1 + \Delta x_2) \cdot \frac{L}{b} + \Delta x_1 = 3.288 \text{ mm}$$

Displacement at top of pile from joint

Joint stiffness of test pile 10, calculation vs. measured

$$F := 73.1 \text{ kN}$$

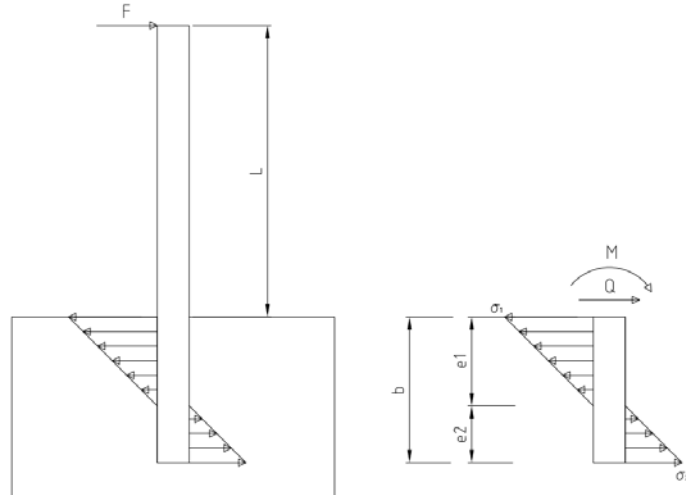
$$L := 1.97 \text{ m} = 1.97 \text{ m}$$

$$a := 219.1 \text{ mm}$$

$$b := 1000 \text{ mm}$$

$$e := \frac{b}{2} = 500 \text{ mm}$$

Load distance from center

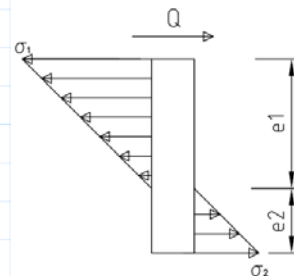


From shear force

$$\sigma_{1Q} := \frac{F}{a \cdot b} \cdot \left(1 + \frac{6 \cdot e}{b} \right) = 1.335 \text{ MPa}$$

[Rakentajain kalenteri 2004]

$$\sigma_{2Q} := -\frac{F}{a \cdot b} \cdot \left(1 - \frac{6 \cdot e}{b} \right) = 0.667 \text{ MPa}$$



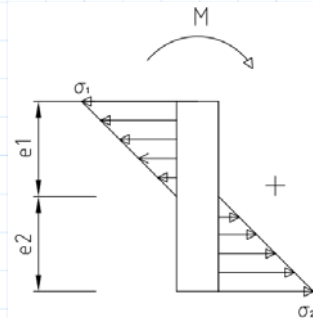
From bending moment

$$M := F \cdot L = 144.007 \text{ m} \cdot \text{kN}$$

$$e_1 := \frac{b}{2} = 0.5 \text{ m}$$

$$e_2 := \frac{b}{2} = 0.5 \text{ m}$$

$$e_{12} := \frac{2}{3} e_1 + \frac{2}{3} e_2 = 0.667 \text{ m}$$



Distance between force resultants

$$M_{\text{support}} := M$$

Supporting moment = external moment

$$M_{support} := 2 \cdot \boxed{F_1} \cdot \frac{e_{12}}{2}$$

$$M_{support} := M = 144.007 \text{ kN} \cdot \text{m}$$

In that case $F_1 = F_2$ and $e_1 = e_2$
otherwise $M = \frac{2}{3} \cdot F_1 \cdot e_1 + \frac{2}{3} \cdot F_2 \cdot e_2$

$$F_1 := \frac{\sigma_{1M}}{2} \cdot e_1 \cdot a$$

$$\sigma_{1M} := 2 \cdot \frac{F_1}{e_1 \cdot a}$$

$$\sigma_{1M} := 2 \cdot \frac{M_{support}}{e_{12} \cdot e_{12} \cdot a} = 2.958 \text{ MPa}$$

$$\sigma_{2M} := \sigma_{1M} = 2.958 \text{ MPa}$$

From shear force and moment

$$\sigma_1 := \sigma_{1Q} + \sigma_{1M} = 4.292 \text{ MPa}$$

Very near to joint limit, FEM calculation indicates same

$$\sigma_2 := \sigma_{2Q} + \sigma_{2M} = 3.625 \text{ MPa}$$

Horizontal displacement due from joint. Pile assumed to be extremely stiff

$$d_{oversize} := 27 \text{ mm}$$

Oversize of the drilling on one side of the pile

$$E_{grout} := 24.3 \text{ GPa}$$

$$\varepsilon_1 := \frac{\sigma_1}{E_{grout}} = 0.0002$$

$$\varepsilon_2 := \frac{\sigma_2}{E_{grout}} = 0.0001$$

$$\Delta x_1 := \varepsilon_1 \cdot d_{oversize} = 0.005 \text{ mm}$$

Displacement at rock level

$$\Delta x_2 := \varepsilon_2 \cdot d_{oversize} = 0.004 \text{ mm}$$

Displacement at toe of pile

$$\Delta x := \left(\Delta x_1 + \Delta x_2 \right) \cdot \frac{L}{b} + \Delta x_1 = 0.022 \text{ mm}$$

Displacement at top of pile from joint

Not even close to measured 38 mm-24.7 mm=13.3 mm -> pile deflection in the drilling hole plays major role when drilled deep into bedrock



Lari Hannukainen, puh. 040-8490302

17-12-2013

Leo-Ville Miettinen**SAVINÄYTTEIDEN PETROGRAFINEN KUVAUS**

Näytteet	2 kpl, Savinäytteet (TTY:n työnumero 150036/408/2013). Näytteenotto ja näytteen edustavuus ovat tilaajan vastuulla.
Näytteiden esikäsittely	Näytteet hienonnettiin huhmareella ja sekoitettiin ionivaihdettuun veteen suspension muodostamiseksi. Näytesuspensioista pipetoitiin testinäytteet lasilevyille. Testinäytteiden vesi haihdutettiin huoneenlämmössä.
Testausmenetelmät	Lasilevyille laskeutettujen näytteiden mineralogia tutkittiin PANalytical Empyrean-röntgendiffraktiolaitteella PANK 2301 ohjeen mukaisesti (kvalitatiivinen analyysi).
Tulokset	<p>Tutkimus on tehty 4.12.2013.</p> <p><u>Näyte 408/23:</u> Kvartsi, kloriitti, plagioklaasi, muskoviitti</p> <p><u>Näyte 408/24:</u> Kalsiitti, Portlandiitti, Kvartsi, Kalsiumsilikaatti</p> <p>Tulokset pätevät ainoastaan testatuille näytteille. Testausselostuksen saa kopioida ainoastaan kokonaisuudessaan.</p>

JAKELU:

Asiakas
TTY

TAMPEREEN TEKNILLINEN YLIOPISTO
MPR

KALKKIKIVIJAUHEEN LIUKOISUUS SUOLAHAPPOON

PANK-2405

Punnitaan 10 g kuivattua näytettä dekantterilasiin. Mitataan mittalasiin 50ml vettä ja 25ml väkevää suolahappoa. Liuos kaadetaan varovasti näytteen päälle.

Näyte kuumennetaan ja keitetään n. 10min.

Suodatetaan kuivatun ja punnitun suodatinpaperin läpi. Huuhdotaan.

Paperi kuivataan. Punnitaan

Näyte	408_27
pvm	19.12.2013
tekijä	NL

	A	B
näytteen paino g m	10,012	10,0353
näyte + suodatinpaperi + astia g m ₁	6,4822	6,2509
suodatinpaperi + astia g m ₂	3,2357	3,1824

Liukoisuusprosentti $S = ((1-(m_1-m_2)/m))*100$	67,57	69,42
--	-------	-------

Keskiarvo %	68,50
-------------	-------

Tampereen teknillinen yliopisto
Maa- ja pohjarakenteet
PL 600, 33101 Tampere

Tilaaaja: **Ruukki Construction Oy**
Työnumero: **408/2013**

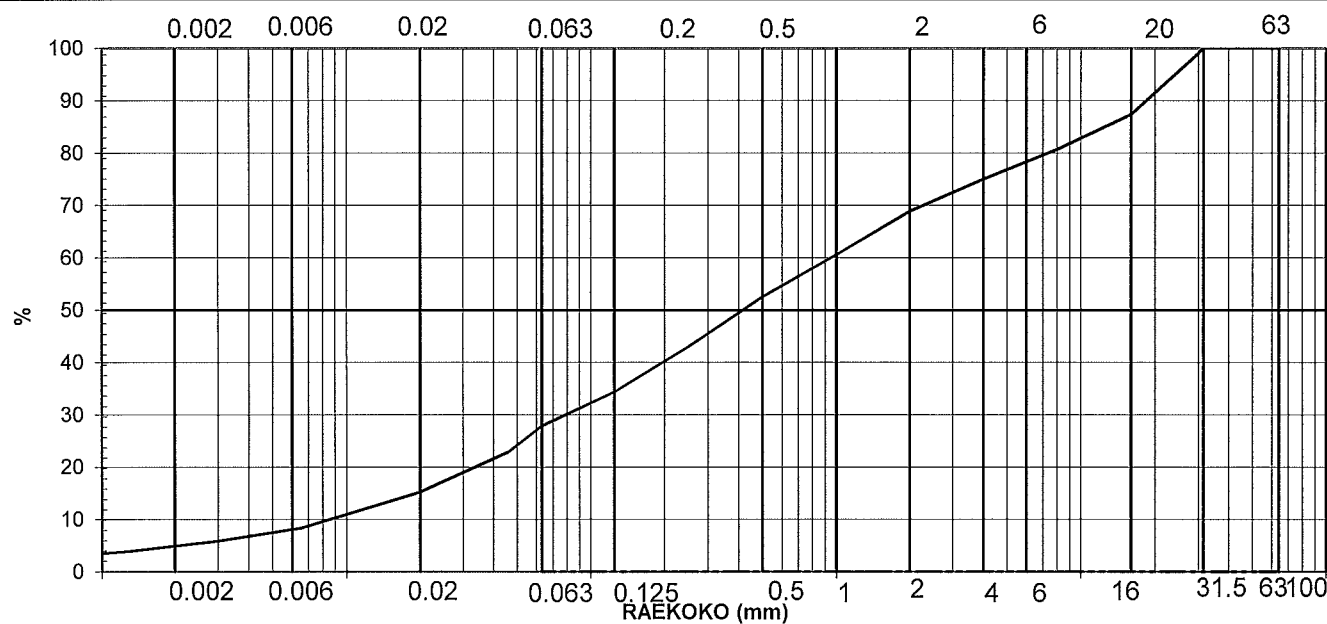
Tutkimus:

Työkohte:

Diplomiotyö

Kunta:

Näytteen tunnus	a	b	c
Näytenumero			
paalu/km	2		
syvyys			
korkeustaso			
ottoaika			
Irtotiheys kuiva			
Irtotiheys märkä			
Kiintotiheys			
Vesipitoisuus %			
Polttohäviö %			
Humuspitoisuus %			
Humus NaOH			
Hienoainespitoisuus (-0.063)			
Routivuus, routim, routiva			
Kantavuusluokka			
Kapillaarisuus			
Maalaji SFS (Geo)			
GEO SAVI SILTTI HIEKKA SORA KIVET			



Huomautuksia:

Päiväys:

Tutki:

Tarkasti:

Tampereen teknillinen yliopisto
Maa- ja pohjarakenteet
PL 600, 33101 Tampere

Tilaaaja: **Ruukki Construction Oy**
Työnumero: **408/2013**

Tutkimus:

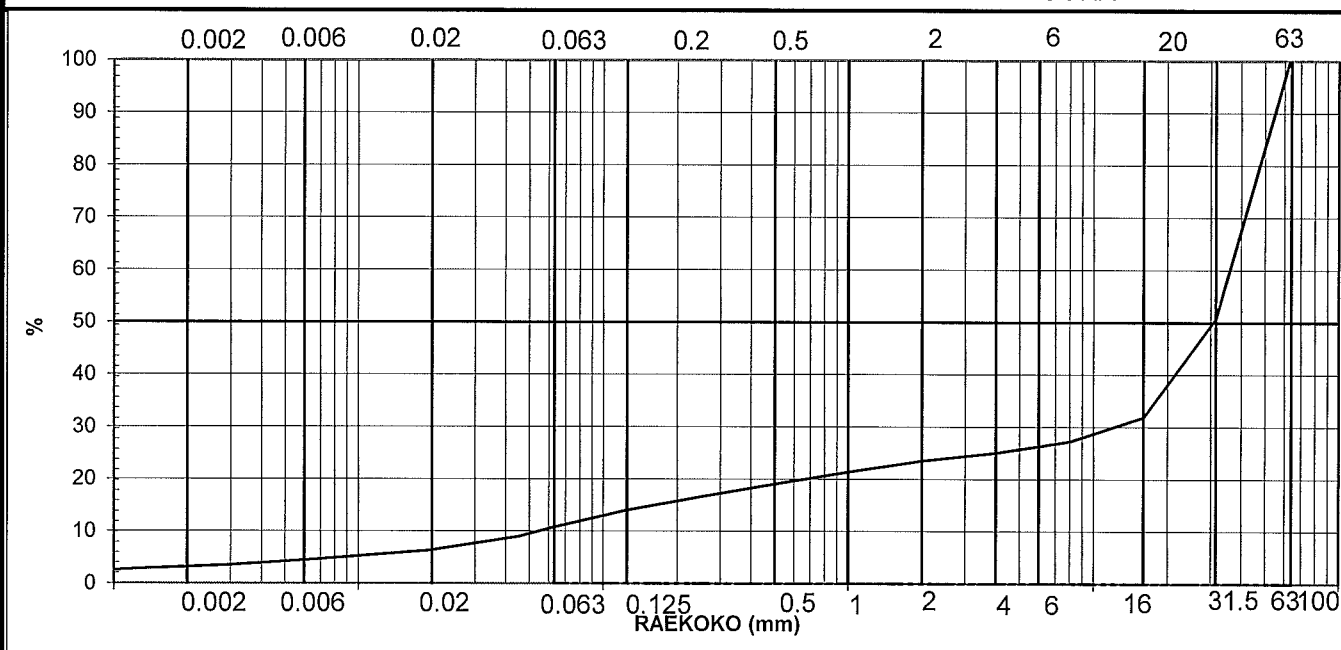
Työkohde:

Diplomiotyö

Kunta:

Näytteen tunnus	a	b	c
Näytenumero			
paalu/km	3		
syvyys			
korkeustaso			
ottoaika			
Irtotiheys kuiva			
Irtotiheys märkä			
Kiintotiheys			
Vesipitoisuus %			
Polttohäviö %			
Humuspitoisuus %			
Humus NaOH			
Hienoainespitoisuus (-0.063)			
Routivuus, routim, routiva			
Kantavuusluokka			
Kapillaarisuus			
Maalaji SFS (Geo)			

GEO| SAVI | SILTTI | HIEKKA | SORA | KIVET



Huomautuksia:

Päiväys:

Tutki:

Tarkasti:

Tampereen teknillinen yliopisto
Maa- ja pohjarakenteet
PL 600, 33101 Tampere

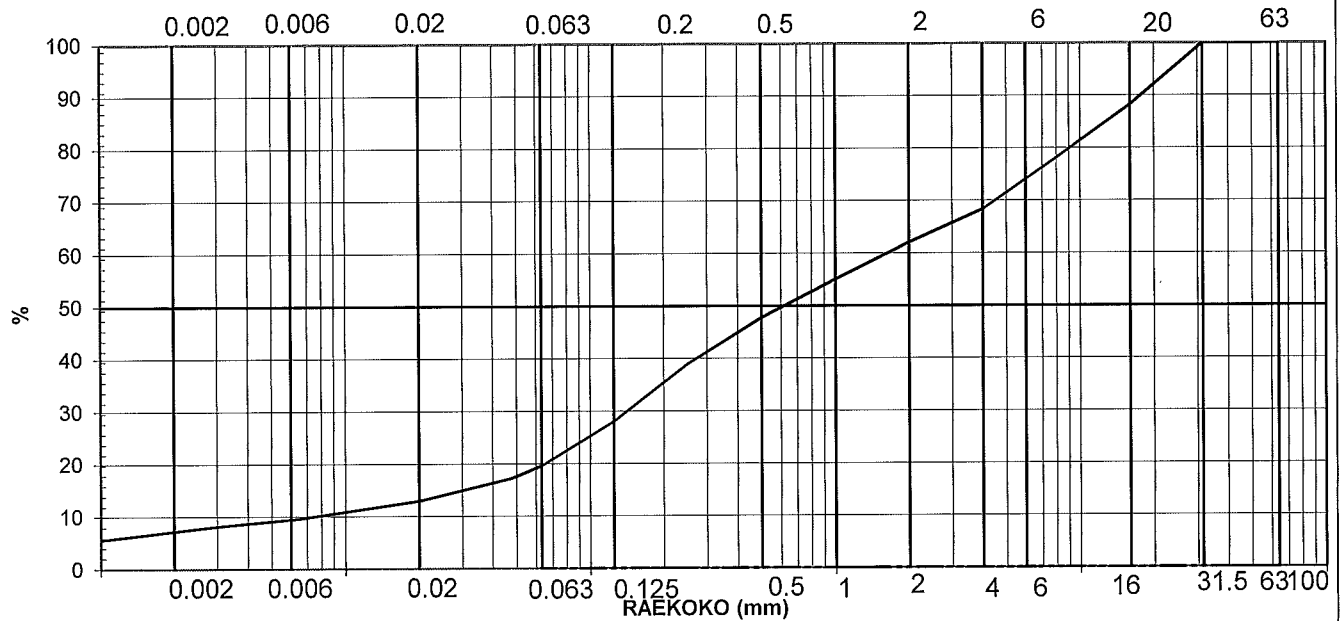
Tilaaaja: Ruukki Construction Oy
Työnumero: 408/2013

Tutkimus:

Työkohte: Diplomiotyö Kunta: _____

Näytteen tunnus	a	b	c
Näyttenumero			
paalu/km	9		
syvyys			
korkeustaso			
ottoaika			
Irtotiheys kuiva			
Irtotiheys märkä			
Kiintotiheys			
Vesipitoisuus %			
Polttohäviö %			
Humuspitoisuus %			
Humus NaOH			
Hienoainespitoisuus (-0.063)			
Routivuus, routim, routiva			
Kantavuusluokka			
Kapillaarisuus			
Maalaji SFS (Geo)			

GEO| SAVI | SILTTI | HIEKKA | SORA | KIVET



Huomautuksia:

Päiväys:

Tutki:

Tarkasti:

Tampereen teknillinen yliopisto
Maa- ja pohjarakenteet
 PL 600, 33101 Tampere

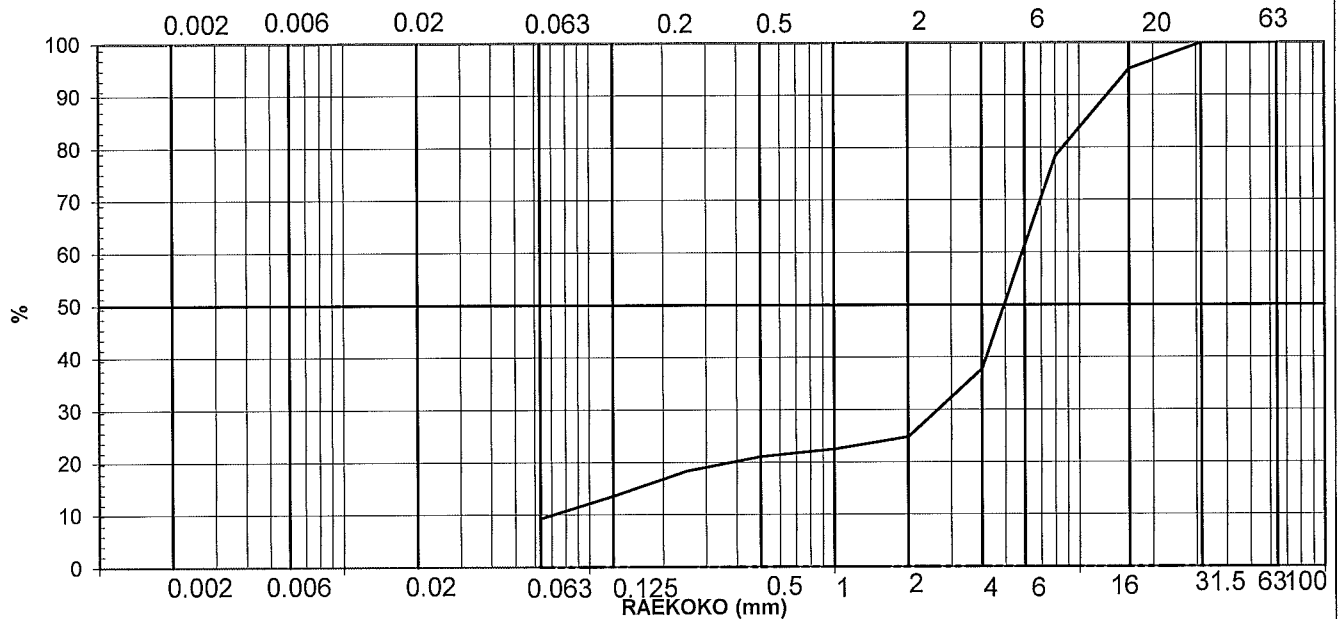
Tilaaaja: Ruukki Construction Oy
Työnumero: 408/2013

Tutkimus:

Työkohde: Diplomiotyö Kunta: _____

Näytteen tunnus	a	b	c
Näyttenumero			
paalu/km	10		
syvyys			
korkeustaso			
ottoaika			
Irtotiheys kuiva			
Irtotiheys märkä			
Kiintotiheys			
Vesipitoisuus %			
Polttohäviö %			
Humuspitoisuus %			
Humus NaOH			
Hienoaainepitoisuus (-0.063)			
Routivuus, routim, routiva			
Kantavuusluokka			
Kapillaarisuus			
Maalaji SFS (Geo)			

GEO | SAVI | SILTTI | HIEKKA | SORA | KIVET



Huomautuksia:

Päiväys:

Tutki:

Tarkasti:

Tampereen teknillinen yliopisto Maa- ja pohjarakenteet PL 600, 33101 Tampere	Tilaaaja: Ruukki Construction Oy Työnumero: 408/2013
---	---

Tutkimus	
Työkohde:	Diplomiotyö Kunta: _____

Näytteen tunnus	a _____	b -----	c_
Työnumero			
Näytteen ottopaikka (Paalu)	2		
- syvyys			
- korkeustaso			
Näytteen massa kuivana	829,79		
Näytteen massa pesun jälkeen	606,211		
Pesutappio	223,58		
Kiviä ja lohkareita	%	%	%
20-64			
64-200			
200-600			
> 600			

Seulonta									
Seula	jäi (g)	jäi (%)	läp (%)	jäi (g)	jäi (%)	läp (%)	jäi (g)	jäi (%)	läp (%)
mm									
63	0,00	0,0	100,0						
31,5	0,00	0,0	100,0						
16	104,80	12,6	87,4						
8	55,10	6,6	80,7						
4	47,10	5,7	75,0						
2	50,35	6,1	69,0						
1	69,27	8,4	60,6						
0,5	66,62	8,0	52,6						
0,25	78,96	9,5	43,0						
0,125	71,67	8,6	34,4						
0,063	53,59	6,5	27,9						
pohja	7,79	0,9							
pohja+pesutappio	231,37								
Yhteensä	828,84								

Areometrikoe		4								
Näyttemäärä		100								
Aika	°C	lukema	raekoko	läp%	lukema	raekoko	läp%	lukema	raekoko	läp%
Alku										
1 min	22	22,5	0,0460	37,6						
6 min	22	14,5	0,0197	24,8						
1 h	22	7,5	0,00653	13,7						
5 h	22	5,0	0,00299	9,6						
1 d	21	3,0	0,00130	6,4						
4 d	21	2,0	0,00070	4,8						

Huomautuksia:

Tampereen teknillinen yliopisto Maa- ja pohjarakenteet PL 600, 33101 Tampere	Tilaaaja: Ruukki Construction Oy Työnumero: 408/2013
--	---

Tutkimus	
Työkohte:	Diplomi työ Kunta: _____

Näytteen tunnus	a _____	b -----	c _____.____.
Työnumero			
Näytteen ottopaikka (Paalu)	3		
- syvyys			
- korkeustaso			
Näytteen massa kuivana	863,69		
Näytteen massa pesun jälkeen	774,119		
Pesutappio	89,57		
Kiviä ja lohkareita	%	%	%
20-64			
64-200			
200-600			
> 600			

Seulonta

Seula	jäi (g)	jäi (%)	läp (%)	jäi (g)	jäi (%)	läp (%)	jäi (g)	jäi (%)	läp (%)
mm									
63	0,00	0,0	100,0						
31,5	425,20	49,2	50,8						
16	163,00	18,9	31,9						
8	40,30	4,7	27,2						
4	19,20	2,2	25,0						
2	12,78	1,5	23,5						
1	18,58	2,2	21,4						
0,5	19,99	2,3	19,1						
0,25	21,22	2,5	16,6						
0,125	22,42	2,6	14,0						
0,063	28,05	3,2	10,8						
pohja	3,57	0,4							
pohja+pesutappio	93,14								
Yhteensä	863,89								

Areometrikoe		4									
Näytemäärä		100									
Aika	°C	lukema	raekoko	läp%	lukema	raekoko	läp%	lukema	raekoko	läp%	
Alku											
1 min	22	26,0	0,0450	43,1							
6 min	22	18,0	0,0193	30,4							
1 h	22	12,5	0,00634	21,6							
5 h	22	9,5	0,00291	16,8							
1 d	21	7,5	0,00127	13,5							
4 d	21	5,5	0,00068	10,4							

Huomautuksia:

Tampereen teknillinen yliopisto Maa- ja pohjarakenteet PL 600, 33101 Tampere	Tilaaaja: Ruukki Construction Oy Työnumero: 408/2013
---	---

Tutkimus		
Työkohde:	Diplomiotyö	Kunta: _____

Näytteen tunnus	a _____	b -----	c _____.____.
Työnumero			
Näytteen ottopaikka (Paalu)	9		
- syvyys			
- korkeustaso			
Näytteen massa kuivana	289,06		
Näytteen massa pesun jälkeen	236,536		
Pesutappio	52,52		
Kiviä ja lohkareita	%	%	%
20-64			
64-200			
200-600			
> 600			

Seulonta									
Seula	jäi (g)	jäi (%)	läp (%)	jäi (g)	jäi (%)	läp (%)	jäi (g)	jäi (%)	läp (%)
mm									
63	0,00	0,0	100,0						
31,5	0,00	0,0	100,0						
16	33,90	11,7	88,3						
8	29,20	10,1	78,1						
4	28,10	9,7	68,4						
2	18,27	6,3	62,1						
1	20,19	7,0	55,1						
0,5	21,04	7,3	47,8						
0,25	25,56	8,9	38,9						
0,125	31,52	10,9	28,0						
0,063	24,33	8,4	19,6						
pohja	3,98	1,4							
pohja+pesutappio	56,51								
Yhteensä	288,62								

Areometrikoe		4									
Näytemäärä		100									
Aika	°C	lukema	raekoko	läp%	lukema	raekoko	läp%	lukema	raekoko	läp%	
Alku											
1 min	22	17,0	0,0476	28,8							
6 min	22	12,5	0,0200	21,6							
1 h	22	9,0	0,00647	16,0							
5 h	22	7,5	0,00295	13,6							
1 d	21	5,5	0,00128	10,3							
4 d	21	4,0	0,00069	8,0							

Huomautuksia:	
---------------	--

Tampereen teknillinen yliopisto
Maa- ja pohjarakenteet
PL 600, 33101 Tampere

Tilaaaja: Ruukki Construction Oy
Työnumero: 408/2013

Tutkimus

Työkohde:

Diplomiotyö

Kunta:

Näytteen tunnus	a	b	c
Työnumero			
Näytteen ottopaikka (Paalu)	10		
- syvyys			
- korkeustaso			
Näytteen massa kuivana	324,25		
Näytteen massa pesun jälkeen	298,1		
Pesutappio	26,15		
Kiviä ja lohkareita	%	%	%
20-64			
64-200			
200-600			
> 600			

Seulonta

Seula	jäi (g)	jäi (%)	läp (%)	jäi (g)	jäi (%)	läp (%)	jäi (g)	jäi (%)	läp (%)
mm									
63	0,00	0,0	100,0						
31,5	0,00	0,0	100,0						
16	16,10	5,0	95,0						
8	53,90	16,6	78,4						
4	131,80	40,6	37,8						
2	42,10	13,0	24,8						
1	7,60	2,3	22,5						
0,5	4,50	1,4	21,1						
0,25	8,90	2,7	18,3						
0,125	15,40	4,7	13,6						
0,063	14,00	4,3	9,3						
pohja	3,90	1,2							
pohja+pesutappio	30,05								
Yhteensä	324,35								

Areometrikoe

4

Näytemäärä

Aika	°C	lukema	raekoko	läp%	lukema	raekoko	läp%	lukema	raekoko	läp%
Alku										
1 min	20									
6 min	20									
1 h	20									
5 h	21									
1 d	20									
4 d	20									

Huomautuksia:

SULJETTU KOLMIAKSIALIKOE

TTY	ASIAKAS	Ruukki Construction Oy
Maa- ja pohjarakenteet	KOHDE	Injektointikohde
PL 600 33101 TAMPERE	TYÖNUMERO	408/2013 (H408)

KOKEEN / KOSELLIN N:O	5	5		
PISTE, PAALU	Näyte 1	Näyte 1	Näyte 1	
SYVYYS [m]	-	-	-	
TIEDOSTO	H408 S1	H408 S2	-	
NOPEUS [mm/min]	0,015	0,015	0,015	
KOKEEN ALUSSA SULLOTTUNA: pmv 17.10.-13 21.10.-13				
NÄYTTEEN HALKAISIJA [mm]	51	51	50	
NÄYTTEEN KORKEUS [mm]	97,7	96,4		
NÄYTTEEN POIKKIP.-ALA [cm**2]	20,43	20,43	19,63	
NÄYTTEEN TILAVUUS [cm**3]	199,58	196,93		
NÄYTTEEN PAINO [g]	336,00	336,00	159,13	
Kokoonpuristuma konsolidoinnissa [mm]	2,34	3,53		
Poistunut vesi konsolidoinnissa [ml],[g]	6,2	11,2		
Näytteen paino konsolidoituneena [g]	329,80	324,80		
Kuivan näytteen paino [g]	210,60	216,54	107,59	
ARVIO VESI [g]	125,40	119,46	51,54	
ARVIO VESIPITOISUUS [%]	59,5	55,2	47,90	
IRTOTIHEYS [g/cm**3]	1,68	1,71		
TILAVUUSPAINO [kN/m**3]	16,5	16,7		
ARVIO KUIVA IRTOTIHEYS [g/cm**3]	1,06	1,10		
ARVIO KUIVATILAVUUSPAINO [kN/m**3]	10,4	10,8		
ARVIOITA				
KYLLÄSTYSASTE Sr, oletus [%]	100,00	100,00	100,00	
KIINTOTIHEYS [g/cm**3]	2,84	2,80		
HUOKOSLUKU e	1,69	1,54		
OMINAISTILAVUUS v	2,69	2,54		
KIINTOTIHEYS, oletus [g/cm**3]	2,65	2,65	2,65	
KYLLÄSTYSASTE Sr [%]	104,4	103,7		
HUOKOSLUKU e	1,51	1,41		
OMINAISTILAVUUS v	2,51	2,41		
KONSOLIDOITUNEENA:	101 kPa	298 kPa	- kPa	
TILAVUUSPAINO [kN/m**3]	16,7	17,2		
KUIVATILAVUUSPAINO [kN/m**3]	10,7	11,4		
KOKEEN LOPUSSA:				
ASTIAN NUMERO	H408 S1	H408 S2	-	
KOSTEA NÄYTE [g]	311,45	310,01	159,13	
Kuivan näytteen paino [g]	210,60	216,54		
VESI [g]	100,85	93,47		
VESIPITOISUUS [%]	47,9	43,2		

TUTKI:

TAMPERE

PAIKKA

PÄIVÄYS

Niko Levo

Laboratoriomestari

TARKASTI:

TAMPERE

PAIKKA

PÄIVÄYS

NUUTTI VUORIMIES

Projektipaällikkö, DI

SULJETTU KOLMIAKSIAALIKOE

TTY

Maa- ja pohjarakenteet

PL 600 33101 TAMPERE

ASIAKAS

KOHDE

TYÖNUMERO

Ruukki Construction Oy

Injektointikohde

408/2013 (H408)

Laskennallinen paino = kokeen loppupaino + konsolidoinnissa poistunut vesi + leikkauksessa poistunut vesi

KOKEEN / KOSELLIN N:O	5	5	
PISTE, PAALU	Näyte 1	Näyte 1	
SYVYYS	-	-	
TIEDOSTO	H408 S1	H408 S2	
NOPEUS [mm/min]	0,015	0,015	

LASKENNALLISESTI 20 kPa:n sellipaineessa ennen konsolidointia:

NÄYTTEEN HALKAISIJA [mm]	51	51	
NÄYTTEEN KORKEUS [mm]	97,7	96,4	
NÄYTTEEN POIKKIP.-ALA [cm**2]	20,43	20,43	
NÄYTTEEN TILAVUUS [cm**3]	199,58	196,93	
NÄYTTEEN PAINO LASKENNALLISESTI [g]	317,7	321,2	
Kokoonpuristuma konsolidoinnissa [mm]	2,34	3,53	
Poistunut vesi konsolidoinnissa [ml],[g]	6,2	11,2	
Näytteen paino konsolidoituneena [g]	311,45	310,01	
Kuivan näytteen paino [g]	210,60	216,54	
VESI [g]	107,05	104,67	
VESIPITOISUUS [%]	50,8	48,3	
IRTOTIHEYS [g/cm**3]	1,59	1,63	
TILAVUUSPAINO [kN/m**3]	15,6	16,0	
KUIVA IRTOTIHEYS [g/cm**3]	1,06	1,10	
KUIVATILAVUUSPAINO [kN/m**3]	10,4	10,8	

KYLLÄSTYSASTE Sr, oletus [%]	100,0	100,0	
KIINTOTIHEYS [g/cm**3]	2,28	2,35	
HUOKOSLUKU e	1,16	1,13	
OMINAISTILAVUUS v	2,16	2,13	

KIINTOTIHEYS, oletus [g/cm**3]	2,65	2,65	
KYLLÄSTYSASTE Sr [%]	89,1	90,8	
HUOKOSLUKU e	1,51	1,41	
OMINAISTILAVUUS v	2,51	2,41	

KONSOLIDOITUNEENA:	101 kPa	298 kPa	
"TILAVUUSPAINO" [kN/m**3]	15,8	16,4	
KUIVATILAVUUSPAINO [kN/m**3]	10,7	11,4	

KOKEEN LOPUSSA:

ASTIAN NUMERO	H408 S1	H408 S2	
KOSTEA NÄYTE [g]	311,45	310,01	
Kuivan näytteen paino [g]	107,59	216,54	
VESI [g]	203,86	93,47	
VESIPITOISUUS [%]	189,5	43,2	

0

0

Laskennallinen paino = Koekpl:een paino kokeen lopussa + konsolidoinnissa poistunut vesi (ei välttämättä oikein)

TUTKI:

TAMPERE

PAIKKA

PÄIVÄYS

Niko Levo

Laboratoriomestari

TARKASTI:

TAMPERE

PAIKKA

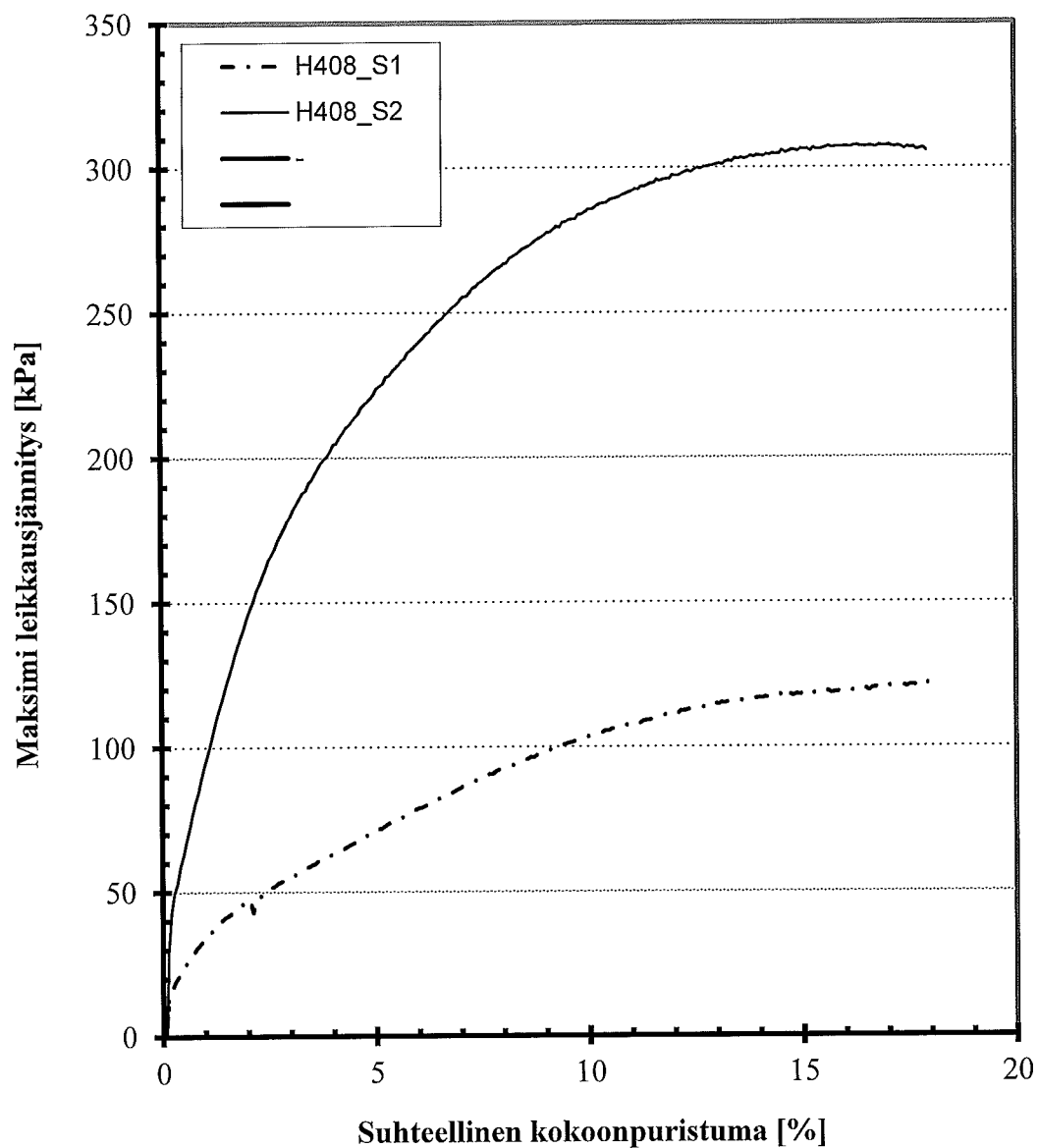
PÄIVÄYS

NUUTTI VUORIMIES

Projektipäällikkö, DI

KOLMIAKSIAALIKOE**TTY****Maa- ja pohjarakenteet****PL 600 33101 TAMPERE****ASIAKAS****KOHDE****TYÖNUMERO****Ruukki Construction Oy****Injektointikohde****408/2013 (H408)****Piste Näyte 1**

Nro	Sellipaine	Tiedosto	Syvyys
1	101	H408_S1 -	
2	298	H408_S2 -	
3	-	-	-



KOLMIAKSIAALIKOE

TTY

Maa- ja pohjarakenteet

PL 600 33101 TAMPERE

ASIAKAS

KOHDE

TYÖNUMERO

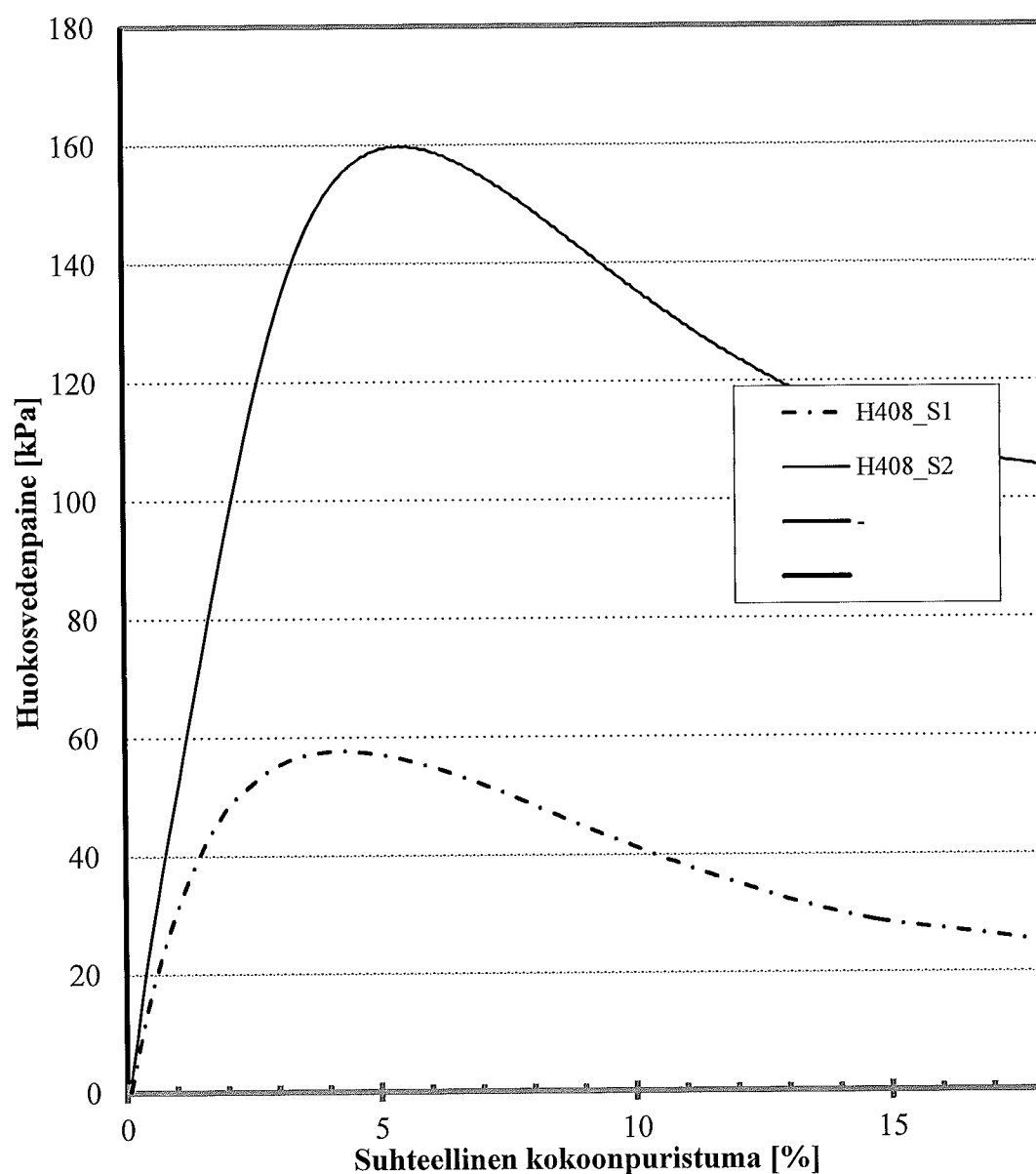
Ruukki Construction Oy

Injektointikohde

408/2013 (H408)

Piste Näyte 1

Nro	Sellipaine	Tiedosto	Syvyys
1	101	H408_S1 -	
2	298	H408_S2 -	
3	-	-	-



KOLMIAKSIAALIKOE

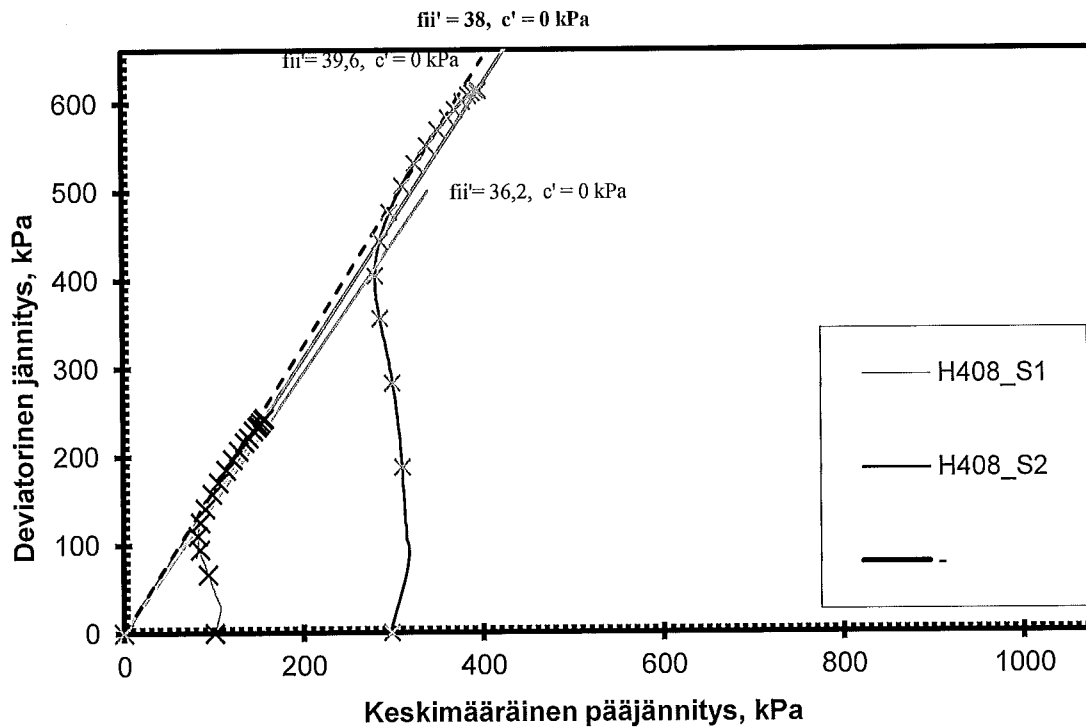
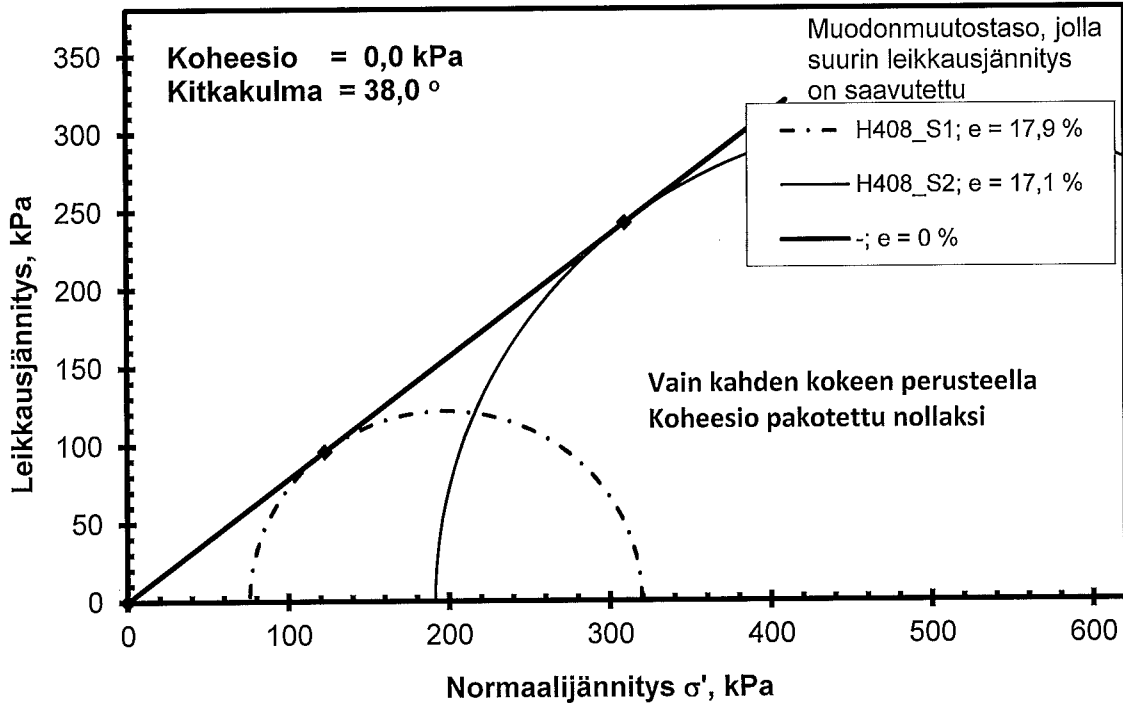
TTY
Maa- ja pohjarakenteet
PL 600 33101 TAMPERE

ASIAKAS
KOHDE
TYÖNUMERO

Ruukki Construction Oy
Injektointikohde
408/2013 (H408)

Piste Näyte 1

Syvyys



Tampereen teknillinen yliopisto
Maa- ja pohjarakenteet
PL 600, 33101 Tampere

Tilaaaja: Ruukki Construction Oy
Työnumero: 408/2013

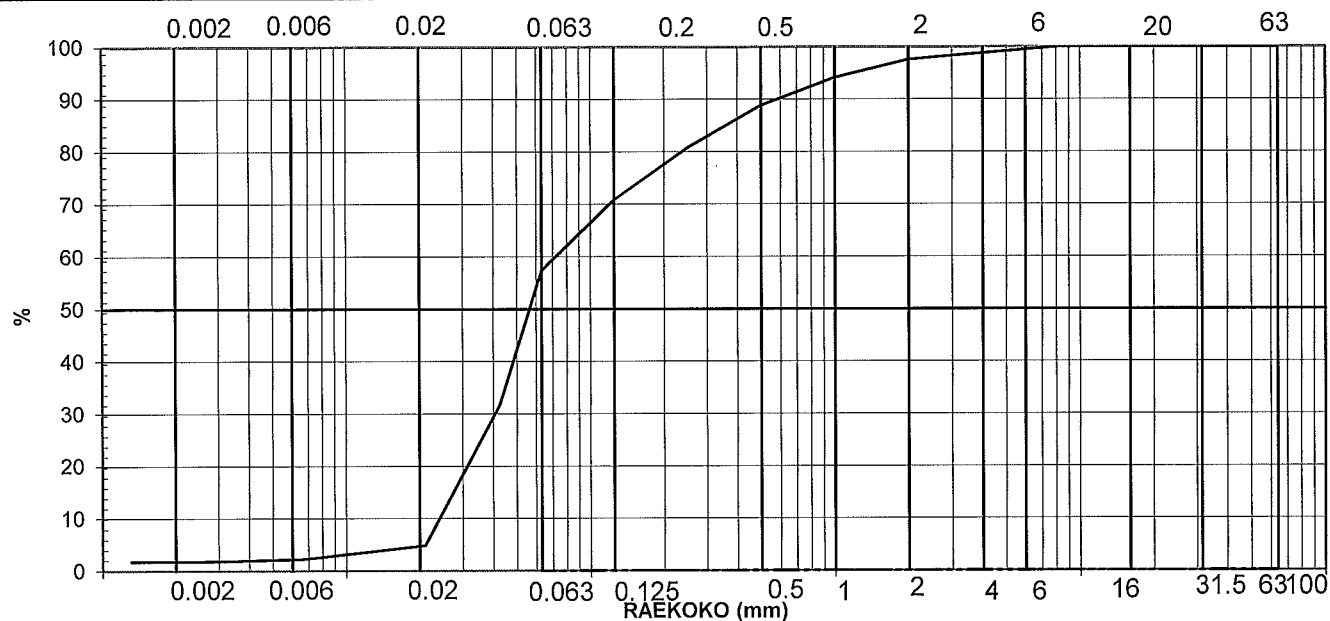
Tutkimus:

Työkohde:

Diplomityö

Kunta:

Näytteen tunnus	a	b	c
Näyttenumero			
paalu/km	1		
syvyys			
korkeustaso			
ottoaika			
Irtotiheys kuiva			
Irtotiheys märkä			
Kiintotiheys			
Vesipitoisuus %			
Polttohäviö %			
Humuspitoisuus %			
Humus NaOH			
Hienoainespitoisuus (-0.063)			
Routivuus, routim, routiva			
Kantavuusluokka			
Kapillaarisuus			
Maalaji SFS (Geo)			
GEO SAVI SILTTI HIEKKA SORA KIVET			



Huomautuksia:

Osa materiaalista "klimppiytyy" ja kaikki ei liukene tasaisesti veteen

Päiväys:

Tutki:

Tarkasti:

Tampereen teknillinen yliopisto Maa- ja pohjarakenteet PL 600, 33101 Tampere	Tilaaaja: Ruukki Construction Oy Työnumero: 408/2013
---	---

Tutkimus	
Työkohde:	Diplomityö Kunta:

Näytteen tunnus	a	b	c
Työnumero			
Näytteen ottopaikka (Paalu)	1		
- syvyys			
- korkeustaso			
Näytteen massa kuivana	107,59		
Näytteen massa pesun jälkeen	49,41		
Pesutappio	58,18		
Kiviä ja lohkareita	%	%	%
20-64			
64-200			
200-600			
> 600			

Seulonta									
Seula	jäi (g)	jäi (%)	läp (%)	jäi (g)	jäi (%)	läp (%)	jäi (g)	jäi (%)	läp (%)
mm									
63	0,00	0,0	100,0						
31,5	0,00	0,0	100,0						
16	0,00	0,0	100,0						
8	0,00	0,0	100,0						
4	1,26	1,2	98,8						
2	1,32	1,2	97,6						
1	3,68	3,4	94,2						
0,5	5,78	5,4	88,8						
0,25	8,72	8,1	80,7						
0,125	10,61	9,8	70,9						
0,063	14,49	13,5	57,4						
pohja	3,68	3,4							
pohja+pesutappio	61,85								
Yhteensä	107,70								

Areometrikoe		4									
Näytemäärä		100		100							
Aika	°C	lukema	raekoko	läp%	lukema	raekoko	läp%	lukema	raekoko	läp%	
Alku											
1 min	22	35,5	0,0424	58,2							
6 min	22	4,5	0,0211	8,9							
1 h	22	1,5	0,00674	4,1							
5 h	22	1	0,00306	3,3							
1 d	22	1	0,00130	3,2							
4 d	21										

Huomautuksia:	Osa materiaalista "klimppiytyy" ja kaikki ei liukene tasaisesti veteen
---------------	--

KOLMIAKSIAALIKOE

TTY

Maa- ja pohjarakenteet

PL 600 33101 TAMPERE

ASIAKAS

KOHDE

TYÖNUMERO

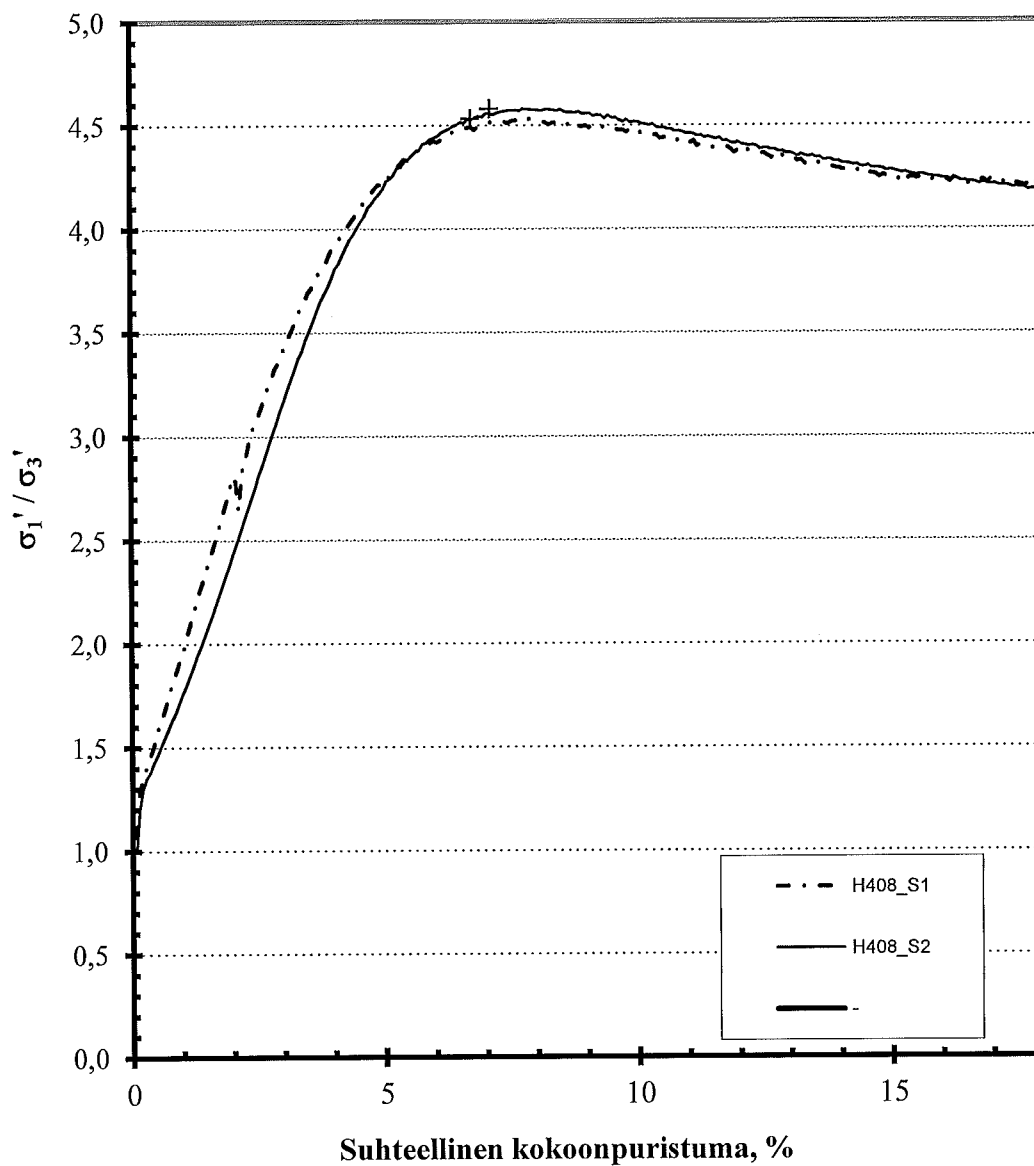
Ruukki Construction Oy

Injektointikohde

408/2013 (H408)

Piste Näyte 1

Nro	Sellipaine	Tiedosto	Syvyys
1	101	H408_S1 -	
2	298	H408_S2 -	
3	-	-	-



KOLMIAKSIAALIKOE

TTY

Maa- ja pohjarakenteet

PL 600 33101 TAMPERE

ASIAKAS

KOHDE

TYÖNUMERO

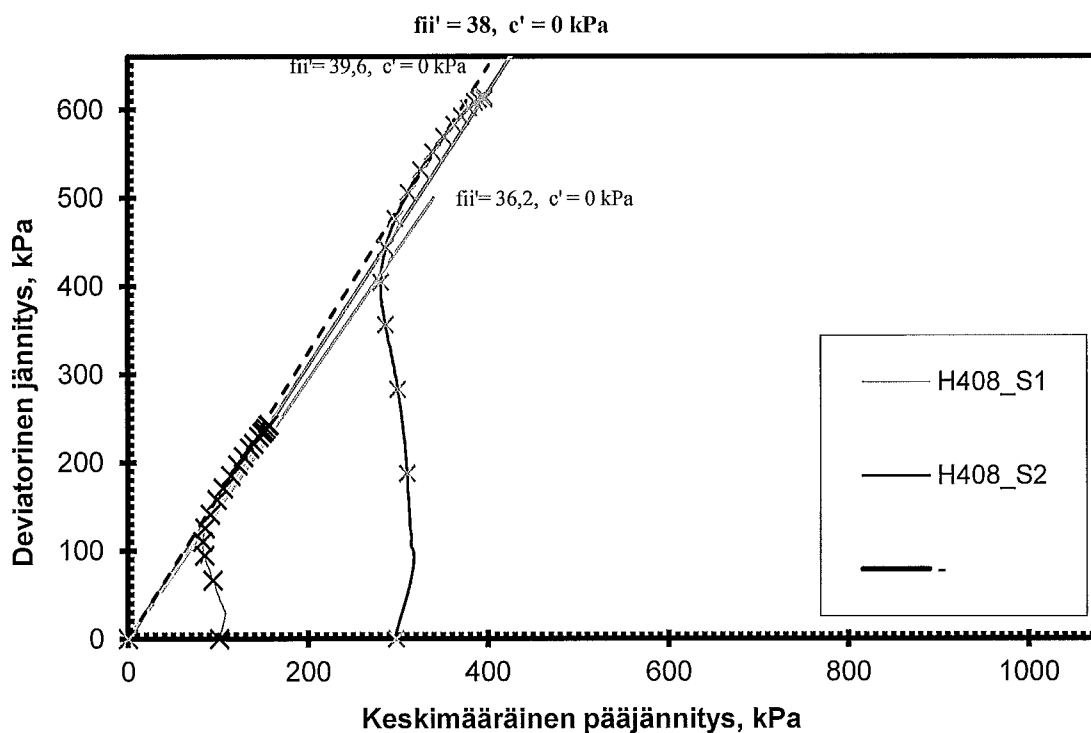
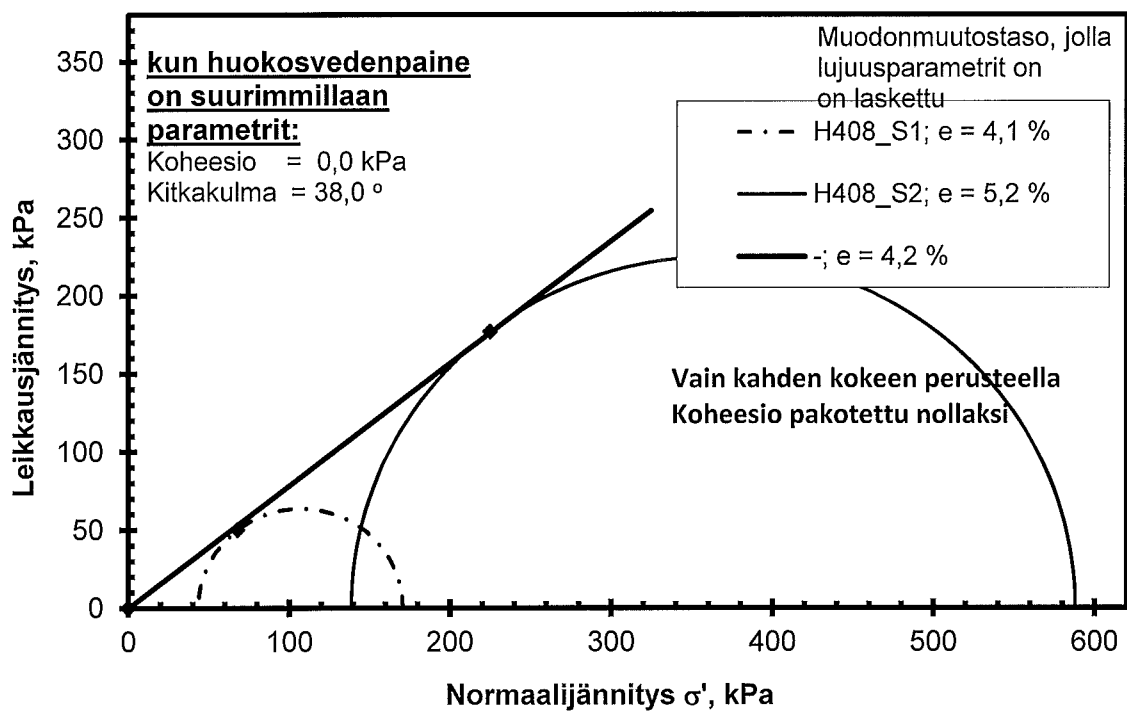
Ruukki Construction Oy

Injektointikohde

408/2013 (H408)

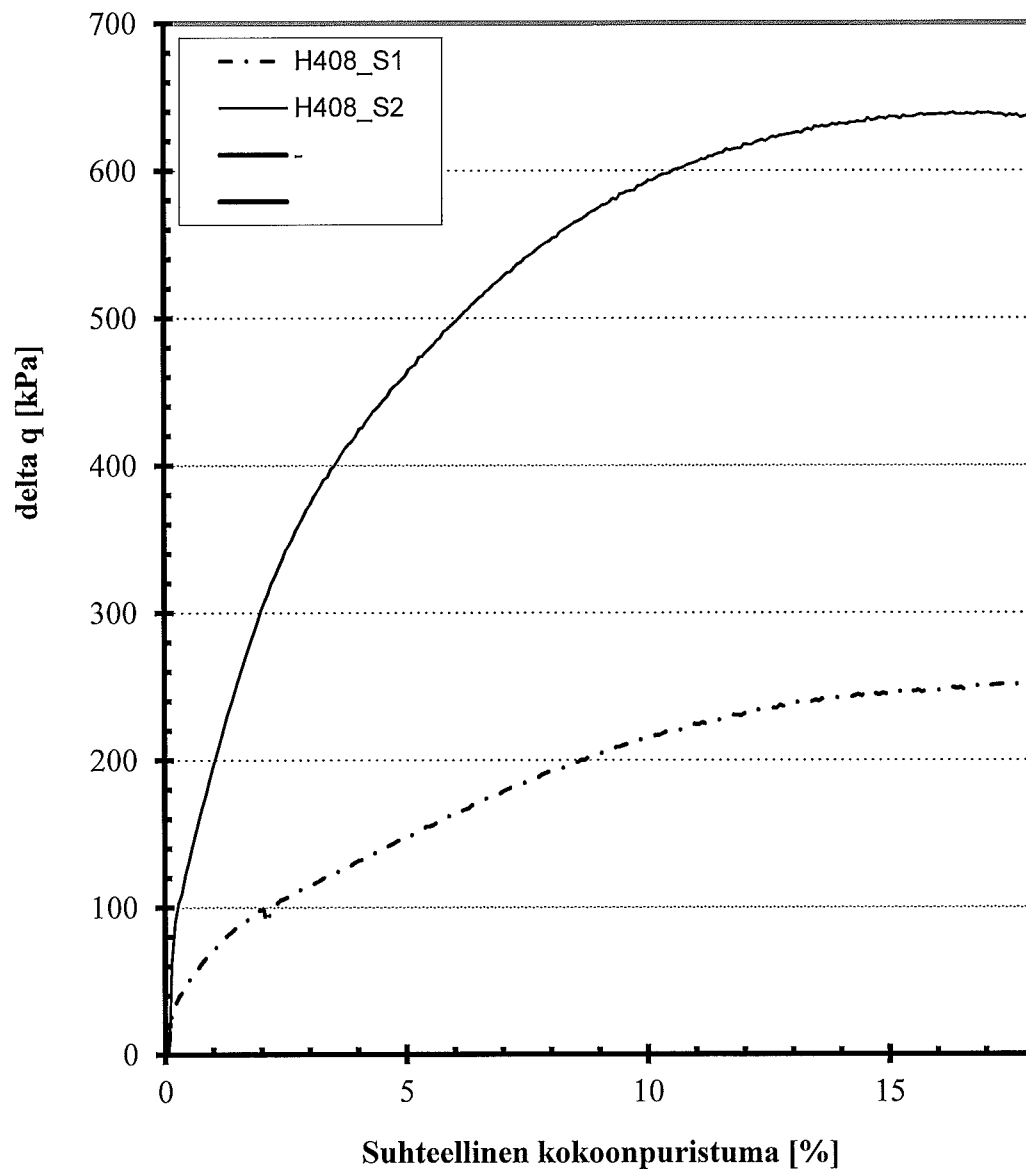
Piste Näyte 1

Syvyys



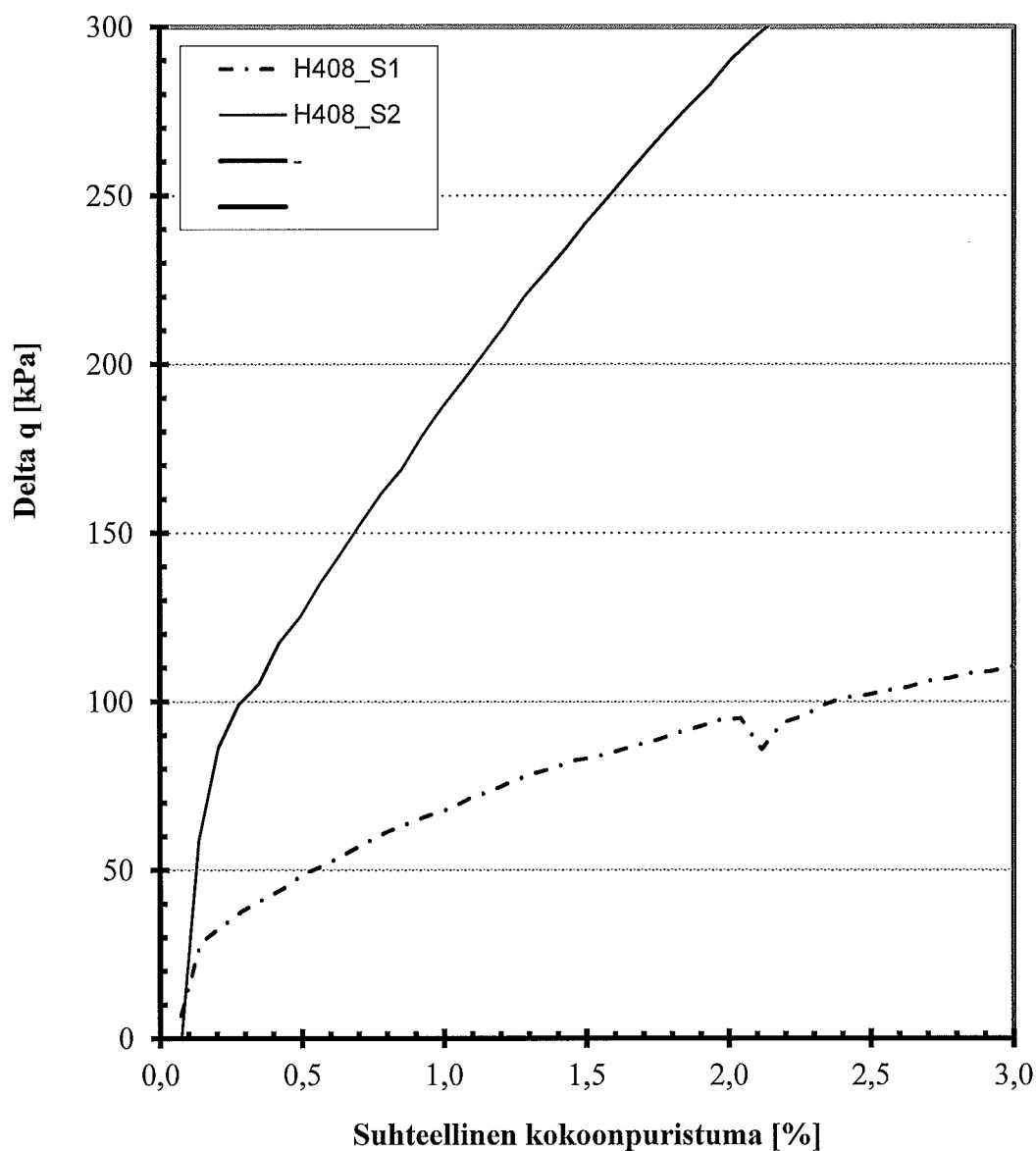
KOLMIAKSIAALIKOE**TTY****Maa- ja pohjarakenteet****PL 600 33101 TAMPERE****ASIAKAS****KOHDE****TYÖNUMERO****Ruukki Construction Oy****Injektointikohde****408/2013 (H408)****Piste Näyte 1**

Nro	Sellipaine	Tiedosto	Syvyys
1	101	H408_S1	-
2	298	H408_S2	-
3	-	-	-



KOLMIAKSIAALIKOE**TTY****Maa- ja pohjarakenteet****PL 600 33101 TAMPERE****ASIAKAS****KOHDE****TYÖNUMERO****Ruukki Construction Oy****Injektointikohde****408/2013 (H408)****Piste Näyte 1**

Nro	Sellipaine	Tiedosto	Syvyys
1	101	H408_S1	-
2	298	H408_S2	-
3	-	-	-



ÖDOMETRIKOE

TTY	ASIAKAS	Ruukki Construction
Maa- ja pohjarakenteet	KOHDE	Injektointikohde
PL 600 33101 TAMPERE	TYÖNUMERO	408/2013 (H408)

ÖDOMETRIN N:O / KOETYYPPI	p12/puntti			
PISTE, PAALU	Näyte 23			
SYVYYS [m]				
TIEDOSTO	H408 P1			
NOPEUS				

KOKEEN ALUSSA:	pvm	9.10.-13		
NÄYTTEEN KORKEUS [mm]		20		
NÄYTTEEN POIKKIP.-ALA [cm**2]		10		
NÄYTTEEN TILAVUUS [cm**3]		20,00		
NÄYTE + RENGAS [g]		66,84		
RENKAAN PAINO [g]		30,55		
KOSTEA NÄYTE [g]		36,29		
KUIVA NÄYTE [g]		28,17		
VESI [g]		8,12		
VESIPITOISUUS [%]		28,8		
IRTOTIHEYS [g/cm**3]		1,81		
TILAVUUSPAINO [kN/m**3]		17,8		
KUIVA IRTOTIHEYS [g/cm**3]		1,41		
KUIVATILAVUUSPAINO [kN/m**3]		13,8		

KYLLÄSTYSASTE Sr [%]	100,00	100,00	100,00	
KIINTOTIHEYS [g/cm**3]	2,37			
HUOKOSLUKU e	0,68			
OMINAISTILAVUUS v	1,68			

KIINTOTIHEYS [g/cm**3]	2,70	2,70	2,70	
KYLLÄSTYSASTE Sr [%]	84,9			
HUOKOSLUKU e	0,92			
OMINAISTILAVUUS v	1,92			

*1)

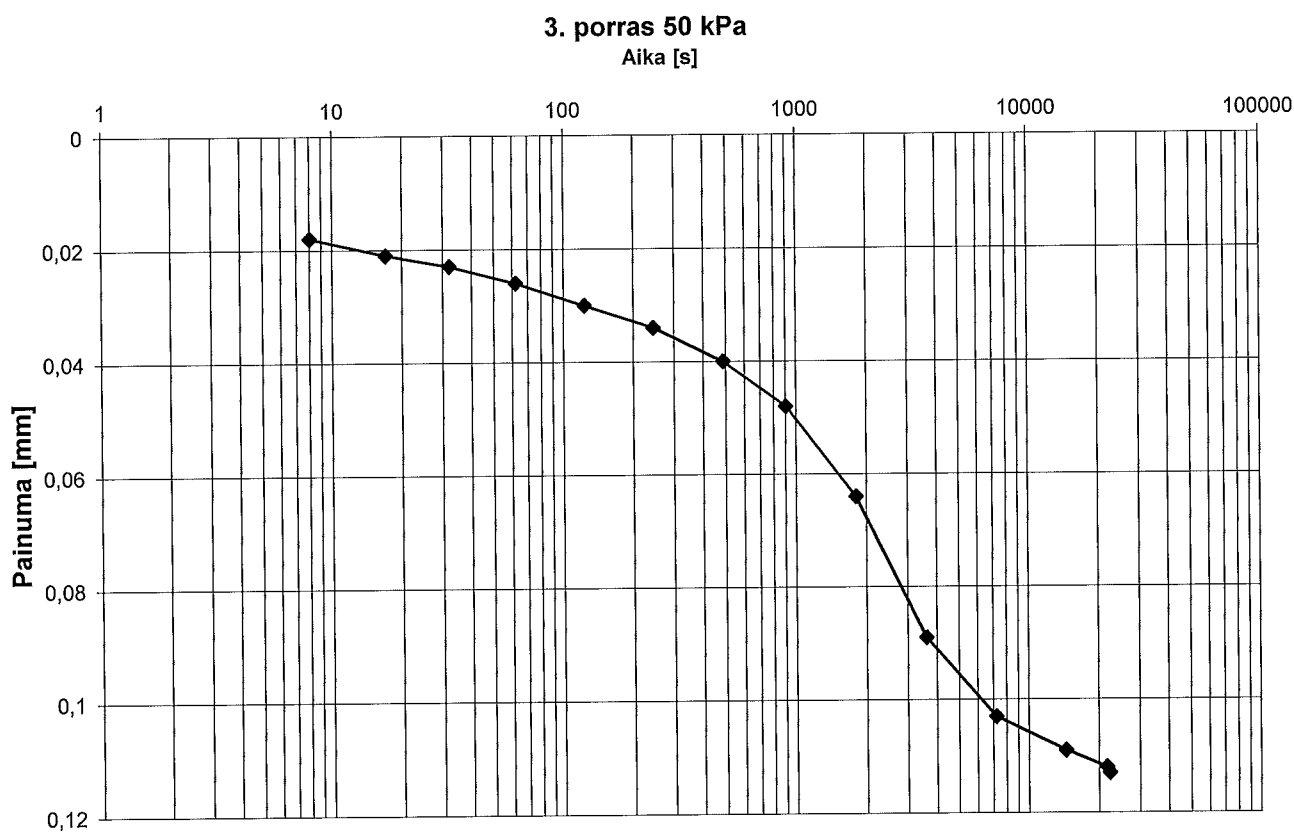
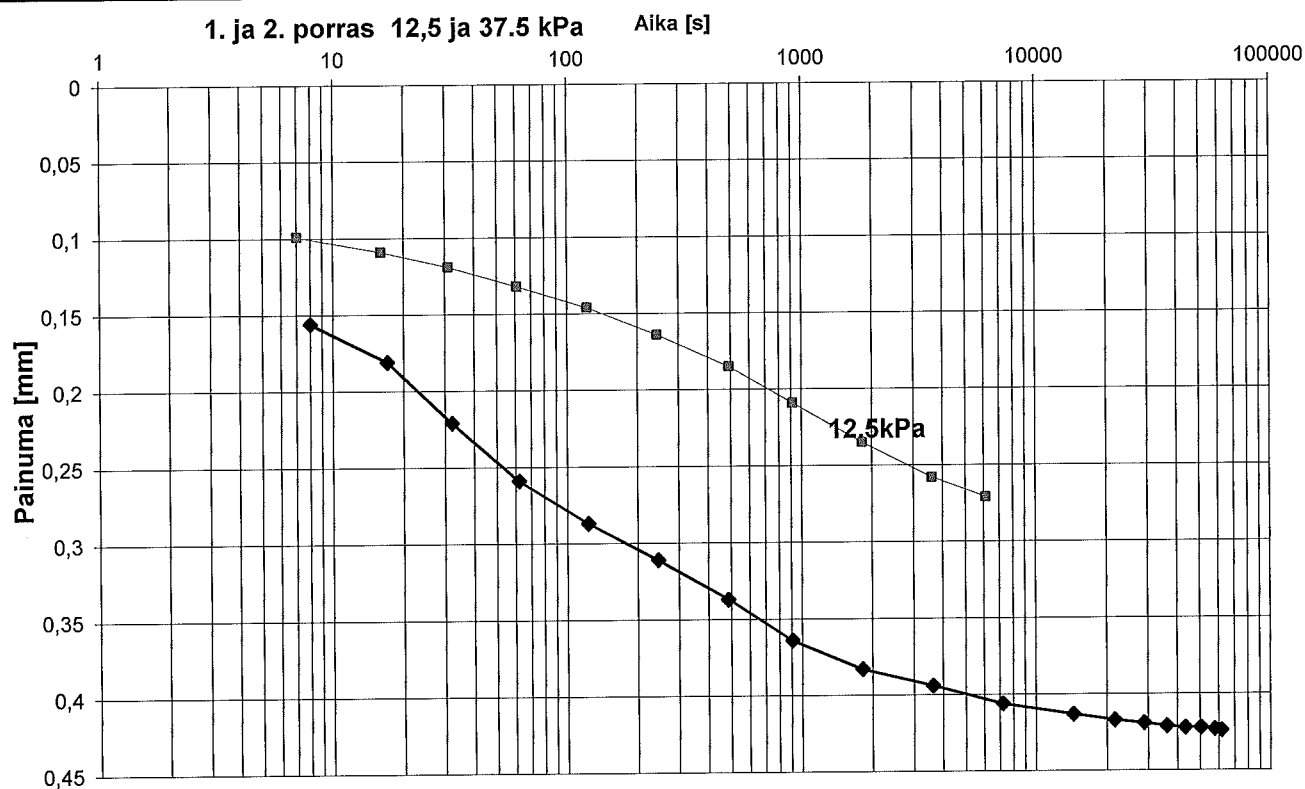
KOKEEN LOPUSSA:				
ASTIAN NUMERO	H408 P1	0,00	0,00	
KOSTEA NÄYTE [g]	34,20			
KUIVA NÄYTE [g]	28,17			
VESI [g]	6,03			
VESIPITOISUUS [%]	21,4			

*1) Häiriintynyt näyte tehty paakusta, jota kostutettiin ennen koekappaleen tekemistä. Näytettä paikattu ödometrirengaaseen
Näyte ei ollut täysin kyllästynyt

TUTKI:	TAMPERE			
	PAIKKA	PÄIVÄYS	Saara Hainari	
			Tutkimusapulainen, tekn yo	
TARKASTI:	TAMPERE			
	PAIKKA	PÄIVÄYS	Nuutti Vuorimies	
			Projektipäällikkö, DI	

ODOMETRIKOE

1/5

TTY**Maa- ja pohjarakenteet****PL 600****33101 TAMPERE****ASIAKAS****KOHDE****PISTE****SYVYYS****TIEDOSTO****Ruukki Contruction****Injektointikohde****Näyte 23****H408_P1.DA4**

ODOMETRIKOE

2/5

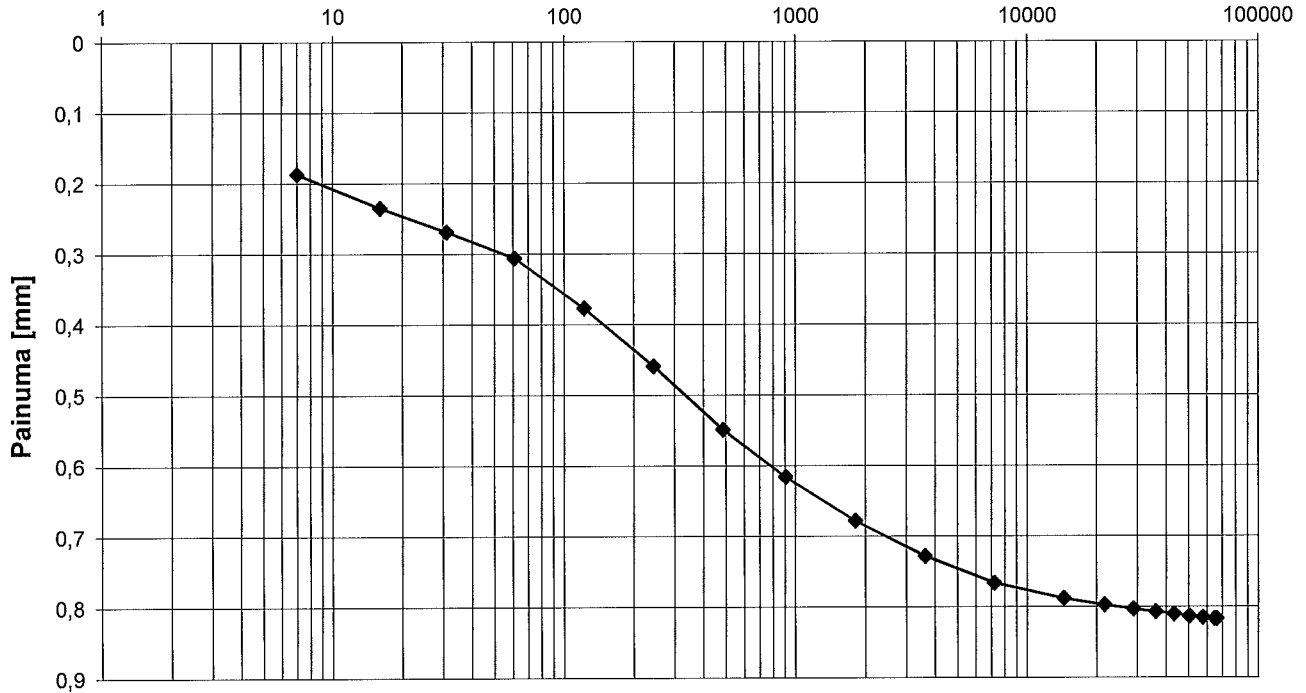
TTY
Maa- ja pohjarakenteet
PL 600
33101 TAMPERE

ASIAKAS
KOHDE
PISTE
SYVYYS
TIEDOSTO

Ruukki Contruction
Injektointikohde
Näyte 23
-
H408_P1.DA4

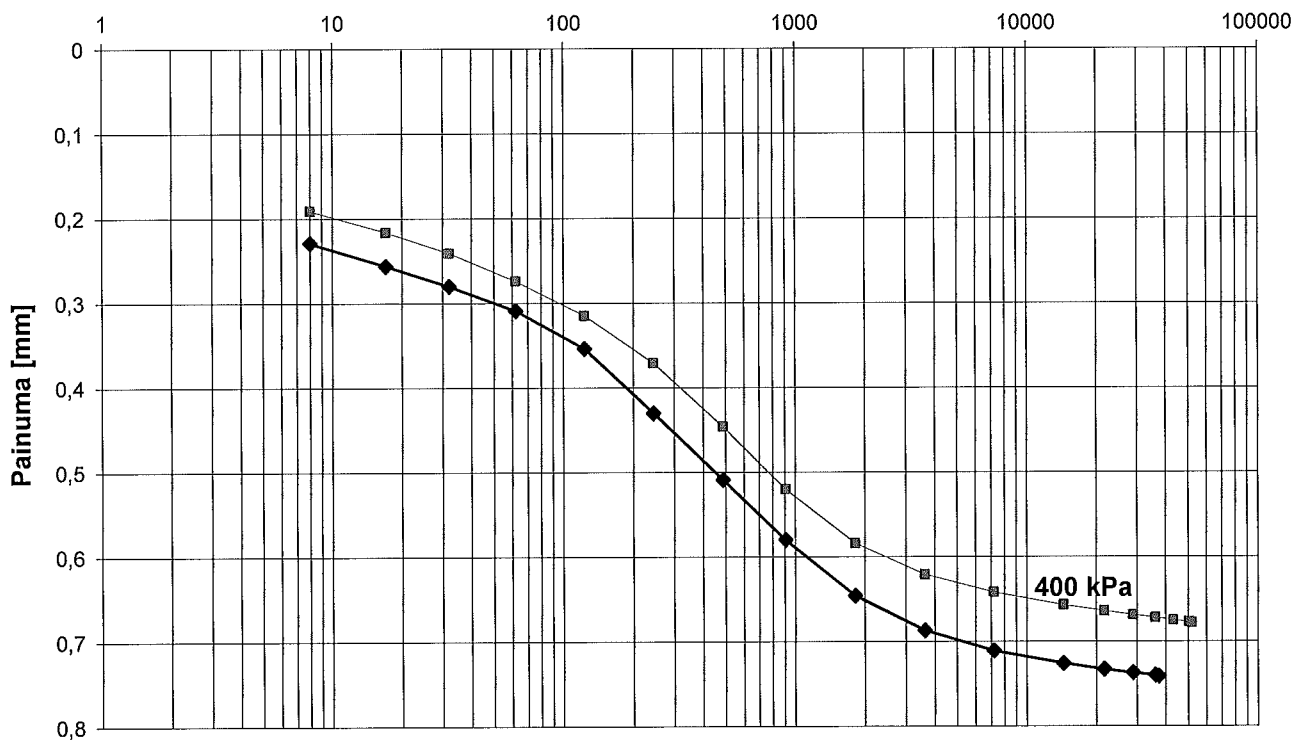
4. porras 100 kPa

Aika [s]



5. ja 6. porras 200 ja 400 kPa

Aika [s]



ODOMETRIKOE

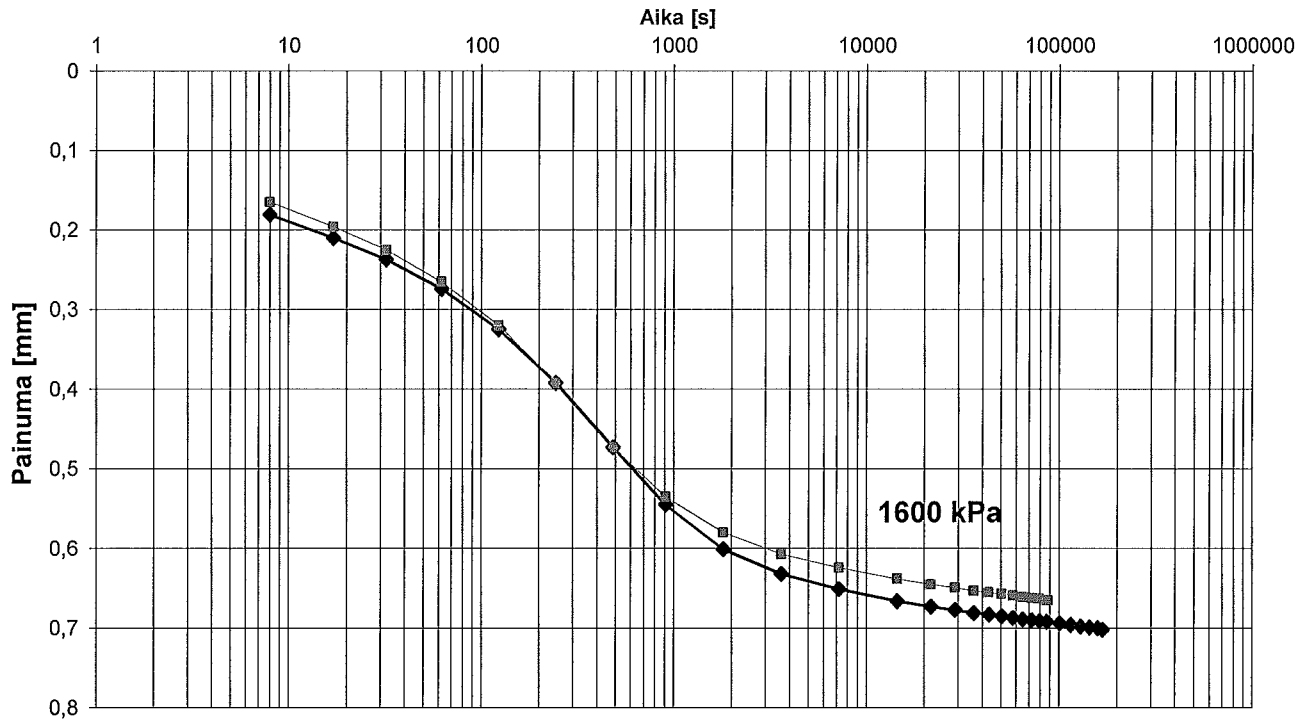
3/5

TTY
Maa- ja pohjarakenteet
PL 600
33101 TAMPERE

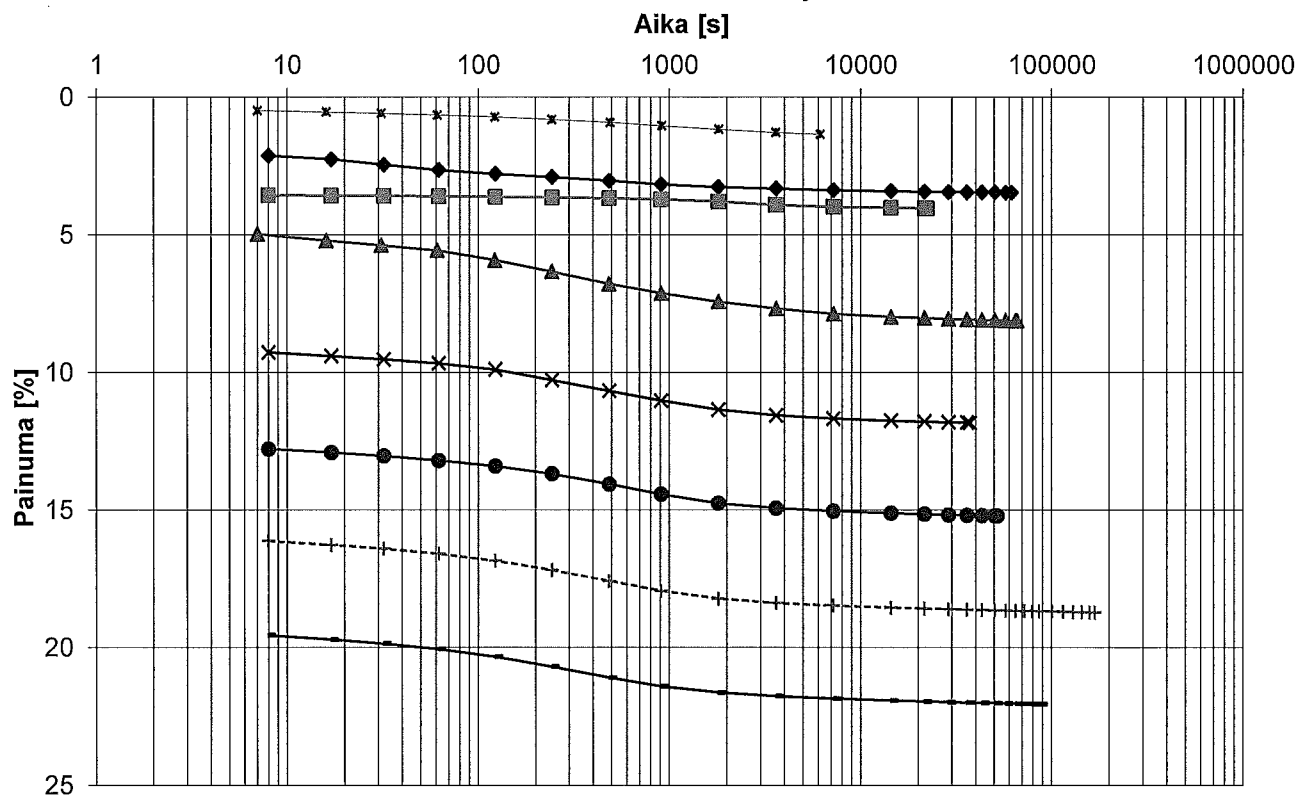
ASIAKAS
KOHDE
PISTE
SYVYYS
TIEDOSTO

Ruukki Contruction
Injektointikohde
Näyte 23
-
H408_P1.DA4

7. porras 800 ja 1600 kPa



Portaat 6.25, 12.5, 25, 50, 100, 200 ja 400 kPa



ODOMETRIKOE

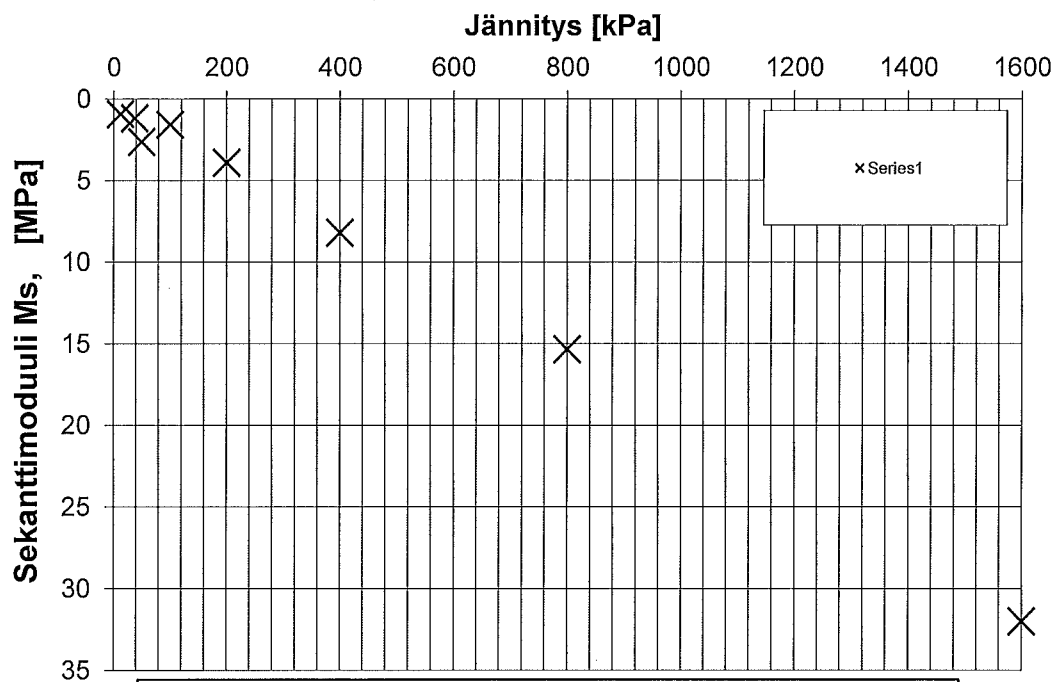
4/5

TTY
Maa- ja pohjarakenteet
PL 600
33101 TAMPERE

ASIAKAS
KOHDE
PISTE
SYVYYS
TIEDOSTO

Ruukki Contruction
Injektointikohde
Näyte 23
-
H408_P1.DA4

Numeerisen menetelmän sovitus



Koekappale ei ollut täysin kyllästynyt

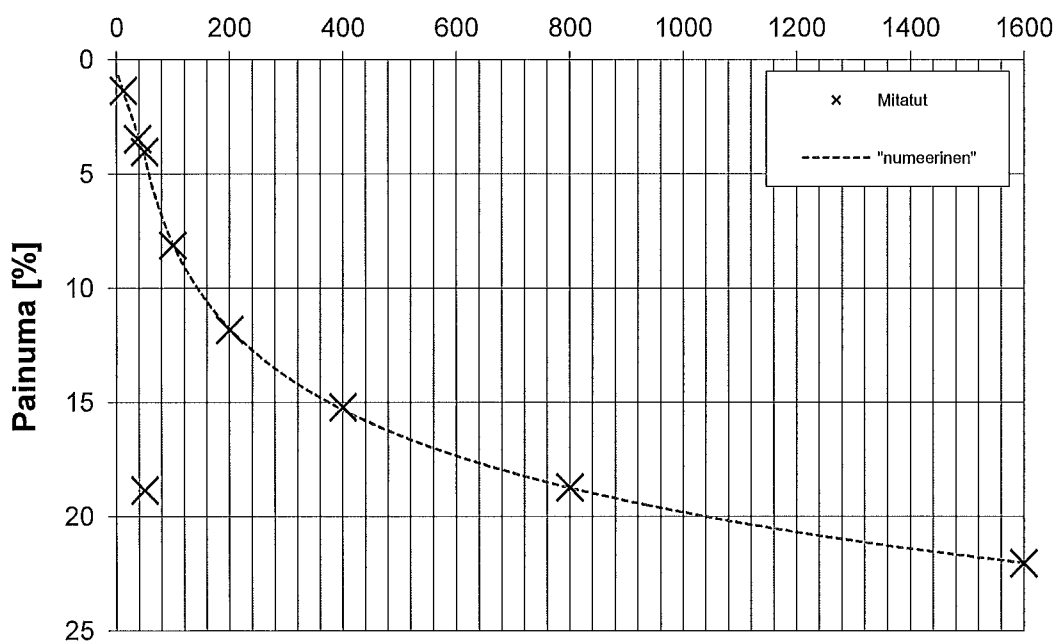
Konsolidaatiokerroin
Casagrande
porras c_v , m²/a

100	11
200	7,3
400	6,4
800	7,5
1600	6,9

Vedenläpäisevyyskerroin
Casagrande
porras k , m/s

100	2,1E-09
200	5,8E-10
400	2,4E-10
800	1,5E-10
1600	6,7E-11

Numeerisen menetelmän sovitus



Numer. sovitus
 $\beta = -0,06$
 $m = 18,4$
 $\sigma'_c = 50,0$
 $\beta_2 = 1,0$
 $m_2 = 13,5$
palaut.= 484,4

Konsolidaatiokerroin
Taylor
porras c_v , m²/a

100	16
200	11
400	11
800	9
1600	11

Tampere

päiväys

Nuutti Vuorimies, tutkija

ODOMETRIKOE

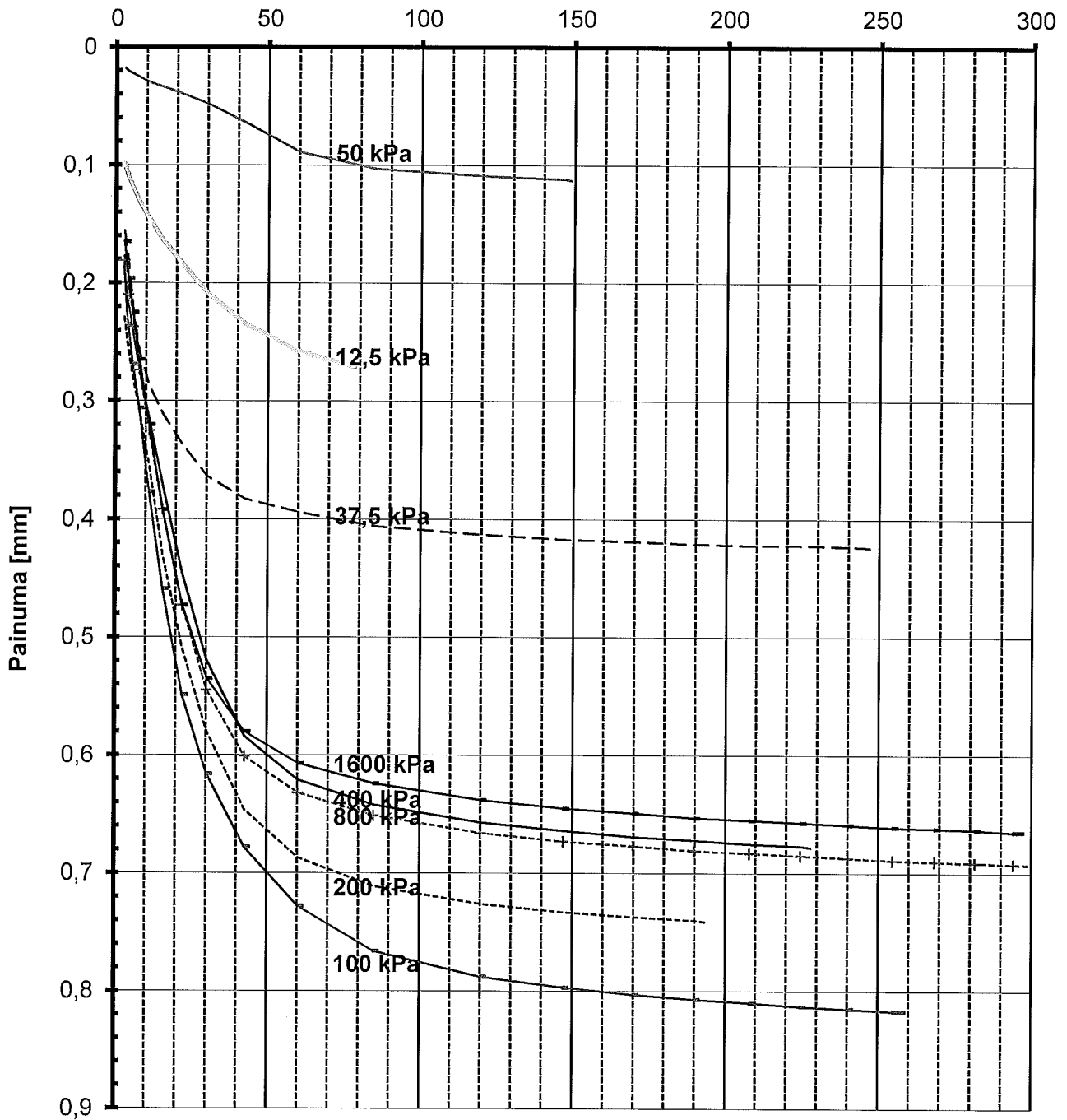
5/5

TTY
Maa- ja pohjarakenteet
PL 600
33101 TAMPERE

ASIAKAS
KOHDE
PISTE
SYVYYS
TIEDOSTO

Ruukki Contruction
Injektointikohde
Näyte 23
-
H408_P1.DA4

Portaat 6.25, 12.5, 25, 50, 100, 200 ja 400 kPa
SQRT Aika [s]



Appendix 21: rotational stiffness of test piles versus FEM calculation

Pile	Pile length [m]	Material in the gap of the drilling hole in bedrock	Max elastic force [kN]	Measured displacement at max elastic force [mm]	Displacement due to FEM without extra springs and large deflection allowed, friction 0.5	FEM displacement compared to tested	Displacement from joint, measured	Comment		Non-linear 0.5 friction vs. reality TOTAL	Non-linear 0.5 friction vs. reality JOINT	Displacement due to FEM without extra springs and large deflection allowed, linear model 0.1 friction	Linear 0.1 friction vs. reality TOTAL	Linear 0.1 friction vs. reality JOINT
10	1.97	Grouted	73.1	38	35.9	-5.5 %	13.3	sand above rock level		-5.5 %	-15.8 %	37.3	-1.8 %	-5.3 %
11	1.99	Drilling mud	72.4	38.9	36.2	-6.9 %	14.2	sand above rock level		-6.9 %	-19.0 %	37.2	-4.4 %	-12.0 %
20	2	Grouted	72	41.3	37.5	-9.2 %	16.6	clay above rock level		-9.2 %	-22.9 %	37.9	-8.2 %	-20.5 %
22**	1.98	Grout/clay	72.7	108.1	39.4	-63.6 %	83.4	clay above rock level		-63.6 %	-82.4 %	38.3	-64.6 %	-83.7 %
22***	1.98	Grout/clay	72.7	108.1	95.7	-11.5 %	83.4	clay above rock level		-11.5 %	-14.9 %	108.5	0.4 %	0.5 %

*Non-grouted tight, drilling mud

**weakest clay-concrete sample values

***weakest clay-concrete sample values/1000

Master of Science Thesis: THE ROTATIONAL STIFFNESS AND WATERTIGHTNESS OF RD PILE WALLS IN THE BEDROCK AND PILE INTERFACE, Leo-Ville Miettinen

Appendix 22: Interview memo 27 November 2013, translated into English from conversations conducted in Finnish.

6 May 2013 Western metro line, Koivusaari, Antti Westerlund

-Grouting pipe ended at about the level of interlock toe, in some piles pipe was even longer. As such, grouting pipe ended approximately 50 mm above pipe toe. Grouting pipe diameter was 20 mm. Grouting pipe was located at the ground side of the wall (not excavation side).

-Grouting working order: Piles concreted inside, curtain grouting, clearing the grouting channel by using pressurized air and then grouting via injection pipe.

-Approximately 50% of grouting pipes allowed grout to pass, rest could not be opened with pressurized air. Could be assumed that at least some if not all blockings were caused by curtain grouting, which was done before grouting via channel. Curtain grouting reached to the drilling hole gap even as deep as 4 meter deep from bedrock.

-Finishing pressure in grouting was 10 bar, can be verified in report.

-Grouting consumption was documented in grouting record, ask for record from Anniina.

-Drilling depths into bedrock were 1.5 to 2 meters, differed from 0.5 meters in design. The reason for deeper drilling depths was that bedrock was more fractured than assumed.

-Rock bolts 50 mm in diameter were extended 500 mm into the pile and 1500 mm into the bedrock. Rock bolts were used probably due to preparation for collision.

Watertightness:

Water leakage through interlocks was mainly insignificant, mainly completely watertight. Sealant used in interlocks was bitumen-based mass (this can be checked somewhere) and welded steel piece. WOM/WOF interlocks were used. **Leo-Ville Miettinen 19 December 2013 additional comment: Bitumen sealant was Beltan, same mass was used in Trondheim**

There was no need for sealing afterwards.

-Water penetration test:

5 bar overpressure for 5 minutes. Water penetration record can be requested from Anniina.

Connection points of pile wall were executed by using smaller piles drilled aside wall and welded together by using steel pieces to seal wall. There were 8 connection points in the wall.

-Additional remarks:

Master of Science Thesis: THE ROTATIONAL STIFFNESS AND WATERTIGHTNESS OF RD PILE WALLS IN THE BEDROCK AND PILE INTERFACE, Leo-Ville Miettinen

One or two interlocks were opened while drilling piles. The reason was that pile was not fully vertical when drilling started. The start is most important when drilling RD pile wall. The fault was fixed like connection point of the pile.

Every second pile had a grouting pipe and only 4m from surface in esker. **Leo-Ville Miettinen 27**

November 2013 additional comment: This means that only every second pile had a grouting pipe which was only 4 meters long. Therefore, the pipe did not reach the bedrock. The purpose was to grout background soil to minimize the settlement of soil and therefore prevent damaging the building next to the excavation.

6 May 2013 Western metro line, Urheilupuisto, project manager Erkki Virtanen, Peab

-To allow concrete to flow into the drilling hole gap, there was a plan to raise the pile. We noticed, though, that concrete flowed even from one pile to another, so it was assumed that concrete had flowed into the gap. To prevent concrete from flowing from one pile to other piles, they were vibrated. Concrete flow to piles unready reinforcement was not desired.

-After three weeks it was assumed that bedrock is visible next to RD pile wall. Ask Kauko Korpela

Technical specialist, Veli-Matti Uotinen Ruukki 27 May 2013

-In Western metro line, Koivusaari 100 mm casing was left inside the concrete in RD pile wall. After that hole into the bedrock was drilled from inside the casing, curtain grouting was done at several stages starting from the bottom of drilling hole. Afterwards, a grouting water penetration test was executed. After the water penetration test, the bedrock was grouted again until the required watertightness was achieved.

Erkki Virtanen Peab, summer 2013

-Self compacting K40, S5, max 16 mm aggregate concrete was used in RD piles

-Pile wall has been watertight, water flow may be restricted by sheet pile wall behind the RD pile wall. Anchors were drilled through the sheet piles so that the water pressure would be the same behind the RD pile wall.

-Material may be used in Master's thesis.

Nuutti Vuorimies, project manager, TTY 19 December 2013, comment for Master's thesis

The sample size should be increased so that the sample is sufficiently representative and the individual granules do not have too large an effect on the big picture. For 32 mm maximum grain size of the sample a sample of approximately 10 kg is required. For 4mm grain size sample about 200 g is sufficient quantity. Sample 1 had sufficient amount of material, others did not.

Master of Science Thesis: THE ROTATIONAL STIFFNESS AND WATERTIGHTNESS OF RD PILE WALLS IN THE BEDROCK AND PILE INTERFACE, Leo-Ville Miettinen

-Table 3.2.2.1.2: Water permeability is not measured. Coefficient of consolidation was defined by Casagrande method from oedometer test

-Table 3.2.2.1.3: Mention that the measurements were made up to 1600 kPa and that the rest was estimated